ABC Imagem Cardiovascular

Volume 38 | Number 1

January/February/March 2025

Sociedade Brasileira de Cardiologia
ISSN-2675-312X

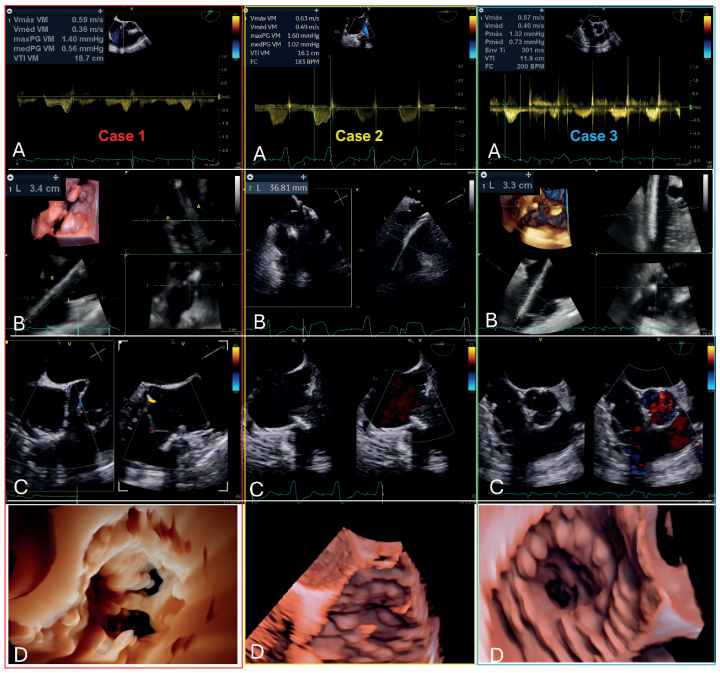

Central Illustration of the article: First Percutaneous Orthotopic Tricuspid Valve Implantations using the LuX-Valve Plus Device in Latin America: Report of the First Three Cases

DIC | SBC Sociedade Brasileira de Cardiologia 1943 | ABC Imagem Cardiovascular

Contents

Click on the title to read the article

Image

Departament of Cardiovascular Imaging

President
Silvio Henrique Barberato - PR

Vice President of Echocardiography
Daniela do Carmo Rassi Frota - GO

Vice President of Nuclear Cardiology
Cláudio Tinoco Mesquita – RJ

Vice President of Vascular Echography
Salomon Israel do Amaral – RJ

Vice President of Magnetic Resonance Imaging
Isabela Bispo Santos da Silva Costa – SP

Vice President of Computed Tomography
Jorge Andion Torreão – BA

Vice President of Congenital Heart Disease and Pediatric Cardiology
Andressa Mussi Soares – ES

Managing Director
Adenalva Lima de Souza Beck – DF

Financial Director
Gláucia Maria Penha Tavares - SP

Journal Editor
Marcelo Dantas Tavares de Melo – PB

Consulting Board

Members
André Luiz Cerqueira de Almeida - BA
Arnaldo Rabischoffsky - RJ
Carlos Eduardo Rochitte - SP
Marcelo Luiz Campos Vieira - SP
Samira Saady Morhy - SP

Scientific Committee

Coordinator
Daniela do Carmo Rassi Frota - GO

Members
Andressa Mussi Soares - ES
Cláudio Tinoco Mesquita - RJ
Isabela Bispo Santos da Silva Costa - SP
Jorge Andion Torreão - BA
Salomon Israel do Amaral - RJ

Echocardiography Certification Committee

Coordinator
Tatiane Mascarenhas Santiago Emerich - ES
Andrea de Andrade Vilela - SP

Adult Echo Members
Antonio Amador Calvilho JR. - SP
Antonio Tito Paladino Filho - SP
Eliza de Almeida Gripp - RJ
Jaime Paula Pessoa Linhares Filho - CE
João Carlos Moron Saes Braga - SP
Marcio Mendes Pereira - MA
Paulo Henrique Nunes Pereira - PA
Renato de Aguiar Hortegal - SP
Tiago Costa Bignoto - SP
Wanessa Nakamura Guimarães - DF

Congenital Echo Members
Barbara Neiva Tanaka - MA
Daniela Lago Kreuzig - SP
Danielle Lopes Rocha - ES
Halsted Alarcao Gomes Pereira da Silva - SP
Leandro Alves Freire - SP
Marcio Miranda Brito - TO
Maria Elisa Martini Albretch - SP

Seniors
Andrea de Andare Vilela - SP
Glaucia Maria Penha Tavares - SP
José Luiz Barros Pena - MG
Maria Estefania Bosco Otto - DF
Mohamed Hassan Saleh - SP
Solange Bernardes Tatani - SP

Social Media Committee

Coordinator
Alex dos Santos Félix - RJ
Antonio Carlos Leite de Barros Filho - SP

Members
Barbara Athayde Linhares Martins Vrandecic - MG
Cristiane Nunes Martins - MG
José Roberto Matos Souza - SP
Simone Cristina Soares Brandão - PE

Professional Defense and Institutional Relations Committee

Members
Fabio Cañellas Moreira - RS
Jorge Yussef Afiune - DF
Marcelo Haertel Miglioranza - RS
Mohamed Hassan Saleh - SP
Wagner Pires de Oliveira Júnior - DF

Committee of Education and Accreditation

Coordinator
Edgar Bezerra de Lira Filho - SP

Members
Andrea de Andare Vilela - SP
Sandra Nívea dos Reis Saraiva Falcão - CE

Intersociety Committee

Coordinator
Marcelo Luiz Campos Vieira - SP

Members
Ana Cristina de Almeida Camarozano - PR
José Luiz Barros Pena - MG
Marcelo Haertel Miglioranza - RS

DIC Youth Committee

Coordinator
Bruna Morhy Borges Leal Assunção - SP
Márcio Miranda Brito - TO

Adult Echo Members
Carolina da Costa Mendes - SP
Manoela Falsoni - SP
Talita Beithum Ribeiro Mialski - PR
Tauin Raoni Do Couto - PA

CR/MR Members
Maria Júlia Silveira Souto - SP

Vascular Ultrasound Member
Larissa Chaves Nunes de Carvalho - SP

Member Of Congenital Heart Diseases
Isabela de Sousa Lobo Silva - SP

Committee on Echocardiography, Congenital and Pediatric Cardiology

Coordinator
Andressa Mussi Soares - ES

Members
Cláudia Regina Pinheiro de Castro Grau - SP
Laura Mercer Rosa - USA
Márcia Ferreira Alves Barberato - PR

PORTAL DIC

Coordinator
Alex dos Santos Félix - RJ

ABC Imagem Cardiovascular

Volume 38, Nº 1, January/February/March 2025

Indexing: Lilacs (Latin American and Caribbean Health Sciences Literature), Latindex (Regional Cooperative Online Information System for Scholarly Journals from Latin America, the Caribbean, Spain and Portugal) and DOAJ (Directory of Open Access Journals)

Address: Av. Marechal Câmara, 160 - 3º andar - Sala 330
20020-907 • Centro • Rio de Janeiro, RJ • Brazil
Phone.: (21) 3478-2700
E-mail: abcimaging@cardiol.br
https://www.abcimaging.org/

Commercial Department
Phone: (11) 3411-5500
E-mail: comercialsp@cardiol.br

Editorial Production
SBC - Scientific Department

Graphic Design and Diagramming
SBC - Scientific Department

Association of Noonan Syndrome, Noncompaction of the Myocardium, Hypertrophic Cardiomyopathy, and Long QT Syndrome: A Case Series

Anna Luisa de Melo Lula Lins Pimentel,[1] Érika Alves da Silva,[1] Marcelo Dantas Tavares de Melo,[1] Vera Maria Cury Salemi[2]

Universidade Federal da Paraíba,[1] João Pessoa, PB – Brazil
Hospital Sírio Libanês,[2] São Paulo, SP – Brazil

Abstract

Background: The Noonan syndrome (NS) is a rare genetic disorder characterized by manifestations such as short stature, a webbed neck, micrognathia, and hypertelorism. Although NS predisposes to cardiac disorders such as hypertrophic cardiomyopathy (HCM), it has only rarely been associated with noncompaction cardiomyopathy (NCCM), an embryonic anomaly defined by excessive trabeculation and formation of deep myocardial recesses. The clinical presentation of NCCM ranges from asymptomatic to severe thromboembolic events. This study aims to describe cardiovascular changes and outcomes in patients with NS and NCCM followed at the cardiology department of a Brazilian hospital.

Methods: Observational, longitudinal, prospective follow-up of three adult patients with the NS phenotype. All underwent echocardiography and cardiac magnetic resonance imaging (CMR). Data such as age, sex, family history, symptom onset, and outcomes of interest, such as thromboembolic events, heart transplantation (HTx), and death, were analyzed.

Results: All three patients followed (one male-female sibling pair and one unrelated male) had NCCM with ventricular dysfunction. The female patient also had the long QT syndrome (LQTS). All developed apical thrombi, in the left ventricle in two cases. The female patient underwent successful HTx, while the two males died after decompensation of heart failure (HF) progressing to cardiogenic shock.

Conclusion: This case series highlights the need for early diagnosis and family screening of patients with NS to optimize treatment and improve prognosis. There is no prior record in the literature of the association of all conditions described herein in the same patient.

Keywords: Noonan Syndrome; Isolated Noncompaction of the Ventricular Myocardium; Long QT Syndrome.

Introduction

The Noonan syndrome (NS) is a rare, predominantly autosomal genetic condition characterized by distinct phenotypic features, including short stature, a webbed neck, hypertelorism, micrognathia, low-set ears, and pectus carinatum.[1,2] NS is frequently associated with heart diseases, such as hypertrophic cardiomyopathy (HCM), arrhythmias, and conduction disorders, having been described only once—in 2016—in association with noncompaction cardiomyopathy (NCCM).[2,3] NCCM, also known as noncompaction of the myocardium, is a complex embryonic disorder characterized by excessive trabeculation of the myocardium, resulting in formation of deep ventricular recesses that fill with blood. The clinical picture of NCCM can range from asymptomatic to severe thromboembolic complications.[4] The diagnostic criteria for this cardiomyopathy are not yet fully established. The use of echocardiography and cardiac magnetic resonance imaging (CMR) for diagnosis is widespread, especially using the Zurich criteria (described by Jenni in 2001) and the Petersen criteria.[4-6]

The prevalence of cardiac disease in adults with NS is not well studied, but the syndrome is known to affect multiple organs, which means clinicians must be aware of and have a high index of suspicion for serious events arising from the most prevalent causes.[2] The present report describes three clinical cases (including one sibling pair) of patients simultaneously affected by the NS, HCM, and NCCM, all followed at the outpatient cardiology clinic of a Brazilian public hospital. One of the patients also had long QT syndrome (LQTS), a condition that compromises ventricular repolarization; the association of NS, NCCM, and LQTS is heretofore undescribed in the literature.[7] Furthermore, the

Mailing Address: Marcelo Tavares •
Universidade Federal da Paraíba. Cidade Universitária, sn, Conj. Pres. Castelo Branco III. Postal code: 58051-900. João Pessoa, PB – Brazil
E-mail: marcelo_dtm@yahoo.com.br
Manuscript received October 25, 2024; revised October 28, 2024; accepted October 28, 2024
Editor responsible for the review: Marcelo Tavares

DOI: https://doi.org/10.36660/abcimg.20240107i

Central Illustration: Association of Noonan Syndrome, Noncompaction of the Myocardium, Hypertrophic Cardiomyopathy, and Long QT Syndrome: A Case Series

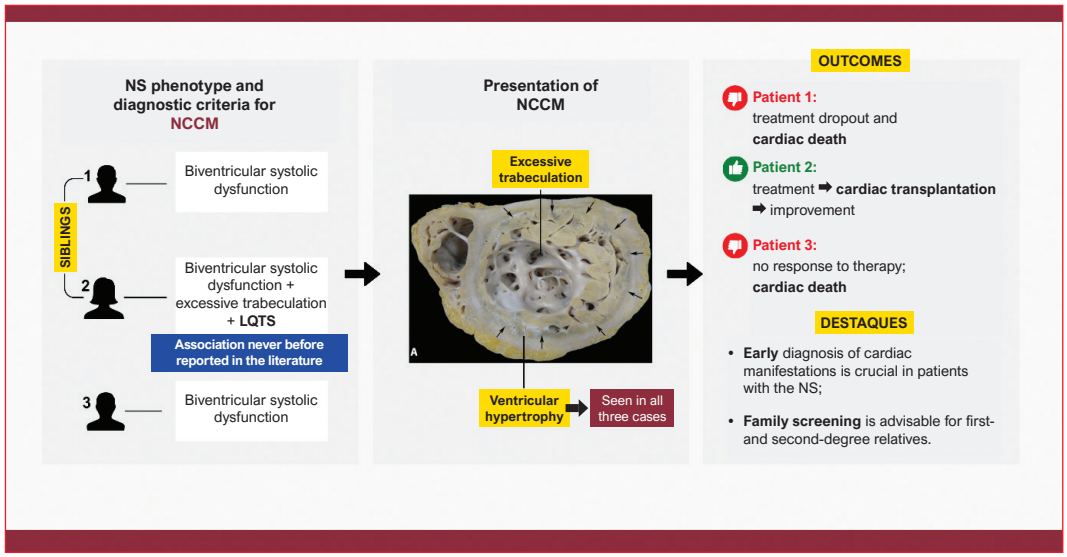

Arq Bras Cardiol: Imagem cardiovasc. 2025;38(1):e20240107

NS: Noonan syndrome; NCCM: noncompaction cardiomyopathy; HCM: hypertrophic cardiomyopathy; LQTS: long QT syndrome.

outcomes of each case were analyzed to highlight similarities and differences, considering the rarity and heterogeneity of this association. Given the growing need to elucidate the interactions between genotype and phenotype in NS, this report also highlights the importance of early diagnosis of cardiac anomalies, which is essential to improving the prognosis and quality of life of these patients. We chose to provide a detailed description of each individual patient, due to their particular features.

Methods

This observational, longitudinal, prospective study was based on the follow-up of three adult patients with the NS treated at Quaternary Hospital.

In addition to a detailed review of systems and physical examination to collect clinical data, patients also underwent diagnostic testing to assess cardiovascular function and possible complications, including plain chest radiography, electrocardiography, 24-hour Holter monitoring, transthoracic echocardiography, and CMR — the latter two being the preferred imaging methods for assessing myocardial noncompaction. In echocardiography, the most commonly used initial method, a suspected diagnosis of NCCM is assessed by criteria such as Jenni's, which compares the proportion between compacted (C) and noncompacted (NC) layers of the myocardium, with measurements taken during systole, in which a NC/C ratio > 2 is considered diagnostic.[5] CMR provides improves spatial definition, aiding in visualization of trabeculae and possible thrombi, especially apical ones. In CMR, the Petersen criterion defines as diagnostic an NC:C myocardium ratio > 2.3.[6] Diagnosis of the LQTS was established by electrocardiography and 24-hour Holter monitoring. For diagnostic confirmation, all imaging findings and test results were reassessed by a second, experienced specialist.

Parameters of interest included age, sex, past medical history, family history, age at onset of cardiac symptoms, current medications, imaging findings and laboratory test results, and the following endpoints: development or decompensation of heart failure (HF), thromboembolic events, cardiac events, heart transplantation (HTx), and death.

The study was approved by the institutional Research Ethics Committee with decision no. 0103/09. All three participants provided written informed consent in accordance with the provisions of Brazilian National Health Council Resolution 466/2012.

Results

Case presentation

Case 01:

A 26-year-old male was diagnosed with dilated cardiomyopathy (DCM) of unknown etiology. Symptoms had developed 5 years before with lower-extremity edema, palpitations, and progressive dyspnea. He denied chest pain, syncope, or paroxysmal nocturnal dyspnea. However, he had a history of pulmonary thromboembolism (PE) and was positive for the NS phenotype (webbed neck, hypertelorism, micrognathia, low-set ears, and right-sided cryptorchidism).

The family history included a sister with heart disease of unclear etiology and the same NS phenotype. Their parents were healthy and non-consanguineous; there were no other cases in the family. He also denied a history of hypertension, diabetes mellitus (DM), dyslipidemia, or problem alcohol use, and did not use tobacco or take illicit drugs. Medications for the past 6 months included warfarin, carvedilol, losartan, spironolactone, and furosemide.

At the first clinic visit, the patient was in no acute distress, afebrile, with pink and moist mucous membranes and no dyspnea at rest. Cardiovascular examination revealed visible jugular venous distension when supine, a regular rhythm with no third heart sound, and a grade II/IV systolic murmur in the mitral area. The heart rate (HR) was 60 beats per minute and the blood pressure (BP) 100/80 mmHg. The respiratory rate was normal, and the lungs were clear to auscultation. The extremities were warm and well-perfused, with grade II/IV lower-limb edema.

Plain radiography of the chest showed an enlarged heart shadow, and the initial electrocardiogram was notable for evidence of biventricular hypertrophy and first-degree atrioventricular block; 24-hour Holter monitoring recorded several runs of nonsustained ventricular tachycardia (NSVT). Echocardiography revealed marked biventricular systolic dysfunction, pulmonary hypertension, mild mitral and moderate tricuspid regurgitation, and a filling defect consistent with an apical thrombus in the right ventricle (RV). CMR confirmed biventricular systolic impairment (LVEF: 0.25; RVEF: 0.21) and increased myocardial thickness, as well as positive criteria for NCCM (NC/C ratio: 2.7) (Figure 1).

The patient experienced initial improvement in symptoms but was then lost to follow-up for 2 years. When next seen, he was in fair condition, pale, with poor peripheral perfusion, anasarca, palpitations, and dyspnea at rest, and was hospitalized for acute decompensated HF. Cardiovascular examination revealed jugular venous distension in the seated position and muffled heart sounds (regular S1/S2 rhythm). The HR was 88 beats per minute and the BP 90/60 mmHg. The respiratory rate was 30 breaths per minute; bibasilar crackles were heard on lung auscultation. Laboratory tests were notable for evidence of acute kidney injury and leukocytosis. During hospitalization, PE was once again suspected but ruled out by CT angiography. Within 36 hours, cardiogenic shock developed despite high-dose vasopressors, standard measures for septic shock, and intra-aortic balloon pump placement. He died in cardiac arrest with pulseless electrical activity.

Postmortem examination confirmed the Noonan phenotype and myocardial involvement consistent with NCCM. Extensive intramural fibrosis in the ventricular myocardium and thrombi in the right atrium were found (Figure 2). Changes secondary to congestive HF were seen in the lungs (passive pulmonary congestion, dilatation of the pulmonary artery), liver (chronic passive congestion, centrilobular hepatic necrosis), and spleen (chronic passive congestion), in addition to anasarca (ascites, pleural effusion, and pericardial effusion). Multiple thromboembolic phenomena were also identified, including organizing thrombi in the right atrium and posterior wall of the right atrium, healed cortical infarcts in both kidneys, multiple splenic infarcts, and widespread petechiae, as well as diffuse alveolar damage and massive hemorrhage in both lungs.

Case 02:

A 33-year-old female presented for HCM screening after the death of her brother (Case 01). She reported sporadic palpitations as her only symptom. There was an established history of infertility and the NS phenotype (Figure 3). The family history was as for Case 01. She denied hypertension, DM, dyslipidemia, and use of alcohol, tobacco, or other substances. She took no medications. At the first visit, the patient was in no acute distress, afebrile, with pink and moist mucous membranes and no dyspnea at rest. Cardiovascular examination was unremarkable except for a grade I/IV systolic murmur in the mitral area; the rhythm was regular with no third heart sound and there was no appreciable jugular venous distension. The HR was 72 beats per minute and the BP 110/80 mmHg. The respiratory rate was normal, the lungs were clear to auscultation, and the extremities were warm and well-perfused, with no peripheral edema.

A plain radiograph of the chest showed an enlarged cardiac shadow and evidence of pulmonary congestion (Figure 4). The initial electrocardiogram showed regular sinus rhythm with evidence of biatrial enlargement, RV hypertrophy, and septal hypertrophy (Figure 5); 24-hour Holter monitoring showed prolongation of the QT interval, as well as a single episode of NSVT. CMR was notable for significant ventricular hypertrophy (septal thickness 17 mm and lateral wall thickness 16 mm) and excessive trabeculation of the anterior, lateral, and inferior walls—findings consistent with NCCM (NC/C ratio: 2.4). There was also prominent dilatation of the pulmonary trunk, vena cava, and hepatic veins, as well as an apical thrombus in the left ventricle (Figure 6).

The patient was started on warfarin, carvedilol, and enalapril and reported improvement of palpitations. Seven months later, she suddenly developed pain in the left leg with associated malaise and right-sided paresthesias (including the face). She presented to the emergency department and was diagnosed with a transient ischemic attack involving multiple cerebral segments. Neuroimaging was consistent with subtotal occlusion of the proximal segment of the left middle cerebral artery (Figure 7). Chemical thrombolysis was performed uneventfully, and she recovered with no residual motor or cognitive deficits. During the same hospitalization, arteriography of the left lower extremity confirmed acute arterial occlusion in the left femoral artery, which was treated by surgical thrombectomy. After discharge, the patient experienced several further episodes of acute decompensated HF, NSVT, and QT prolongation, ultimately requiring placement of an implantable cardioverter/defibrillator. Despite optimization of medical therapy, over the following year she required frequent hospitalization for decompensated HF; HTx was indicated and performed successfully. As of the time of writing, she remains stable under close outpatient follow-up.

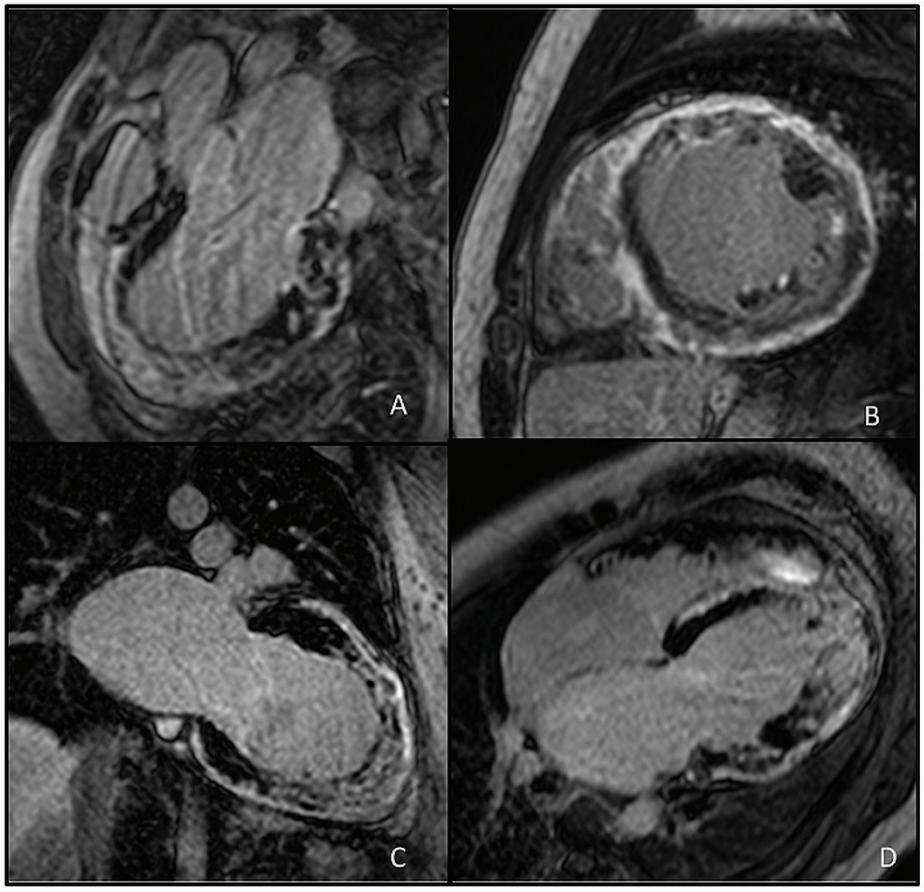

Figure 1 – *Late gadolinium enhancement CMR of Patient 1 showing diffuse delayed hyperenhancement of prominent left ventricular trabeculations, suggesting fibrosis. This patient showed overlap of findings consistent with HCM and NCCM.*

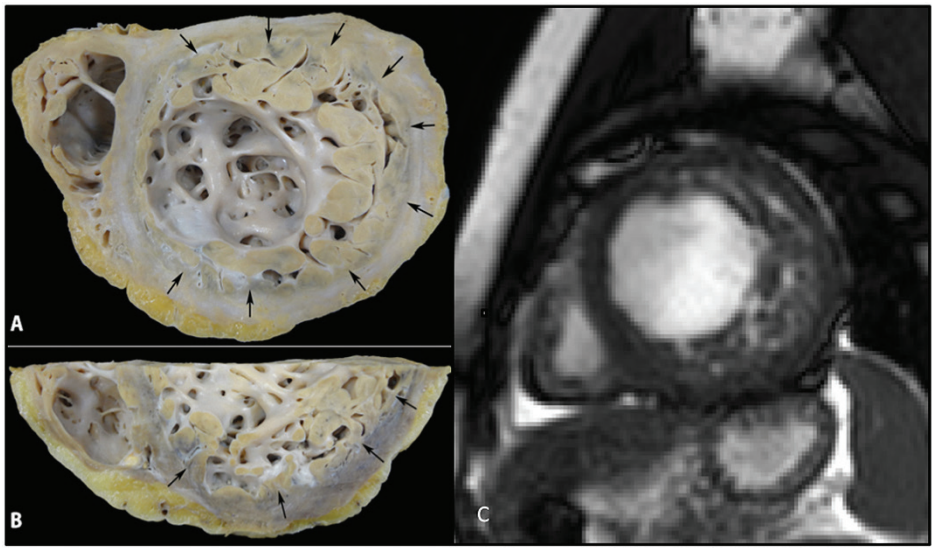

Figure 2 – *Axial (A) and coronal (B) sections through the cardiac ventricles of Patient 1 showing apical views of the left ventricular cavity with polypoid, anastomosing trabeculations (arrows) of the subendocardial layer. Short-axis cine CMR images (C) of the same patient, showing overlap between HCM and NCCM findings.*

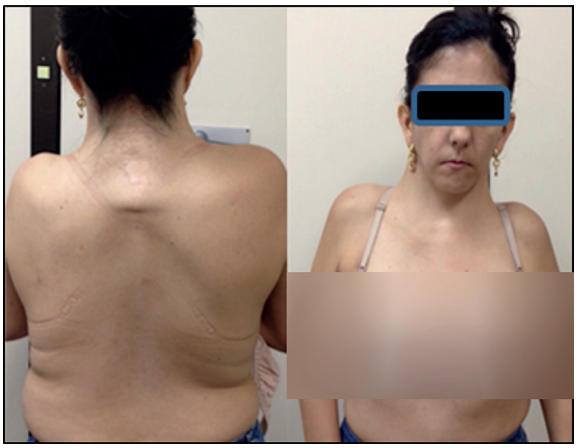

Figure 3 – *Photographs of Patient 2 (A and B). Note the webbed neck, low-set ears, pectus carinatum, scoliosis, and micrognathia.*

Case 03:

A 24-year-old male presented with a history of cardiomyopathy of unknown etiology, diagnosed at 3 years of age. He had been well until age 20, when he experienced a sudden deterioration of functional class requiring successive hospitalizations for acute decompensated HF. Physical examination was notable for the NS phenotype (short stature, webbed neck, hypertelorism, micrognathia, and low-set ears). There were no other cases in the family. Both parents were healthy and non-consanguineous. There was no psychomotor retardation. The patient denied hypertension, DM, dyslipidemia, and use of alcohol, tobacco, or other substances. Medications included bisoprolol, ivabradine, captopril, furosemide, spironolactone, hydrochlorothiazide, and warfarin. He was referred to our hospital for admission due to acute HF decompensation with dyspnea at rest, orthopnea, paroxysmal nocturnal dyspnea, and right upper quadrant pain. He reported no palpitations, chest pain, or syncope.

At the first visit, the patient was afebrile and well-hydrated but appeared acutely ill, with grade II/IV pallor and dyspnea at rest. Cardiovascular examination was notable for a grade I/IV systolic murmur in the mitral area, a regular rhythm with no third heart sound, and visible jugular venous distension while seated. The HR was 72 beats per minute and the BP 80/50 mmHg. He was tachypneic (RR 29 breaths per minute) and pulmonary auscultation revealed bibasilar crackles. The extremities were cold, clammy, and poorly perfused, with marked (grade III/IV) lower-limb edema.

Plain chest radiographs showed an enlarged cardiac shadow. The initial electrocardiogram showed evidence of biatrial and RV enlargement; 24-hour Holter monitoring recorded runs of NSVT. Transthoracic echocardiography showed increased myocardial thickness consistent with HCM, significant biventricular systolic dysfunction, marked LV diastolic dysfunction with a restrictive pattern (Figure 8), pulmonary hypertension, and a filling defect suggestive of apical thrombus in the LV. CMR confirmed biventricular systolic impairment (LVEF: 0.24; RVEF: 0.28) and increased myocardial thickness, as well as positive criteria for NCCM (NC/C ratio: 3.4). Late gadolinium enhancement was seen in the mesocardial layer mid-apically and in the epicardial layer circumferentially.

The patient had a stormy course complicated by bronchopneumonia, cardiac tamponade due to pericardial effusion requiring drainage, acute kidney injury, and mixed cardiogenic-septic shock, dying on the 62nd hospital day.

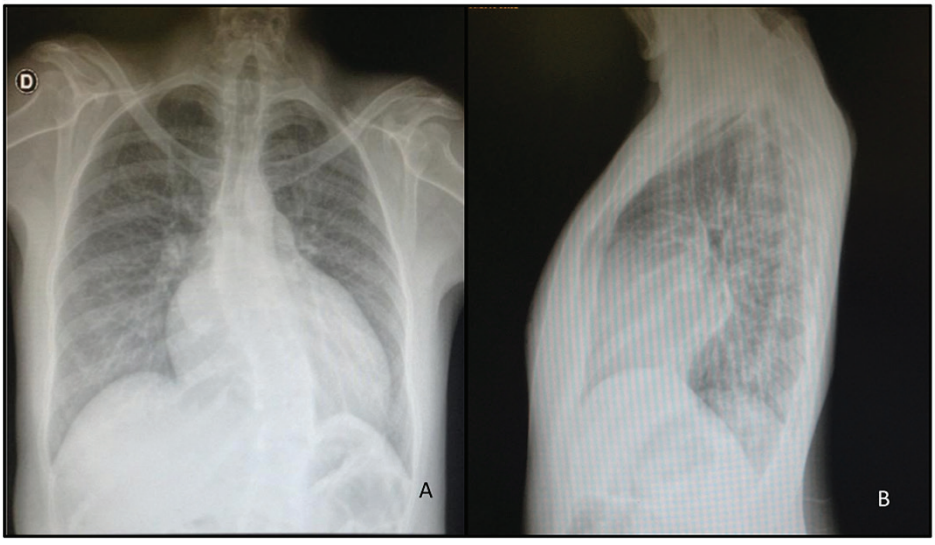

Figure 4 – *Patient 2 - PA (A) and lateral (B) chest radiographs showing pectus carinatum, scoliosis, cardiomegaly, and evidence of pulmonary congestion.*

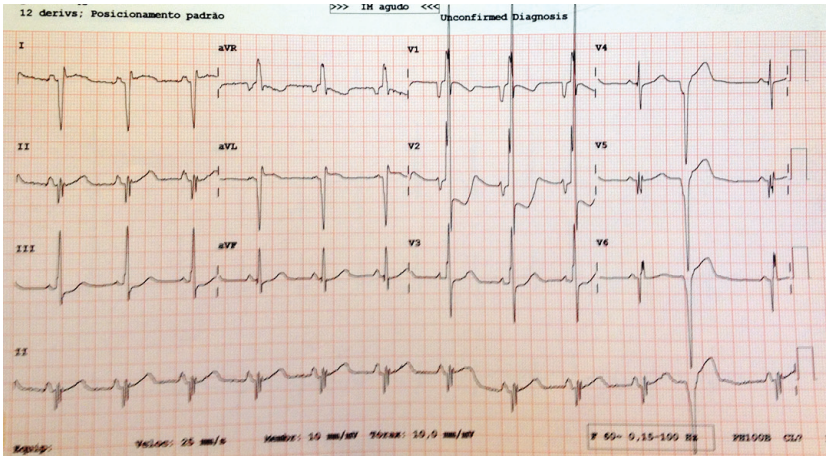

Figure 5 – *Patient 2 - 12-lead ECG showing sinus rhythm, evidence of biatrial and right ventricular enlargement, and severe septal hypertrophy.*

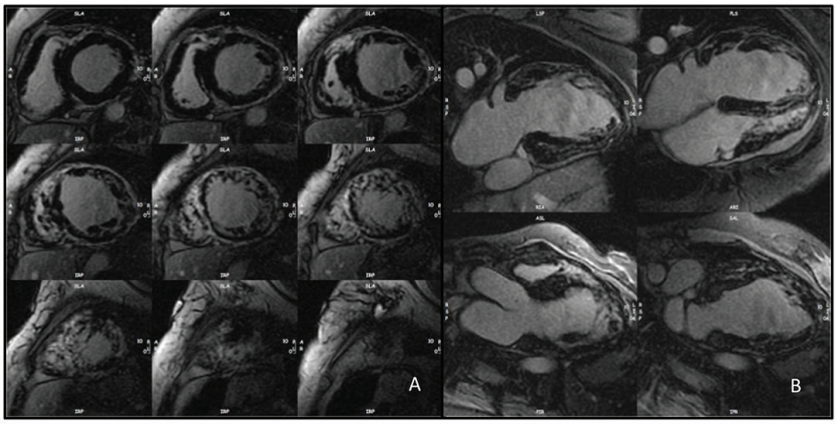

Figure 6 – *Patient 2 - CMR showing severe ventricular hypertrophy, excessive trabeculation of the anterior, lateral, and inferior myocardial walls (NC/C ratio: 2.4), and an enlarged left ventricle with significant systolic dysfunction (LVEF: 0.20). A non-ischemic delayed enhancement pattern is visible. There is also an apical thrombus in the left ventricle.*

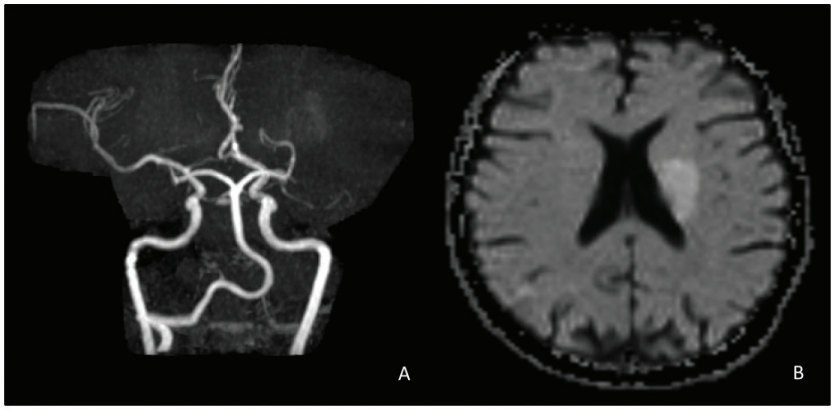

Figure 7 – *Brain MRI: ischemic stroke secondary to involvement of multiple cerebral vascular territories. Imaging is consistent with subtotal occlusion of the proximal segment of the left middle cerebral artery (A). The periventricular region, internal capsule, part of the caudate nucleus, posterior putamen, and subinsular region on the left are all involved (B).*

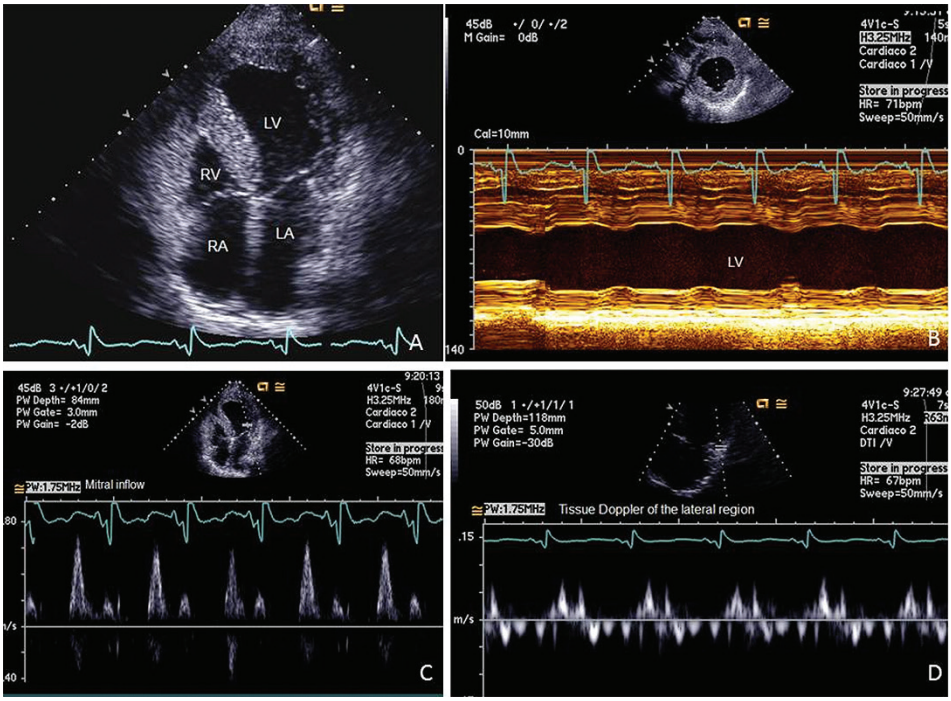

Figure 8 – *Two-dimensional and M-mode transthoracic echocardiography showing biventricular hypertrophy, LV trabeculation (A and B), and a restrictive diastolic dysfunction pattern (C and D).*

Analysis of common findings

All patients had the NS phenotype and met diagnostic criteria for NCCM. Of the 3 patients, 1 was female and 2 were male (66.6%), with a mean (SD) age of 27.6 (3.8) years. The female patient and the first male patient were siblings, while the other male patient had no family history of NS or cardiomyopathy; none of the patients had consanguineous parents. All had an established diagnosis of cardiomyopathy, with the second male patient having been diagnosed at 3 years of age. The presenting symptoms were dyspnea (n=2), palpitations (n=2), lower-limb edema (n=2), paroxysmal nocturnal dyspnea (n=1), and anasarca (n=1). All patients denied hypertension, DM, dyslipidemia, and use of alcohol, tobacco, or illicit substances. Physical examination was notable for a regular rhythm with no third heart sound, systolic murmur in the mitral area, and jugular venous distension while seated in all three patients, as well as muffled heart sounds in one.

Plain chest radiographs showed an enlarged cardiac shadow in 100% of cases (n=3). Electrocardiography revealed biventricular enlargement and first-degree atrioventricular block (n=1), normal sinus rhythm with evidence of biatrial enlargement (n=1), and biatrial enlargement with no prominent sinus rhythm (n=1), right ventricular hypertrophy (n=2), and septal hypertrophy (n=1). All patients had runs of NSVT on 24-hour Holter monitoring; the female patient also had prolongation of the QT interval. Echocardiography was performed in only two patients, revealing significant biventricular systolic dysfunction (n=2), LV dysfunction with a restrictive pattern (n=1), pulmonary hypertension (n=2), mitral regurgitation (n=1), and tricuspid regurgitation (n=1). All patients had evidence of apical thrombi, two confirmed by echocardiography and the third by CMR; two were in the left ventricle and one in the RV.

CMR showed increased myocardial thickness in 100% of cases (n=3), with a mean NC/C myocardium ratio of 2.8 (SD = 0.4). One patient showed excessive trabeculation of the anterior, lateral, and inferior walls.

All patients presented with HF (n=3) and acute decompensation. Pulmonary congestion was present in two cases, as was pericardial effusion. Optimized medical therapy was attempted in all patients; one discontinued treatment and was lost to follow-up and two had an inadequate response to treatment. Thromboembolic events occurred in 66.6% of cases (n=2), in the form of PE (n=1) and transient ischemic attack (n=1). The outcomes were implantable cardioverter/defibrillator placement with subsequent HTx in one case and death in cardiogenic shock in the two others. The patient who underwent HTx has since experienced significant improvement in her condition.

Discussion

NS is an autosomal dominant genetic disorder with a wide range of phenotypic presentations, including short stature, webbed neck, facial dysmorphism, delayed puberty, and skeletal and cardiovascular anomalies. Its incidence ranges from 1 in 1000 to 1 in 2500 live

births, being the second leading genetic cause of heart defects.[1,2,8] Although its clinical manifestations are not yet fully understood, cardiovascular changes are common, with pulmonary artery stenosis being most prevalent, which highlights the importance of cardiology follow-up throughout adulthood.[2,8,9] Outcomes similar to those of our series were found in a cohort studied by Shaw et. al., with 112 individuals followed for 12 years; 19% of them developed HCM, with one undergoing HTx, and three deaths due to myocardial infarction secondary to HCM.[10] The association of NS with NCCM is exceedingly rare, having been reported only by Nakamura et al. in a rat model in 2007 and by Sun et al. in a 12-year-old child in 2016.[3,11] Heart disease is the worst prognostic factor in patients with NS and, therefore, that most associated with mortality, as demonstrated in the three cases described herein, where the two male patients died in cardiogenic shock and the female patient ultimately required HTx.[2]

The American Heart Association considers NCCM a genetic disorder, with great genotypic and phenotypic variability.[12] Candidate genes have already been identified, such as *MYH7*, *TNNT2*, *TNNI3*, and *ACTC*, with those associated with defects in the genesis of sarcomere proteins being most common.[13-16] NCCM is characterized by the arrest of myocardial compaction during embryogenesis, leading to varying degrees of trabeculation, creating deep recesses that predispose to the formation of thrombi and consequent thromboembolic events. CMR performed alongside echocardiography is currently the method of choice for diagnosis.[5, 6, 17] Imaging shows thickening of the LV myocardial wall with two distinct layers: a thin, compact epicardial layer (C) and a thick, NC endocardial layer (NC) filled with blood from the ventricular cavity. Using the Petersen criterion, a ratio of NC to compacted myocardium (NC/C) > 2.3 confirms the diagnosis.[6] NCCM usually progresses to microcirculatory dysfunction and ventricular systolic dysfunction. It may be associated with other genetic conditions such as Ebstein's anomaly, bicuspid valve, HCM, septal defects, and neuromuscular disorders, such as the Barth and Becker syndromes.[1,2,18] Other family members can be involved at rates ranging from 18 to 50% in the literature, which highlights the importance of family screening.[13, 18]

HCM is the most prevalent cardiomyopathy (1:500 live births). It is inherited in an autosomal dominant pattern and leads to thickening of the myocardial walls, although function is often initially preserved.[19] Recent research has demonstrated similar genetic anomalies in sarcomeres and beta-myosin heavy chain in patients with HCM and NCCM, such as the L620P mutation in *MYH7*, suggesting there may be genetic overlap in the different presentations of these two cardiomyopathies—which appears to be in agreement with the cases reported herein.[13-16] Some cases of comorbid HCM and NCCM have been described in the same individual or separately in different members of the same family, such as children of patients with NCCM who have HCM or NCCM/HCM overlap and vice versa.[15, 20]

LQTS affects ventricular repolarization, leading to serious arrhythmias such as *torsades de pointes* and ventricular fibrillation; it is associated with a high risk of sudden death. Although it may be caused by drug interactions or genetic mutations – such as the *KCNQ1* mutation –, it has only rarely been reported in association with NCCM, making genetic screening essential for diagnosis and intervention.[7, 21] As of the time of writing, the co-occurrence of NS, NCCM, and LQTS had not been reported.

The symptoms reported by the patients in our series were similar to those found in the literature on NCCM, such as dyspnea, chest pain, and clinical manifestations of HF.[18] Areas of delayed enhancement on imaging have been suggested as a criterion for preventive implantable cardioverter/defibrillator placement,[17] as was required by one of our patients. The literature shows that mortality and heart transplantation rates in isolated noncompaction of the myocardium are similar to those found in idiopathic cardiomyopathy. However, our patient presented with NCCM in association with NS and other cardiac dysfunction, with additional complications and a worse prognosis. The simultaneous co-occurrence of all of these conditions has not been previously reported in the literature.

Conclusion

This paper describes three cases (including one sibling pair) of NS and NCCM with significant ventricular dysfunction and other associated conditions. The association of all conditions reported herein in the same patient has not been previously described in the literature. We highlight the importance of early screening for heart disease in patients with NS. Family screening should be recommended for all first- and second-degree relatives. Early diagnosis and treatment can improve prognosis in these cases.

Author Contributions

Conception and design of the research: Tavares M, Salemi VMC; acquisition of data: Pimentel ALL, Tavares M; analysis and interpretation of the data: Pimentel ALL, Tavares M, Silva EA, Salemi VMC; obtaining financing: Salemi VMC; writing of the manuscript: Pimentel ALL, Tavares M, Silva EA; critical revision of the manuscript for intellectual content: Pimentel ALL, Silva EA.

Potential Conflict of Interest

No potential conflict of interest relevant to this article was reported.

Sources of Funding

There were no external funding sources for this study.

Study Association

This article is part of the thesis of Doctoral submitted by Marcelo Dantas Tavares de Melo, from Incor - USP.

Ethics Approval and Consent to Participate

This study was approved by the Ethics Committee of the Análise de Projetos de Pesquisa-CAPPesq da Diretoria Clínica do Hospital das Clínicas da Faculdade de Medicina da Universidade de São Paulo under the protocol number 0103/09. All the procedures in this study were in accordance with the 1975 Helsinki Declaration, updated in 2013. Informed consent was obtained from all participants included in the study.

References

1. Mendez HM, Opitz JM. Noonan Syndrome: A Review. Am J Med Genet. 1985;21(3):493-506. doi: 10.1002/ajmg.1320210312.
2. Smpokou P, Tworog-Dube E, Kucherlapati RS, Roberts AE. Medical Complications, Clinical Findings, and Educational Outcomes in Adults with Noonan Syndrome. Am J Med Genet A. 2012;158A(12):3106-11. doi: 10.1002/ajmg.a.35639.
3. Sun XL, Zhao JX, Chen XJ, Zeng Z, Chen YC, Zhang Q. A Unique Case of a 12-Year-Old Boy with Noonan Syndrome Combined with Noncompaction of the Ventricular Myocardium. Int Heart J. 2016;57(2):258-61. doi: 10.1536/ihj.15-343.
4. Gerecke BJ, Engberding R. Noncompaction Cardiomyopathy-History and Current Knowledge for Clinical Practice. J Clin Med. 2021;10(11):2457. doi: 10.3390/jcm10112457.
5. Jenni R, Oechslin E, Schneider J, Jost CA, Kaufmann PA. Echocardiographic and Pathoanatomical Characteristics of Isolated Left Ventricular Non-Compaction: A Step Towards Classification as a Distinct Cardiomyopathy. Heart. 2001;86(6):666-71. doi: 10.1136/heart.86.6.666.
6. Petersen SE, Selvanayagam JB, Wiesmann F, Robson MD, Francis JM, Anderson RH, et al. Left Ventricular Non-Compaction: Insights from Cardiovascular Magnetic Resonance Imaging. J Am Coll Cardiol. 2005;46(1):101-5. doi: 10.1016/j.jacc.2005.03.045.
7. Moss AJ, Schwartz PJ, Crampton RS, Tzivoni D, Locati EH, MacCluer J, et al. The Long QT Syndrome. Prospective Longitudinal Study of 328 Families. Circulation. 1991;84(3):1136-44. doi: 10.1161/01.cir.84.3.1136.
8. Prendiville TW, Gauvreau K, Tworog-Dube E, Patkin L, Kucherlapati RS, Roberts AE, et al. Cardiovascular Disease in Noonan Syndrome. Arch Dis Child. 2014;99(7):629-34. doi: 10.1136/archdischild-2013-305047.
9. van der Burgt I. Noonan Syndrome. Orphanet J Rare Dis. 2007;2:4. doi: 10.1186/1750-1172-2-4.
10. Shaw AC, Kalidas K, Crosby AH, Jeffery S, Patton MA. The Natural History of Noonan Syndrome: A Long-term Follow-up Study. Arch Dis Child. 2007;92(2):128-32. doi: 10.1136/adc.2006.104547.
11. Nakamura T, Colbert M, Krenz M, Molkentin JD, Hahn HS, Dorn GW 2nd, et al. Mediating ERK 1/2 Signaling Rescues Congenital Heart Defects in a Mouse Model of Noonan Syndrome. J Clin Invest. 2007;117(8):2123-32. doi: 10.1172/JCI30756.
12. Maron BJ, Towbin JA, Thiene G, Antzelevitch C, Corrado D, Arnett D, et al. Contemporary Definitions and Classification of the Cardiomyopathies: An American Heart Association Scientific Statement from the Council on Clinical Cardiology, Heart Failure and Transplantation Committee; Quality of Care and Outcomes Research and Functional Genomics and Translational Biology Interdisciplinary Working Groups; and Council on Epidemiology and Prevention. Circulation. 2006;113(14):1807-16. doi: 10.1161/CIRCULATIONAHA.106.174287.
13. Oechslin E, Jenni R. Left Ventricular Non-compaction Revisited: A Distinct Phenotype with Genetic Heterogeneity? Eur Heart J. 2011;32(12):1446-56. doi: 10.1093/eurheartj/ehq508.
14. Klaassen S, Probst S, Oechslin E, Gerull B, Krings G, Schuler P, et al. Mutations in Sarcomere Protein Genes in Left Ventricular Noncompaction. Circulation. 2008;117(22):2893-901. doi: 10.1161/CIRCULATIONAHA.107.746164.
15. Laaroussi L, Halima AN, Boukhris M, Addad F, Kachboura S. Left Ventricular Non-compaction Associated with Hypertrophic Cardiomyopathy in the Same Patient. Kardiol Pol. 2017;75(4):397. doi: 10.5603/KP.2017.0064.
16. Lorca R, Martín M, Gómez J, Santamarta E, Morís C, Reguero JJ, et al. Hypertrophic Cardiomyopathy and Left Ventricular Non-compaction: Different Manifestations of the Same Cardiomyopathy Spectrum? Int J Cardiol. 2015;190:26-8. doi: 10.1016/j.ijcard.2015.04.138.
17. Zuccarino F, Vollmer I, Sanchez G, Navallas M, Pugliese F, Gayete A. Left Ventricular Noncompaction: Imaging Findings and Diagnostic Criteria. AJR Am J Roentgenol. 2015;204(5):W519-30. doi: 10.2214/AJR.13.12326.
18. Rosa LV, Salemi VMC, Alexandre LM, Mady C. Miocardiopatia não compactada: uma visão atual. Arq Bras Cardiol. 2011;97(1):13-9. doi: 10.1590/S0066-782X2011000900021.
19. Iio C, Ogimoto A, Nagai T, Suzuki J, Inoue K, Nishimura K, et al. Association between Genetic Variation in the SCN10A Gene and Cardiac Conduction Abnormalities in Patients with Hypertrophic Cardiomyopathy. Int Heart J. 2015;56(4):421-7. doi: 10.1536/ihj.14-411.
20. Hoedemaekers YM, Caliskan K, Michels M, Frohn-Mulder I, van der Smagt JJ, Phefferkorn JE, et al. The Importance of Genetic Counseling, DNA Diagnostics, and Cardiologic Family Screening in Left Ventricular Noncompaction Cardiomyopathy. Circ Cardiovasc Genet. 2010;3(3):232-9. doi: 10.1161/CIRCGENETICS.109.903898.
21. Nakashima K, Kusakawa I, Yamamoto T, Hirabayashi S, Hosoya R, Shimizu W, et al. A Left Ventricular Noncompaction in a Patient with Long QT Syndrome Caused by a KCNQ1 Mutation: A Case Report. Heart Vessels. 2013;28(1):126-9. doi: 10.1007/s00380-012-0235-8.

Original Article

Misinterpretation of Indeterminate Diastolic Function: Awareness and Insights from a Survey among Brazilian Cardiologists

Daniela do Carmo Rassi,[1,2] Salvador Rassi,[1] Jorge Eduardo Assef,[3] Alex dos Santos Felix,[4] Adenalva Lima de Souza Beck,[5] Cecília Beatriz Bittencourt Viana Cruz,[6] Silvio Henrique Barberato[7,8]

Faculdade de Medicina da Universidade Federal de Goiás,[1] Goiânia, GO – Brazil
Hospital São Francisco de Assis,[2] Goiânia, GO – Brazil
Instituto Dante Pazzanese de Cardiologia,[3] São Paulo, SP – Brazil
Instituto Nacional de Cardiologia,[4] Rio de Janeiro, RJ – Brazil
Instituto de Cardiologia e Transplantes do Distrito Federal,[5] Brasília, DF – Brazil
Universidade de São Paulo, Instituto do Coração,[6] São Paulo, SP – Brazil
Cardioeco – Centro de Diagnóstico Cardiovascular,[7] Curitiba, PR – Brazil
Quanta Diagnóstico por Imagem,[8] Curitiba, PR – Brazil

Abstract

Background: Diastolic dysfunction (DD) is highly prevalent and is associated with significant morbidity and mortality. More recent guidelines have introduced the classification of Indeterminate Diastolic Function or Indeterminate Diastolic Dysfunction (IDF or IDD). Nevertheless, both diagnoses are still poorly understood in clinical practice, with variable prevalence.

Objectives: Assess the understanding of IDF and IDD among non-echocardiographer cardiologists in Brazil.

Methods: A nationwide online survey was conducted among non-echocardiography readers cardiologists via mobile messaging platforms. A brief and anonymous questionnaire on knowledge and interpretation of Diastolic Function.

Results: A total of 570 cardiologists from all regions of Brazil participated in the study. Most participants (64.21%) had more than ten years of clinical experience. While 71% correctly identified grades 2 or 3 as indicative of elevated filling pressures, only 34.21% accurately understood the diagnostic criteria for IDF or IDD. Among the mistakes associated with the indeterminate classification, the following stand out: attribution of this status to conditions that interfere with the assessment of diastole (49.12%), technical limitations of the echocardiography equipment (3.33%), and alleged lack of knowledge by echocardiographers (4.91%). In addition, 46.7% reported finding this diagnosis rarely in the reports, 33.5% believed that this classification influenced clinical conduct, and 43.5% considered that the examination could have been better performed.

Conclusion: Despite knowledge about diastolic function, misinterpretation of IDF or IDD is still common among non-echocardiographer cardiologists. Investment in education, sharing these concepts with clinicians, and clear guidelines are essential to optimize the use and diagnostic accuracy of echocardiography.

Keywords: Diastole; Echocardiography; Practice Guidelines as Topic.

Introduction

The analysis of left ventricular (LV) diastolic function is key in an echocardiographic examination and is performed using echocardiography, which has been established as the main imaging tool for this evaluation.[1] Although invasive methods for measuring ventricular relaxation and filling pressures are considered the gold standard, echocardiography is widely preferred due to its high temporal resolution, reproducibility, validation of measurements, and wide availability at the bedside, and because it does not require invasive procedures or does not expose the patient to ionizing radiation.[2]

Left Ventricular Diastolic Dysfunction (LVDD) is highly prevalent, especially among the elderly, and is associated with significant morbidity and mortality. Furthermore, DD may contribute to the development and progression of Heart Failure with preserved Ejection Fraction (HFpEF), a condition characterized by increased LV filling pressures.[3,4]

Ventricular Diastole can be classified as normal or presenting Diastolic Dysfunction (DD) in grades 1, 2, or 3, or even as indeterminate, when it is not possible to establish its presence or severity. The guidelines of the American Society of Echocardiography (ASE) and the European Association of Cardiovascular Imaging (EACVI), published in 2016, sought to simplify this assessment, with clearer and more objective criteria, compared to the previous version.[5]

Mailing Address: Daniela do Carmo Rassi •
Hospital São Francisco de Assis. Rua 9ª. Postal code: 74075-250. Goiânia, GO – Brazil
E-mail: dani.rassi@hotmail.com
Manuscript received February 13, 2025; revised February 14, 2025; accepted February 14, 2025
Editor responsible for the review: Marcelo Tavares

DOI: https://doi.org/10.36660/abcimg.20250013i

CONTENTS

Central Illustration: Misinterpretation of Indeterminate Diastolic Function: Awareness and Insights from a Survey among Brazilian Cardiologists

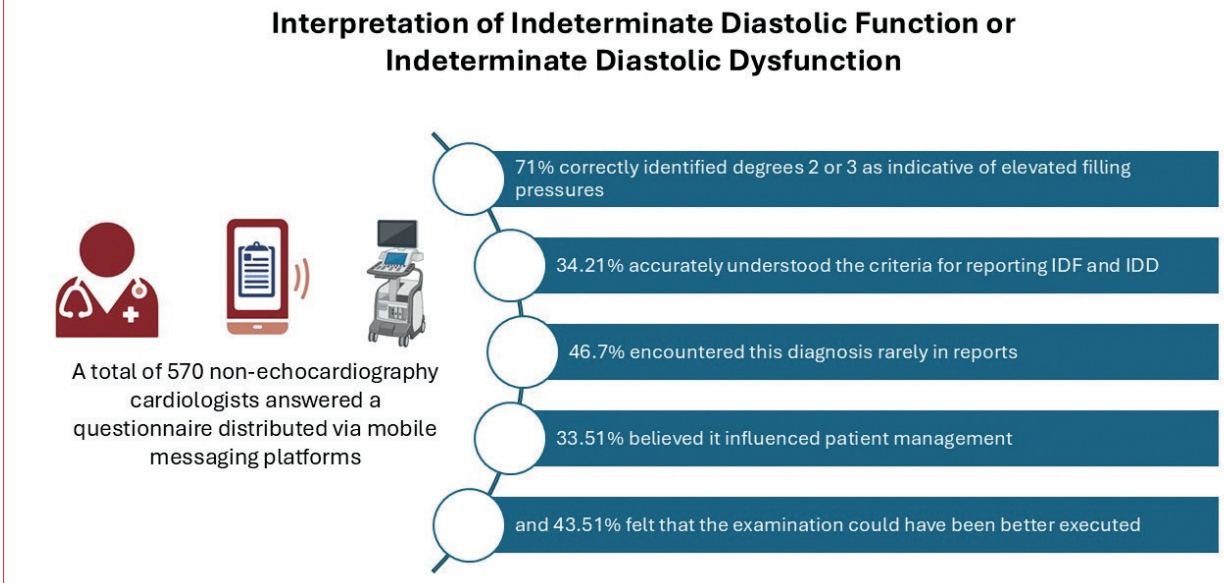

Arq Bras Cardiol: Imagem cardiovasc. 2025;38(1):e20250013

IDF: Indeterminate Diastolic Function; IDD: Indeterminate Diastolic Dysfunction.

However, the analysis of Diastolic Function and Left Ventricular Filling Pressures (LVFP) by echocardiography can be challenging, especially in patients with preserved LV ejection fraction, due to the need to evaluate multiple parameters for an accurate diagnosis. Despite all diagnostic efforts, a considerable proportion of patients are still classified as having indeterminate diastolic function (IDF), with prevalence ranging from 10% to 20% of the cases, according to previous studies.[6] This can be frustrating both for the professionals who perform the examination and for clinical cardiologists, who often depend on this diagnosis to define a therapeutic approach for the patient.

Thus, the objective of this study was to evaluate the understanding of the diastolic function or indeterminate diastolic dysfunction (IDD) classification in echocardiography reports by cardiologists not specialized in echocardiography in Brazil and analyze the knowledge these professionals have about diastolic function classification.

Methods

A nationwide, voluntary, online survey applied to cardiologists not specialized in echocardiography was conducted via mobile messaging platforms from June 1 to June 30. A brief online questionnaire was applied using the SurveyMonkey platform, anonymously, with no option for personal identification. There was no financial or material compensation for the participation in the research. The questionnaire consisted of seven questions (https://pt.surveymonkey.com/r/Y8NN97F), which were mandatory to complete, about time since medical training, region of practice, general knowledge about Diastolic Function, and how the result of a report impacts medical practice. The questions were multiple choice, with no possibility of open answers.

The complete questionnaire can be found in "Supplementary Material". Under the recommendation of Resolution 510 of the National Health Council, this questionnaire was not forwarded for evaluation by the CEP/CONEP system, as it is a public opinion survey with unidentified participants. The data obtained were described as categorical variables, with their absolute values, percentages, or proportions.

Results

General data

A total of 570 cardiologists accessed and answered the questionnaire, with the following distribution across the regions of Brazil: Southeast (29.65%), Midwest (23.80%), Northeast (18.77%), South (16.14%), and North (11.58%).

The participants were distributed according to their time since medical training: up to 5 years (23.33%), 6 to 10 years (12.46%), 11 to 20 years (26.14%), and more than 20 years (38.07%).

Knowledge about diastolic function analysis

Regarding diastolic function grading in which the patient has elevated LVEP, 1.75% responded that this would occur when diastole was classified as indeterminate, 22.16% as

grade 1, 70% as grade 2 or 3, and 5.09% did not know how to respond.

Regarding the understanding of what leads an echocardiographer to classify IDF or IDD in the report, the majority (49.12%) chose an inadequate option, which indicated that an indeterminate classification would be caused by pathologies that interfere with the correct assessment (e.g.: pacemaker rhythm, mitral prosthesis). The second most chosen option (34.21%) was the correct answer, which indicated that it was not possible to determine diastolic function due to the absence of sufficient criteria for classification (Figure 1).

Observed frequency of diagnosis in reports and impact on clinical management

Regarding the frequency observed in echocardiography reports, concerning the report of IDF or IDD, 29.30% said they had never seen this phrase in the report, 46.67% said they rarely see it, and 24.04% said they frequently see it.

Regarding the impact of this diagnosis on adequate patient management, 33.51% responded that it had an impact, 21.23% that it did not, 33.86% occasionally, and 11.40% considered the diagnosis to be a source of confusion.

Faced with the diagnosis of IDF or IDD, 45.82% of the participants feel satisfied. However, a significant percentage of cardiologists, 44.51%, suspect that the exam could have been conducted in a more effective way (Figure 2).

Discussion

This study provides important and unprecedented information on the interpretation, understanding, observed frequency, impact on patient management, and the perception of cardiologists when faced with an IDF or IDD diagnosis.

There was good representation among the five regions of Brazil, which contributes to a more balanced assessment of this perception, minimizing the risk of bias associated with the concentration of knowledge in areas with greater access to resources and updates, compared to regions with more limitations in this regard.

Most of the cardiologists surveyed had more than 10 years of training, which reflects good experience in reading essential cardiological exams, such as echocardiography, and in patient management care.

When grading Diastolic Function in which the patient has elevated LV filling pressures, the vast majority confirmed that this occurs in grades 2 and 3 of DD according to the guidelines of the ASE and the EACVI.[5]

These guidelines are the most widely used to analyze Diastolic Function. In the absence of a myocardial disease, four echocardiographic signs are evaluated: the early diastolic tissue velocity of the septal and lateral mitral annulus (e'), the indexed left atrial volume, the ratio between the maximum mitral E velocity (early diastolic) and the mean of the velocities of the septal and lateral e' wave, and the maximum velocity of tricuspid regurgitation. If most available data are within the normal range, LV Diastolic Function is considered normal. Otherwise, DD is observed and LV filling pressure can be estimated. If the criteria are insufficient or there is disagreement in the classification, the diastolic function is considered indeterminate.[4,5,7]

If there is a myocardial disease or DD after the evaluation described above, filling pressures should be estimated and DD classified. The algorithm for assessing LV filling pressure first measures mitral wave velocities. If the mitral E wave velocity is < 0.5 m/s and the E/A ratio is ≤ 0.8, LV filling pressure is likely normal or low, so DD is classified as grade 1, whereas a tall E wave and E/A ≥ 2 indicates elevated

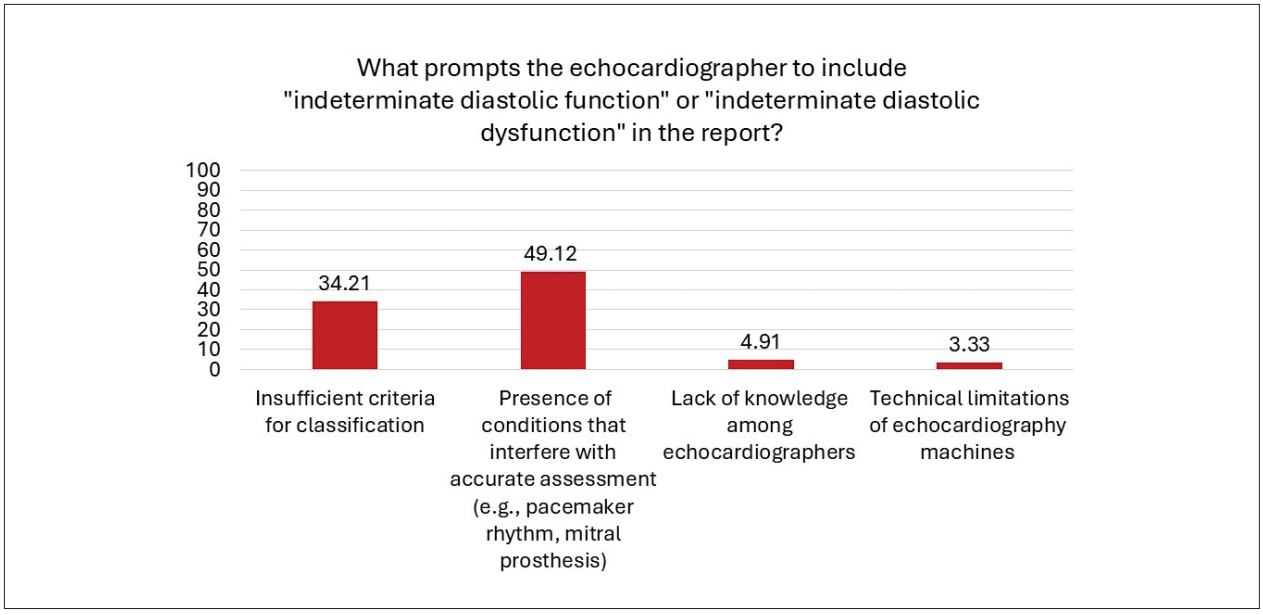

Figure 1 – *The cardiologist's understanding of the echocardiographic criteria used for the report of indeterminate diastolic function or indeterminate diastolic dysfunction.*

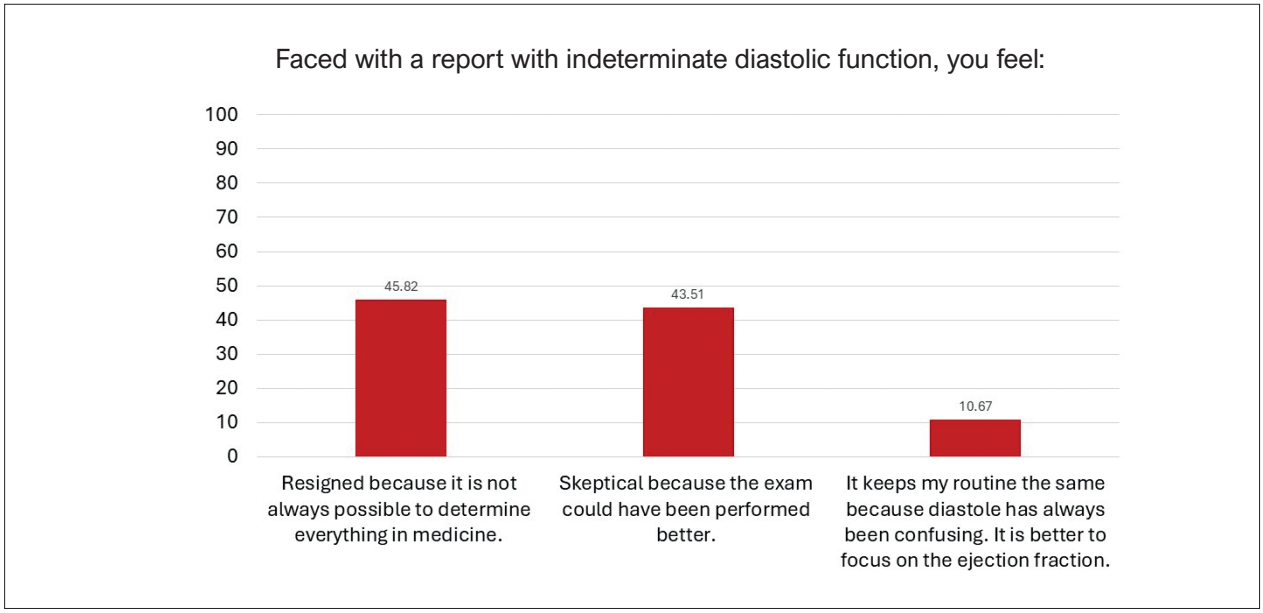

Figure 2 – *How the cardiologist feels about the report of indeterminate diastolic function or indeterminate diastolic dysfunction.*

LV filling pressure and is classified as grade 3 DD. When the mitral E/A ratio is between 0.8 and 2.0, additional criteria are needed to assess LV filling pressure. These include mean E/e' ratio > 14, peak tricuspid regurgitation velocity > 2.8 m/s, and indexed LA volume > 34 mL/m^2. If ≥ 2 of the criteria are above the cutoff value, LV filling pressure is most likely elevated, classifying DD as grade 2. If ≥ 2 of the criteria are below the cutoff value, LV filling pressure is most likely normal and is therefore classified as grade 1. However, if all of these additional measurements, especially tricuspid regurgitation, are not available and there is discordance between the two existing measurements, DD is considered indeterminate.[4,5,7]

The proportion of cases with IDF is reduced when specific Doppler findings are carefully considered, including changes in mitral inflow velocities and E/A ratio with the Valsalva maneuver, flow velocity and duration in the pulmonary veins, including the reversed wave, and the presence of an L wave in mitral inflow with velocity ≥ 50 cm/s.[7]

Therefore, it is clear that the diagnosis of IDF or IDD is associated with the lack of sufficient criteria or discordance between criteria.

However, most cardiologists attribute this diagnosis to conditions that make it impossible to adequately analyze diastolic function, mainly because they interfere with the velocities of the mitral E waves and the tissue waves of the mitral annulus. Among these conditions, the following stand out: pacemaker rhythm, the presence of a mitral valve prosthesis, significant mitral valve diseases (stenosis or insufficiency), and left bundle branch block.[4,5]

The perception of the frequency of this diagnosis in echocardiography reports was low, with almost a third of cardiologists never having observed this description. However, this contrasts with the reported prevalence of this finding in reports, which ranges from 10% to 20%.[3]

Furthermore, there is an important bias: several echocardiographers hesitate to classify diastole as indeterminate for fear that this definition would be misinterpreted by the clinical cardiologist. There is concern that this may create distrust about the examination quality, especially since the diagnosis of IDF or IDD is still not widely understood by cardiologists who do not specialize in echocardiography. This can lead to an underdiagnosis of this pattern of DD, with a tendency to classify the patient differently in a way that does not correspond to their true classification. On the other hand, Left Atrial strain has been suggested as a useful method in reclassifying cases of DD considered indeterminate by the traditional ASE-EACVI algorithm.[1,2,8,9]

This reasoning is in line with the perception of cardiologists when faced with the diagnosis of IDF or IDD. Most of them accept this classification, recognizing that determining all aspects of medicine is not always possible. However, a significant percentage, numerically close to that of the previous response, expresses distrust, suspecting that the exam could have been performed in a more effective way.

Although most people are unaware of the real reason for including this diagnosis in the report, the general perception is that IDF or IDD compromises, even occasionally, effective patient management. This highlights the importance of better interaction and understanding between the echocardiography report, echocardiographers, and clinical cardiologists.

Study limitations

This research involved a relatively small sample of cardiologists, which may limit the generalizability of the results. Furthermore, based on the alternatives chosen, it was not possible to assess regional differences and training time differences, which could offer a more detailed analysis of the results obtained.

Conclusion

Despite general knowledge about Diastolic Function, misinterpretation of IDF or IDD persists among non-echocardiographer cardiologists. Investments in education, sharing these concepts with clinicians, and clear guidelines are essential to optimize the use of the exam and diagnostic accuracy of echocardiography.

Author Contributions

Conception and design of the research and critical revision of the manuscript for intellectual content: Rassi DC, Rassi S, Assef JE, Barberato SH; acquisition of data: Rassi DC, Rassi S, Assef JE, Felix AS, Cruz C, Beck ALS, Barberato SH; analysis and interpretation of the data: Rassi DC, Rassi S, Beck ALS, Barberato SH; statistical analysis and writing of the manuscript: Rassi DC, Rassi S, Barberato SH.

Potential Conflict of Interest

No potential conflict of interest relevant to this article was reported.

Sources of Funding

There were no external funding sources for this study.

Study Association

This study is not associated with any thesis or dissertation work.

Ethics Approval and Consent to Participate

This article does not contain any studies with human participants or animals performed by any of the authors.

References

1. Barberato SH, Romano MMD, Beck ALS, Rodrigues ACT, Almeida ALC, Assunção BMBL, et al. Position Statement on Indications of Echocardiography in Adults - 2019. Arq Bras Cardiol. 2019;113(1):135-81. doi: 10.5935/abc.20190129.
2. Robinson S, Ring L, Oxborough D, Harkness A, Bennett S, Rana B, et al. The Assessment of Left Ventricular Diastolic Function: Guidance and Recommendations from the British Society of Echocardiography. Echo Res Pract. 2024;11(1):16. doi: 10.1186/s44156-024-00051-2.
3. Kumar S, Desai N, Gona OJ, Kumar VK, Madbu B M. Impact of Updated 2016 ASE/EACVI VIS-À-VIS 2009 ASE Recommendation on the Prevalence of Diastolic Dysfunction and LV Filling Pressures in Patients with Preserved Ejection Fraction. J Cardiovasc Imaging. 2021;29(1):31-43. doi: 10.4250/jcvi.2020.0117.
4. Smiseth OA, Morris DA, Cardim N, Cikes M, Delgado V, Donal E, et al. Multimodality Imaging in Patients with Heart Failure and Preserved Ejection Fraction: An Expert Consensus Document of the European Association of Cardiovascular Imaging. Eur Heart J Cardiovasc Imaging. 2022;23(2):e34-e61. doi: 10.1093/ehjci/jeab154.
5. Nagueh SF, Smiseth OA, Appleton CP, Byrd BF 3rd, Dokainish H, Edvardsen T, et al. Recommendations for the Evaluation of Left Ventricular Diastolic Function by Echocardiography: An Update from the American Society of Echocardiography and the European Association of Cardiovascular Imaging. J Am Soc Echocardiogr. 2016;29(4):277-314. doi: 10.1016/j.echo.2016.01.011.
6. Chung YJ, Choi KH, Lee SH, Shin D, Hong D, Park S, et al. Prognostic Impact of Indeterminate Diastolic Function in Patients with Functionally Insignificant Coronary Stenosis. J Am Soc Echocardiogr. 2023;36(3):295-306.e5. doi: 10.1016/j.echo.2022.11.014.
7. Nagueh SF. Diastology: 2020-A Practical Guide. Echocardiography. 2020;37(11):1919-25. doi: 10.1111/echo.14742.
8. Singh A, Addetia K, Maffessanti F, Mor-Avi V, Lang RM. LA Strain for Categorization of LV Diastolic Dysfunction. JACC Cardiovasc Imaging. 2017;10(7):735-43. doi: 10.1016/j.jcmg.2016.08.014.
9. Barberato SH, Borsoi R. Left Atrial Reserve Function in Assessing Indeterminate Diastolic Function. Arq Bras Cardiol: Imagem Cardiovasc. 2021;34(2):eabc196. doi: 10.47593/2675-312X/20213402eabc196 .

***Supplemental Materials**

For additional information, please click here.

Original Article

Variations in Myocardial FDG Uptake and Metformin Use: Implications for Survival during Immunotherapy

Matheus Coelho Torres,[1] *Juliana Goes Martins Fagundes,*[2] *Luís Fábio Barbosa Botelho,*[1] *Alinne Fernanda Amaral Verçosa,*[3] *Marcelo Dantas Tavares de Melo*[1]

Universidade Federal da Paraíba,[1] *João Pessoa, PB – Brazil*
Grupo Oncoclínicas,[2] *João Pessoa, PB – Brazil*
Nova Diagnóstico por Imagem,[3] *João Pessoa, PB – Brazil*

Abstract

Background: The rise of immune checkpoint inhibitors (ICIs) has significantly improved lung cancer outcomes; however, there is a lack of response prediction protocols. Furthermore, preclinical studies have indicated a promising association between metformin, β-blockers (BBs), and improved cancer patient outcomes.

Objectives: The primary objective of this study was to investigate metformin's impact on survival outcomes. The secondary objectives included assessing myocardial FDG uptake variation (change in standardized uptake value [ΔSUV]) during ICI treatment and evaluating the effects of smoking, diabetes, hypertension, and BB usage on survival outcomes.

Methods: This single-arm, unicentric retrospective cohort study evaluated lung cancer patients who started using ICIs from July 2016 to December 2021. Inclusion criteria were age 18 years or above, lung cancer treated with ICIs (CTLA-4, PD-1, and PD-L1 inhibitors), and having undergone at least two positron emission tomography-computed tomography (PET-CT) scans.

Results: Fifty-eight patients fulfilled all the inclusion criteria. Metformin users presented a 759-day increase in overall survival (OS) (p = 0.015). A trend of a 161-day increase in progression-free survival was observed in patients with positive myocardial ΔSUV compared to the negative ΔSUV group (p = 0.066), along with a trend of a 285-day increase in favor of BB users (p=0.886).

Conclusion: The significant association between metformin use and increased OS suggests metformin as a promising adjuvant for ICI therapy. A trend of positive myocardial ΔSUV and improved outcomes may suggest a potential role of PET-CT in response prediction; however, larger studies are necessary to solidify this hypothesis.

Keywords: Immune Checkpoint Inhibitors; Positron Emission Tomography-Computed Tomography; Metformin; Cardio-Oncology; Cardiotoxicity.

Introduction

Immune system evasion represents a pivotal mechanism in carcinogenesis, whereby tumor cells employ various mechanisms to elude immune surveillance. These mechanisms encompass the downregulation of tumor antigen presentation and the exposure of molecules that impede directed immune response.[1] Notably, lung cancer, the leading cause of global cancer-related deaths, is frequently approached by the utilization of immune checkpoint inhibitors (ICIs) as a treatment modality. These therapeutic agents function by impeding the detrimental regulatory mechanisms enacted by the tumor, thus fostering an enhanced immune defense against malignant growth.

Despite limited improvements in 5-year survival rates among lung cancer patients, 2-year survival rates have significantly increased.[2] This improvement can be largely attributed to the well-documented efficacy of ICI therapy in enhancing long-term overall survival (OS) and progression-free survival (PFS).[3,4] In addition to the stand-alone effectiveness of ICI therapy, the safety and effectiveness of combination regimens involving immunotherapy and chemotherapy,[5] platinum-based regimens,[6,7] and/or radiotherapy[8,9] have been extensively reported.

However, predicting immunotherapy response and the impact of synergistic drugs on treatment outcomes remains uncertain. Although some evidence supports the safety and efficacy of adjuvant drugs such as β-blockers (BBs),[10] metformin,[11] and albendazole[12] through murine models, retrospective data, and meta-analyses, high-quality clinical trials are still needed.

As further research is needed to establish the role of these adjuvant drugs, their potential to complement ICI therapy and contribute to improved patient outcomes remains a

Mailing Address: Matheus Coelho Torres •
Universidade Federal da Paraíba. Bacharel José de Oliveira Curchatuz, 15. Postal code: 58036-130. João Pessoa, PB – Brazil
E-mail: matheuscoelhotorres@gmail.com
Manuscript received October 26, 2024; revised October 28, 2024; accepted October 28, 2024
Editor responsible for the review: Marcelo Tavares

DOI: https://doi.org/10.36660/abcimg.20240108i

Central Illustration: Variations in Myocardial FDG Uptake and Metformin Use: Implications for Survival during Immunotherapy

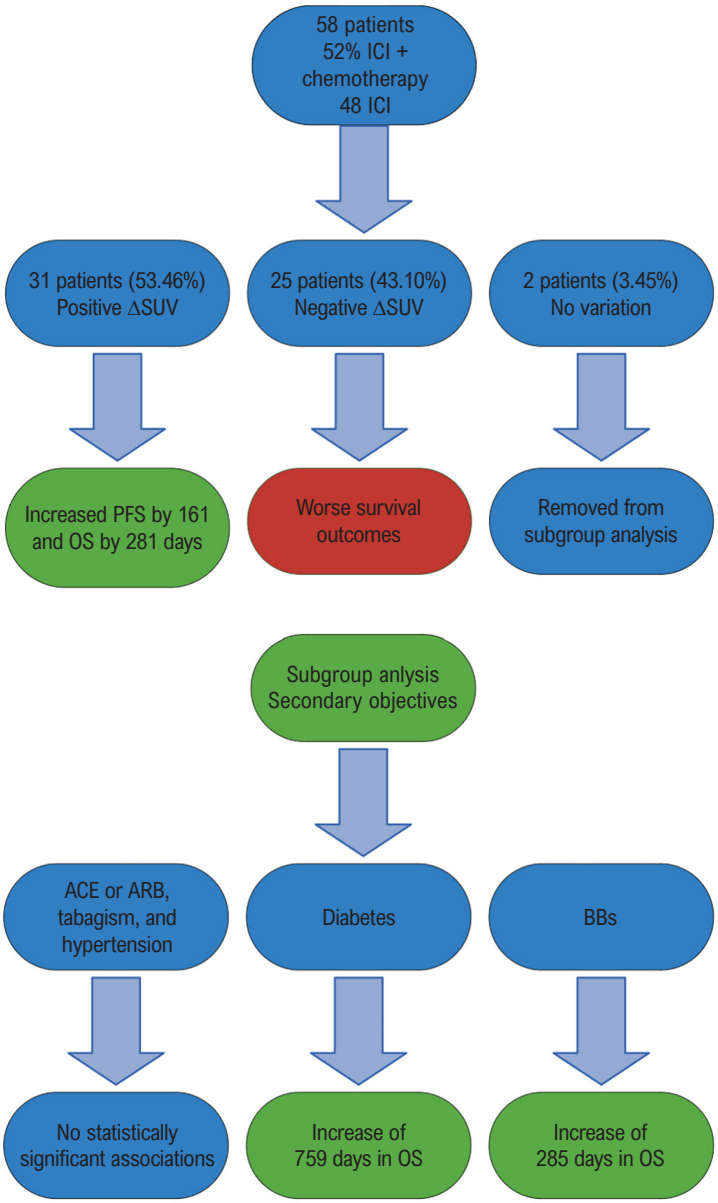

Arq Bras Cardiol: Imagem cardiovasc. 2025;38(1):e20240108

subject of hypotheses and speculation. Certain positron emission tomography-computed tomography (PET-CT) models have been proposed to predict immunotherapy response by analyzing standardized uptake value variation (ΔSUV) and employing PET tracers targeting ICIs, including PD-L1. Nevertheless, the absence of standardized evidence and ambiguous implications for clinical practice present ongoing challenges.[13-15]

Thus, we propose to evaluate the role of adjuvant drugs, such as metformin, on ICI therapy prognosis and to assess changes in myocardial FDG uptake (MGU) rate in advanced lung cancer patients undergoing ICI treatment. Our investigation aims to explore MGU's potential as a monitoring tool for immunotherapy response and the effects of metformin, BBs, and other drugs on survival in immunotherapy.

Methods

Study design and participants

This retrospective cohort study is a single-arm, unicentric investigation that utilized electronic medical records and PET-CT images to evaluate lung cancer patients who initiated ICI treatment between July 2016 and December 2021. Inclusion criteria included age 18 or above, lung cancer treated with ICIs (Cytotoxic T-lymphocyte associated protein 4 - CTLA-4, Programmed Death 1 PD-1, and Programmed-Death Ligand 1 PD-L1 inhibitors), and having undergone at least two PET-CT scans – one at baseline and another during the course of treatment.

The primary objective of the study was to assess the variation in MGU rate, measured by the ΔSUV, during the administration of ICIs and their impact on survival outcomes. The secondary objectives aimed to investigate the potential positive or negative effects associated with smoking, diabetes, hypertension, metformin usage, and BB usage on survival outcomes.

Ethical approval for this research was obtained from the ethics committee under the registration number CAAE 47402321.9.0000.5186

Statistical analysis

Descriptive statistics for numerical variables were presented as median and interquartile range, while categorical variables were described using absolute and relative frequencies. The Mann-Whitney test was employed to compare medians between groups. PFS and OS were estimated using the Kaplan-Meier method, and the log-rank test was utilized to compare survival curves. The significance level (alpha) was set at 0.05.

Results

Among the 114 patients with lung cancer who underwent immunotherapy at our medical center, 58 patients met the inclusion criteria. Of these, 25 were female and 33 were male, with a median age of 68 years (standard deviation [SD] ±10). The median body mass index was 26 (SD ±4), and the median interval from baseline PET scan to treatment start was 27 days (SD ±47).

Nearly 52% of the patients received immunotherapy in combination with chemotherapy, while the remaining 48% received immunotherapy alone. Within our sample, 31 patients (53.45%) exhibited a positive ΔSUV, indicating an increase in MGU. Conversely, 25 patients (43.10%) showed a negative ΔSUV, indicating a decrease in MGU. Two patients (3.45%) had no SUV variation and were excluded from the subgroup analysis. The subgroups with positive and negative ΔSUV were comparable, except for a prolonged interval between baseline PET scan and treatment start in the negative ΔSUV group. Detailed clinical and demographic data are shown in Table 1, and Table 2 shows the histological and treatment characteristics of the study population.

Table 1 – Demographic characteristics and subgroup distribution of the study population (n = 58), +δSUV and –δSUV subgroups.

	Global study population		ΔSUV+		ΔSUV–	
	Median	SD	Median		Median	
Age, yrs	68	±10	67.0096		68.5336	
BMI, kg/m^2	26	±4	26.01		26.26	
Interval between baseline PET and treatment start, days	27	±47	31.58		52.52	
Sex	N	%	N	%	N	%
Female	25	43	14	45.16	10	40
Male	33	57	17	54.84	15	60
Comorbidities	N	%	N	%	N	%
Hypertension	28	48	14	45.16	12	48
Diabetes	12	21	5	16.12	7	28
Tabagism	43	74	21	67.74	20	80
Coronary disease	4	7	2	6.45	2	8
Heart failure (HF)	1	2	0	0	1	4
Drug usage	N	%	N	%	N	%
BBs	14	24	7	22.58	6	24
ACE/ARB	17	29	9	29.03	7	28
Metformin	8	14	3	9.68	4	16
Anticoagulants	3	5	3	9.68	0	0

SUV: standardized uptake value; SD: standard deviation; BMI: PET: positron emission tomography-computed tomography; HF: Heart failure; BB: β-blockers; ACE/ARB: angiotensin-converting enzyme/Angiotensin II receptor blockers.

Table 2 – Histological and treatment characteristics of the study population.

	Global study population		ΔSUV+		ΔSUV–	
Histology	N	%	N	%	N	%
Adenocarcinoma	43	74	23	74.19	18	72
SCC	4	7	2	6.45	2	8
NSCLC	5	9	2	6.45	2	8
Others	6	10	4	12.9	3	12
Immunotherapy	N	%	N	%	N	%
Atezolizumab	14	24	6	19.35	8	32
Durvalumab	5	9	3	9.68	1	4
Nivolumab	13	22	7	22.58	6	24
Pembrolizumab	26	45	15	48.38	10	40
Treatment type	N	%	N	%	N	%
QT-IO	30	52	17	54.84	12	48
IO	28	48	14	45.16	13	52
Treatment line	N	%	N	%	N	%
1st line	35	60	19	61.29	14	56
Subsequent lines	23	40	12	38.71	11	44
Tumor genetic analysis	N	%	N	%	N	%
ALK/EGFR	9	15	4	12.9	4	16
Without mutation	23	40	14	45.16	10	40
Unknown	26	45	13	41.94	11	44
PD-L1: >50%	8	14	3	9.68	4	16
PD-L1: 1%–50%	9	15	8	25.81	1	4
PD-L1: <1%	10	17	6	19.35	7	28
PD-L1: unknown	31	53	14	45.16	13	52

SUV: standardized uptake value; SCC: squamous cell carcinoma; NSCLC: Non-small cell lung cancer; QT-IO: Chemotherapy in combination with Immunotherapy; ALK/EGFR: Anaplastic Lymphoma Kinase (ALK) or Epidermal Growth Factor Receptor (EGFR) mutations.

Among the documented comorbidities, the highest prevalence was observed for tabagism (74%), followed by hypertension (48%) and diabetes (21%). The most commonly used drugs were angiotensin-converting enzyme (ACE) inhibitors or Angiotensin II receptor blockers (ARBs) (29%), BBs (24%), and metformin (14%).

Regarding the primary outcome, the overall median ΔSUV was +0.05. Within the disease control group, the median ΔSUV was +0.48, indicating an increase in MGU. In contrast, the disease progression group exhibited a median ΔSUV of –0.66.

When comparing patients with a positive myocardial ΔSUV to those with a negative ΔSUV, there was a median prolongation of PFS by 161 days in favor of the positive myocardial ΔSUV group (p = 0.066). Additionally, an increase of 281 days in OS was observed in the positive myocardial ΔSUV group (p = 0.256) (Figure 1).

Furthermore, diabetic patients demonstrated a noteworthy increase of 759 days in OS (p = 0.023). In subgroup analysis, a trend toward even more favorable outcomes was observed in metformin users (p = 0.015) (Figure 2). Additionally, a non-statistically significant trend of prolongation in OS by 285 days was noticed among BB users (p = 0.886) (Figure 3).

However, no statistically significant associations were found between the usage of ACE inhibitors or ARBs, tobacco use, or hypertension and OS or PFS.

Discussion

The well-documented ability of Fluorodeoxyglucose F 18 (18F-FDG) PET-CT to identify tissue inflammation—a hallmark of immune-related adverse events (irAEs)—indicates its potential for the early detection of subclinical irAEs. Moreover, PET-CT may play a crucial role in confirming suspected irAEs, including myocarditis, by revealing heterogeneous and moderate-to-high increases in 18F-FDG uptake within the left ventricle (LV).[16,17]

The disparity observed in the average cardiac ΔSUV between the disease control group and the disease progression group within our study suggests a potential association between increased SUV following treatment and improved responses to immunotherapy. This finding is further substantiated by the median prolongation of 161 days in PFS (p = 0.066) and 281

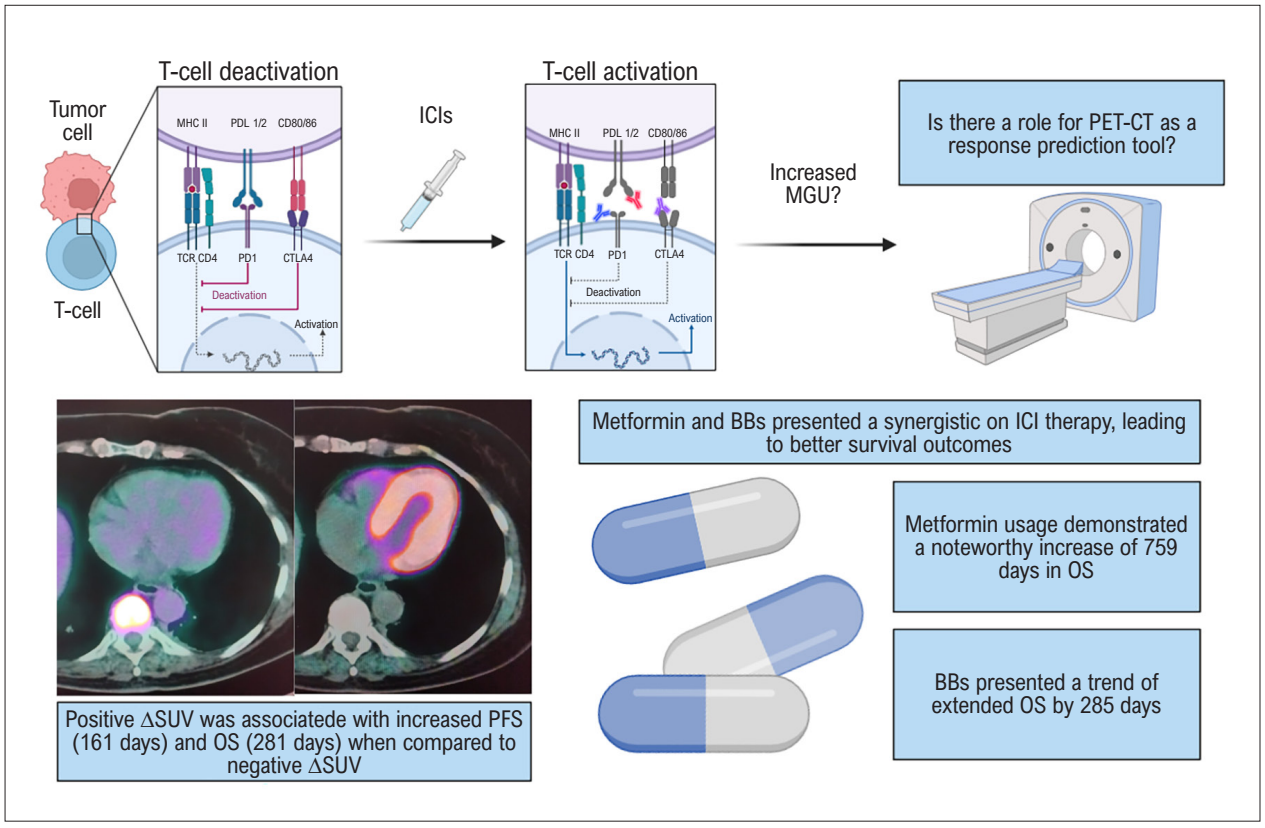

Figure 1 – *ICI: immune checkpoint inhibitors; PET-CT: positron emission tomography-computed tomography; BBs: β-blockers; PFS: progression-free survival; SUV: standardized uptake value; OS: Overall Survival.*

days in OS (p = 0.256) among patients exhibiting a positive ΔSUV. These results highlight the potential utility of ΔSUV as a predictive marker for treatment response and prognosis in patients undergoing immunotherapy.

Although the precise mechanism underlying irAEs is not yet fully understood, it is known that ICIs enhance the immune response against tumors, leading to inflammatory side effects through the recognition of shared antigens between tumor cells and normal tissues. Thus, it is hypothesized that the increase in 18F-FDG uptake, known in inflammatory processes, along with the presence of irAEs, could estimate response to immunotherapy and be associated with positive clinical outcomes.

Our findings align with a recent systematic review and meta-analysis, which demonstrated a correlation between irAEs and improved OS, PFS, and objective response rates (ORRs) in ICI-treated patients. The increase in SUV was identified as the main irAE marker on PET-CT.[18,19] Similarly, it was found that patients who experienced low- to mid-grade irAEs during atezolizumab-containing treatment regimens exhibited longer OS compared to those with high-grade irAEs or no irAEs at all.[20] These findings further support the notion that the occurrence of irAEs, along with changes in MGU, can serve as a valuable prognostic indicator and predictor of treatment response in patients undergoing immunotherapy.

A significant correlation was observed between increased OS and the usage of metformin (p = 0.015). The relationship between metformin and cancer immunity has been postulated to involve various mechanisms. These include the activation of adenosine monophosphate-activated protein kinase (AMPK)-dependent and AMPK-independent signaling pathways, which exert anti-tumor effects, and the elevation of the exhaustion threshold of cytotoxic T-lymphocytes (CTLs), thereby enhancing immune surveillance. Furthermore, metformin has been shown to impede the immune-inhibitory signaling of PD-L1 through the phosphorylation of PD-L1 associated with AMPK-dependent signaling activation,[21] as well as the glycosylation and degradation of PD-L1 within the endoplasmic reticulum.[22] These findings support the potential role of metformin as a modulator of cancer immunity and suggest its potential benefits in improving patient outcomes, particularly in terms of OS.

Consistent with our findings, several studies have demonstrated enhanced treatment outcomes when ICIs are combined with metformin in preclinical models of metastatic melanoma,[23] non-small cell lung cancer (NSCLC),[24] and breast cancer.[21] These studies provide further evidence supporting the potential synergistic effects of combining ICIs with metformin, leading to improved therapeutic responses in various cancer types.

Furthermore, the combination of metformin with PD-1 blockade has shown promising results in enhancing tumor

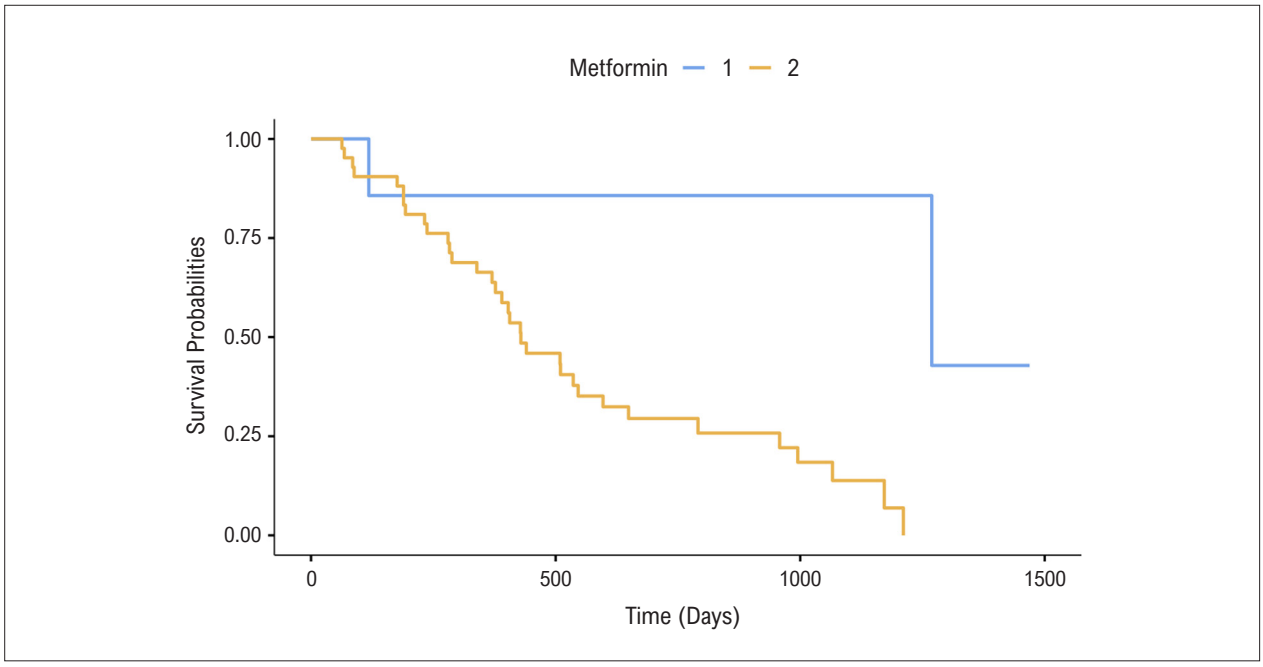

Figure 2 – *Overall survival comparison between metformin users and non-metformin users.*

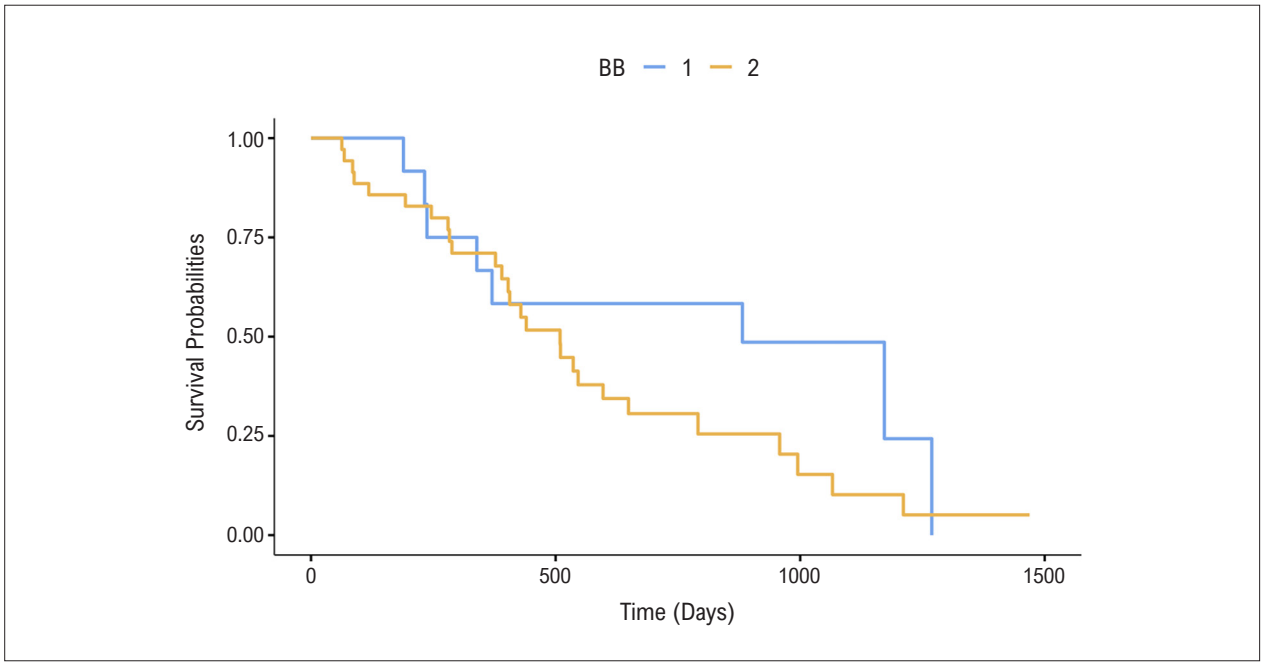

Figure 3 – *Overall survival comparison between β-blocker users and non-β-blocker users.*

clearance and improving T-cell function by mitigating tumor-induced hypoxia, which acts as an inhibitory factor for T-cell activity.[25] Moreover, in murine models, the synergistic effect of metformin and vaccine immunotherapy has been demonstrated to reduce PD-L1 expression on tumor cells.[11] These findings highlight the potential of metformin in modulating the tumor microenvironment, alleviating hypoxia-associated immune suppression, and augmenting the efficacy of immunotherapeutic approaches.

In the same manner, investigations have examined the potential of combining metformin with anti-PD-1 monotherapy or a combination of anti-VEGFR2 and anti-PD-1 to restore sensitivity to immunotherapies in Nonalcoholic Steatohepatitis-Hepatocellular Carcinoma

(NASH-HCC) tumors, which are typically characterized by limited responsiveness. Notably, these studies conducted in mice demonstrated the enhanced therapeutic efficacy achieved through such combinations, providing further support for exploring the synergistic effects of metformin and immunotherapies in overcoming resistance and improving treatment outcomes in challenging tumor types.[26,27]

Although limited in number, the available studies investigating the combination of metformin and ICIs in human subjects have yielded promising results. In an Italian study involving 40 patients, the concomitant administration of metformin and nivolumab was well tolerated and deemed safe. Notably, higher metformin doses (>1,000 mg daily) were associated with longer OS (p = 0.037) and PFS (p = 0.021) and improved response rates, corroborating our own findings.[28] Similarly, the combination of metformin with ICIs demonstrated potentially favorable clinical outcomes, although statistical significance was not reached, likely due to the small sample size.[23] Furthermore, metformin has been shown to enhance natural killer cell functions in head-and-neck squamous cell carcinoma.[29] These preliminary findings suggest that the combination of metformin with ICIs holds promise as a therapeutic strategy, warranting further investigation in larger clinical studies to establish its efficacy and safety profile on humans.

Hence, based on the multitude of pathways and immunologic mechanisms proposed in preclinical studies and its favorable results, it can be reasonably concluded that metformin may play a significant role as a safe, well-tolerated, and readily available adjuvant therapy in the management of solid cancers when used in conjunction with ICIs.

The potential role of beta-blockers (BBs) in cancer treatment has been widely investigated, with conflicting evidence found in the literature. Some older retrospective studies have demonstrated improved treatment outcomes in patients with breast cancer, especially in triple-negative,[30,31] ovarian,[32] bladder,[33] and NSCLCs.[34]

Moreover, a possible mechanism of action for BBs in cancer has been proposed in the literature, where beta-adrenergic signaling was found to be related to reduced proliferation of CD8+ T-cells and immune suppression mediated by regulatory T-cells and myeloid-derived suppressor cells.[10]

While the observed data regarding BB usage and OS did not reach statistical significance, potentially due to the limited sample size, the trend toward a 285-day increase in OS suggests a possible role for BBs as adjuvant therapy to ICIs in cancer treatment. Further studies with larger sample sizes are warranted to elucidate the underlying mechanism of action and determine whether BBs should be considered as a complementary drug for all patients undergoing immune checkpoint blockade.

Despite conflicting evidence in the literature regarding the impact of BBs on OS, PFS, and ORRs, similar findings to ours were reported in a recent meta-analysis that included 10,156 patients. The meta-analysis revealed that BB usage was associated with better ORRs to ICIs (odds ratio [OR] = 0.42 [0.19−0.94], p = 0.036), particularly in the subgroup of lung cancer patients (OR = 0.25 [0.08−0.83], p = 0.024). However, no significant association was found between BBs and OS or PFS in the pooled analysis.[29]

In summary, while the literature on the relationship between BBs and cancer treatment outcomes remains inconclusive, our findings, along with the meta-analysis results, suggest that BBs may have a potential role as adjunctive therapy to ICIs in cancer treatment that should be further studied.

Study limitations

The study has certain limitations that need to be acknowledged. First, the sample size was relatively small, primarily due to the limited number of lung cancer patients who received ICI therapy at our center. Consequently, the statistical significance of some findings may be compromised. Further research involving larger cohorts is essential to strengthen the validity and generalizability of our results.

Moreover, additional investigations are required to establish the underlying mechanisms of action and determine the clinical significance of using BBs in combination with ICIs. Furthermore, the importance of ΔSUV on survival outcomes also needs to be explored in future studies. These aspects will provide a more comprehensive understanding of the therapeutic potential and prognostic implications associated with the combined use of metformin, BBs, and ICIs in the context of lung cancer treatment.

Conclusions

Although further studies are needed to comprehensively assess the relationship between increased MGU and improved outcomes in patients undergoing ICI therapy, the role of PET-CT as a valuable tool for evaluating treatment response and irAEs is well established. Our findings highlight a significant association between increased OS and metformin use. This suggests that metformin could serve as an important adjuvant treatment option for patients undergoing ICI therapy, regardless of their diabetic or hyperglycemic status. Metformin's synergistic effects through multiple pathways, coupled with its accessibility, minimal side effects, and favorable safety profile, underscore its potential in enhancing treatment outcomes.

Author Contributions

Conception and design of the research: Torres MC, Martins J, Tavares M; acquisition of data: Torres MC, Martins J, Verçosa A, Tavares M; analysis and interpretation of the data and writing of the manuscript: Torres MC, Martins J, Verçosa A, Botelho LF, Tavares M; statistical analysis: Torres MC, Botelho LF, Tavares M; obtaining financing: Martins J, Tavares M; critical revision of the manuscript for intellectual content: Torres MC, Martins J, Verçosa A, Botelho LF, Tavares M.

Potential Conflict of Interest

No potential conflict of interest relevant to this article was reported.

Sources of Funding

There were no external funding sources for this study.

Study Association

This study is not associated with any thesis or dissertation work.

Ethics Approval and Consent to Participate

This study was approved by the Ethics Committee of the Secretaria de Saúde do Estado da Paraíba – SES/PB under the protocol number 47402321.9.0000.5186. All the procedures in this study were in accordance with the 1975 Helsinki Declaration, updated in 2013. Informed consent was obtained from all participants included in the study.

References

1. Zitvogel L, Kroemer G, editors. Oncoimmunology: A Practical Guide for Cancer Immunotherapy. Cham: Springer International Publishing; 2018.
2. American Cancer Society. Global Cancer Facts & Figures 2023. Atlanta: American Cancer Society; 2023.
3. Reck M, Remon J, Hellmann MD. First-Line Immunotherapy for Non-Small-Cell Lung Cancer. J Clin Oncol. 2022;40(6):586-97. doi: 10.1200/JCO.21.01497.
4. Zulfiqar B, Farooq A, Kanwal S, Asghar K. Immunotherapy and Targeted Therapy for Lung Cancer: Current Status and Future Perspectives. Front Pharmacol. 2022;13:1035171. doi: 10.3389/fphar.2022.1035171.
5. Zouein J, Haddad FG, Eid R, Kourie HR. The Combination of Immune Checkpoint Inhibitors and Chemotherapy in Advanced Non-Small-Cell Lung Cancer: The Rational Choice. Immunotherapy. 2022;14(2):155-67. doi: 10.2217/imt-2021-0014.
6. Qian L, Ding X, Li FQ, Tian HM, Chen X, Han FJ, et al. Cellular Immunotherapy Combined with Platinum-Based Chemotherapy Prolongs Survival for Non-Small Cell Lung Cancer Patients. Neoplasma. 2023;70(2):251-9. doi: 10.4149/neo_2023_230127N44.
7. Bianco A, Campbell SFM. Atezolizumab Plus Platinum-Based Regimen and Bevacizumab: Is it Time to Consider Immunotherapy in a Concurrent Approach for Lung Cancer? Transl Cancer Res. 2019;8(Suppl 2):103-5. doi: 10.21037/tcr.2018.11.06.
8. Arina A, Gutiontov SI, Weichselbaum RR. Radiotherapy and Immunotherapy for Cancer: From "Systemic" to "Multisite". Clin Cancer Res. 2020;26(12):2777-82. doi: 10.1158/1078-0432.CCR-19-2034.
9. Zhang Z, Liu X, Chen D, Yu J. Radiotherapy Combined with Immunotherapy: The Dawn of Cancer Treatment. Signal Transduct Target Ther. 2022;7(1):258. doi: 10.1038/s41392-022-01102-y.
10. Oh MS, Guzner A, Wainwright DA, Mohindra NA, Chae YK, Behdad A, et al. The Impact of Beta Blockers on Survival Outcomes in Patients with Non-Small-Cell Lung Cancer Treated with Immune Checkpoint Inhibitors. Clin Lung Cancer. 2021;22(1):e57-e62. doi: 10.1016/j.cllc.2020.07.016.
11. Munoz LE, Huang L, Bommireddy R, Sharma R, Monterroza L, Guin RN, et al. Metformin Reduces PD-L1 on Tumor Cells and Enhances the Anti-Tumor Immune Response Generated by Vaccine Immunotherapy. J Immunother Cancer. 2021;9(11):e002614. doi: 10.1136/jitc-2021-002614.
12. Zhu L, Kuang X, Zhang G, Liang L, Liu D, Hu B, et al. Albendazole Induces Immunotherapy Response by Facilitating Ubiquitin-Mediated PD-L1 Degradation. J Immunother Cancer. 2022;10(5):e003819. doi: 10.1136/jitc-2021-003819.
13. Léger MA, Routy B, Juneau D. FDG PET/CT for Evaluation of Immunotherapy Response in Lung Cancer Patients. Semin Nucl Med. 2022;52(6):707-19. doi: 10.1053/j.semnuclmed.2022.04.010.
14. Mu W, Jiang L, Shi Y, Tunali I, Gray JE, Katsoulakis E, et al. Non-Invasive Measurement of PD-L1 Status and Prediction of Immunotherapy Response Using Deep Learning of PET/CT Images. J Immunother Cancer. 2021;9(6):e002118. doi: 10.1136/jitc-2020-002118.
15. Evangelista L, Sepulcri M, Pasello G. PET/CT and the Response to Immunotherapy in Lung Cancer. Curr Radiopharm. 2020;13(3):177-84. doi: 10.2174/1874471013666191220105449.
16. Cherk MH, Nadebaum DP, Barber TW, Beech P, Haydon A, Yap KS. 18 F-FDG PET/CT Features Of Immune-Related Adverse Events and Pitfalls Following Immunotherapy. J Med Imaging Radiat Oncol. 2022;66(4):483-94. doi: 10.1111/1754-9485.13390.
17. Tatar G, Alçin G, Samanci NS, Fenercioglu ÖR, Beyhan E, Cermik TF. Diagnostic Impact of 18F-FDG PET/CT Imaging on the Detection Of Immune-Related Adverse Events in Patients Treated with Immunotherapy. Clin Transl Oncol. 2022;24(10):1903-13. doi: 10.1007/s12094-022-02840-9.
18. Fan Y, Xie W, Huang H, Wang Y, Li G, Geng Y, ET AL. Association of Immune Related Adverse Events with Efficacy of Immune Checkpoint Inhibitors and Overall Survival in Cancers: A Systemic Review and Meta-Analysis. Front Oncol. 2021;11:633032. doi: 10.3389/fonc.2021.633032.
19. Zhou X, Yao Z, Yang H, Liang N, Zhang X, Zhang F. Are Immune-Related Adverse Events Associated with the Efficacy of immune Checkpoint Inhibitors in Patients with Cancer? A Systematic Review and Meta-Analysis. BMC Med. 2020;18(1):87. doi: 10.1186/s12916-020-01549-2.
20. Socinski MA, Jotte RM, Cappuzzo F, Nishio M, Mok TSK, Reck M, ET AL. Association of Immune-Related Adverse Events with Efficacy of Atezolizumab in Patients with Non-Small Cell Lung Cancer: Pooled Analyses of the Phase 3 IMpower130, IMpower132, and IMpower150 Randomized Clinical Trials. JAMA Oncol. 2023;9(4):527-35. doi: 10.1001/jamaoncol.2022.7711.
21. Cha JH, Yang WH, Xia W, Wei Y, Chan LC, Lim SO, et al. Metformin Promotes Antitumor Immunity via Endoplasmic-Reticulum-Associated Degradation of PD-L1. Mol Cell. 2018;71(4):606-620.e7. doi: 10.1016/j.molcel.2018.07.030.
22. Ma R, Yi B, Riker AI, Xi Y. Metformin and Cancer Immunity. Acta Pharmacol Sin. 2020;41(11):1403-9. doi: 10.1038/s41401-020-00508-0.
23. Afzal MZ, Mercado RR, Shirai K. Efficacy of Metformin in Combination with Immune Checkpoint Inhibitors (anti-PD-1/anti-CTLA-4) in Metastatic Malignant Melanoma. J Immunother Cancer. 2018;6(1):64. doi: 10.1186/s40425-018-0375-1.
24. Shen X, Zhao Y, Liu G, Zhou HL, Fan J, Zhang L, et al. Upregulation of Programmed Death Ligand 1 by Liver Kinase B1 and its Implication in Programmed Death 1 Blockade Therapy in Non-Small Cell Lung Cancer. Life Sci. 2020;256:117923. doi: 10.1016/j.lfs.2020.117923.
25. Scharping NE, Menk AV, Whetstone RD, Zeng X, Delgoffe GM. Efficacy of PD-1 Blockade Is Potentiated by Metformin-Induced Reduction of Tumor Hypoxia. Cancer Immunol Res. 2017;5(1):9-16. doi: 10.1158/2326-6066.CIR-16-0103.
26. Lujambio A, Sarobe P. Metformin Keeps CD8+ T Cells Active and Moving in NASH-HCC Immunotherapy. J Hepatol. 2022;77(3):593-5. doi: 10.1016/j.jhep.2022.05.038.
27. Wabitsch S, McCallen JD, Kamenyeva O, Ruf B, McVey JC, Kabat J, et al. Metformin Treatment Rescues CD8+ T-Cell Response To Immune Checkpoint Inhibitor Therapy In Mice with NAFLD. J Hepatol. 2022;77(3):748-60. doi: 10.1016/j.jhep.2022.03.010.
28. Ciccarese C, Iacovelli R, Buti S, Primi F, Astore S, Massari F, et al. Concurrent Nivolumab and Metformin in Diabetic Cancer Patients: Is It Safe and More Active? Anticancer Res. 2022;42(3):1487-93. doi: 10.21873/anticanres.15620.

29. Crist M, Yaniv B, Palackdharry S, Lehn MA, Medvedovic M, Stone T, et al. Metformin Increases Natural Killer Cell Functions in Head and Neck Squamous Cell Carcinoma Through CXCL1 Inhibition. J Immunother Cancer. 2022;10(11):e005632. doi: 10.1136/jitc-2022-005632.

30. Løfling LL, Støer NC, Sloan EK, Chang A, Gandini S, Ursin G, et al. β-Blockers and Breast Cancer Survival by Molecular Subtypes: A Population-Based Cohort Study and Meta-Analysis. Br J Cancer. 2022;127(6):1086-96. doi: 10.1038/s41416-022-01891-7..

31. Caparica R, Bruzzone M, Agostinetto E, De Angelis C, Fêde Â, Ceppi M, et al. Beta-Blockers in Early-Stage Breast Cancer: A Systematic Review and Meta-Analysis. ESMO Open. 2021;6(2):100066. doi: 10.1016/j.esmoop.2021.100066.

32. Watkins JL, Thaker PH, Nick AM, Ramondetta LM, Kumar S, Urbauer DL, et al. Clinical Impact of Selective and Nonselective Beta-Blockers on Survival in Patients with Ovarian Cancer. Cancer. 2015;121(19):3444-51. doi: 10.1002/cncr.29392.

33. Udumyan R, Botteri E, Jerlstrom T, Montgomery S, Smedby KE, Fall K. Beta-Blocker Use and Urothelial Bladder Cancer Survival: A Swedish Register-Based Cohort Study. Acta Oncol. 2022;61(8):922-930. doi: 10.1080/0284186X.2022.2101902.

34. Yan X, Liu P, Li D, Hu R, Tao M, Zhu S, et al. Novel Evidence for the Prognostic Impact of β-Blockers in Solid Cancer Patients Receiving Immune Checkpoint Inhibitors. Int Immunopharmacol. 2022;113(Pt A):109383. doi: 10.1016/j.intimp.2022.109383.

Metformin in Combination with Immune Checkpoint Inhibitors: Myocardial FDG Uptake Can Predict Prognosis?

Claudio Tinoco Mesquita,[1,2,3] *Ana Beatriz Couto,*[4] *Marina Schmid Nunes,*[4] *Fernanda Azevedo Silva*[4]

ACAMERJ,[1] *Niterói, RJ – Brazil*

Universidade Federal Fluminense, Departamento de Radiologia,[2] *Niterói, RJ – Brazil*

Hospital Universitário Antonio Pedro, Health, Science & Education Lab,[3] *Niterói, RJ – Brazil*

Universidade Federal Fluminense,[4] *Niterói, RJ – Brazil*

Short Editorial related to the article: Variations in Myocardial FDG Uptake and Metformin Use: Implications for Survival During Immunotherapy

In Brazil, the estimate for 2023-2025 indicates that there will be 704,000 new cancer cases in the country, 221,000 of which will be non-melanoma skin cancers, cited as the most common type. After this type of cancer, breast cancer has the highest incidence, with 74,000 cases, followed by prostate cancer, with 72,000 cases, colorectum cancer, with 46,000 cases, and lung cancer, with 32,000 new cases.[1] The cancer epidemiological profile in Brazil is like countries with a high income; however, it differs when analyzed by region, indicating significant regional inequalities. While in the country's more developed regions (South and Southeast), the age-adjusted incidence rates range between 180 and 190 cases per 100,000 inhabitants, in less developed regions (North and Northeast), these rates vary from 157 to 164 cases per 100,000 inhabitants.[1] The highest cancer mortality in Brazil is due to lung cancer (13.7% of cancer deaths), followed by colorectum cancer (10.4% of cancer deaths), and then breast cancer (8% of cancer deaths).[2]

Immune checkpoints, like PD-1, PD-L1, and CTLA-4, regulate the immune system and help to equilibrate immune activation and suppression. They act by avoiding a strong immune response that could attack normal cells. Tumor cells can use these mechanisms to elude the immune system, decreasing its response.[3] The mechanisms used for immune system evasion in lung cancer are linked to PD-1 inhibition, which reduces the activity of tumor immunity cells.[4] Additionally, there is a decrease in T-lymphocyte proliferation and cytokine production (IL-2 and IFN-γ), allowing neoplastic cells to proliferate.

Immune Checkpoint Inhibitors (ICIs) are drugs that block checkpoint proteins and increase immunological defenses against cancer, by permitting a larger response.[5] This block permits T-cells to recognize and destroy neoplastic cells effectively. A few examples of ICI are nivolumab, pembrolizumab, and ipilimumab, which inhibit PD-1 and CTLA-4, respectively. These drugs have been used to treat non-small cell lung cancer, melanoma, renal cell carcinoma, lymphoma, and other types of cancer with success, even in metastatic and chemotherapy-resistant cancer.[5]

One of the most typical Adverse Effects (AE) of the ICIs are the Immune-related Adverse Events (irAEs), that occur due to the suppression of immune inhibitory functions. It is uncommon but there is the potential for a higher grade of severity in 10–15% of cases and clinical manifestations usually start within the first few weeks to months after the onset of treatment. ICI myocarditis is reported at an incidence rate of 0.06% to 1.14%. The cardiovascular system can be affected by irAEs also as takotsubo syndrome, pericardial disease, acute coronary syndromes, thromboembolic events, and arrhythmias.[6]

Metformin has become a research target in oncology due to its properties in improving prognosis and promoting tumor growth regression.[2-4,7,8] In addition to its use in the treatment of type II diabetes, studies have reported evidence of metformin's action in tumors by reducing neoplastic cell proliferation.[8,9] One of the treatment strategies for cancer cells with mutations in the Epidermal Growth Factor Receptor (EGFR) involves the use of an EGFR Tyrosine Kinase Inhibitor (TKI). The combination of metformin with TKI shows a synergistic effect, delaying tumor resistance.[10] The transmembrane tyrosine-protein kinase receptor (IGF-1R) is expressed in various cells with mitogenic potential.[10,11] In this context, metformin acts by restoring the sensitivity of EGFR-TKI-resistant cells, inhibiting the IGF-1R pathway and the expression of IGFBP3, a gene that encodes the growth factor protein.[12] This regulation negatively impacts synergistic antitumor effects mediated by BIM, one of the apoptotic regulatory proteins involved in the control of tumorigenesis.[13]

An 18F-fluorodeoxyglucose positron emission tomography/computed tomography (18F-FDG PET/CT) is commonly used in the assessment of cancer therapy responses. Some studies are suggesting that 18F-FDG PET/CT may also be used as a tool for detecting irAEs.[14]

In this issue of the ABC Imaging, Torres *et al.*, evaluated the role of metformin as an adjuvant therapy with ICIs on the prognosis of advanced lung cancer patients and assessed the associated changes in myocardial FDG uptake rate (MGU).[15] Interestingly the authors found that metformin users presented a significant increase in Overall Survival (OS). Also, patients with a positive variation in myocardial

Keywords

Immune Checkpoint Inhibitors; Positron-Emission Tomography; X-Ray Computed Tomography; Metformin; Cardio-Oncology

Mailling Address: Claudio Tinoco Mesquita •
Universidade Federal Fluminense, Hospital Universitário Antonio Pedro. Av. Marquês do Paraná, 303. Postal code: 24033-900. Niterói, RJ – Brazil
E-mail: claudiotinocomesquita@gmail.com

DOI: https://doi.org/10.36660/abcimg.20240111i

SUV (a quantitative measure of tissue glucose uptake) had an increase in progression-free survival (PFS). The authors concluded that metformin has the potential to be an important adjuvant treatment option for patients undergoing ICI therapy. Also, they hypothesize that an increase in myocardial SUV could be a potential marker for ICI beneficial effects.[15] These findings are interesting and draw attention to the complex interactions between the immune system and cancer treatment, in which activation of immune cells can bring benefits but there is also a risk that overactivation can cause significant complications. PET/CT with 18F-FDG can identify patients at higher risk of cardiac complications from cancer treatment, as demonstrated by Dourado *et al* in ABC Cardiol, identifying a phenotype of patients with cardiotoxicity.[16,17] Could the inflammation observed in these patients be considered a prognostic predictor of response? Could this uptake in the myocardium be an indication of systemic activation of the immune system? Could metformin protect the heart from the AEs of therapy given the absence of clinically relevant cases of myocarditis in the sample? There are limitations to the study, such as the absence of a formal control group, the absence of serial troponin measurements, or monitoring of left ventricular function with speckle-tracking echocardiography. This information would provide additional data to understand the findings. In any case, the authors should be congratulated for this hypothesis-generating study, and we suggest that studies of ICIs that include metformin as an adjuvant should perform serial monitoring of cardiac parameters, including measurement of FDG uptake in the myocardium, as a way of understanding whether these parameters can contribute to the management of cancer patients receiving immunotherapy.

References

1. Santos MO, Lima FCS, Martins LFL, Oliveira JFP, Almeida LM, Cancela MC. Estimativa de Incidência de Câncer no Brasil, 2023-2025. Rev Bras Cancerol. 2023;69(1):1-12. doi: 10.32635/2176-9745.RBC.2023v69n1.3700.
2. Ferlay J, Ervik M, Lam F, Laversanne M, Colombet M, Mery L, et al. Global Cancer Observatory: Cancer Today. Lyon: International Agency for Research on Cancer; 2024.
3. Johnson DB, Nebhan CA, Moslehi JJ, Balko JM. Immune-checkpoint Inhibitors: Long-term Implications of Toxicity. Nat Rev Clin Oncol. 2022;19(4):254-67. doi: 10.1038/s41571-022-00600-w.
4. Tang S, Qin C, Hu H, Liu T, He Y, Guo H, et al. Immune Checkpoint Inhibitors in Non-small Cell Lung Cancer: Progress, Challenges, and Prospects. Cells. 2022;11(3):320. doi: 10.3390/cells11030320.
5. Naimi A, Mohammed RN, Raji A, Chupradit S, Yumashev AV, Suksatan W, et al. Tumor Immunotherapies by Immune Checkpoint Inhibitors (ICIs); The Pros and Cons. Cell Commun Signal. 2022;20(1):44. doi: 10.1186/s12964-022-00854-y.
6. Thuny F, Naidoo J, Neilan TG. Cardiovascular Complications of Immune Checkpoint Inhibitors for Cancer. Eur Heart J. 2022;43(42):4458-68. doi: 10.1093/eurheartj/ehac456.
7. Han K, Pintilie M, Lipscombe LL, Lega IC, Milosevic MF, Fyles AW. Association between Metformin Use and Mortality after Cervical Cancer in Older Women with Diabetes. Cancer Epidemiol Biomarkers Prev. 2016;25(3):507-12. doi: 10.1158/1055-9965.EPI-15-1008.
8. Yousef M, Tsiani E. Metformin in Lung Cancer: Review of in Vitro and in Vivo Animal Studies. Cancers. 2017;9(5):45. doi: 10.3390/cancers9050045.
9. Pollak MN. Investigating Metformin for Cancer Prevention and Treatment: The End of the Beginning. Cancer Discov. 2012;2(9):778-90. doi: 10.1158/2159-8290.CD-12-0263.
10. Wang H, Yang X, Sun Y, Li Y, Dong Y, Shan D, et al. Synergistic Effect of Metformin and EGFR-TKI in the Treatment of Non-small Cell Lung Cancer. Transl Cancer Res. 2020;9(1):372-81. doi: 10.21037/tcr.2019.11.09.
11. Martin JL, Baxter RC. Signalling Pathways of Insulin-like Growth Factors (IGFs) and IGF Binding Protein-3. Growth Factors. 2011;29(6):235-44. doi: 10.3109/08977194.2011.614237.
12. Cortot AB, Repellin CE, Shimamura T, Capelletti M, Zejnullahu K, Ercan D, et al. Resistance to Irreversible EGF Receptor Tyrosine Kinase Inhibitors Through a Multistep Mechanism Involving the IGF1R Pathway. Cancer Res. 2013;73(2):834-43. doi: 10.1158/0008-5472.CAN-12-2066.
13. Harada H, Grant S. Targeting the Regulatory Machinery of BIM for Cancer Therapy. Crit Rev Eukaryot Gene Expr. 2012;22(2):117-29. doi: 10.1615/critreveukargeneexpr.v22.i2.40.
14. Karlsen W, Akily L, Mierzejewska M, Teodorczyk J, Bandura A, Zaucha R, et al. Is 18F-FDG-PET/CT an Optimal Imaging Modality for Detecting Immune-Related Adverse Events after Immune-Checkpoint Inhibitor Therapy? Pros and Cons. Cancers. 2024;16(11):1990. doi: 10.3390/cancers16111990.
15. Torres MC, Martins J, Botelho LF, Verçosa A, Tavares M. Variações na captação miocárdica de FDG e uso de metformina: implicações para a sobrevivência durante a imunoterapia. Arq Bras Cardiol: Imagem cardiovasc. 2025;38(1):e20240108. DOI: https://doi.org/10.36660/abcimg.20240108
16. Mesquita CT, Rezende MF. Precision Medicine: Can 18F-FDG PET Detect Cardiotoxicity Phenotypes? Arq Bras Cardiol. 2022;119(1):109-10. doi: 10.36660/abc.20220393.
17. Dourado MLC, Dompieri LT, Leitão GM, Mourato FA, Santos RGG, Almeida PJ Filho, et al. Chemotherapy-induced Cardiac18F-FDG Uptake in Patients with Lymphoma: An Early Metabolic Index of Cardiotoxicity? Arq Bras Cardiol. 2022;118(6):1049-58. doi: 10.36660/abc.20210463.

Left Ventricular Global Longitudinal Strain: an Early Marker of Diabetic Cardiomyopathy

Ana Carolina Saran,[1] Stephanie Corradini Tormin,[1] Jennifer Vogel,[1] Rogério Krakauer,[1] João Eduardo Nunes Salles[1]

Faculdade de Ciências Médicas da Santa Casa de São Paulo,[1] São Paulo, SP – Brazil

Abstract

Background: Diabetic cardiomyopathy (DCM) leads to abnormal myocardial structure and function in the absence of cardiac risk factors. Screening in the pre-clinical phase is not well established. Global longitudinal strain (GLS) has been measured as an important echocardiography parameter in asymptomatic patients.

Objective: To describe the presence of early parameters of DCM in patients with type 2 diabetes (T2DM) without cardiovascular disease and to compare results against 2 control groups (CT groups).

Methods: A total of 58 patients were divided into the following 3 groups: T2DM (n = 20); heart failure (HF) with preserved ejection fraction (HFpEF) without T2DM (n = 19); and control without T2DM or HFpEF (n = 19). Patients with cardiovascular disease and those using SGLT2 inhibitors, pioglitazone or saxagliptin were excluded.

Results: The mean overall prevalence of GLS was 16% (standard deviation [SD] ± 2.9), and 41% of participants had abnormal values, comprising 10 (50%) patients from the T2DM, 11 (58%) from the HFpEF, and 3 (16%) from the CT groups (p = 0.019). Mean GLS values in the T2DM, HFpEF, and CT groups were 16.1%, 14.8%, and 17.5%, respectively (p = 0.015). There was a negative moderate association between HbA1c levels and GLS values in the T2DM group (p = 0.043).

Conclusions: GLS proved to be a potential early marker of left ventricular (LV) cardiac changes in patients with T2DM, given the similarity between this patient group and the HFpEF group studied.

Keywords: Diabetes Mellitus; Diabetic Cardiomyopathies; Echocardiography; Ventricular Dysfunction.

Introduction

Type 2 diabetes mellitus (T2DM) is a chronic heterogeneous disease characterized by persistent hyperglycemia caused by metabolic disturbances, resulting in impaired insulin secretion and/or action.[1] The condition is increasingly recognized as a complex cardio-renal-metabolic disease, promoted by a positive energy balance.[2]

Persistent hyperglycemia is associated with a host of cardiovascular complications.[1] Even in the absence of valvulopathies or coronary heart diseases, T2DM alone can cause structural and functional cardiac changes, generally referred to as diabetic cardiomyopathy (DCM)[3-5] (Central Figure).

The pathogenesis of DCM is multifactorial and not yet fully elucidated. Several elements appear to play a role in cardiac dysfunctions in this patient group: mitochondrial dysfunction, activation of the renin-angiotensin-aldosterone system, oxidative stress, myocardial fibrosis, microangiopathy, inflammatory cytokines, and the underlying hyperglycemia.[3] These patients can consequently develop relaxation difficulties, changes in left ventricular (LV) pressure and stiffness and left atrial enlargement.[4]

These alterations are referred to as diastolic dysfunction (DD), an echocardiographic finding recognized as an early marker of DCM that can be associated with preserved or reduced fraction ejection (FE). Screening for DD in the pre-clinical stage is important given the benefits of early intervention in these individuals, with the aim of preventing progression to the symptomatic form of the disease.

Mechanisms for diagnosing patients with DCM in the asymptomatic stage are inadequate owing to the clinical complexity of the condition. The use of imaging scans allows monitoring and/or stratifying the degree of ventricular dysfunction.[5] Tissue Doppler echocardiogram is a highly accessible, relatively non-invasive imaging method that provides early detection of structural and functional cardiac dysfunctions in patients at risk of heart failure (HF), the symptomatic progression of DCM.[6]

Useful parameters for assessing the presence of ventricular remodeling include indexed LV mass, indexed left atrial volume, and the ratio of early diastolic transmitral inflow to early diastolic mitral annular velocity (E/E' mitral), which aid

Correspondência: Ana Carolina Saran •
Faculdade de Ciências Médicas da Santa Casa de São Paulo. Rua Dr. Cesário Motta Jr., 61. CEP: 01221-020. São Paulo, SP - Brasil
E-mail: anasaran@hotmail.com
Manuscript received October 30, 2024; revised October 30, 2024; accepted October 30, 2024
Editor responsible for the review: Marcelo Tavares

DOI: https://doi.org/10.36660/abcimg.20240082i

Central Illustration: Left Ventricular Global Longitudinal Strain: an Early Marker of Diabetic Cardiomyopathy

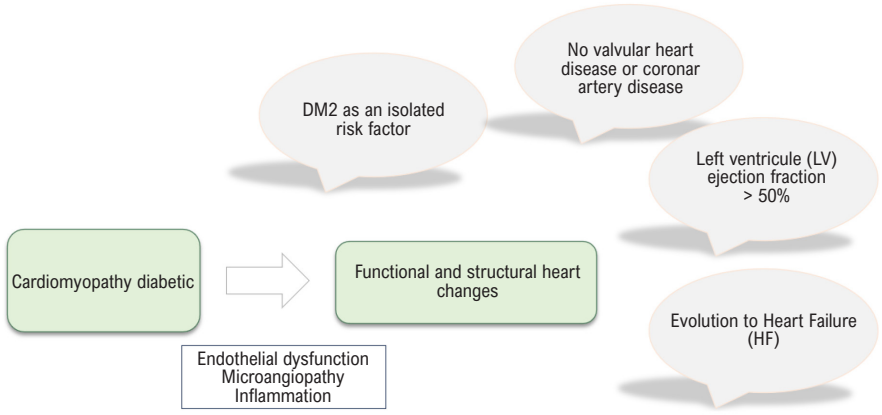

Arq Bras Cardiol: Imagem cardiovasc. 2025;38(1):e20240082

diagnosis and offer high specificity for characterizing elevated LV diastolic pressures.[7]

However, the emergence of new echocardiographic methods, such as LV global longitudinal strain (GLS), can offer even greater sensitivity for early DCM diagnosis. GLS constitutes a measure of myocardial deformity and provides greater diagnostic sensitivity, particularly in asymptomatic patients. Currently, GLS is considered a better predictor of risk than EF.[8]

Thus, this raises the possibility of using LV GLS as an echocardiographic marker of changes present in DCM (not widely recognized by health professionals) which manifest early in patients with T2DM in the absence of known cardiovascular disease. Therefore, this study sought to establish a potential association between clinical characteristics of patients with T2DM and LV GLS, in addition to similarities and differences on comparisons with 2 control groups (CT groups) of patients without T2DM.

Materials and methods

A cross-sectional study was conducted of patients recruited from the Endocrinology Outpatient Clinic, with clinically confirmed diagnosis of T2DM, as defined by the 2023 criteria of the American Diabetes Association.[1] Control subjects, matched for age, body mass index (BMI), and comorbidities, were recruited from the Endocrinology, Cardiology and/or Internal Medicine Outpatient Clinics to form 2 CT groups: patients without T2DM or suspected symptoms of HF with preserved ejection fraction (HFpEF); and patients without T2DM investigated for HFpEF, as per the criteria of the European Society of Cardiology.[9] In conjunction with medical chart review, participants underwent clinical examination, imaging scans and laboratory tests.

Patients with history of previous ischemic or hemorrhagic stroke, cardiovascular disease, confirmed infectious cardiomyopathies, collagen disorders, and/or granulomatous diseases were excluded. Patients using SGLT-2 inhibitors, pioglitazone, or saxagliptin for more than 1 month and patients with atrial fibrillation, LVEF < 50%, or severe valve disease as classified by the criteria of the American Society of Echocardiography (ASE) were also excluded.[10]

A Doppler transthoracic echocardiogram was performed and assessed by the same physician assistant of the cardiology sector, blinded to participants´ clinical data. Echocardiographic assessments and reports were based on the 2016 ASE Guidelines,[10] using a Vivid™ iq Ultra Edition GE HealthCare device. GLS was analyzed by 2D speckle tracking, using the software Echo-PAC, version 113, with 3 apical standard views. Apical images were divided into 6 standard deformation segments and times, yielding corresponding deformation curves. The cutoff point defined for LV GLS was < 16%.

Blood samples were collected from participants to test glycated hemoglobin (HbA1c) by turbidimetry, levels of natriuretic peptide using chemiluminescence, and kidney function (urea and creatine, automated glomerular filtration rate calculated using the CKD-EPI equation at ml/min/1.73 m^2). Only patients with T2DM underwent triage for nephropathy screening based on microalbuminuria in a spot sample using immunoturbidimetry (positivity defined as > 30 mg albumin/gram of creatinine) and diabetic retinopathy.

A retinography scan was carried out using a Phelcon Eyer NM Top device with photographic documentation and classified according to the international 2018 ETDRS (Early Treatment Diabetic Retinopathy Study) classification[11] by a vitreoretinal specialist ophthalmologist. The study was approved by the Research Ethics Committee (CAAE permit number: 26182819.5.0000.5479).

A total of 104 patients with clinically confirmed T2DM were randomly selected from the Endocrinology Outpatient Clinic.

Retrospective analysis of patient electronic medical records and application of the inclusion and exclusion criteria led to the assignment of 20 participants into the group with T2DM (T2DM group).

The CT group comprised an initial 20 patients randomly selected from the Internal Medicine Outpatient Clinic, with 1 subject subsequently excluded for EF < 50% on echocardiogram, resulting in 19 participants. For the group with suspected HFpEF (HFpEF group), an initial 24 patients were recruited from the Cardiology Outpatient Clinic, with subsequent exclusion of 5 patients for EF < 50% on the echocardiogram, resulting in 19 patients. Thus, a final total of 58 patients were analyzed. The study design is depicted in Figure 1.

For descriptive analysis, categorical variables were expressed as frequencies and percentages, and continuous variables as measures of central tendency (mean, standard deviation [SD], minimum and maximum).

For inferential analysis, categorical variables were compared using the chi-square test or Fisher's exact test. Continuous variables were assessed using Student's t test, or by the Mann-Whitney non-parametric test when data had a non-normal distribution. A 5% level of significance was adopted for all tests. All statistical analyses were performed using the software IBM SPSS Statistics for Windows, version 25.0.

Results

Of the total 58 participants, 64% were female, and groups had a similar sex distribution. For the overall sample, mean age was 56 (SD ± 12) years and 97% had preserved renal function (creatinine clearance > 60 ml/min). Regarding BMI, 51.8% of participants had some degree of obesity (BMI > 30 kg/m^2), with the highest prevalence in the T2DM group. The demographic characteristics of the population analyzed are presented in Table 1.

T2DM group

Mean age of patients in the T2DM group was 62 (SD ± 7.5) years, and 65% were female. With respect to disease duration, 11 patients had been diagnosed more than 10 years prior, and 45% were using insulin. Mean HbA1c level was 7.6% (SD ± 1.8). Of the patients assessed, 30% had microalbuminuria, and 35% had some degree of retinopathy.

Among the comorbidities assessed, systemic arterial hypertension and dyslipidemia were more prevalent in the T2DM group. The characteristics of the T2DM group are given in Table 2.

Echocardiographic data

Overall, mean GLS in the groups was 16% (SD ± 2.9; median 17%). Of all patients analyzed, 24 had abnormal strain (41%), comprising 10 (50%) from the T2DM group, 11 (58%) from the HFpEF group, and 3 (16%) from the CT group (p = 0.019). Median strain by group was 16.5% in the T2DM group, 15% in the HFpEF group, and 17.9% in the CT group (p = 0.015), with the largest statistical difference occurring between the HFpEF and CT groups (p = 0.012).

In the T2DM group, a negative association was found between HbA1c levels and strain. Patients with higher HbA1c levels had GLS < 16% (p = 0.043), as shown in Figure 2.

Regarding the association of microvascular complications and abnormal LV GLS, 4 (40%) patients testing positive for microalbuminuria (p = 0.628) and 5 patients (50%) with retinopathy (p = 0.350) had strain < 16%. Among patients with some degree of obesity, 90% had abnormal LV GLS values (p = 0.087). The results of the subanalyses of the T2DM group are presented in Table 3. The mean and SD for the variables investigated are given in Table 4.

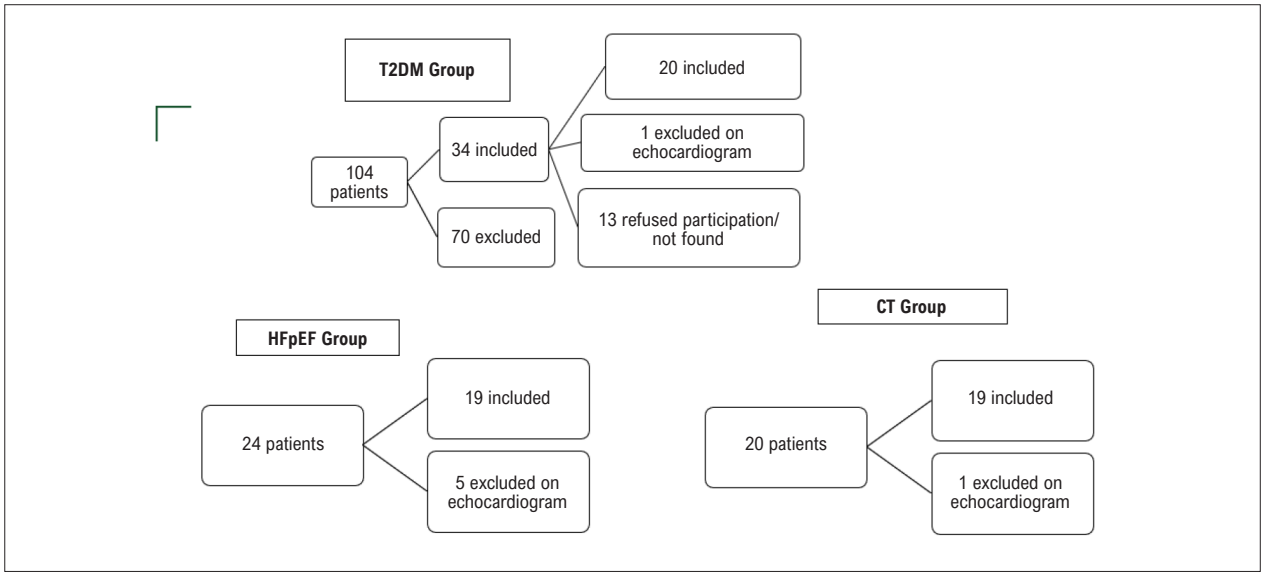

Figure 1 – *Study design CT: control; HFpEF: heart failure with preserved ejection fraction; T2DM: type 2 diabetes mellitus.*

Table 1 – Main demographic characteristics of overall study population and by group

Characteristics	Total	T2DM	HFpEF	Control	p value
n	58	20	19	19	
Sex					
Female	37 (64%)	13 (65%)	11 (58%)	13 (68%)	0.789
Male	21 (36%)	7 (35%)	8 (42%)	6 (32%)	
Age range (years)					0.001
≤ 40	6 (10%)	0 (0%)	1 (5%)	5 (26%)	
41 to 50	10 (17%)	0 (0%)	6 (32%)	4 (21%)	
51 to 60	18 (31%)	10 (50%)	2 (11%)	6 (32%)	
61 to 70	18 (31%)	6 (30%)	8 (42%)	4 (21%)	
> 70	6 (10%)	4 (20%)	2 (11%)	0 (0%)	
BMI					0.404
Normal	10 (17%)	4 (20%)	4 (21%)	2 (11%)	
Overweight	18 (31%)	2 (10%)	7 (37%)	9 (47%)	
Obese	30 (52%)	14 (70%)	8 (42%)	8 (42%)	
Tobacco use					0.015
No	50 (86%)	18 (90%)	13 (68%)	19 (100%)	
Yes	8 (14%)	2 (10%)	6 (32%)	0 (0%)	
SAH					<0.001
No	26 (45%)	4 (20%)	6 (32%)	16 (84%)	
Yes	32 (55%)	16 (80%)	13 (68%)	3 (16%)	
Dyslipidemia					<0.001
No	31 (53%)	3 (15%)	13 (68%)	15 (79%)	
Yes	27 (47%)	17 (85%)	6 (32%)	4 (21%)	
CrCl					0.006
≥ 60	47 (81%)	12 (60%)	16 (84%)	19 (100%)	
60 a 30	9 (16%)	6 (30%)	3 (16%)	0 (0%)	
30 a 15	2 (3%)	2 (10%)	0 (0%)	0 (0%)	
< 15	0 (0%)	0 (0%)	0 (0%)	0 (0%)	

BMI: body mass index; CrCl: creatinine clearance; HFpEF: heart failure with preserved ejection fraction; SAH: systemic arterial hypertension; T2DM: type 2 diabetes mellitus.

Discussion

T2DM is one of the most prevalent diseases worldwide, and not only represents a risk factor for the development of HF but can exacerbate the progression of the existing disease.[12] Studies involving patients with T2DM and HF have shown the positive impact of treatment on disease progression.[13-15] The 2015 EMPAREG study, comparing the use of empagliflozin against placebo, found a 35% reduction in the number of hospital admissions for HF.[14] A similar result was seen in the 2017 CANVAS study, which reported a 33% decrease in hospitalizations for decompensated HF.[15] Some of these patients were unaware that they hard HFpEF.[13]

It is believed that, through early diagnosis of DCM in the asymptomatic stage, early damage can be reversed and progression to the symptomatic disease averted. Currently, specific therapies are available which can improve the prognosis of the disease.[16]

The characteristics of patients with DD secondary to diabetes, in the early stages, are both complex and challenging to diagnose. Currently, there is no consensus on screening or when to start treatment in asymptomatic patients, although several factors can be considered, including disease duration, insulin use, glycemic control, and presence of microvascular complications.[17]

The physiopathology of DCM is not fully understood, and one of the main hypotheses is the progression of diastolic to systolic dysfunction, concomitant with LV remodeling and hypertrophy. Metabolic changes secondary to hyperglycemia and insulin resistance begin to promote

Table 2 – Main demographic characteristics of T2DM group

	T2DM (n = 20)
Disease duration (years)	
≤ 5	2 (10%)
5 to 10	7 (35%)
> 10	11 (55%)
Insulin use	
No	11 (55%)
Yes	9 (45%)
HbA1c	
< 6.5%	7 (35%)
6.5% to 7.5%	5 (25%)
7.5% to 9.0%	3 (15%)
9.0% to 11%	3 (15%)
> 11%	2 (10%)
MAB (> 30 mg)	
No	14 (70%)
Yes	6 (30%)
Retinopathy	
Absent	12 (60%)
Mild non-proliferative	3 (15%)
Moderate non-proliferative	2 (10%)
Severe non-proliferative	1 (5%)
Proliferative	1 (5%)
Inconclusive	1 (5%)
Post-laser	0 (0%)

HbA1c: glycated hemoglobin; MAB: microalbuminuria; T2DM: type 2 diabetes mellitus.

gradual changes in the heart, and, owing to compensatory adaptation, changes are evident only at a structural and cellular level.[17]

LV GLS serves as a predictor of hospitalization for HF and cardiovascular death, correlating strongly with LV stiffness and biomarkers.[18] Strain is believed to be the best marker of subclinical DD in DCM.[8]

In a systematic review, da Silva et al.[8] reported that around 40% of asymptomatic T2DM patients exhibited abnormal strain values. Mirroring the present findings, the study by Karagöz et al.,[19] comparing T2DM patients with control subjects, observed lower strain results in the T2DM group.

The relationship between microvascular complications and low GLS is also well established. Many studies have demonstrated the association of diabetic retinopathy, for example, with the development of DD and HF.[8,20] By contrast, Karagöz et al.[19] failed to identify this association. Although the present study was unable to confirm this association in the sample assessed, a tendency towards a greater incidence of abnormal strain values among patients testing positive for microalbuminuria was evident. The mean HbA1c of 7.6% and lower prevalence of microvascular complications in the patient sample might explain the absence of this association in the study.

The association between T2DM duration and LV GLS is controversial.[21] Silverii et al.[21] assessed patients with T2DM and was unable to establish this relationship. In the present analysis, although the association could not be confirmed, 60% of patients with GLS < 16% had T2DM for more than 10 years. Moreover, the cited study also established an inverse correlation of HbA1c with GLS, a finding corroborated by the current results in the T2DM group.

Obesity is associated with abnormal GLS values, irrespective of the concomitant presence of T2DM. In the series by Mochizuki et al.,[20] patients with T2DM concomitant with obesity had abnormal GLS values, a correlation also observed in the present analysis.

Study limitations

The research was initially planned to assess at least 30 patients for each group to provide a significant confidence interval for the variables investigated. However, the start of data collection and patient recruitment coincided with the COVID-19 outbreak. The pandemic led to delays in data collection and problems inviting patients due to the lockdown and social distancing measures, where most patients were deemed a high-risk group.

Notably, patients in the T2DM group had HbA1c values averaging 7.6% The low number of echocardiographic abnormalities observed in the present study may have been attributed to the apparently better controlled T2DM in the patient population studied.

Lastly, given that the tertiary hospital handled cases of greater complexity, factors such as systemic arterial hypertension and obesity were more prevalent in the patient group compared to the CT groups, representing factors which also correlate with cardiac dysfunctions.

Conclusion

LV relaxation abnormalities are important echocardiographic findings in patients with T2DM and a diagnostic component of the early stages of DD.

LV GLS proved a valuable early marker of LV abnormalities, where the results obtained for T2DM group were similar to those of the HFpEF group, yet differed from the control population. Further, these abnormalities were also more prevalent in patients with diabetes, obesity, and associated microvascular complications. However, the limiting factors of the study may have had a statistical impact on the results obtained.

Thus, future studies involving a larger patient sample and fewer confounding factors are needed for a more accurate assessment of the impact of employing LV GLS as an early marker of DCM in the pre-clinical phase.

Acknowledgments

The authors extend their thanks to the staff at the Endocrinology, Internal Medicine, and Cardiology Outpatient

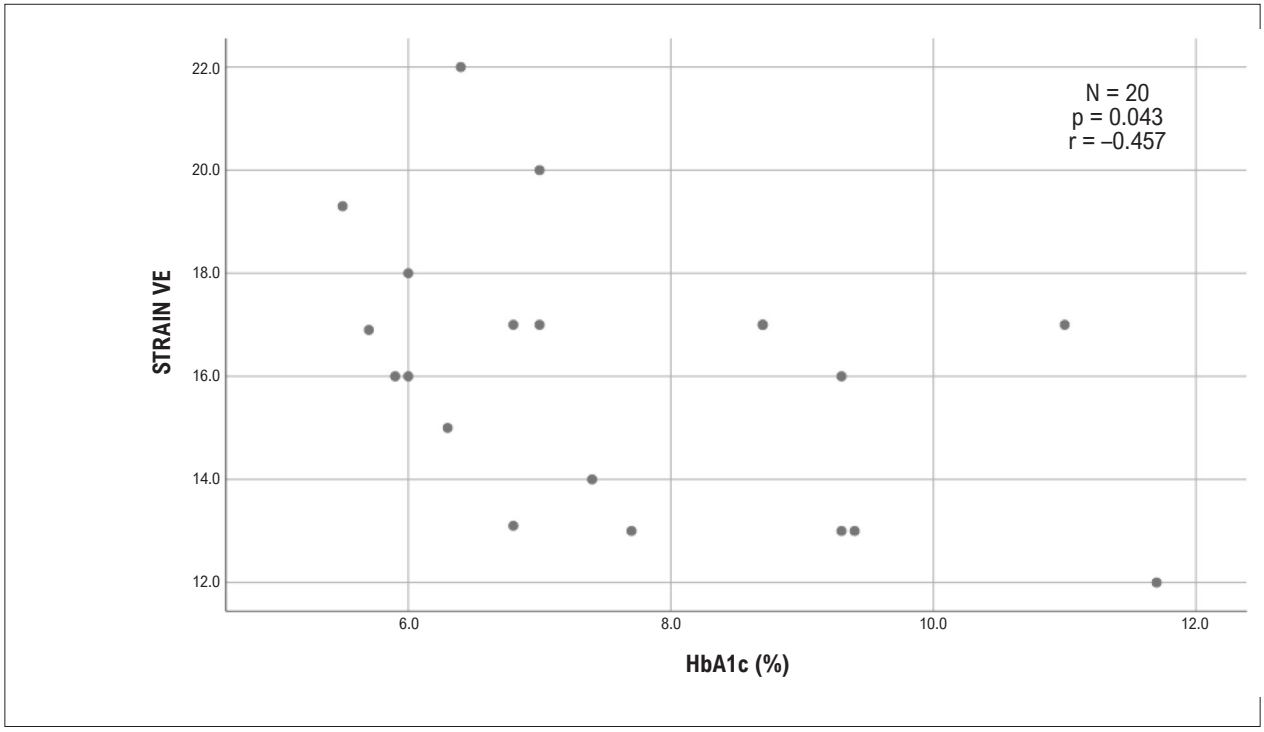

Figure 2 – *Dot plots of negative moderate correlation between LV GLS and HbA1c. HbA1c: glycated hemoglobin; LV GLS: left ventricular global longitudinal strain.*

Table 3 – Descriptive analysis of T2DM group and association with LV GLS

	LV GLS			p value	Test used
	Total	> 16%	< 16%		
n	20	10	10	-	-
Insulin				1.000	Fisher's exact
No	11 (55%)	5 (50%)	6 (60%)		
Yes	9 (45%)	5 (50%)	4 (40%)		
MAB				0.628	Fisher's exact
No	14 (70%)	8 (80%)	6 (60%)		
Yes	6 (30%)	2 (20%)	4 (40%)		
Retinopathy				0.350	Fisher's exact
Absent	12 (60%)	7 (70%)	5 (50%)		
Present	7 (35%)	2 (20%)	5 (50%)		
Inconclusive	1 (5%)	1 (10%)	0 (0%)		
BMI				0.087	Fisher's exact
Normal	4 (20%)	4 (40%)	0 (0%)		
Overweight	2 (10%)	1 (10%)	1 (10%)		
Obese	14 (70%)	5 (50%)	9 (90%)		
Disease duration (years)				1.000	Fisher's exact
≤ 5	2 (10%)	1 (10%)	1 (10%)		
5 to 10	7 (35%)	4 (40%)	3 (30%)		
> 10	11 (55%)	5 (50%)	6 (60%)		

BMI: body mass index; LV GLS: left ventricular global longitudinal strain; MAB: microalbuminuria in spot sample; T2DM: type 2 diabetes mellitus.

Table 4 – Mean and SD of variables analyzed

Variable	Total (n = 58)	T2DM (n = 20)	HFpEF (n = 19)	Control (n = 19)	p value
Age	55.9 (± 11.6)	61.6 (± 7.5)	57.2 (± 12.2)	48.8 (± 11.6)	0.001
CrCl (value)	72.22 (± 25)	-	-	-	
BNP (value)	27.9 (± 32.8)	33.5 (± 40)	34.9 (± 33.7)	13.6 (± 13.2)	0.048
LAV	26.6 (± 8.3)	29.4 (± 9.5)	25.8(± 7.9)	24.6 (± 7.1)	0.176
E/e'	8.6 (± 2.5)	9.1 (± 2.3)	8.8 (± 2.5)	7.5 (± 2.7)	0.274
LV GLS	16 (± 2.9)	16.1 (± 2.6)	14.8 (± 3.2)	17.5 (± 2.5)	0.015
LV mass	87.5 (± 20)	92 (± 17.7)	89.3 (± 20.6)	80.4 (± 21.9)	0.185

BNP: natriuretic peptide; CrCl: Creatinine clearance; E/e': ratio of E diastolic mitral inflow velocity to e' diastolic mitral annulus velocity (abnormal > 14); HFpEF: heart failure with preserved ejection fraction; LAV: indexed left atrial volume (abnormal > 34 ml/²); LV GLS: left ventricular global longitudinal strain; LV mass: left ventricular mass (abnormal > 95 g/m² in females and > 115 g/m² in males); T2DM: type 2 diabetes mellitus.

Clinics and the Clinical Analysis Laboratory. Thanks also go to the physician assistants of the Ophthalmology Team.

Author Contributions

Conception and design of the research and critical revision of the manuscript for intellectual content: Saran AC, Tormin SC, Krakauer R, Salles JEN; acquisition of data: Saran AC, Tormin SC, Vogel J, Krakauer R; analysis and interpretation of the data: Saran AC, Tormin SC, Vogel J, Krakauer R, Salles JEN; statistical analysis and writing of the manuscript: Saran AC, Tormin SC, Vogel J, Krakauer R, Salles JEN.

Potential Conflict of Interest

No potential conflict of interest relevant to this article was reported.

Sources of Funding

There were no external funding sources for this study.

Study Association

This article is part of the thesis of master submitted by Ana Carolina Saran, from Faculdade de Ciências Médicas da Santa Casa de São Paulo.

Ethics Approval and Consent to Participate

This study was approved by the Ethics Committee of the Santa Casa de São Paulo under the protocol number 26182819.5.0000.5479. All the procedures in this study were in accordance with the 1975 Helsinki Declaration, updated in 2013. Informed consent was obtained from all participants included in the study.

References

1. El Sayed NA, Aleppo G, Aroda VR, Bannuru RR, Brown FM, Bruemmer D, et al. Introduction and Methodology: Standards of Care in Diabetes-2023. Diabetes Care. 2023;46(Suppl 1):1-4. doi: 10.2337/dc23-Sint.
2. Okemah J, Peng J, Quiñones M. Addressing Clinical Inertia in Type 2 Diabetes Mellitus: A Review. Adv Ther. 2018;35(11):1735-45. doi: 10.1007/s12325-018-0819-5.
3. Jia G, Hill MA, Sowers JR. Diabetic Cardiomyopathy: An Update of Mechanisms Contributing to This Clinical Entity. Circ Res. 2018;122(4):624-38. doi: 10.1161/CIRCRESAHA.117.311586.
4. McHugh K, De Vore AD, Wu J, Matsouaka RA, Fonarow GC, Heidenreich PA, et al. Heart Failure with Preserved Ejection Fraction and Diabetes: JACC State-of-the-art Review. J Am Coll Cardiol. 2019;73(5):602-11. doi: 10.1016/j.jacc.2018.11.033.
5. Okoshi K, Guimarães JF, Di Muzio BP, Fernandes AA, Okoshi MP. Diabetic Cardiomyopathy. Arq Bras Endocrinol Metabol. 2007;51(2):160-7. doi: 10.1590/s0004-27302007000200004.
6. Lorenzo-Almorós A, Tuñón J, Orejas M, Cortés M, Egido J, Lorenzo Ó. Diagnostic Approaches for Diabetic Cardiomyopathy. Cardiovasc Diabetol. 2017;16(1):28. doi: 10.1186/s12933-017-0506-x.
7. Mesquita ET, Jorge AJ. Understanding Asymptomatic Diastolic Dysfunction in Clinical Practice. Arq Bras Cardiol. 2013;100(1):94-101. doi: 10.1590/s0066-782x2013000100015.
8. Silva TRW, Silva RL, Martins AF, Marques JLB. Role of Strain in the Early Diagnosis of Diabetic Cardiomyopathy. Arq Bras Cardiol: Imagem Cardiovasc. 2022;35(2):eabc293. doi:10.47593/2675-312X/20223502eabc293.
9. McDonagh TA, Metra M, Adamo M, Gardner RS, Baumbach A, Böhm M, et al. 2023 Focused Update of the 2021 ESC Guidelines for the Diagnosis and Treatment of Acute and Chronic Heart Failure. Eur Heart J. 2023;44(37):3627-39. doi: 10.1093/eurheartj/ehad195.
10. Lang RM, Badano LP, Mor-Avi V, Afilalo J, Armstrong A, Ernande L, et al. Recommendations for Cardiac Chamber Quantification by Echocardiography in Adults: An Update from the American Society of Echocardiography and the European Association of Cardiovascular Imaging. J Am Soc Echocardiogr. 2015;28(1):1-39.e14. doi: 10.1016/j.echo.2014.10.003.
11. Wong TY, Sun J, Kawasaki R, Ruamviboonsuk P, Gupta N, Lansingh VC, et al. Guidelines on Diabetic Eye Care: The International Council of Ophthalmology Recommendations for Screening, Follow-up, Referral, and Treatment Based on Resource Settings. Ophthalmology. 2018;125(10):1608-22. doi: 10.1016/j.ophtha.2018.04.007.
12. Stratton IM, Adler AI, Neil HA, Matthews DR, Manley SE, Cull CA, et al. Association of Glycaemia with Macrovascular and Microvascular Complications of Type 2 Diabetes (UKPDS 35): Prospective Observational Study. BMJ. 2000;321(7258):405-12. doi: 10.1136/bmj.321.7258.405.

13. Anker SD, Butler J, Filippatos G, Ferreira JP, Bocchi E, Böhm M, et al. Empagliflozin in Heart Failure with a Preserved Ejection Fraction. N Engl J Med. 2021;385(16):1451-61. doi: 10.1056/NEJMoa2107038.

14. Zinman B, Wanner C, Lachin JM, Fitchett D, Bluhmki E, Hantel S, et al. Empagliflozin, Cardiovascular Outcomes, and Mortality in Type 2 Diabetes. N Engl J Med. 2015;373(22):2117-28. doi: 10.1056/NEJMoa1504720.

15. Neal B, Perkovic V, Matthews DR. Canagliflozin and Cardiovascular and Renal Events in Type 2 Diabetes. N Engl J Med. 2017;377(21):2099. doi: 10.1056/NEJMc1712572.

16. Redfield MM, Borlaug BA. Heart Failure with Preserved Ejection Fraction: A Review. JAMA. 2023;329(10):827-38. doi: 10.1001/jama.2023.2020.

17. Zhao X, Liu S, Wang X, Chen Y, Pang P, Yang Q, et al. Diabetic Cardiomyopathy: Clinical Phenotype and Practice. Front Endocrinol. 2022;13:1032268. doi: 10.3389/fendo.2022.1032268.

18. Hotta VT, Rassi DDC, Pena JLB, Vieira MLC, Rodrigues ACT, Cardoso JN, et al. Critical Analysis and Limitations of the Diagnosis of Heart Failure with Preserved Ejection Fraction (HFpEF). Arq Bras Cardiol. 2022;119(3):470-9. doi: 10.36660/abc.20210052.

19. Karagöz A, Bezgin T, Kutlutürk I, Külahçıoğlu S, Tanboğa IH, Güler A, et al. Subclinical Left Ventricular Systolic Dysfunction in Diabetic Patients and its Association with Retinopathy: A 2D Speckle Tracking Echocardiography Study. Herz. 2015;40(Suppl 3):240-6. doi: 10.1007/s00059-014-4138-6.

20. Mochizuki Y, Tanaka H, Matsumoto K, Sano H, Toki H, Shimoura H, et al. Clinical Features of Subclinical Left Ventricular Systolic Dysfunction in Patients with Diabetes Mellitus. Cardiovasc Diabetol. 2015;14:37. doi: 10.1186/s12933-015-0201-8.

21. Silverii GA, Toncelli L, Casatori L, Bossini R, Nannelli F, Pala L, et al. Assessment of Left Ventricular Global Longitudinal Strain in Patients with Type 2 Diabetes: Relationship with Microvascular Damage and Glycemic Control. Nutr Metab Cardiovasc Dis. 2022;32(4):994-1000. doi: 10.1016/j.numecd.2022.01.014.

Clinical and Echocardiographic Characterization of Patients with ATTR VAL142Ile

Tonnison de Oliveira Silva,[1,2] Tonnison de Oliveira Silva Filho,[3] Lara Tavares Cardoso dos Santos,[1] Maria Luisa Fialho,[1] Gabriel de Souza Santos Pereira,[1] Ellen Beatriz Menezes,[1] Enzo Galeffi Rodrigues,[1] Marcelo Tavares,[4] Marcela Câmara Machado Costa,[1,2] Luiz Eduardo Fonteles Ritt[1,2]

Escola Bahiana de Medicina e Saúde Pública,[1] Salvador, BA – Brazil
Cardio Pulmonary Hospital,[2] Salvador, BA – Brazil
Universidade Federal da Bahia,[3] Salvador, BA – Brazil
Universidade Federal da Paraíba,[4] João Pessoa, PB – Brazil

Abstract

Background: **Transthyretin (TTR) amyloid cardiomyopathy associated with the VAL142Ile variant typically presents in patients in their sixth or seventh decades of life. It is among the most common hereditary forms of cardiac amyloidosis. This study aims to characterize the clinical, laboratory, and echocardiographic features observed in patients with the VAL142Ile variant, contributing to a deeper understanding of the phenotypic expression of this genetic variant.**

Method: **Cross-sectional study of 31 patients diagnosed with HF due to transthyretin amyloidosis (ATTR) VAL142Ile. Functional class, presence of atrial fibrillation (AF) and carpal tunnel syndrome (CTS), and NT-proBNP value were assessed. Diastolic and systolic dimensions, septum, posterior wall (PW), left atrial volume, ejection fraction (EF), diastolic function and global longitudinal strain (GLS) were quantified. Statistical analysis was performed using SPSS software version 26.0.**

Results: **Mean age at symptoms onset was 74.3 years (±5.9 years), with 61% being male. A total of 14 (45%) were identified with AF and 17 (55%) with CTS. Regarding New York Heart Association (NYHA) classification, 19 (61%) were in FC II and 8 (25.8%) in FC III. Measurements were diastolic diameter (DD) of 50.6 mm (±8.5), systolic diameter (SD) of 35.2 mm (±7.8), pw = 13.5 mm (±2.1) and ivs = 14.8 mm (±2.4). The left atrial volume was 54.3 mL/m² (±12) and the EF was 47.3% (±15.1). A total of 8 (25%) underwent strain echocardiography, and 7 (87.5%) showed apical sparing. Diastolic dysfunction grade II was observed in 8 (47%), and 14 (45%) had AF. The mean NT-proBNP was 3026 pg/mL (±1941 pg/mL).**

Conclusion: **Our findings underscore the importance of characterizing this population, highlighting the potential for early disease onset even with the VAL142Ile variant. Elevated NT-proBNP levels, along with the presence of AF and CTS, further elucidate the phenotypic patterns of patients with the ATTR VAL142Ile variant.**

Keywords: **Cardiac amyloidosis due to transthyretin, genetic variant Val142Ile, heart failure.**

Introduction

Transthyretin amyloidosis (ATTR) is an infiltrative, progressive, and often underdiagnosed disease caused by amyloid protein deposits in tissues, primarily affecting the heart and resulting in cardiomyopathy, heart failure, and arrhythmias.[1,2] There are two forms of ATTR: the hereditary form, caused by variants in the transthyretin (TTR) gene, and the wild-type form, which occurs independently of genetic mutations. The VAL142Ile genetic variant is prevalent in individuals of African descent, affecting up to 3.4% of this population, with a higher incidence in the elderly. In the United States, this condition accounts for up to 10% of heart failure cases among African Americans over age 65.[3] Amyloid cardiomyopathy associated with VAL142Ile generally appears in the sixth or seventh decades of life and is a leading hereditary form of cardiac amyloidosis,[3] clinically characterized by increased ventricular mass, heart failure symptoms, and arrhythmias. The slow progression of the disease and nonspecific symptoms make early diagnosis challenging, resulting in a high mortality rate when not treated appropriately.[1-4]

This study seeks to enhance the understanding of the clinical, laboratory, and echocardiographic profiles of patients with the VAL142Ile genetic variant, broadening our insight into its phenotypic manifestations (Central Illustration).

Mailing Address: Tonnison de Oliveira Silva •
Escola Bahiana de Medicina e Saúde Publica. Rua Dom João VI. Postal Code: 40285-001. Brotas, Salvador, BA – Brazil
E-mail: tonnisonsilva@hotmail.com
Manuscript received November 1, 2024; revised November 5, 2024; accepted November 5, 2024
Editor responsible for the review: Marcelo Tavares

DOI: https://doi.org/10.36660/abcimg.20240116i

Central Illustration: Clinical and Echocardiographic Characterization of Patients with ATTR VAL142Ile

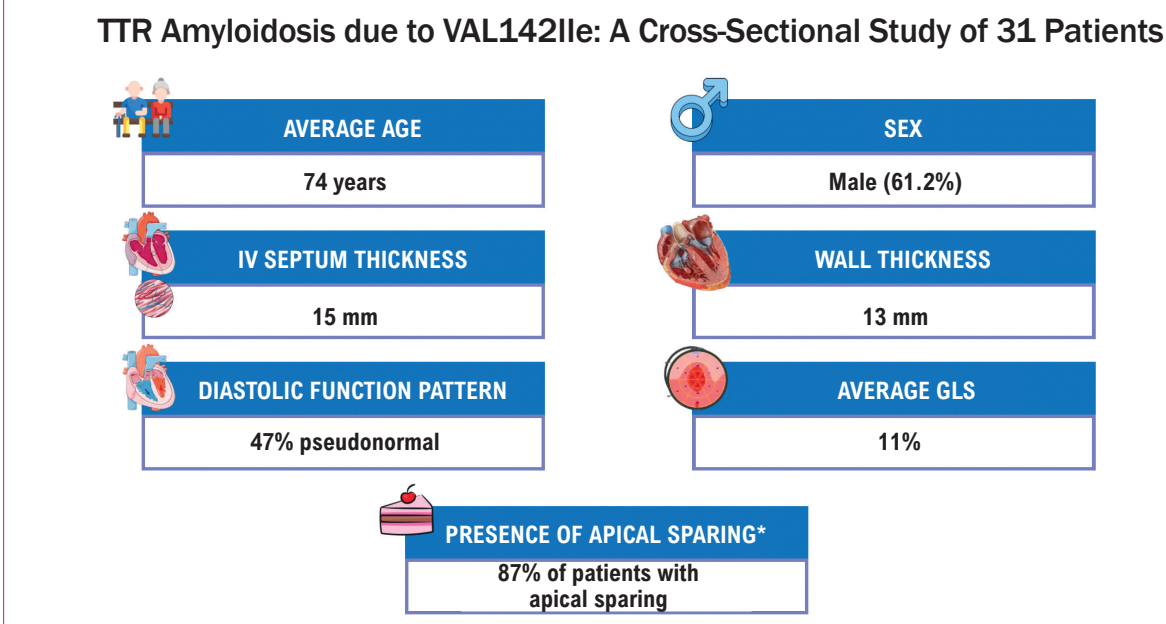

Arq Bras Cardiol: Imagem cardiovasc. 2025;38(1):e20240116

TTR: Transthyretin; GLS: global longitudinal strain.

Notably, limited data are available in the medical literature, specifically addressing this increasingly prevalent variant in our population.

Methods

This is a cross-sectional, retrospective cohort study conducted at the Teaching-Care Outpatient Clinic of the Bahiana School of Medicine and Public Health (Salvador, Bahia). Data collection was conducted from February 2023 to September 2024 and included 31 patients diagnosed with VAL142Ile-associated cardiac amyloidosis. Diagnoses were based on clinical suspicion and confirmed by 12-lead electrocardiograms (ECG), echocardiography, cardiac resonance imaging, pyrophosphate scintigraphy, and genetic testing, in line with the latest diagnostic guidelines.[5-9] Exclusion criteria included patients with light chain (AL) amyloidosis. Clinical data collected included age, sex, New York Heart Association (NYHA) functional class, presence of atrial fibrillation (AF), and history of carpal tunnel syndrome (CTS). The age at symptoms onset was defined as the first event related to heart failure (signs and symptoms of HF, hospitalization due to HF, or emergency room visit due to congestive symptoms). NT-proBNP levels were measured as a prognostic marker and indicator of hemodynamic overload. The cutoff value of 3000 pg/mL was used as an indicator of severe ventricular dysfunction[1] (Table 1).

Echocardiographic measurements, including ejection fraction (EF), diastolic diameter (DD), systolic diameter (SD), septal thickness (S), and posterior wall thickness (PW), were calculated according to recommendations from the American Society of Echocardiography (ASE). Global longitudinal strain (GLS) was assessed per the Brazilian Society of Cardiology's Position Statement on Myocardial Deformation Imaging.[10] Apical sparing was identified in patients with preserved strain in the apical region compared to the basal and mid-myocardial areas.[11,12] Diastolic dysfunction was classified based on mitral flow and tissue Doppler criteria, with particular attention to the E/e' ratio, peak mitral annular velocity, and transmitral filling patterns (Table 2).

Statistical Analysis

Statistical analysis was performed using SPSS software version 26.0. Continuous variables, such as age at onset of symptoms, EF, GLS, and NT-proBNP levels, were described using mean, median, and standard deviation. Absolute and percentage frequencies were calculated for categorical variables, such as NYHA functional class, presence of AF, and CTS.

Results

Analysis of a sample of 31 patients diagnosed with VAL142Ile cardiac amyloidosis showed an average age of symptom onset at 74.3 years (±5.9 years), with males comprising approximately 68% of the sample. Among the patients studied, 14 (45%) had AF, and 17 (55%) reported a

Table 1 – Clinical characteristics of patients diagnosed with cardiac amyloidosis

Patient	Sex	Age at onset of symptoms	Functional class (NYHA)	CTS	AF	NT-proBNP
1	Male	72	II	Yes	No	Not performed
2	Male	70	III	No	No	Not performed
3	Female	77	II	No	No	Not performed
4	Male	74	II	No	Yes	Not performed
5	Male	78	III	No	No	Not performed
6	Female	74	II	No	Yes	Not performed
7	Female	76	II	No	No	Not performed
8	Male	70	II	No	No	Not performed
9	Male	78	III	Yes	No	Not performed
10	Male	66	II	Yes	No	2460 pg/mL
11	Male	71	I	Yes	Yes	Not performed
12	Male	79	III	Yes	Yes	3600 pg/mL
13	Male	79	II	No	No	Not performed
14	Female	81	III	No	Yes	Not performed
15	Male	72	II	Yes	Yes	Not performed
16	Female	81	II	No	No	Not performed
17	Female	72	II	Yes	Yes	3900 pg/mL
18	Female	75	III	No	Yes	4332 pg/mL
19	Female	79	II	Yes	No	650 pg/mL
20	Male	80	II	Yes	Yes	Not performed
21	Female	78	I	Yes	No	450 pg/mL
22	Male	69	II	No	No	1940 pg/mL
23	Female	74	III	Yes	Yes	4250 pg/mL
24	Male	69	IV	Yes	Yes	3900 pg/mL
25	Male	70	II	No	No	Not performed
26	Female	87	I	Yes	No	3100 pg/mL
27	Male	78	II	Yes	No	3747 pg/mL
28	Male	56	III	Yes	Yes	6471 pg/mL
29	Male	71	II	Yes	No	1400 pg/mL
30	Male	74	III	Yes	Yes	3203 pg/mL
31	Female	75	II	No	Yes	2000 pg/mL

CTS: Carpal Tunnel Syndrome; AF: Atrial fibrillation; NYHA: New York Heart Association.

history of CTS. Regarding functional class, 19 patients (61%) were in NYHA FC II, 8 (25.8%) in FC III, 3 (9.7%) in FC I, and 1 (3.2%) in FC IV. Mean measurements for left ventricular structure included a DD of 50.6 mm (±8.5), a SD of 35.2 mm (±7.8), a PW thickness of 13.5 mm (±2.1), and an interventricular septum thickness of 14.8 mm (±2.4). The mean left atrial volume indexed by body surface area was 54.3 mL/m² (±12) and the EF was 47.3% (±15.1). Of the 31 participants, 8 (25%) underwent echocardiography with assessment of ventricular deformation and of these, 7 (87.5%) had apical sparing visualized on echocardiography. Diastolic dysfunction was observed in 17 (55%) of the participants, with grades I (changed relaxation), II (pseudonormal) and III (restrictive), respectively in 3 (18%), 8 (47%), and 6 (35%) patients. Fourteen (45%) of the total 31 had a diagnosis of AF, and it was not possible to assess the left ventricular filling

Table 2 – Echocardiographic data of patients diagnosed with cardiac amyloidosis

Patient	EF	S	PW	DD	SD	Left Atrial Volume	Diastolic Function Pattern	Apical Sparing	GLS
1	60%	12	12	40	21	44 mL/m²	Pseudonormal	Present	14%
2	20%	18	16	60	54	64 mL/m²	Restrictive	N/A	N/A
3	48%	14	13	48	36	48 mL/m²	Pseudonormal	N/A	N/A
4	30%	14	14	59	50	64 mL/m²	N/A	N/A	N/A
5	27%	14	13	62	54	55 mL/m²	N/A	N/A	N/A
6	26%	12	12	50	44	52 mL/m²	N/A	N/A	N/A
7	33%	16	16	42	43	50 mL/m²	Restrictive	N/A	N/A
8	40%	16	16	48	33	42 mL/m²	Restrictive	N/A	N/A
9	38%	14	13	54	44	60 mL/m²	Restrictive	N/A	N/A
10	56%	14	15	54	38	26 mL/m²	Relaxation Alteration	N/A	N/A
11	60%	14	15	40	27	42 mL/m²	N/A	N/A	N/A
12	42%	17	14	45	37	50 mL/m²	N/A	Present	12%
13	68%	15	15	55	34	42 mL/m²	Relaxation Alteration	N/A	N/A
14	52%	14	12	55	40	47 mL/m²	N/A	N/A	N/A
15	41%	16	13	51	36	46 mL/m²	N/A	Present	8%
16	48%	11	11	52	40	42 mL/m²	Restrictive	N/A	N/A
17	56%	13	12	48	34	62 mL/m²	N/A	Present	10%
18	47%	22	18	46	35	71 mL/m²	N/A	Present	12%
19	62%	15	14	50	33	40 mL/m²	Pseudonormal	N/A	N/A
20	62%	15	15	50	32	80 mL/m²	N/A	N/A	N/A
21	80%	13	13	39	20	45 mL/m²	Pseudonormal	N/A	N/A
22	41%	18	12	43	39	52 mL/m²	Pseudonormal	Present	10%
23	55%	16	15	41	27	46 mL/m²	N/A	N/A	N/A
24	30%	19	18	64	55	84 mL/m²	N/A	N/A	N/A
25	50%	12	13	48	36	38 mL/m²	Pseudonormal	N/A	N/A
26	52%	14	14	49	36	50 mL/m²	Pseudonormal	Present	12%
27	60%	13	10	53	36	64 mL/m²	Relaxation Alteration	N/A	N/A
28	14%	11	11	68	64	50 mL/m²	N/A	Absent	7.2%
29	57%	16	15	40	28	54 mL/m²	Restrictive	N/A	N/A
30	46%	16	12	45	30	74 mL/m²	N/A	N/A	N/A
31	65%	12	12	48	31	40 mL/m²	N/A	N/A	N/A

EF: Ejection Fraction; S: Septum; PW: Posterior Wall; DD: Diastolic Diameter; GLS: Global Longitudinal Strain, SD: systolic diameter; N/A: doesn't apply.

pattern. NT-proBNP levels varied between patients, with an average of 3026 pg/mL (±1941 pg/mL) (Table 3).

Discussion

The findings of this sample reveal characteristics consistent with the findings in the literature on ATTR associated with the VAL142Ile variant.[3,4] The mean age of 74.3 years at symptoms onset and male predominance align with previous studies demonstrating a late manifestation and a greater impact on the male sex.[3,4] The patient in this cohort who presented the latest onset of HF symptoms was 87 years old, while the youngest developed heart failure due to TTR amyloidosis at the age of 56. This patient was homozygous for the TTR genetic variant, a condition that appears to have caused this pathology to manifest earlier.[3] The history

Table 3 – Results of clinical and echocardiographic evaluation

Variables	Mean	N (%)	Standard deviation
Male		19 (61%)	
Age	74.3 years		±5.9 years
Functional Class (NYHA)			
I		3 (9.7%)	
II		19 (61%)	
III		8 (25.8%)	
IV		1 (3.2%)	
DD	50.6 mm		±8.5 mm
SD	35.2 mm		±7.8 mm
Septum	14.8 mm		±2.4 mm
PW	13.5 mm		± 2.1 mm
EF	47.3%		±15.1%
Atrial volume	54.3 mL/m²		±12mL/m²
GLS	11%		
Apical sparing		7 (87.5%)	
CTS		17 (55%)	
AF		14 (45%)	
NT-proBNP	3026 pg/mL		±1941 pg/mL

GLS: Global Longitudinal Strain; N: Sample Number; CTS: carpal tunnel syndrome; EF: ejection fraction; AF: atrial fibrillation; NYHA: New York Heart Association; DD: diastolic diameter; SD: systolic diameter; PW: posterior wall.

of CTS in 55% of patients reinforces the association of TTR deposits in tendons and peripheral nerves, a marker that aids in the early diagnosis of the disease.[1,2,4,5] The mean EF was 47.3%, indicating a left ventricular systolic function impairment, which is usually seen in more advanced stages of this restrictive cardiomyopathy.[1,2,4,5] The increased thickness of the PW and interventricular septum reflect the deposition of amyloid in the interstitial space, with increased ventricular mass, diastolic dysfunction, and subsequent systolic dysfunction. In this study, diastolic dysfunction was prevalent, with most patients displaying grade II or higher dysfunction. This finding is expected regardless of the type of TTR-related genetic variant since amyloid infiltration in the myocardium causes ventricular stiffness and progressive impairment of diastolic function and HFpEF.[1,2,5] The reduced GLS value associated with apical sparing in approximately 87% of cases highlights the importance of GLS assessment in the diagnostic flow of patients with suspected ATTR. The presence of concentric left ventricular hypertrophy, atrial dilation, and the apical sparing pattern provides an echocardiographic profile that aids in distinguishing ATTR from other cardiomyopathies, such as hypertensive or hypertrophic types.[10-12] In this study, patients with NT-proBNP levels exceeding 3000 pg/mL showed lower GLS and more severe diastolic dysfunction, reflecting a higher degree of cardiac impairment. This finding aligns with previous studies that identified similar cutoff values for risk stratification in CA.[1] The AF (45%) among patients is consistent with other studies, which point to an association between amyloidosis and atrial arrhythmias.[1-4]

Although this study provides valuable information on the clinical manifestation of cardiac amyloidosis associated with the VAL142Ile variant, there are some limitations. The sample size was relatively small, and the lack of longitudinal follow-up prevents the evaluation of the temporal progression of clinical and echocardiographic markers. Additionally, underutilization of myocardial strain due to limited echocardiographic windows and availability may have affected the accuracy of GLS values and apical sparing detection in this subgroup with the VAL142Ile variant.

Conclusion

In conclusion, this study emphasizes the importance of characterizing this population and the potential for early onset, even in VAL142Ile variant cases. Furthermore, findings such as increased ventricular wall thickness, significant atrial dilation, reduced EF, and markedly low GLS (11%) indicate a late-stage diagnosis, a known marker of poor prognosis. High NT-proBNP levels, along with the presence of AF and CTS in a substantial proportion of patients, contribute to our understanding of the phenotypic patterns in patients with ATTR VAL142Ile.

Author Contributions

Conception and design of the research: Silva TO, Silva Filho TO, Tavares M, Ritt LEF; acquisition of data: Silva TO, Santos LTC, Fialho ML, Pereira GSS, Menezes EB, Rodrigues EG; analysis and interpretation of the data: Silva TO, Ritt LEF;

Statistical analysis: Silva TO; writing of the manuscript: Silva TO, Silva Filho TO, Santos LTC; critical revision of the manuscript for intellectual content: Silva TO, Tavares M, Machado MC, Ritt LEF.

Potential Conflict of Interest

No potential conflict of interest relevant to this article was reported.

Sources of Funding

There were no external funding sources for this study.

Study Association

This study is not associated with any thesis or dissertation work.

Ethics Approval and Consent to Participate

This study was approved by the Ethics Committee of the Escola Bahiana de Medicina e Saúde Pública under the protocol number 743825235.0000.5544. All the procedures in this study were in accordance with the 1975 Helsinki Declaration, updated in 2013. Informed consent was obtained from all participants included in the study.

References

1. Garcia-Pavia P, Bengel F, Brito D, Damy T, Duca F, Dorbala S, et al. Expert Consensus on the Monitoring of Transthyretin Amyloid Cardiomyopathy. Eur J Heart Fail. 2021;23(6):895-905. doi: 10.1002/ejhf.2198.
2. Kottam A, Hanneman K, Schenone A, Daubert MA, Sidhu GD, Gropler RJ, et al. State-of-the-art Imaging of Infiltrative Cardiomyopathies: A Scientific Statement from the American Heart Association. Circ Cardiovasc Imaging. 2023;16(11):e000081. doi: 10.1161/HCI.0000000000000081.
3. Chandrashekar P, Alhuneafat L, Mannello M, Al-Rashdan L, Kim MM, Dungu J, et al. Prevalence and Outcomes of p.Val142Ile TTR Amyloidosis Cardiomyopathy: A Systematic Review. Circ Genom Precis Med. 2021;14(5):e003356. doi: 10.1161/CIRCGEN.121.003356.
4. Ruberg FL, Grogan M, Hanna M, Kelly JW, Maurer MS. Transthyretin Amyloid Cardiomyopathy: JACC State-of-the-art Review. J Am Coll Cardiol. 2019;73(22):2872-91. doi: 10.1016/j.jacc.2019.04.003.
5. Simões MV, Fernandes F, Marcondes-Braga FG, Scheinberg P, Correia EB, Rohde LEP, et al. Position Statement on Diagnosis and Treatment of Cardiac Amyloidosis - 2021. Arq Bras Cardiol. 2021;117(3):561-98. doi: 10.36660/abc.20210718.
6. Dorbala S, Ando Y, Bokhari S, Dispenzieri A, Falk RH, Ferrari VA, et al. ASNC/AHA/ASE/EANM/HFSA/ISA/SCMR/SNMMI Expert Consensus Recommendations for Multimodality Imaging in Cardiac Amyloidosis: Part 1 of 2-Evidence Base and Standardized Methods of Imaging. J Nucl Cardiol. 2019;26(6):2065-123. doi: 10.1007/s12350-019-01760-6.
7. Dorbala S, Ando Y, Bokhari S, Dispenzieri A, Falk RH, Ferrari VA, et al. ASNC/AHA/ASE/EANM/HFSA/ISA/SCMR/SNMMI Expert Consensus Recommendations for Multimodality Imaging in Cardiac Amyloidosis: Part 2 of 2-Diagnostic Criteria and Appropriate Utilization. J Card Fail. 2019;25(11):854-65. doi: 10.1016/j.cardfail.2019.08.002.
8. Singh V, Falk R, Di Carli MF, Kijewski M, Rapezzi C, Dorbala S. State-of-the-art Radionuclide Imaging in Cardiac Transthyretin Amyloidosis. J Nucl Cardiol. 2019;26(1):158-73. doi: 10.1007/s12350-018-01552-4.
9. Gillmore JD, Maurer MS, Falk RH, Merlini G, Damy T, Dispenzieri A, et al. Nonbiopsy Diagnosis of Cardiac Transthyretin Amyloidosis. Circulation. 2016;133(24):2404-12. doi: 10.1161/CIRCULATIONAHA.116.021612.
10. Almeida ALC, Melo MDT, Bihan DCSL, Vieira MLC, Pena JLB, Del Castillo JM, et al. Position Statement on the Use of Myocardial Strain in Cardiology Routines by the Brazilian Society of Cardiology's Department Of Cardiovascular Imaging - 2023. Arq Bras Cardiol. 2023;120(12):e20230646. doi: 10.36660/abc.20230646.
11. Phelan D, Collier P, Thavendiranathan P, Popović ZB, Hanna M, Plana JC, et al. Relative Apical Sparing of Longitudinal Strain Using Two-dimensional Speckle-tracking Echocardiography is Both Sensitive and Specific for the Diagnosis of Cardiac Amyloidosis. Heart. 2012;98(19):1442-8. doi: 10.1136/heartjnl-2012-302353.
12. Pagourelias ED, Mirea O, Duchenne J, Van Cleemput J, Delforge M, Bogaert J, et al. Echo Parameters for Differential Diagnosis in Cardiac Amyloidosis: A Head-to-head Comparison of Deformation and Nondeformation Parameters. Circ Cardiovasc Imaging. 2017;10(3):e005588. doi: 10.1161/CIRCIMAGING.116.005588.

Original Article

First Percutaneous Orthotopic Tricuspid Valve Implantations using the LuX-Valve Plus Device in Latin America: Report of the First Three Cases

Fernanda Esteves,[1,2] Vinícius Esteves,[3] Marcio Mendes Pereira,[4] Frederico José Neves Mancuso,[2,5] Marden Tebet,[1,2,6] Sergio Kreimer,[1,2,6] Edmur Carlos de Araújo,[7] Francisco Monteiro de Almeida Magalhães[1]

Hospital Vila Nova Star,[1] São Paulo, SP – Brazil
Hospital e Maternidade São Luiz,[2] São Paulo, SP – Brazil
Rede D'Or,[3] São Paulo, SP – Brazil
UDI Hospital,[4] São Luis, MA – Brazil
Universidade Federal de São Paulo,[5] São Paulo, SP – Brazil
Hospital e Maternidade Brasil,[6] Santo André, SP – Brazil
Hospital do Coração do Brasil,[7] Brasília, DF – Brazil

Abstract

Background: Severe tricuspid regurgitation (TR) is associated with high morbidity and mortality, especially in patients with contraindications for surgery. Transcatheter tricuspid valve replacement has emerged as a minimally invasive alternative for this population, with the LuX-Valve Plus device designed for orthotopic implantation via the transjugular route.

Objective: To report the first 3 cases of transcatheter tricuspid valve replacement using the LuX-Valve Plus device in Latin America, assessing the feasibility, safety, and immediate clinical outcomes.

Methods: The study included 3 female patients with torrential TR and high surgical risk. Pre-procedure assessment included transesophageal echocardiography, 3-dimensional transthoracic echocardiography (3D TEE), computed tomography, and cardiac catheterization. The procedure was performed via transjugular access, under general anesthesia, with 3D TEE and fluoroscopy guidance. Implant efficacy was assessed as resolution of TR, transprosthetic gradient, and post-procedure complications.

Results: The implants were successful in all cases, with complete resolution of TR, absence of paravalvular leaks, and adequate transprosthetic gradient. Right ventricular function was preserved, and all patients were discharged 3 to 4 days after the procedure with no significant complications.

Conclusion: Transcatheter tricuspid valve replacement using the LuX-Valve Plus was shown to be a viable and safe alternative for patients with severe TR and high surgical risk. The use of 3D TEE was essential to the planning and execution of the implant. Further studies are needed to assess durability and long-term clinical outcomes.

Keywords: Tricuspid Valve; Tricuspid Valve Insufficiency; Transcatheter Aortic Valve Replacement; Transesophageal Echocardiography.

Introduction

Tricuspid regurgitation (TR) is frequently functional, resulting from dilation of the tricuspid annulus in conditions such as valvular heart disease, cardiomyopathy, and pulmonary hypertension. Primary cases may be associated with rheumatic disease or post-surgical complications. When severe and untreated, TR leads to right ventricular dysfunction, worsening prognosis and increasing morbidity and mortality.[1] Tricuspid valve replacement surgery is characterized by high risk in patients with comorbidities, such as right heart failure and pulmonary hypertension. Transcatheter replacement has emerged as a promising alternative, but there are still challenges related to the complex anatomical characteristics of the tricuspid valve.[2]

The LuX-Valve Plus device (Figure 1) is a self-expandable prosthesis implanted via a transjugular approach that was designed to overcome these limitations. This article reports the first 3 cases of transcatheter tricuspid valve replacement using the LuX-Valve Plus in Latin America, assessing the feasibility, safety, and immediate clinical outcomes.[3]

Methods

Three female patients with torrential TR were treated. Two had atrial functional TR, and the third had mixed

Mailing Address: Marcio Mendes Pereira •
UDI Hospital. AV. Prof. Carlos Cunha, 2000. Postal Code: 65076-820. Jaracti, São Luis, MA – Brazil
E-mail: marciomp50@hotmail.com
Manuscript received December 3, 2024; revised February 16, 2025; accepted February 17, 2025
Editor responsible for the review: Marcelo Tavares

DOI: https://doi.org/10.36660/abcimg.20240124i

Central Illustration: First Percutaneous Orthotopic Tricuspid Valve Implantations using the LuX-Valve Plus Device in Latin America: Report of the First Three Cases

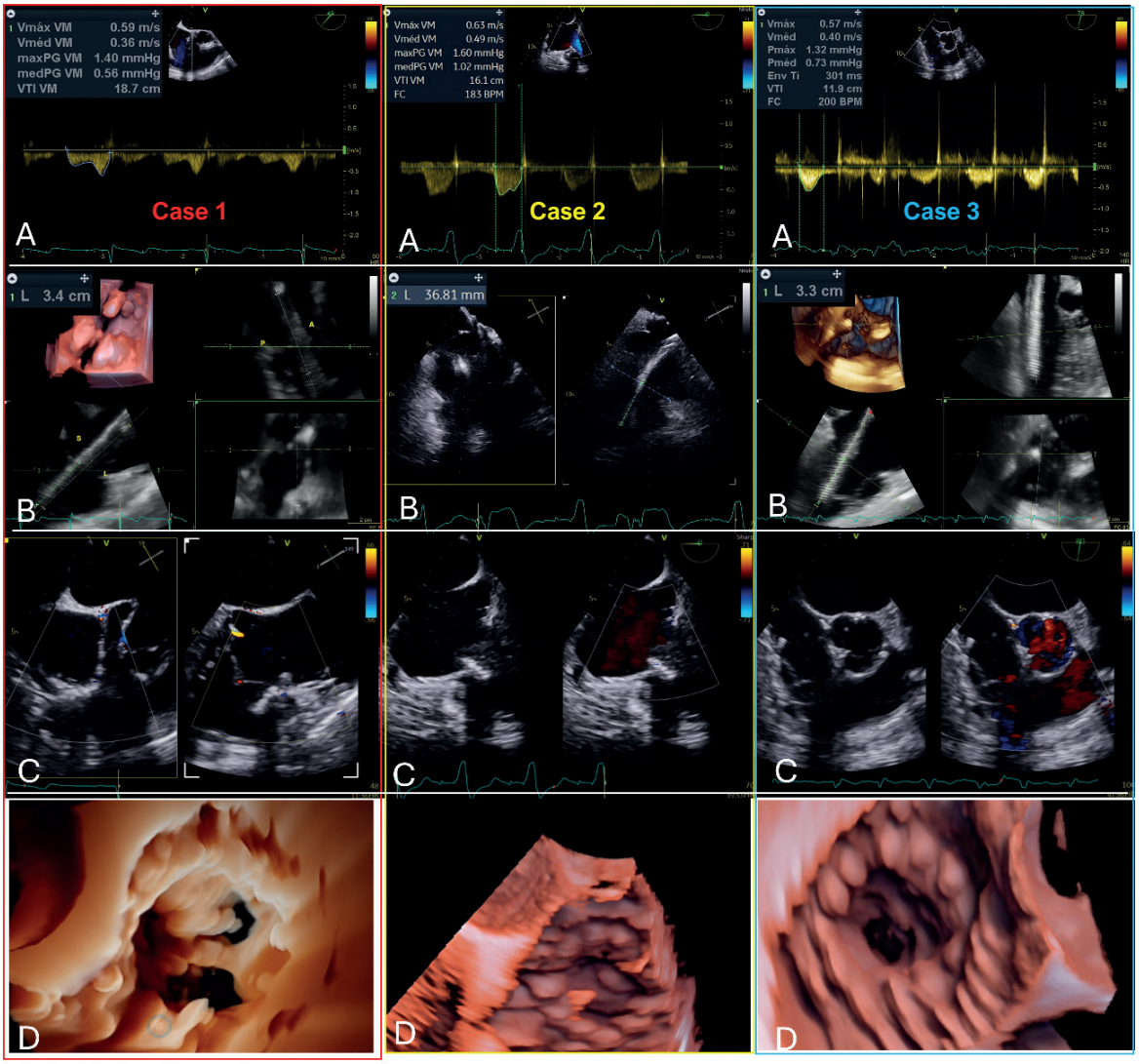

Arq Bras Cardiol: Imagem cardiovasc. 2025;38(1):e20240124

Echocardiographic assessment after LuX-Valve Plus implantation in the 3 cases, illustrating the following: (A) the mean gradient, (B) the positioning of the delivery system, (C) the resolution of TR, and (D) 3-dimensional reconstructions of the implanted valve, demonstrating the efficacy of the transcatheter approach.

etiology related to mitral prosthesis and pacemaker leads. All patients had a history of decompensated heart failure, with predominance of systemic congestive symptoms.

The decision for transcatheter treatment was based on high surgical risk and favorable anatomy. Assessment included transthoracic and transesophageal echocardiography, computed tomography, and right chamber catheterization, allowing for detailed planning. Three-dimensional transesophageal echocardiography (3D TEE) was essential for analysis of regurgitation, valve anatomy, and right ventricular function.

Transcatheter procedure

Procedures were performed via transjugular access, under general anesthesia, with 3D TEE and fluoroscopy guidance. Critical steps included the following:

1. Positioning of the delivery system in the right atrium (Figure 2).
2. Centering and coaxiality in the tricuspid annulus (Figure 3).
3. Implantation and anchoring of the device in the interventricular septum (Figures 4 and 5).

4. Final assessment to rule out paravalvular leaks and obstructions (Figures 6 and 7).

Prosthesis sizes ranged from 30/50 mm, 30/55 mm, and 30/45 mm, adjusted to tricuspid anatomy. Intraoperative echocardiographic monitoring was crucial for successful implantation and rapid patient recovery.

Results

All 3 transcatheter tricuspid valve replacement procedures with the LuX-Valve Plus device were conducted successfully, by means of transjugular access with 3D TEE and fluoroscopy guidance. Implantation was performed without significant complications, with appropriate prosthesis positioning in all cases.

Following the procedure, complete resolution of TR was observed in all 3 patients, accompanied by preserved right ventricular function. The mean transvalvular gradient remained within physiological limits, with no evidence of relevant stenosis. Moreover, the patients showed rapid clinical recovery, without requiring hemodynamic support and no serious complications during the initial follow-up period.

Echocardiographic analysis demonstrated adequate adaptation of the prosthesis to the tricuspid annulus, without signs of displacement or valve dysfunction. These findings reinforce the safety and efficacy of the minimally invasive approach using the LuX-Valve Plus device in patients with high surgical risk (Central Illustration).

Discussion

Severe TR, previously considered of minor clinical relevance, has been associated with worse cardiovascular outcomes, including right ventricular dysfunction and increased morbidity and mortality. Multiple recent studies have demonstrated that the severity of TR is directly correlated with worse clinical outcomes, regardless of other parameters, such as pulmonary artery pressure and left ventricular ejection fraction.[4] Moreover, a large retrospective study found that even mild TR is associated with significantly worse clinical outcomes compared with the absence of any trace of regurgitation, reinforcing the need for early and effective therapeutic approaches.[5,6]

Transcatheter approaches, such as the LuX-Valve Plus, represent an important advance in cardiovascular medicine, offering new therapeutic perspectives for a challenging condition, with a substantial impact on patient quality of life and morbidity. Although conventional treatment, which includes medical therapy and open surgery, has shown limited benefits in many cases, transcatheter alternatives, such as implantation of tricuspid valve repair devices, have emerged as promising options, promoting a minimally invasive approach. These interventions have the potential to significantly expand therapeutic options for patients with refractory TR, especially those who are not ideal candidates for traditional surgery.[2,7,8]

A recent study including 76 patients undergoing LuX-Valve Plus implantation observed a significant reduction in TR to ≤ 2+ in 94.7% of cases and ≤ 1+ in 90.8%, with sustained results after 1 month. In-hospital mortality was 5.3%, and major events were infrequent, demonstrating the safety and efficacy of the transcatheter approach, even in complex anatomies.[9]

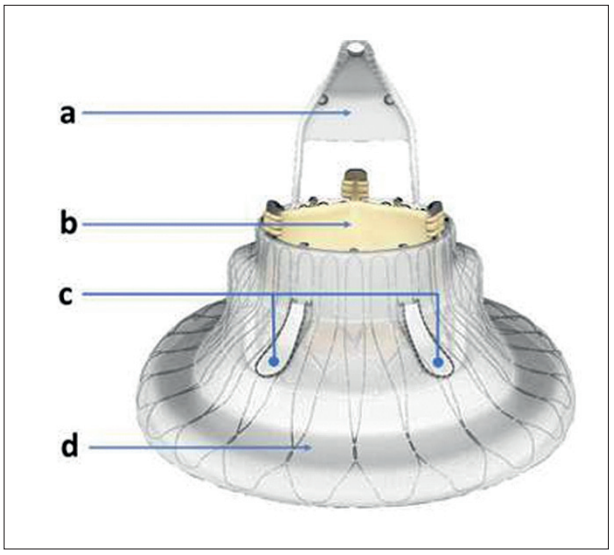

Figure 1 – *The LuX-Valve Plus device: (a) bird tongue-shaped ventricular septal anchor; (b) bovine pericardial prosthetic valve; (c) leaflet graspers; (d) a self-expanding nitinol valve stent consisting of an atrial disc.*

In this report, the device demonstrated safety and efficacy, with positive immediate outcomes, standing out as a promising option for the management of TR. The use of 3D TEE was essential to planning and execution, allowing detailed visualization of the tricuspid annulus and accurate guidance of the delivery system.

Compared to existing transcatheter alternatives, the LuX-Valve Plus offers benefits due to its anatomical adaptation and post-implant stability; however, long-term studies are needed to evaluate its durability and late clinical outcomes.

Conclusion

Transcatheter tricuspid valve replacement using the LuX-Valve Plus was shown to be an effective and safe alternative for patients with severe TR and high surgical risk. This pioneering report in Latin America reinforces the role of transcatheter therapies in managing complex valve conditions, highlighting the importance of echocardiography in planning and monitoring these procedures. Further studies are needed to consolidate its clinical application and establish criteria for patient selection.

Author Contributions

Conception and design of the research and acquisition of data: Esteves F, Esteves V, Pereira MM, Araújo EC, Tebet M, Mancuso FJN, Kreimer S, Magalhães FMA; Analysis and interpretation of the data, statistical analysis, writing of the manuscript and critical revision of the manuscript for intelectual content: Esteves F, Esteves V, Pereira MM.

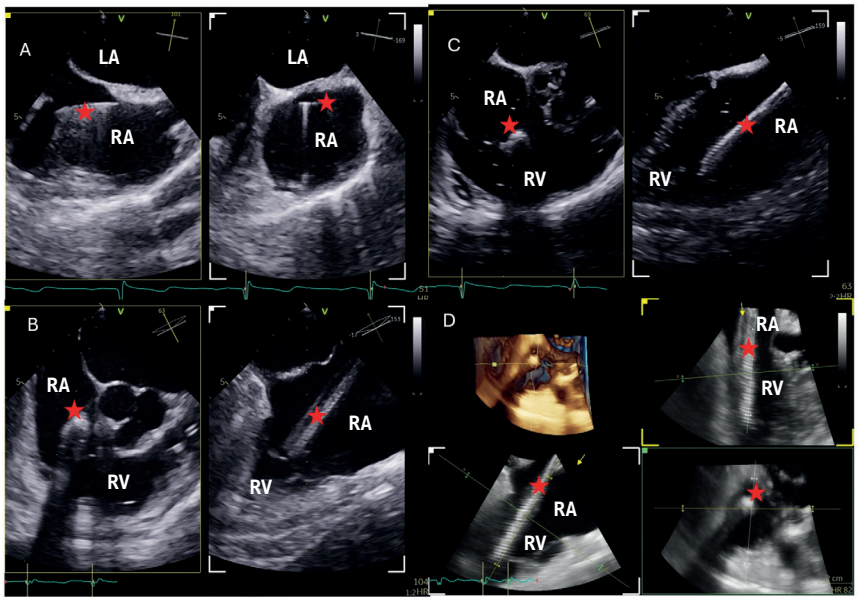

Figure 2 – *Two-dimensional transesophageal echocardiography with biplane images (multi-D or X-plane) based on the short-axis view, showing the process of guiding the delivery system (red star) through the valve and into the right ventricle. (A) The super stiff guidewire advancing into the right atrium (red star). (B) The delivery system has reached the tricuspid valve orifice. (C) The delivery system has crossed the tricuspid valve. (D) After crossing the tricuspid valve, 3-dimensional transesophageal echocardiography imaging with multiplane reconstruction to guide the coaxiality of the delivery system. LA: left atrium; RA: right atrium; RV: right ventricle.*

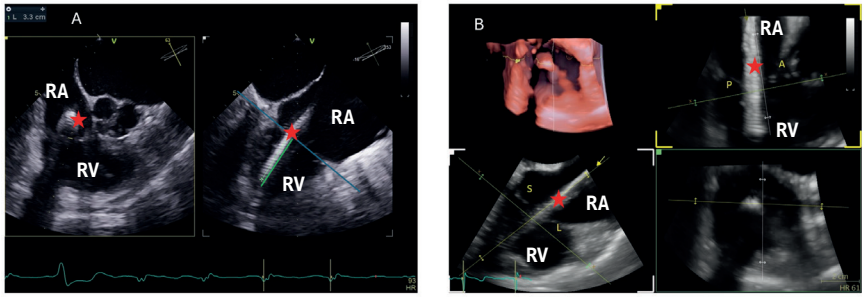

Figure 3 – *(A) Measurement of the insertion depth of the delivery system (red star). The implantation depth is 3.3 cm. (B) After coaxialization, the delivery system was positioned in the central axis of the tricuspid valve, perpendicular to the annular plane. RA: right atrium; RV: right ventricle.*

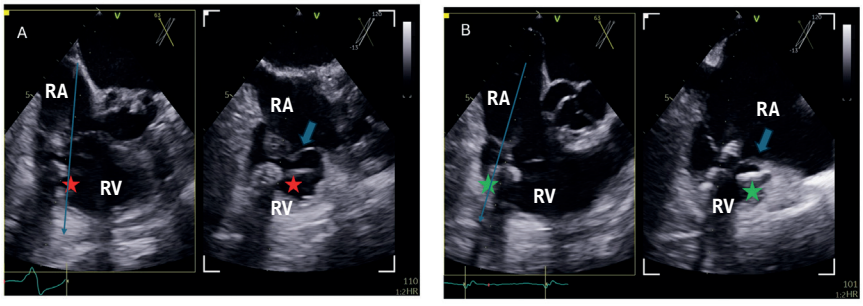

Figure 4 – *Confirmation of leaflet capture by grasper. In the short-axis view, two graspers (red and green stars) can be observed. (A) In the multi-D or X-plane in the RV inflow-outflow view, the sampling cursor is first positioned on the anterior grasper (red star) near the aorta. The grasper can be seen below the anterior tricuspid leaflet (blue arrow) in the corresponding orthogonal plane. (B) In the multi-D or X-plane in the RV inflow-outflow view, the sampling cursor is positioned on the posterior grasper (green star) away from the aorta. The grasper can be seen below the posterior tricuspid leaflet (blue arrow) in the corresponding orthogonal plane. RA: right atrium; RV: right ventricle.*

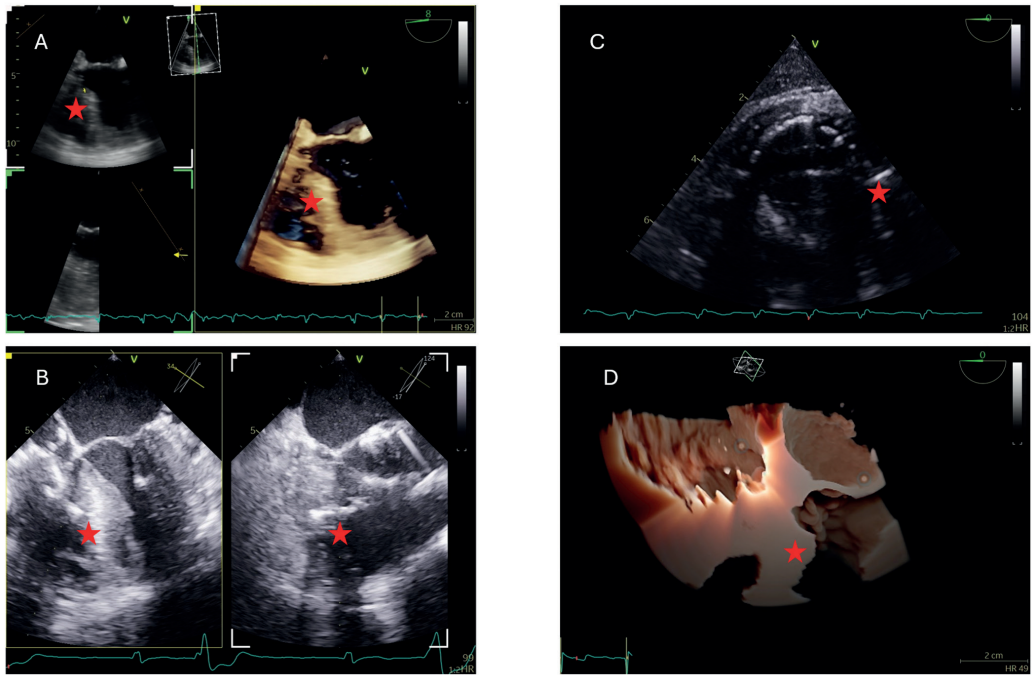

Figure 5 – *Different ways to analyze septal anchoring. (A) Real-time 3-dimensional transesophageal echocardiography imaging, mid-esophageal 4-chamber view, showing septal anchorage (red star). (B) Multi-D or X-plane 4-chamber view of the mid-esophagus. Left: the anchor aligns parallel and attaches to the septum (red star). Right: the anchor attaches to the septum (red star). (C) Short-axis view of the right ventricle through the transgastric window showing septal anchorage (red star). (D) Real-time 3-dimensional transesophageal echocardiography imaging, mid-esophageal 4-chamber view, showing septal anchoring (red star).*

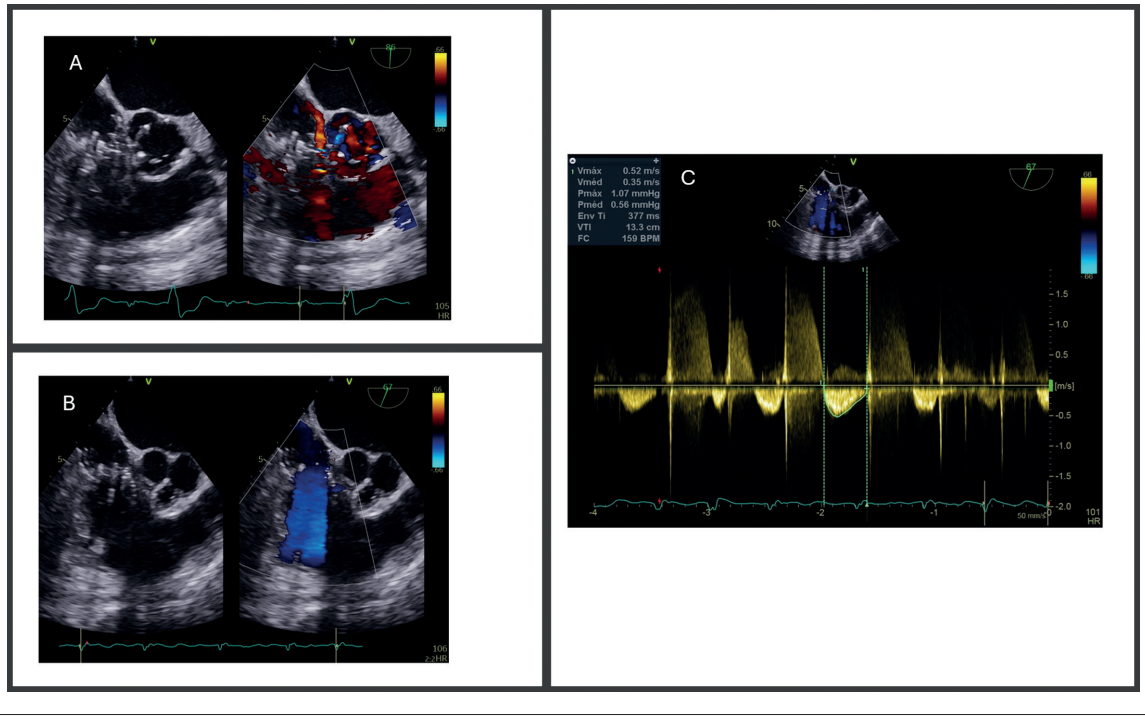

Figure 6 – *Assessment of prosthetic valve function. (A) Determination of the position and degree of paravalvular regurgitation. In the biplane RV inflow-outflow view, a mild paravalvular leak was observed, located in the anterior topography. (B) After fine adjustment and repositioning of the prosthesis, it was possible to correct the paravalvular leak with an excellent final result. (C) Analysis of transprosthetic gradients. RV: right ventricle.*

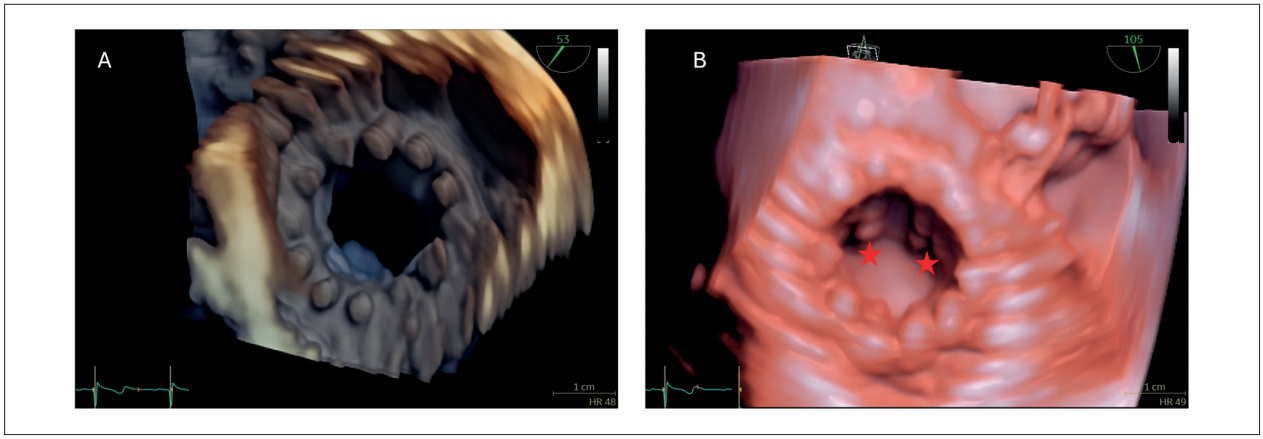

Figure 7 – *Assessment of prosthetic valve function. (A) Three-dimensional imaging of the atrial face of the LuX-Valve Plus, showing the right atrial disc (D-shaped) and stent (the circular structure in the middle). (B) Three-dimensional imaging of the ventricular face of the LuX-Valve Plus, showing 2 graspers, known as "rabbit ears" (red star).*

Potential Conflict of Interest

No potential conflict of interest relevant to this article was reported.

Sources of Funding

There were no external funding sources for this study.

Study Association

This study is not associated with any thesis or dissertation work.

Ethics Approval and Consent to Participate

This article does not contain any studies with human participants or animals performed by any of the authors.

References

1. Tarasoutchi F, Montera MW, Ramos AIO, Sampaio RO, Rosa VEE, Accorsi TAD, et al. Update of the Brazilian Guidelines for Valvular Heart Disease - 2020. Arq Bras Cardiol. 2020;115(4):720-75. doi: 10.36660/abc.20201047.
2. Sun Z, Li H, Zhang Z, Li Y, Zhang L, Xie Y, et al. Twelve-Month Outcomes of the LuX-Valve for Transcatheter Treatment of Severe Tricuspid Regurgitation. EuroIntervention. 2021;17(10):818-26. doi: 10.4244/EIJ-D-21-00095.
3. Esteves V, Andrade PB, Kreimer S, Esteves FA, Magalhães FMA, Modine T. First Performance of Transjugular Transcatheter Tricuspid Valve Replacement with the Lux-Valve Plus System in Latin America. A Case Report. Arq Bras Cardiol. 2024;121(10):e20240201. doi: 10.36660/abc.20240201.
4. Hahn RT, Lawlor MK, Davidson CJ, Badhwar V, Sannino A, Spitzer E, et al. Tricuspid Valve Academic Research Consortium Definitions for Tricuspid Regurgitation and Trial Endpoints. J Am Coll Cardiol. 2023;82(17):1711-35. doi: 10.1016/j.jacc.2023.08.008.
5. Hahn RT, Asch F, Weissman NJ, Grayburn P, Kar S, Lim S, et al. Impact of Tricuspid Regurgitation on Clinical Outcomes: The COAPT Trial. J Am Coll Cardiol. 2020;76(11):1305-14. doi: 10.1016/j.jacc.2020.07.035.
6. Sala A, Hahn RT, Kodali SK, Mack MJ, Maisano F. Tricuspid Valve Regurgitation: Current Understanding and Novel Treatment Options. J Soc Cardiovasc Angiogr Interv. 2023;2(5):101041. doi: 10.1016/j.jscai.2023.101041.
7. Seligman H, Vora AN, Haroian NQ, Puri R, Heng EL, Smith RD, et al. The Current Landscape of Transcatheter Tricuspid Valve Intervention. J Soc Cardiovasc Angiogr Interv. 2023;2(6):101201. doi: 10.1016/j.jscai.2023.101201.
8. Wang Y, Zhai M, Mao Y, Yang T, Zhu G, Liu Y, et al. Transcatheter Tricuspid Valve Replacement for Functional Tricuspid Regurgitation after Left-Sided Valve Surgery: A Single-Center Experience. Catheter Cardiovasc Interv. 2024;103(4):626-36. doi: 10.1002/ccd.30972.
9. Stolz L, Cheung A, Boone R, Fam N, Ong G, Villablanca P, et al. Transjugular Transcatheter Tricuspid Valve Replacement: Early Compassionate Use Outcomes. JACC Cardiovasc Interv. 2024;17(16):1936-45. doi: 10.1016/j.jcin.2024.06.014.

Mitral Annulus Diameter's Relevance in the Diagnosis of Atrial Etiology in Mitral Regurgitation: A Comparative Analysis

Alexandre Costa Souza,[1,2] Bruna de Mattos Ivo Junqueira,[1,2] Stephanie de Azevedo Drubi,[1,2] Laila Caroline Gomes,[1,2] Marcus Vinicius Freire,[1,2] Priscila Pinheiro,[1,2] Alessandra Ghattas Basile,[1,2] Marco André Moraes Sales,[1,2] Ricardo André Sales Pereira Guedes,[1,2] Carolina Thé Macêdo[1,2]

Hospital São Rafael/ Rede DOr,[1] Salvador, BA – Brazil

Instituto D'Or de ensino e pesquisa,[2] Idor, Salvador, BA – Brazil

Abstract

Background: Atrial Functional Mitral Regurgitation (FMR) is defined by mitral annular dilation and functional alterations without structural impairment of the leaflets or subvalvular apparatus. It is associated with higher cardiovascular mortality, being often characterized as an exclusion diagnosis due to the absence of more precise diagnostic criteria. Therefore, it is crucial to identify markers that distinguish it from other Mitral Regurgitation (MR) types.

Objective: To assess the accuracy of the intercommissural diameter of the mitral annulus and its value indexed to body surface area in differentiating atrial etiology in patients with MR.

Methods: This is an observational cross-sectional study with 109 patients diagnosed with moderate or severe MR. Data were obtained between October 2022 and January 2024, from transesophageal echocardiograms performed at a referral hospital in the city of Salvador-BA.

Results: The mean age was 69 ± 15, with 67 males and 28 cases of atrial etiology. The comparison between patients with MR of Atrial etiology versus Non-atrial etiology revealed significantly increased diameters of the intercommissural mitral annulus and its indexed value, with considerably larger diameters in the Atrial group (p = 0.009; 95% CI: 0.501 to 3.507). The receiver operating characteristic (ROC) curve analysis identified an optimal cut-off value of 20.8750, in which the sensitivity and specificity were 67.9%.

Conclusion: Indexing the mitral annular diameter to the body surface area improves diagnostic accuracy in identifying the atrial etiology of MR compared to diameter alone, supporting its potential role in more comprehensive diagnostic algorithms.

Keywords: Mitral Valve Insufficiency; Heart Failure; Atrial Fibrillation.

Introduction

Mitral Regurgitation (MR) is one of the most prevalent valvular diseases in the world, with continuous advances in the understanding of its pathophysiology, diagnosis, and management.[1-4] Among its etiological presentations, Functional Mitral Regurgitation (FMR) of atrial etiology stands out for its clinical relevance, especially in the context of Atrial Fibrillation (AF) and Heart Failure with preserved Ejection Fraction (HFpEF).[1,2,5] It is characterized by mitral annulus dilation and functional alterations of the valve without structural compromise of the leaflets or the subvalvular apparatus. A detailed evaluation of the left atrium and mitral annulus is key for establishing a diagnosis.[1,2,5] The increasing prevalence of AF and HFpEF highlights the importance of more accurate diagnostic and therapeutic strategies for FMR.[1,6] This condition is associated with increased mortality, and interventions such as rhythm control have shown a potential to reduce its frequency.[7]

While AF is commonly associated with FMR, studies suggest that left ventricular diastolic dysfunction also contributes to atrial remodeling, playing a role in the development of this valvular disease.[4,8,9] Its pathophysiological mechanisms include significant anatomical and functional changes. The phenomenon known as hamstringing, characterized by restricted movement of the posterior mitral leaflet, and bending, which is a pathological deformation of the leaflet under hemodynamic stress, directly impairs valve functionality. Moreover, changes in the ratio between the leaflets and mitral annulus area, associated with atrial tethering caused by posterior displacement of the annulus in response to left atrial enlargement, contribute to mitral coaptation deficiency. These changes show that FMR results from combined valve and atrial remodeling, and is not restricted

Mailing Address: Alexandre Costa Souza •
Hospital São Rafael. Avenida São Rafael. Postal Code: 41253-190. Salvador, BA – Brazil
E-mail: alexandrecostahsr@gmail.com
Manuscript received January 15, 2025, revised manuscript January 17, 2025, accepted January 26, 2025
Editor responsible for the review: Marcelo Tavares

DOI: https://doi.org/10.36660/abcimg.20240134i

Central Illustration: Mitral Annulus Diameter's Relevance in the Diagnosis of Atrial Etiology in Mitral Regurgitation: A Comparative Analysis

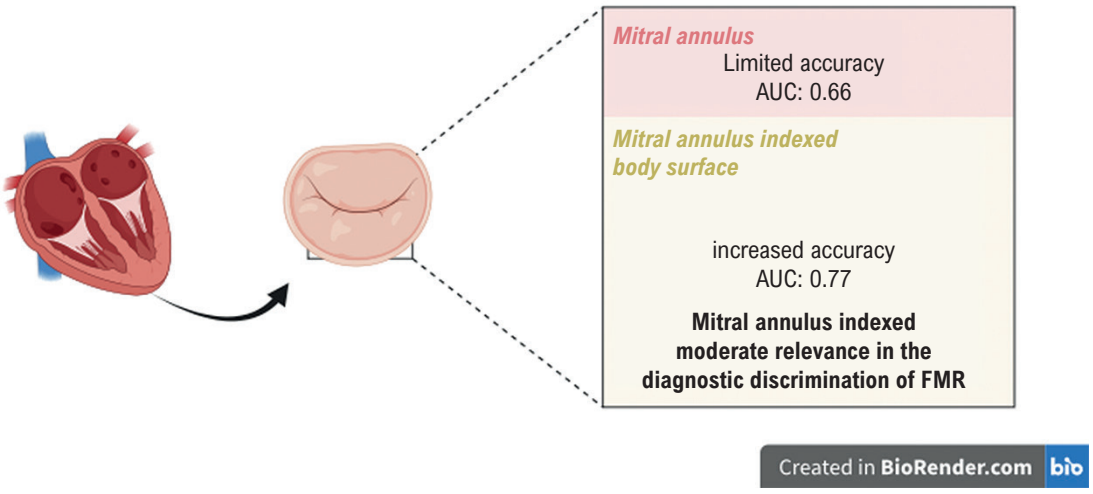

Arq Bras Cardiol: Imagem cardiovasc. 2025;38(1):e20240134

AUC: area under the curve; MR: Mitral Regurgitation.

to the annular dimensions. These processes directly impact valve coaptation and worsen the severity of MR.[10-12]

Although the literature extensively discusses the pathophysiology of MR and its associated clinical and echocardiographic findings, there is a lack of studies focused on refining diagnostic criteria for this specific condition.[5] Given this gap, the present study aimed to determine the accuracy of the intercommissural diameter of the mitral annulus and its value indexed to body surface area, as measured by transesophageal echocardiography, in differentiating atrial etiology in patients with MR.

Method

This is an observational, cross-sectional study, with 109 patients with moderate or severe MR. Echocardiographic images were obtained by transesophageal echocardiography at a referral hospital located in Salvador-BA, in the period between October 2022 and January 2024.

Patients

Patients were selected through a convenience sample based on clinical indications for transesophageal echocardiography as determined by the attending cardiologists. The indication was based on clinical criteria, considering the need for a detailed assessment of the mitral valve and the severity of regurgitation for therapeutic planning. All patients with moderate or severe MR who underwent transesophageal echocardiography between October 2022 and January 2024, in either outpatient or hospital settings, were included. The exclusion criterion was the presence of only mild MR on transesophageal echocardiography or the presence of a prosthetic mitral valve.

The sample consisted of two groups: patients with MR of Atrial etiology (N = 25) and with Non-atrial etiology (N = 84). Between the groups, significant differences were observed in clinical and echocardiographic characteristics. The Atrial group had a higher median age (77 years, 95% CI: 73-84) than the Non-atrial group (67 years, 95% CI: 60-71; $p < 0.001$), in addition to a higher prevalence of AF (72% vs. 34%; $p < 0.001$). 68% vs. 67%, 95% CI: 60-71; $p < 0.001$). The Non-atrial group showed a higher proportion of male patients (68% vs. 68%, 95% CI: 60-71; $p < 0.001$). 42%; $p = 0.019$).

From an echocardiographic point of view, patients in the Atrial group had larger diameters in the mitral annulus, both in linear measurement (46.04 mm vs. 44.37 mm; $p = 0.012$) and in the index adjusted for body surface area (21.63 ± 1.86 vs. 19.36 ± 2.48; $p < 0.001$). Additionally, the left atrial volume was significantly greater in the atrial group (59.02 ml/m² vs. 38.00 ml/m²; $p = 0.08$). Other characteristics, such as Left Ventricular Ejection Fraction (LVEF) and E/e' ratio, were not significantly different between the groups ($p > 0.05$).

Echocardiogram

Transesophageal echocardiography was chosen due to its superior ability to assess both the anatomical and functional aspects of the mitral valve.[13-15] Echocardiographic images were obtained following a standardized protocol with high-resolution equipment (GE Healthcare, E95).

The intercommissural diameter of the mitral annulus was measured using the linear dimension of the intercommissural slice, obtained in a mid-esophageal view at 60º. In addition, two experienced evaluators classified MR into two groups:

Atrial and Non-atrial, according to current guidelines. In cases of disagreement, a third evaluator provided a final classification.[14]

The diagnosis of FMR was based on the following criteria: a dilated mitral annulus on transthoracic echocardiography (> 35 mm in systole on the longitudinal parasternal view), absence of primary mitral valve disease, significant left atrial dilation (indexed volume > 42 ml/m²) and absence of significant ventricular dysfunction (LVEF: > 45%, assessed using the Simpson method).[2,5,16] These criteria were applied to differentiate FMR cases and guide the analysis of the intercommissural diameter relevance as a diagnostic marker.

Statistical Analysis

Statistical analysis was performed using IBM SPSS Statistics for Windows, version 27.0 (IBM Corp, Armonk, NY, USA). In the descriptive analysis, categorical variables were presented as frequencies and percentages, while continuous variables were described by mean and standard deviation. The normality of continuous variables was assessed using the Shapiro-Wilk test, adopting a *p-value*> 0.05 as the criterion for normality.

Comparisons between the Atrial and Non-Atrial groups followed different approaches depending on the variable's nature. For categorical variables, the Pearson's chi-square test was applied. Continuous variables with normal distribution were analyzed using the Student's t-test for independent samples, with the effect size of significant differences being quantified by Cohen's d. In cases of non-normal distribution, the Mann-Whitney's *U* test was used to compare groups. A 95% confidence level was adopted for all tests.

ROC curve analysis was performed to evaluate the diagnostic accuracy of mitral annular diameter and its indexed value in differentiating Atrial from Non-atrial MR. The C statistic was used as a quantitative measure of accuracy, with values above 0.7 indicating good discriminatory capacity. The Youden index was applied to determine the optimal cutoff point for identifying atrial MR based on the indexed mitral annulus.

Results

A total of 109 patients were evaluated, with a mean age of 69 ± 15 years. Most participants were male, with a total of 67 men (61.4%). In the sample, 44% had a known diagnosis of AF, including 20 patients in the Atrial group and 28 in the Non-atrial group. The prevalence of AF differed significantly between the groups ($p < 0.001$) (Table 1).

Patients were categorized based on MR etiology, with 28 (25%) assigned to the Atrial MR group and 81 (75%) to the Non-atrial group. The remaining participants, corresponding to 75% of the sample, formed the composition of the Non-atrial etiology group.

A comparison of echocardiographic measurements between patients with MI of atrial and Non-atrial etiology revealed increased diameters of the intercommissural mitral annulus and its value indexed through the body surface, with larger diameters in the atrial group (Table 1).

The mean intercommissural mitral diameter in the Non-atrial group was 35.067 mm, while in the Atrial group, this value corresponded to 37.071 mm ($p = 0.012$; Cohen's d: 0,580).

Regarding the indexed values, the mean mitral annulus diameter indexed by the body surface area in the Non-atrial group was 19.36 mm/m², while in the Atrial group, this was 21.63 mm/m² ($p < 0.001$; Cohen's d: 0.972) (Table 2).

The diagnostic accuracy of the mitral annulus intercommissural diameter showed an area under the curve (AUC) of 0.659 (95% CI: 0.550 - 0.768), while the ROC curve analysis of the mitral diameter indexed through the body surface exhibited an AUC of 0.767 (95% CI: 0.675 - 0.859). The complementary analysis of the ROC curve identified an optimal cutoff value of 20.8750, at which the sensitivity and specificity were 67.9% (Graph 1).

These findings highlight the relevance of the indexed intercommissural diameter as a potentially superior diagnostic metric to distinguish Atrial from Non-atrial etiologies of MR (Central Illustration).

Discussion

The prevalence of FMR in our study (25%) is consistent with the average number reported in previous observational studies, reflecting the relevance of this condition.[2,7,17] Moreover, the analysis demonstrated that AF is a relevant marker for atrial etiology, with statistically significant differences between the Atrial and Non-atrial groups ($p < 0.001$). AF prevalence reached 71.4% in the atrial MR group, underscoring its strong association with this etiology.[18-20] These findings reinforce the importance of considering AF when identifying the atrial functional etiology in patients with MR.

In this study, a statistically significant difference was observed in the median ages between groups. Patients in the Atrial group had a higher median age (77 years; interquartile range: 73–84) compared to the Non-atrial group (67 years; interquartile range: 60–71; $p < 0.001$). This pattern is in agreement with data previously reported in the literature, which associates advanced age with a greater predisposition to the atrial etiology of MR.[18,21,22] Aging is associated with structural changes such as Left Atrial dilation, which contribute to the development of FMR. These findings reinforce the relevance of age as a relevant pathophysiological factor in determining the etiology of MR.

In the Atrial etiology group, the gender distribution showed 42.9% males and 57.1% females, indicating a slight female predominance. In the Non-atrial group, the proportion of men was considerably higher, representing 67.9% of the participants (55 of 81 individuals). The difference in gender distribution between the groups was statistically significant ($p = 0.019$), suggesting that gender may influence the etiology of MR. Although the exact mechanisms remain unclear, previous studies suggest anatomical and hormonal factors may contribute to atrial remodeling and the atrial etiology of MR development.[3,5] However, these hypotheses still require further investigation.

In the Atrial group, LVEF showed a mean of 56.04 ± 7.53%, while in the Non-atrial group, the mean was significantly lower, reaching 44.42 ± 1.90% ($p < 0.001$). The preservation

Table 1 – Demographic and clinical data

	Atrial group (N=28)	Non-atrial group (N=84)	p-value
Age - years	77 (73-84)	67 (60-71)	< 0.001
Gender: Male, n (%)	12 (48%)	55 (65%)	0.19
AF, n (%)	20 (72%)	28 (33%)	< 0.001
Dyslipidemia, n (%)	21 (75%)	42 (50%)	0.025
Stroke, n (%)	05 (18%)	13 (16%)	0.805
Previous Coronary Artery Disease, n (%)	07 (25%)	34 (40%)	0.141
Diabetes Mellitus, n (%)	07 (25%)	31 (37%)	0.204
Systemic Arterial Hypertension, n (%)	22 (78%)	48 (57%)	0.066
Chronic Renal Failure, n (%)	05 (18%)	14 (17%)	0.976
Weight (kg), n (%)	72.04 (70-74)	73.51 (72-75)	0.632

AF: Atrial Fibrillation.

of the ejection fraction in the atrial group reflects a striking characteristic of this group, since the reduction in LVEF, when present, occurs only in advanced stages of atrial FMR.[21,23-25] FMR is recognized as an important prognostic indicator in patients with AF and HFpEF. This condition is associated with a higher risk of progressive systolic dysfunction and reduced LVEF, factors that contribute to clinical worsening and adverse outcomes.[26] These findings reinforce the need for careful monitoring of left ventricular function in this clinical context.

The behavior of the mitral annulus and the mitral annulus indexed by body surface area was of particular interest in this study. Prior research on the mitral annulus as a diagnostic tool for FMR has yielded conflicting results, with most studies relying on absolute measurements obtained via transthoracic echocardiography.[27] This study utilized transesophageal echocardiography due to its superior precision in assessing the mitral valve, annular complex, and valve morphology.[27-29] Body surface area indexing was used to ensure greater reliability of measurements, especially in heterogeneous populations. This approach allows for a more standardized assessment adjusted to the individuality of patients, expanding its clinical applicability.[20] These factors reinforce the importance of indexing in the context of FMR, where diagnostic accuracy is essential.

The intercommissural mitral annular diameter was compared between atrial and non-atrial MR groups, revealing significant differences in both absolute and indexed measurements. The mean absolute diameter was 35 mm in the Non-atrial group and 37.1 mm in the Atrial group ($p = 0.012$), with a Cohen's d of 0.580, indicating a moderate effect size. When adjusted for body surface area, the difference became even more pronounced, with mean values of 19.35 mm/m² in the non-atrial group and 21.63 mm/m² in the atrial group ($p < 0.001$, Cohen's $d = 0.972$), indicating a large effect size.

These findings confirm that indexing by body surface area enhances the detection of mitral annular changes, standardizing measurements to account for individual patient characteristics. This approach is particularly useful in heterogeneous populations and may improve clinical decision-making by refining the differentiation between atrial and non-atrial MR.[20,29]

The analysis of diagnostic accuracy using the ROC curve for the intercommissural diameter of the mitral annulus revealed an AUC of 0.659 (95% CI: 0.550–0.768), indicating only moderate accuracy in distinguishing between the atrial and non-atrial groups. On the other hand, indexing the mitral diameter by body surface area showed superior relevance, with an AUC of 0.767 (95% CI: 0.675–0.859), reflecting a more robust diagnostic discrimination capacity.

Additionally, the ROC curve analysis identified an optimal cutoff value of 20.8750 mm/m², with sensitivity and specificity of 67.9%. These findings reinforce the potential of indexed diameter as a superior tool when compared to the absolute value of the valve annulus in diagnostic algorithms, offering greater accuracy in differentiating between atrial and non-atrial etiologies of MR.

While indexing the mitral annular diameter increased diagnostic accuracy compared to absolute measurements, limitations remain. The C statistic and Youden index analysis suggest that, when used in isolation, the indexed annular diameter provides only modest diagnostic accuracy. This underscores the need for more comprehensive diagnostic models that integrate indexed diameter with additional clinical and echocardiographic variables to improve atrial MR identification.

Conclusion

The findings support the use of indexed diameter as a superior metric over absolute annular size in diagnostic algorithms, offering greater accuracy in differentiating MR etiologies. However, incorporating this measure into

Table 2 – Echocardiographic Data

	Atrial group (N=28)	Non-atrial group (N=84)	p-value
Linear Measurement of Commissural Mitral Annulus (mm)	37.07 (32-40)	35.06 (25-43)	0.012
Indexed Mitral Annulus (mm/m²)	21.63 ± 1.86	19.36 ± 2.48	< 0.001
Linear Measurement of Left Atrium (mm)	46 (44-49)	44 (41-49)	0.732
Indexed Left Atrial Volume (ml/m²)	59.02 (57-61)	38.00 (35-41)	0.080
LVEF	61 (58-64)	42 (30-54)	< 0.001
E/e' ratio	12 (10-14)	10 (08-12)	0.315

LA: Left Atrium; LVEF: Left Ventricular Ejection Fraction; Kg: Kilograms; m: Meters; HR: Heart Rate; bpm: Beats per Minute.

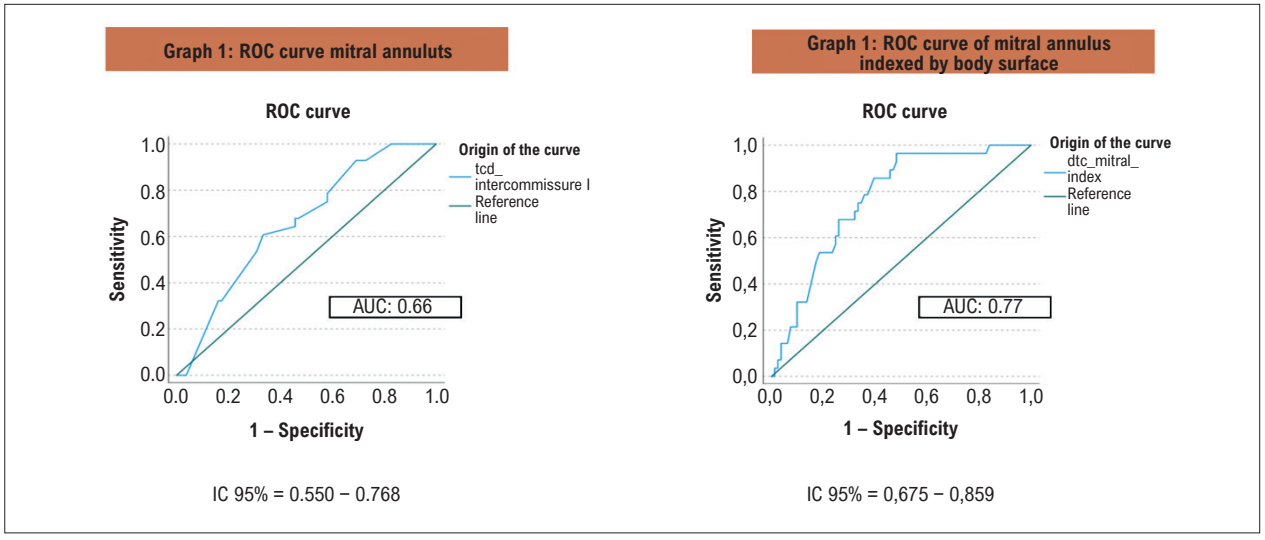

Graph 1 – *ROC Curves for evaluating atrial etiology. (A) Non-indexed mitral annulus: AUC = 0.66 (95% CI: 0.550–0.768), indicating moderate discriminatory ability. (B) Mitral annulus indexed by body surface area: AUC = 0.77 (95% CI: 0.675–0.859), suggesting higher diagnostic accuracy. The reference line represents the absence of discriminatory power (AUC = 0.5). The curves were adjusted based on the dimensions of the mitral annulus (intercommissural length or indexed value) and reflect the population heterogeneity, highlighting the superiority of the adjusted index in distinguishing atrial etiology. AUC: area under the curve; ROC: receiver operating characteristic.*

broader diagnostic frameworks may further enhance its clinical utility.

Author Contributions

Conception and design of the research: Souza AC, Junqueira BMI; acquisition of data: Souza AC, Pinheiro P, Basile AG, Drubi AS; analysis and interpretation of the data and statistical analysis: Souza AC; writing of the manuscript: Gomes LC, Guedes RASP, Sales MAM, Drubi AS, Junqueira BMI; critical revision of the manuscript for intellectual content: Freire MV, Macêdo CT, Guedes RASP, Sales MAM, Junqueira BMI.

Potential Conflict of Interest

No potential conflict of interest relevant to this article was reported.

Sources of Funding

There were no external funding sources for this study.

Study Association

This article is part of the thesis of Doctoral submitted by Alexandre Costa Souza, from Instituto Dor de ensino e pesquisa (Idor).

Ethics Approval and Consent to Participate

This study was approved by the Ethics Committee of the Hospital São Rafael under the protocol number 5722007. All the procedures in this study were in accordance with the 1975 Helsinki Declaration, updated in 2013. Informed consent was obtained from all participants included in the study.

References

1. Deferm S, Bertrand PB, Verbrugge FH, Verhaert D, Rega F, Thomas JD, et al. Atrial Functional Mitral Regurgitation: JACC Review Topic of the Week. J Am Coll Cardiol. 2019;73(19):2465-76. doi: 10.1016/j.jacc.2019.02.061.
2. Pretto AS. Atrial Functional Mitral Regurgitation. Arq Bras Cardiol: Imagem Cardiovasc. 2024;37(1):e20230097. doi: 10.36660/abcimg.20230097i.
3. Doldi P, Stolz L, Orban M, Karam N, Praz F, Kalbacher D, et al. Transcatheter Mitral Valve Repair in Patients with Atrial Functional Mitral Regurgitation. JACC Cardiovasc Imaging. 2022;15(11):1843-51. doi: 10.1016/j.jcmg.2022.05.009.
4. Mesi O, Gad MM, Crane AD, Ramchand J, Puri R, Layoun H, et al. Severe Atrial Functional Mitral Regurgitation: Clinical and Echocardiographic Characteristics, Management and Outcomes. JACC Cardiovasc Imaging. 2021;14(4):797-808. doi: 10.1016/j.jcmg.2021.02.008.
5. Farhan S, Silbiger JJ, Halperin JL, Zhang L, Dukkipati SR, Vogel B, et al. Pathophysiology, Echocardiographic Diagnosis, and Treatment of Atrial Functional Mitral Regurgitation: JACC State-of-the-Art Review. J Am Coll Cardiol. 2022;80(24):2314-30. doi: 10.1016/j.jacc.2022.09.046.
6. Dziadzko V, Dziadzko M, Medina-Inojosa JR, Benfari G, Michelena HI, Crestanello JA, et al. Causes and Mechanisms of Isolated Mitral Regurgitation in the Community: Clinical Context and Outcome. Eur Heart J. 2019;40(27):2194-202. doi: 10.1093/eurheartj/ehz314.
7. Moonen A, Ng MKC, Playford D, Strange G, Scalia GM, Celermajer DS. Atrial Functional Mitral Regurgitation: Prevalence, Characteristics and Outcomes from the National Echo Database of Australia. Open Heart. 2023;10(1):e002180. doi: 10.1136/openhrt-2022-002180.
8. Muraru D, Guta AC, Ochoa-Jimenez RC, Bartos D, Aruta P, Mihaila S, et al. Functional Regurgitation of Atrioventricular Valves and Atrial Fibrillation: An Elusive Pathophysiological Link Deserving Further Attention. J Am Soc Echocardiogr. 2020;33(1):42-53. doi: 10.1016/j.echo.2019.08.016.
9. Hoit BD. Atrial Functional Mitral Regurgitation: The Left Atrium Gets its Due Respect. J Am Coll Cardiol. 2011;58(14):1482-4. doi: 10.1016/j.jacc.2011.06.033.
10. Gertz ZM, Raina A, Saghy L, Zado ES, Callans DJ, Marchlinski FE, et al. Evidence of Atrial Functional Mitral Regurgitation Due to Atrial Fibrillation: Reversal with Arrhythmia Control. J Am Coll Cardiol. 2011;58(14):1474-81. doi: 10.1016/j.jacc.2011.06.032.
11. Silbiger JJ. Mechanistic Insights Into Atrial Functional Mitral Regurgitation: Far More Complicated than Just Left Atrial Remodeling. Echocardiography. 2019;36(1):164-9. doi: 10.1111/echo.14249.
12. Kagiyama N, Mondillo S, Yoshida K, Mandoli GE, Cameli M. Subtypes of Atrial Functional Mitral Regurgitation: Imaging Insights Into Their Mechanisms and Therapeutic Implications. JACC Cardiovasc Imaging. 2020;13(3):820-35. doi: 10.1016/j.jcmg.2019.01.040.
13. Machino-Ohtsuka T, Seo Y, Ishizu T, Sato K, Sugano A, Yamamoto M, et al. Novel Mechanistic Insights Into Atrial Functional Mitral Regurgitation - 3-Dimensional Echocardiographic Study. Circ J. 2016;80(10):2240-8. doi: 10.1253/circj.CJ-16-0435.
14. Zoghbi WA, Adams D, Bonow RO, Enriquez-Sarano M, Foster E, Grayburn PA, et al. Recommendations for Noninvasive Evaluation of Native Valvular Regurgitation: A Report from the American Society of Echocardiography Developed in Collaboration with the Society for Cardiovascular Magnetic Resonance. J Am Soc Echocardiogr. 2017;30(4):303-71. doi: 10.1016/j.echo.2017.01.007.
15. Grayburn PA, Thomas JD. Basic Principles of the Echocardiographic Evaluation of Mitral Regurgitation. JACC Cardiovasc Imaging. 2021;14(4):843-53. doi: 10.1016/j.jcmg.2020.06.049.
16. Zoghbi WA, Levine RA, Flachskampf F, Grayburn P, Gillam L, Leipsic J, et al. Atrial Functional Mitral Regurgitation: A JACC: Cardiovascular Imaging Expert Panel Viewpoint. JACC Cardiovasc Imaging. 2022;15(11):1870-82. doi: 10.1016/j.jcmg.2022.08.016.
17. Naser JA, Alexandrino FB, Harada T, Michelena HI, Borlaug BA, Eleid MF, et al. The Natural History of Atrial Functional Mitral Regurgitation. J Am Coll Cardiol. 2024;83(16):1495-507. doi: 10.1016/j.jacc.2024.02.026.
18. Kihara T, Gillinov AM, Takasaki K, Fukuda S, Song JM, Shiota M, et al. Mitral Regurgitation Associated with Mitral Annular Dilation in Patients with Lone Atrial Fibrillation: An Echocardiographic Study. Echocardiography. 2009;26(8):885-9. doi: 10.1111/j.1540-8175.2009.00904.x.
19. Cramariuc D, Alfraidi H, Nagata Y, Levine RA, van Kampen A, Andrews C, et al. Atrial Dysfunction in Significant Atrial Functional Mitral Regurgitation: Phenotypes and Prognostic Implications. Circ Cardiovasc Imaging. 2023;16(5):e015089. doi: 10.1161/CIRCIMAGING.122.015089.
20. Lang RM, Badano LP, Mor-Avi V, Afilalo J, Armstrong A, Ernande L, et al. Recommendations for Cardiac Chamber Quantification by Echocardiography in Adults: An Update from the American Society of Echocardiography and the European Association of Cardiovascular Imaging. J Am Soc Echocardiogr. 2015;28(1):1-39.e14. doi: 10.1016/j.echo.2014.10.003.
21. Kim DH, Heo R, Handschumacher MD, Lee S, Choi YS, Kim KR, et al. Mitral Valve Adaptation to Isolated Annular Dilation: Insights Into the Mechanism of Atrial Functional Mitral Regurgitation. JACC Cardiovasc Imaging. 2019;12(4):665-77. doi: 10.1016/j.jcmg.2017.09.013.
22. Naser JA, Michelena HI, Lin G, Scott CG, Lee E, Kennedy AM, et al. Incidence, Risk Factors, and Outcomes of Atrial Functional Mitral Regurgitation in Patients with Atrial Fibrillation or Sinus Rhythm. Eur Heart J Cardiovasc Imaging. 2023;24(11):1450-7. doi: 10.1093/ehjci/jead199.
23. Abe Y, Akamatsu K, Ito K, Matsumura Y, Shimeno K, Naruko T, et al. Prevalence and Prognostic Significance of Functional Mitral and Tricuspid Regurgitation Despite Preserved Left Ventricular Ejection Fraction in Atrial Fibrillation Patients. Circ J. 2018;82(5):1451-8. doi: 10.1253/circj.CJ-17-1334.
24. Reddy YNV, Obokata M, Verbrugge FH, Lin G, Borlaug BA. Atrial Dysfunction in Patients with Heart Failure with Preserved Ejection Fraction and Atrial Fibrillation. J Am Coll Cardiol. 2020;76(9):1051-64. doi: 10.1016/j.jacc.2020.07.009.
25. Zakeri R, Chamberlain AM, Roger VL, Redfield MM. Temporal Relationship and Prognostic Significance of Atrial Fibrillation in Heart Failure Patients with Preserved Ejection Fraction: A Community-Based Study. Circulation. 2013;128(10):1085-93. doi: 10.1161/CIRCULATIONAHA.113.001475.
26. Tang Z, Fan YT, Wang Y, Jin CN, Kwok KW, Lee AP. Mitral Annular and Left Ventricular Dynamics in Atrial Functional Mitral Regurgitation: A Three-Dimensional and Speckle-Tracking Echocardiographic Study. J Am Soc Echocardiogr. 2019;32(4):503-13. doi: 10.1016/j.echo.2018.11.009.
27. Akamatsu K, Abe Y, Matsumura Y, Shimeno K, Naruko T, Takahashi Y, et al. Etiology of Atrial Functional Mitral Regurgitation: Insights from Transthoracic Echocardiography in 159 Consecutive Patients with Atrial Fibrillation and Preserved Left Ventricular Ejection Fraction. Cardiology. 2020;145(8):511-21. doi: 10.1159/000508279.
28. Kagiyama N, Toki M, Hara M, Fukuda S, Aritaka S, Miki T, et al. Efficacy and Accuracy of Novel Automated Mitral Valve Quantification: Three-Dimensional Transesophageal Echocardiographic Study. Echocardiography. 2016;33(5):756-63. doi: 10.1111/echo.13135.
29. Ring L, Dutka DP, Boyd J, Parker K, Wendler O, Monaghan MJ, et al. The Normal Mitral Valve Annulus in Humans Defined Using 3-Dimensional Transesophageal Echocardiography. JACC Cardiovasc Imaging. 2018;11(3):510-2. doi: 10.1016/j.jcmg.2017.05.017.

The Role of Objective Assessment of the Mitral Annulus

Minna Moreira Dias Romano[1]

Universidade de São Paulo, Faculdade de Medicina de Ribeirão Preto,[1] *Ribeirão Preto, SP – Brazil*

Short Editorial related to the article: Mitral Annulus Diameter's Relevance in the Diagnosis of Atrial Etiology in Mitral Regurgitation: A Comparative Analysis

The mitral annulus is a complex and dynamic structure responsive to both structural and functional changes involving the mitral valve, as well as those affecting the geometry of the left ventricle (LV) and left atrium (LA). Its bean-shaped or "D"-shaped three-dimensional structure is similar to a horse's saddle, in which the nadir (height) varies throughout the cardiac cycle. The malleability of the mitral annulus is important for valve competence. The posterior portion of the annulus, which is less fibrotic, moves during left ventricular systole, increasing the height of the saddle and reducing its circumferential area. In situations of left atrial dilation and dysfunction, mainly accompanied by atrial fibrillation (AF) and commonly associated with various causes of LV diastolic dysfunction, mitral annulus' dynamics are often compromised. This results in reduced mobility of the posterior leaflet, annulus stiffness, and diminished oscillation of the saddle height, in addition to valve retraction (tethering), which contribute to mitral coaptation failure.[1]

The mitral annulus can be studied using echocardiography, both two-dimensional and three-dimensional, with transesophageal imaging being the preferred approach. Three-dimensional imaging allows for various quantitative measurements facilitated by computational reconstruction software. These measurements can also be dynamic, capturing structural modifications throughout the cardiac cycle in both systole and diastole (Figure 1). Key measurements include annular circumference and area, anteroposterior and inter-commissural diameters, and saddle height. The three-dimensional approach offers significant advantages, particularly when segmentation of valve anatomy is required, such as in cases of mitral valve prolapse that necessitate detailed anatomical analysis of valve bulges.[2] Different etiologies of mitral regurgitation (MR) are accompanied by different degrees of mitral annulus deformation, with the most subtle ones observed in ischemic MR and the most significant in the most advanced spectra of mitral degenerative diseases, such as Barlow's disease.[3] For example, in rheumatic disease—still largely common in Brazil despite its low prevalence in more developed countries—mitral annulus changes are characterized by a "flattening of the saddle shape" and an increased area without a significant change in the perimeter.[4]

The etiological diagnosis of MR, whether functional or primary, can often be challenging. When functional (secondary), regurgitation is commonly related to the enlargement of the left chambers, as well as to the isolated enlargement of the LA in some cases, as occurs in various cardiomyopathies or heart failure with preserved ejection fraction (HFpEF). Regurgitation itself can cause mild secondary valve thickening due to jet lesions, making the etiological diagnosis even more difficult. Distinguishing between MR as a cause or consequence of cardiac chamber dilation remains challenging and often relies on subjective assessments. Addressing this issue is crucial, particularly in the context of primary MR treatments and the evolving role of percutaneous devices for secondary MR. In cases of MR associated with AF but without left ventricular dilation or dysfunction, the possibility of functional or secondary MR (the so-called atrial MR) should be considered, whose etiopathogenesis is not yet well understood.[5] One theory suggests that LA dilation is responsible for the displacement of the posterior mitral annulus towards the LV crest, thus reducing the posterior leaflet's coaptation surface.[6] Other mechanisms of functional MR are also proposed for situations where LV dilation and dysfunction are also present, such as in dilated cardiomyopathies, due to the lack of adequate remodeling/stretching of mitral valve leaflets.

A recent systematic review by Kagiyama et al. provides a comprehensive discussion on functional MR related to AF and the mitral annulus alterations that may accompany left atrial remodeling, even in patients with preserved ventricular function.[1] Based on the published articles, they estimate a 3 to 15% prevalence of atrial MR. The study also revealed that patients with AF presenting atrial MR have more adverse events throughout the clinical evolution. A few studies and publications of isolated cases suggest the role of annuloplasty as a treatment for cases of atrial MR. Furthermore, there is growing clinical interest in the potential role of percutaneous treatments, with some devices under development alongside mitral "clipping," though scientific evidence remains limited. Percutaneous treatments may offer advantages over open surgery, particularly for older patients with AF and multiple comorbidities. This reinforces the relevance of a more detailed assessment of the mitral annulus.

The study by Souza et al.,[7] published in this issue of *ABC Imagem*, analyzed a cohort of 109 patients with significant MR from various etiologies, including 28 cases of atrial MR. Patients were evaluated by two-dimensional transesophageal echocardiography. The linear commissural measurement of the mitral annulus, indexed by CS, obtained from a two-chamber transesophageal image. Patients classified as having "atrial etiology" had preserved left ventricular ejection fraction (LVEF). The commissural measurement power was tested to identify the

Keywords

Mitral Valve Insufficiency; Atrial Fibrillation; Echocardiography.

Mailing Address: Minna Moreira Dias Romano •
Universidade de São Paulo, Faculdade de Medicina de Ribeirão Preto. R. Carlos Rateb Cury, 697. Postal code: 14110-000. Ribeirão Preto, SP – Brazil
E-mail: minna@fmrp.usp.br

DOI: https://doi.org/10.36660/abcimg.20250010i

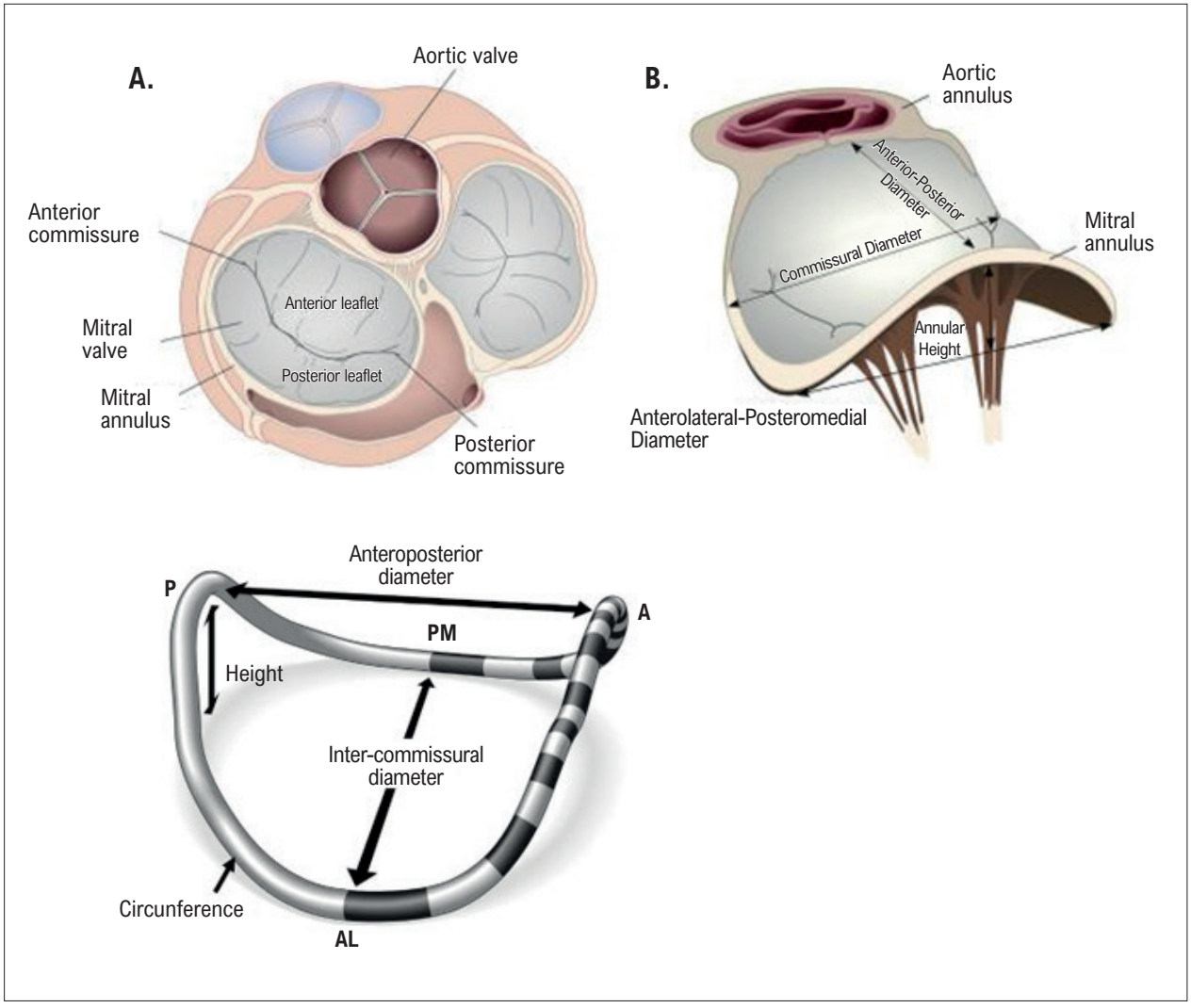

Figure 1 – *Anatomical characteristics of the mitral annulus. Panels A and B demonstrate the mitral annulus anatomy related to other cardiac structures, such as the aortic valve. Panel C highlights the objective measurements that can be performed on the mitral annulus. Figures adapted from Grewal et al. Circulation 2010 and Levine et al. Circulation 1989. PM: posterior-medial; AL: anterior-lateral.*

28 cases of MR of atrial etiology. The authors demonstrated good accuracy of the indexed variable (AUC = 0.77) in identifying patients with MR of atrial etiology, which was slightly superior to the non-indexed linear measurement of the inter-commissural diameter. Despite the small sample size and the use of a single measurement parameter, the results suggest the importance of quantitative mitral annulus assessment, even in patients with preserved LVEF. This approach may aid in differentiating mitral disease etiologies associated with MR.

In conclusion, echocardiography remains a valuable tool for evaluating the mitral annulus, that can be assessed using various parameters, including two-dimensional imaging, and providing even more detail with three-dimensional echocardiography aided by 3D reconstruction software. Studying mitral annulus characteristics in MR cases can assist in distinguishing functional or secondary MR, identifying its etiology, and recognizing a subset of patients with atrial MR related to AF, even in the absence of left ventricular alterations.

References

1. Kagiyama N, Mondillo S, Yoshida K, Mandoli GE, Cameli M. Subtypes of Atrial Functional Mitral Regurgitation: Imaging Insights Into Their Mechanisms and Therapeutic Implications. JACC Cardiovasc Imaging. 2020;13(3):820-35. doi: 10.1016/j.jcmg.2019.01.040.
2. Zekry SB, Lang RM, Sugeng L, McCulloch ML, Weinert L, Raman J, et al. Mitral Annulus Dynamics Early after Valve Repair: Preliminary Observations of the Effect of Resectional versus Non-Resectional Approaches. J Am Soc Echocardiogr. 2011;24(11):1233-42. doi: 10.1016/j.echo.2011.08.010.

3. Kovalova S, Necas J. RT 3D TEE: Characteristics of Mitral Valve in Ischemic Mitral Regurgitation Evaluated by MVQ Program. Cardiol Res. 2011;2(4):168-73. doi: 10.4021/cr63w.

4. Yeong M, Silbery M, Finucane K, Wilson NJ, Gentles TL. Mitral Valve Geometry in Paediatric Rheumatic Mitral Regurgitation. Pediatr Cardiol. 2015;36(4):827-34. doi: 10.1007/s00246-014-1085-1.

5. Lee AP, Jin CN, Fan Y, Wong RHL, Underwood MJ, Wan S. Functional Implication of Mitral Annular Disjunction in Mitral Valve Prolapse: A Quantitative Dynamic 3D Echocardiographic Study. JACC Cardiovasc Imaging. 2017;10(12):1424-33. doi: 10.1016/j.jcmg.2016.11.022.

6. Silbiger JJ. Does Left Atrial Enlargement Contribute to Mitral Leaflet Tethering in Patients with Functional Mitral Regurgitation? Proposed Role of Atriogenic Leaflet Tethering. Echocardiography. 2014;31(10):1310-1. doi: 10.1111/echo.12629.

7. Souza AC, Junqueira BMI, Drubi SA, Gomes LC, Freire MV, Pinheiro P et al. Desempenho do Diâmetro do Anel Mitral no Diagnóstico da Etiologia Atrial na Insuficiência Mitral: Uma Análise Comparativa. Arq Bras Cardiol: Imagem cardiovasc. 2025;38(1):e20240134. doi: 10.36660/abcimg.20240134

8. Grewal J, Suri R, Mankad S, Tanaka A, Mahoney DW, Schaff HV, et al. Mitral Annular Dynamics in Myxomatous Valve Disease: New Insights with Real-Time 3-Dimensional Echocardiography. Circulation. 2010;121(12):1423-31. doi: 10.1161/CIRCULATIONAHA.109.901181.

9. Levine RA, Handschumacher MD, Sanfilippo AJ, Hagege AA, Harrigan P, Marshall JE, et al. Three-Dimensional Echocardiographic Reconstruction of the Mitral Valve, with Implications for the Diagnosis of Mitral Valve Prolapse. Circulation. 1989;80(3):589-98. doi: 10.1161/01.cir.80.3.589.

Permissive Cardiotoxicity: When the Optimal Is the Enemy of the Good

Carolina Maria Pinto Domingues Carvalho Silva,[1] *Juliane Dantas Seabra-Garcez,*[2,3] *Ana Palmira Lima Neves,*[4,5] *Ariane Vieira Scarlatelli Macedo*[6]

Centro Avançado de Pesquisa e Estudos para o Diagnóstico,[1] *Ribeirão Preto, SP – Brazil*
Vitta Oncologia,[2] *Aracaju, SE – Brazil*
Hospital Primavera,[3] *Aracaju, SE – Brazil*
Hospital de Base,[4] *São José do Rio Preto, SP – Brazil*
Santa Casa de Misericórdia de São José do Rio Preto,[5] *São José do Rio Preto, SP – Brazil*
Faculdade de Ciências Medicas da Santa Casa de São Paulo,[6] *São Paulo, SP – Brazil*

Central Illustration: Permissive Cardiotoxicity: When the Optimal Is the Enemy of the Good

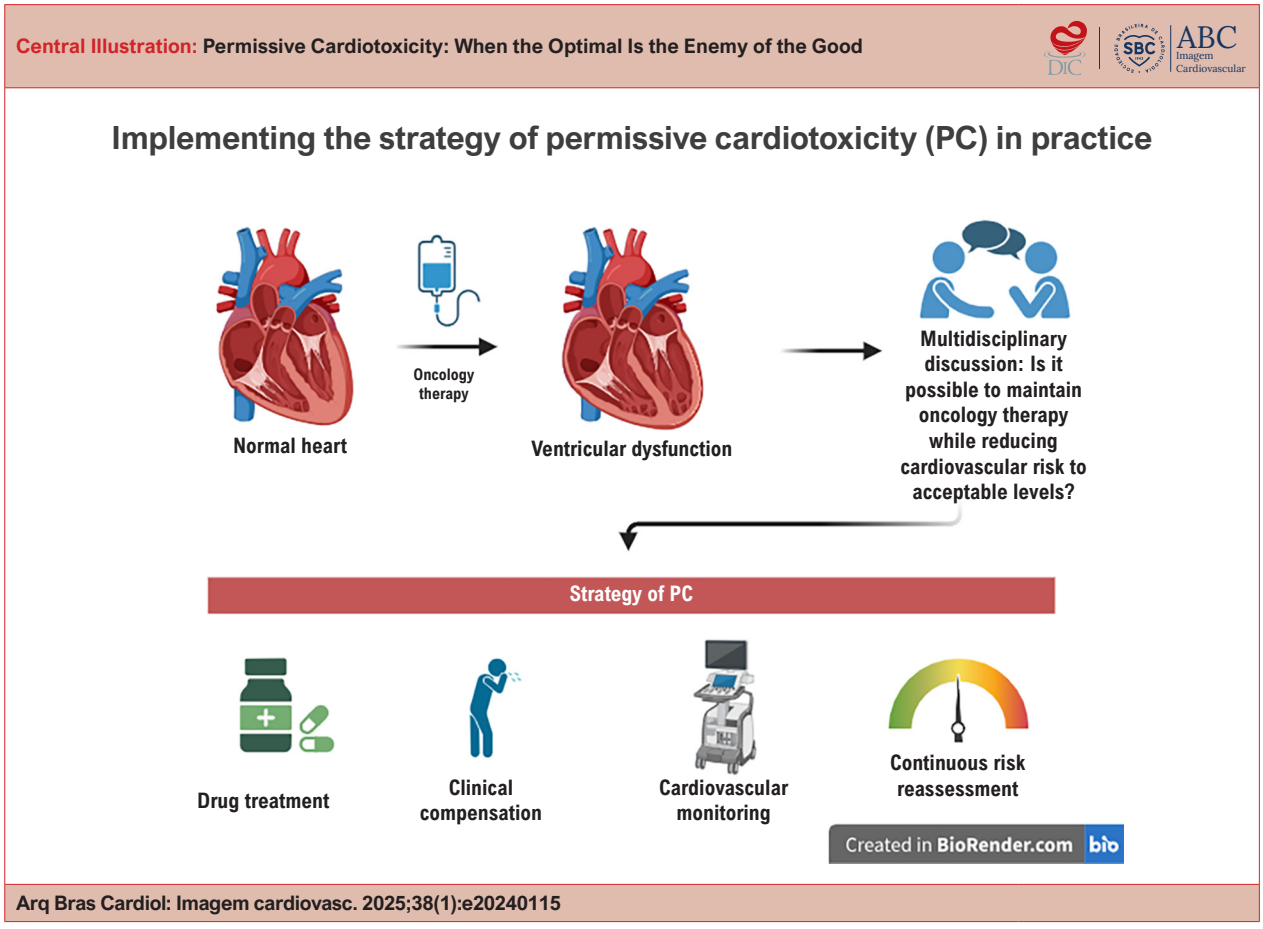

Arq Bras Cardiol: Imagem cardiovasc. 2025;38(1):e20240115

Keywords

Cardiotoxicity; Cardio-Oncology; Ventricular Dysfunction; Antineoplastic Agents; Neoplasms.

Mailing Address: Carolina Maria Pinto Domingues Carvalho Silva •
Centro Avançado de Pesquisa e Estudos para o Diagnóstico. Av. Cel. Fernando Ferreira Leite, 1540. Postal code: 14026-900. Ribeirão Preto, São Paulo, SP – Brazil
E-mail: carolinacsilva@ymail.com
Manuscript received November 11, 2024; revised November 14, 2024; accepted November 19, 2024
Editor responsible for the review: Marcelo Tavares

DOI: https://doi.org/10.36660/abcimg.20240115i

Abstract

Cancer and cardiovascular diseases are the leading causes of mortality worldwide. As these diseases share common metabolic pathways, patients with cancer are currently seen as having subclinical alterations with great potential for developing cardiovascular diseases (and vice versa). This tenuous interrelationship has led to the emergence of cardio-oncology (CO) as an area of study and discussion, with a major impact on the management of these cases.

In clinical practice, CO is dominated by the dilemma of how to best manage cardiovascular toxicity during cancer

treatment. The management of these cases focuses not only on restoring cardiovascular balance, but also on ensuring that the best oncological treatment will be offered, without suspensions or interruptions.

Within this context, the concept of permissive cardiotoxicity (PC) has emerged, proposing the idea of maintaining antitumor treatment in the event that ventricular dysfunction is detected, with no pauses or interruptions, provided that certain premises are respected.

This review aims to examine the concept of PC in depth, contextualizing its emergence, reviewing definitions, and analyzing the evidence from experimental clinical studies. Furthermore, management strategies are detailed, discussing the central role of cardiovascular imaging in guiding this management. Finally, limitations and gaps in the literature in the area are discussed.

Introduction

Cancer and cardiovascular diseases are currently the leading causes of mortality worldwide.[1] These diseases share not only common risk factors (for example, smoking, obesity, sedentary lifestyle, alcohol consumption, diets rich in ultra-processed foods, etc.),[2] but also equivalent metabolic pathways.[3]

Accordingly, patients receiving oncological treatment have come to be seen as having an elevated risk of cardiovascular disease.[4] This fact allows us to predict that, at some point in the oncological journey, heart disease will be part of the list of these patients' comorbidities. In this context, cardiologists have begun to face the challenge of managing cardiovascular events in patients with neoplasia, culminating in the organization of this recent area of study, CO.

Cardio-oncology: a vital field

CO emerged as a result of the intersection between cardiovascular health and cancer treatment.[5] Driven by the growing practical need to manage cardiological events associated with these treatments, CO has rapidly evolved into a field of study and research. This new area brings together specialists who share the common goal of maintaining the most effective oncological treatment available while respecting the premises of cardiovascular safety.

Although the field of CO is vast, with important windows of opportunity for action in the diverse phases of the oncological journey, the main challenge lies in the management of events throughout the active phase of antitumor treatment. The appropriate management of these cases is crucial, as it directly impacts not only cardiovascular, but especially oncological prognosis and survival.

These data, in conjunction with the development of antineoplastic treatments that have significantly increased patient survival rates, have directed the focus of attention to CO, which has become fundamental to ensuring excellence in oncological care.

Cardiotoxicity: what every cardiologist needs to know

We broadly define cardiotoxicity as any pathological alteration of the cardiovascular system induced by oncological treatment.[6] Possible cardiotoxic manifestations thus include all conditions that affect the cardiovascular system, from worsening of cardiovascular risk factors (for example, hypertension, dyslipidemia, metabolic syndrome, etc.) to major events such as acute coronary syndromes, pulmonary thromboembolism, severe ventricular arrhythmias, and others.

Although it has a broad spectrum of manifestations, the main types of cardiotoxic manifestations are presented in the form of the following two clinical syndromes: arrhythmias and chemotherapy-related cardiac dysfunction (CTRCD). Among these, systolic myocardial dysfunction has been the most impactful clinical presentation (due to its severity and risk), making CTRCD a near synonym of "cardiotoxicity." The antineoplastic medications most frequently associated with CTRCD are listed in Table 1.

The most widely accepted and internationally applied definition for CTRCD in clinical practice was standardized by the publication of the Cardio-Oncology Guideline of the European Society of Cardiology in partnership with the International Cardio-Oncology Society in 2016, which defines CTRCD as a drop in left ventricular ejection fraction (LVEF) of ≥ 10% (in relation to the pre-treatment value) in the presence of absolute values < 50%.[7] It is important to mention that CTRCD is a diagnosis of exclusion, making it mandatory to conduct differential diagnosis and rule out other etiologies related to ventricular dysfunction (especially coronary artery disease, which is the most prevalent etiology worldwide).[8]

Permissive cardiotoxicity: a new look for an old concept?

The main challenges of CO include the management of situations in which patients are exposed to a highly effective oncological treatment, but they progress with signs of cardiovascular toxicity. In this scenario, classically, a discussion takes place about whether to pause or suspend antineoplastic treatment, given that this was initially considered the most appropriate course of action. However, questions began to be raised when studies demonstrated that even brief and temporary suspension of oncological treatment resulted in a reduction in its efficacy.[9] The practical observation of the good clinical evolution of patients with discrete drops in LVEF while using trastuzumab (generally oligosymptomatic and with excellent progress after initiating use of cardiovascular medications)[10] provided the pathophysiological rationale for the concept of PC.[11]

The strategy of PC consists of maintaining the antitumor treatment underway when ventricular dysfunction is detected, without pauses or interruptions.[12] This conduct is based on the following pillars: 1 – Maintaining the antineoplastic treatment without temporary pauses or suspension; 2 – Initiating cardiovascular drug treatment that promotes the best cardiological prognosis possible.[12] The strategy of PC assumes the premise that some degree of "manageable" cardiovascular damage (i.e., that does not result in serious cardiovascular events and/or high morbidity and mortality) may be acceptable in the name of maintaining the treatment that results in the best oncological prognosis.

Table 1 – The main antineoplastic medications associated with CTRCD

Pharmacological class	Examples of agents	Indicated tumor types
Anthracyclines	Doxorubicin, epirubicin, daunorubicin, idarubicin, mitoxantrone	Breast, ovarian, lymphomas, and leukemias
Anti-HER therapies	Trastuzumab, T-DM1, pertuzumab, trastuzumab deruxtecan	Breast, gastric
Tyrosine kinase inhibitors	Sorafenib, sunitinib, pazopanib, afatinib, osimertinib, erlotinib	Renal carcinoma, hepatocellular carcinoma, lung cancer
Alkylating agents	Cyclophosphamide, ifosfamide	Lymphomas and leukemias, sarcomas
Immune checkpoint inhibitors	Pembrolizumab, nivolumab, atezolizumab, avelumab, durvalumab, ipilimumab, tremelimumab	Multiple indications, the main ones being: melanoma, bladder cancer, renal carcinoma, lung cancer, hepatocellular carcinoma
Proteasome inhibitors	Carfilzomib, ixazomib, bortezomib	Multiple myeloma
VEGF inhibitors	Bevacizumab, aflibercept	Colorectal cancer and renal carcinoma
MEK/BRAF inhibitors	Dabrafenib/trametinib, vemurafenib/cobimetinib, encorafenib/binimetinib	Melanoma

BRAF: serine/threonine-protein kinase; CTRCD: chemotherapy-related cardiac dysfunction; HER: human epidermal growth factor; MEK: mitogen-activated protein kinase; T-DM1: ado-trastuzumab emtansine; VEGF: vascular endothelial growth factor.

Literally speaking, the strategy of PC is indicated in cases of CTRCD during antitumor treatment. Nonetheless, it can also be applied to candidates who have elevated cardiovascular risk. In this situation, "non-ideal" conditions are tolerated in the name of obtaining a major oncological benefit. In both cases, what differentiates the approaches is the moment when the permissive strategy is instituted: during cancer treatment (in cases of established cardiovascular toxicity) or pre-treatment (in cases of high baseline cardiovascular risk).

The concept of PC assumes that, even in unfavorable cardiological scenarios, the oncological treatment of choice can be maintained as long as the cardiovascular risk is reduced to acceptable levels. It is believed that, in the absence of evidence that proves the benefit of suspending antitumor treatment, clinical optimization provides sufficient conditions to continue to offer the oncological regimen. This concept encourages care teams to change their stances, replacing reactive approaches (modifying or suspending chemotherapy regimens) with proactive approaches (aimed at reducing cardiovascular risk and enabling the continuation of the antitumor regimen). Ultimately, the aim is to achieve a residual cardiovascular risk that is outweighed by the benefits of cancer treatment.[12]

The evidence supporting the PC approach is still scarce and has been published slowly, predominating in the scenario of HER2-positive breast cancer. It is important to underscore that PC is an exceptional approach and that eligible patients are not numerous on a daily basis; therefore, as is the case with rare diseases, it is not a condition that can easily be studied by robust clinical trials with large sample sizes. Table 2 summarizes the data from the experimental studies that are available to date.

These data, although they come from small, single-center, non-randomized studies, reveal the experience of groups who opted not to deprive patients of treatments that modified the natural history of their disease, resulting in a substantial increase in disease-free survival curves.[18]

The PC approach has also been applied in other contexts in oncology. Examples include situations of re-exposure to treatment after episodes of vasospasm with 5-fluorouracil,[19] after myocarditis related to immune checkpoint inhibitors,[20] or even after ventricular dysfunction with carfilzomib.[21] Reports and case series from some centers have demonstrated that strategies of introducing cardioprotective medications before infusion, modifying the route of administration, and adjusting the combination of oncological agents can be useful to ensure continuity of the proposed treatment.[19-21] In these situations, joint work with the CO specialist is fundamental.

Role of cardiovascular imaging in the implementation of the strategy of PC

Cardiovascular imaging tools are essential when implementing the strategy of PC, because they allow for the progressive monitoring of cardiac function during cancer treatment.[22] This monitoring provides information that is essential to decision-making regarding the viability and safety of maintaining antineoplastic treatment.

Among cardiovascular imaging methods, echocardiography stands out as a non-invasive, widely available, and low-cost method, which facilitates regular, serial use in cardiotoxicity monitoring programs. This method's accessibility allows for frequent use for cardiovascular monitoring, making it possible to adjust the therapeutic strategy in real time, which maximizes the efficacy of oncological treatment without compromising patient safety. In this manner, echocardiography has proven to be a valuable resource for the dynamic management of cardiovascular risk in patients who will be exposed to potentially cardiotoxic therapeutic regimens.[23]

Myocardial strain is a quantitative measure of deformation during the cardiac cycle, and it is a sensitive tool for detecting subclinical cardiac dysfunction (before LVEF is affected).[24] The ability to detect these early changes is crucial to the management of PC, as it allows early intervention (such as dose

Table 2 – Data from experimental studies on PC

Author and year	Design	Population	Sample	Results
Nowsheen S. et al, 2018[13]	Retrospective, case-control	Patients with HER-positive breast cancer exposed to trastuzumab	- 20 cases with baseline LVEF < 53% - 408 controls with LVEF ≥ 53%	Group with LVEF < 53% at baseline did not show a higher risk of decreased LVEF
Lynce F. et al, 2019[14] (SAFE-HEaRt Trial)	Prospective, single-arm	Patients with HER-positive breast cancer candidates for T-DM1 or trastuzumab with or without pertuzumab	- 31 patients with baseline LVEF between 40% and 49% - All treated with BB and ACEI	90% of patients completed the planned anti-HER treatment
Leong D. et al, 2019[15] (SCHOLAR Trial)	Prospective, single-arm	Patients with HER-positive breast cancer candidates for trastuzumab	- 20 patients with baseline LVEF between 40% and the lower limit or ≥ 15% drop in LVEF	90% of patients received all planned cycles without interruptions
Khoury K. et al, 2021[16] (SAFE-HEaRt Trial extended)	Prospective, single-arm	Patients with HER-positive breast cancer candidates for T-DM1 or trastuzumab with or without pertuzumab	- 23 cases from the original cohort (8 of them still in continuous anti-HER therapy for metastatic disease) - Follow-up of 42 months	- Improvement in mean LVEF from 44.9% (beginning of the study) to 52.1% (end of study) - 1 case of symptomatic heart failure
Zhou S. et al, 2023[17]	Retrospective, cohort	Patients with HER-positive breast cancer exposed to trastuzumab	- 51 patients managed with PC - Follow-up of 3 years	- 92% completed the treatment - 6% suspended trastuzumab due to severe/symptomatic ventricular dysfunction

ACEI: angiotensin-converting enzyme inhibitor; BB: beta blocker; HER: human epidermal growth factor; LVEF: left ventricular ejection fraction; T-DM1: ado-trastuzumab emtansine; PC: permissive cardiotoxicity.

adjustment or inclusion of cardioprotective drugs) while the patient continues oncological treatment. In clinical practice, a 15% reduction in global longitudinal strain in relation to the baseline value is considered indicative of possible subclinical cardiotoxicity, even in the absence of a decrease in LVEF.[24]

Permissive cardiotoxicity in practice: prerequisites and management strategies

The strategy of PC has not been studied with sufficient methodological rigor to design protocols and guidelines based on scientific data. However, reports of successful experiences and studies conducted in the area[13-17] suggest that some conditions must be met for the strategy to be conducted with due precaution and safety:

1. The concept of PC is applicable in cases of mild to moderate CTRCD (LVEF > 40%), provided that there are no severe symptoms (significant pulmonary congestion with worsening of the respiratory pattern; clinical, electrical, or hemodynamic instability; poor perfusion and/or signs of low output).

2. The strategy of PC applies to manageable cases of CTRCD (patients who have a window for the introduction of cardiovascular medications), always focusing on long-term cardiological safety.

3. It is mandatory to perform strict, regular monitoring of cardiac function during PC, preferably with the same professional and on the same device.

4. It is necessary to pre-define levels of cardiac dysfunction at which it is no longer safe to continue therapy. Routinely, continuation of PC is tolerated as long as LVEF is > 40%. This value varies according to LVEF at the beginning of PC, the magnitude of the drop in LVEF in relation to baseline, and the associated clinical repercussions.

The medical management of these cases should follow the recommendations of the current guidelines for the treatment of heart failure, respecting individual limitations related to the clinical/laboratory context of each case. Below, we will briefly discuss the medical management of CTRCD according to the most recent recommendations.[4,8]

It is suggested that, initially, priority should be given to the introduction of drugs studied for heart failure that also have specific evidence of cardioprotection in patients with cancer, such as beta blockers (BB) and angiotensin-converting enzyme inhibitors (ACEI) or angiotensin receptor blockers (ARBs). Carvedilol and enalapril are the medications with the highest number of favorable studies in CO, and they are the most commonly used medications in practice (although other BB and ACEI/ARB indicated for heart failure also have similar effects). The combination of BB and ACEI/ARB should be initiated at low doses, with progressive escalation up to the maximum tolerated doses. In the case of hypotension that limits concomitant initiation, each medication should be introduced individually; there is no defined order based on evidence, and the choice should be based on each case's characteristics and restrictions. Depending on the presence and degree of associated pulmonary congestion, the prescription of diuretics and/or mineralocorticoid antagonists may be indicated during this first stage of drug management. During a second stage, depending on the clinical response, functional class, presence (or absence) of residual symptoms, and tolerance (also related to laboratory alterations), it is possible to assess the need to add other first-line medications for the treatment of heart failure, with SGLT2 inhibitors and sacubitril/valsartan replacing ACEI or ARB.

The key points for implementing the strategy of PC are summarized in the Central Illustration.

Limitations and gaps in the literature

The strategy of PC has numerous limitations, the main one being the lack of robust scientific evidence to support its use. A borderline context for its implementation is the presence of pre-treatment ventricular dysfunction, since further worsening of LVEF can result in significant impairment. In these cases, drug optimization should be even more immediate and aggressive, and the search for the best oncological outcome should respect the premises of cardiovascular safety. Finally, it is important to underscore that it is not considered appropriate to institute PC in cases that have therapeutic alternatives with similar efficacy or in cases where treatment is optional (a decision that should be delegated exclusively to the oncologist).

Gaps still abound in the literature regarding PC. They include the lack of studies that explore long-term cardiovascular outcomes, the lack of guidelines and standardized protocols for identifying safe levels of ventricular dysfunction to be tolerated, and the identification of specific risk predictors that could help individualize the PC approach.

Conclusions

Correct implementation of the strategy of PC depends on a combination of solid technical expertise in CO, a proactive stance regarding early interventions, and clear and effective communication (involving a medical and multidisciplinary team, patients, and family members). The main objective of this strategy is to offer oncology patients the most effective treatment available, avoiding interruptions or suspension of medications that can save lives. PC seeks to change the mindset when addressing a cardiotoxic event, encouraging professionals to seek ways to maintain cancer treatment with the greatest possible cardiovascular safety.

When facing diagnosis of CTRCD, it is up to cardiologists to weigh, equate, and manage the various factors involved, so that the choice of the PC approach will be appropriate and bring benefits, rather than risks, to the patient. In order to do so, it is essential for the diverse professionals involved in providing care for patients with cancer to share, discuss, and study this topic.

Author Contributions

Conception and design of the research: Silva CMPDC; acquisition of data: Silva CMPDC, Seabra-Garcez JD, Neves APL; writing of the manuscript: Silva CMPDC, Seabra-Garcez JD, Macedo AVS; critical revision of the manuscript for intellectual content: Silva CMPDC, Macedo AVS.

Potential Conflict of Interest

No potential conflict of interest relevant to this article was reported.

Sources of Funding

There were no external funding sources for this study.

Study Association

This study is not associated with any thesis or dissertation work.

Ethics Approval and Consent to Participate

This article does not contain any studies with human participants or animals performed by any of the authors.

References

1. Rache B, Rocha R, Medeiros LA, Okada LM, Ferrari G, Zeng H, et al. Transition Towards Cancer Mortality Predominance Over Cardiovascular Disease Mortality in Brazil, 2000-2019: A Population-Based Study. Lancet Reg Health Am. 2024;39:100904. doi: 10.1016/j.lana.2024.100904.
2. Masoudkabir F, Mohammadifard N, Mani A, Ignaszewski A, Davis MK, Vaseghi G, et al. Shared Lifestyle-Related Risk Factors of Cardiovascular Disease and Cancer: Evidence for Joint Prevention. ScientificWorldJournal. 2023;2023:2404806. doi: 10.1155/2023/2404806.
3. Karlstaedt A, Moslehi J, de Boer RA. Cardio-Onco-Metabolism: Metabolic Remodelling in Cardiovascular Disease and Cancer. Nat Rev Cardiol. 2022;19(6):414-25. doi: 10.1038/s41569-022-00698-6.
4. Marcondes-Braga FG, Moura LAZ, Issa VS, Vieira JL, Rohde LE, Simões MV, et al. Emerging Topics Update of the Brazilian Heart Failure Guideline - 2021. Arq Bras Cardiol. 2021;116(6):1174-212. doi: 10.36660/abc.20210367.
5. Singal PK, Iliskovic N. Doxorubicin-Induced Cardiomyopathy. N Engl J Med. 1998;339(13):900-5. doi: 10.1056/NEJM199809243391307.
6. Chung R, Ghosh AK, Banerjee A. Cardiotoxicity: Precision Medicine with Imprecise Definitions. Open Heart. 2018;5(2):e000774. doi: 10.1136/openhrt-2018-000774.
7. Zamorano JL, Lancellotti P, Muñoz DR, Aboyans V, Asteggiano R, Galderisi M, et al. 2016 ESC Position Paper on Cancer Treatments and Cardiovascular Toxicity Developed under the Auspices of the ESC Committee for Practice Guidelines: The Task Force for Cancer Treatments and Cardiovascular Toxicity of the European Society of Cardiology (ESC). Eur Heart J. 2016;37(36):2768-801. doi: 10.1093/eurheartj/ehw211.
8. McDonagh TA, Metra M, Adamo M, Gardner RS, Baumbach A, Böhm M, et al. 2023 Focused Update of the 2021 ESC Guidelines for the Diagnosis and Treatment of Acute and Chronic Heart Failure. Eur Heart J. 2023;44(37):3627-39. doi: 10.1093/eurheartj/ehad195.
9. Sardesai S, Sukumar J, Kassem M, Palettas M, Stephens J, Morgan E, et al. Clinical Impact of Interruption in Adjuvant Trastuzumab Therapy in Patients with Operable HER-2 Positive Breast Cancer. Cardiooncology. 2020;6(1):26. doi: 10.1186/s40959-020-00081-9.
10. Yu AF, Yadav NU, Eaton AA, Lung BY, Thaler HT, Liu JE, et al. Continuous Trastuzumab Therapy in Breast Cancer Patients with Asymptomatic Left Ventricular Dysfunction. Oncologist. 2015;20(10):1105-10. doi: 10.1634/theoncologist.2015-0125.
11. Solomon SB, Bellavia L, Sweeney D, Piknova B, Perlegas A, Helms CC, et al. Angeli's Salt Counteracts the Vasoactive Effects of Elevated Plasma

Hemoglobin. Free Radic Biol Med. 2012;53(12):2229-39. doi: 10.1016/j.freeradbiomed.2012.10.548.

12. Porter C, Azam TU, Mohananey D, Kumar R, Chu J, Lenihan D, et al. Permissive Cardiotoxicity: The Clinical Crucible of Cardio-Oncology. JACC CardioOncol. 2022;4(3):302-12. doi: 10.1016/j.jaccao.2022.07.005.

13. Nowsheen S, Aziz K, Park JY, Lerman A, Villarraga HR, Ruddy KJ, et al. Trastuzumab in Female Breast Cancer Patients with Reduced Left Ventricular Ejection Fraction. J Am Heart Assoc. 2018;7(15):e008637. doi: 10.1161/JAHA.118.008637.

14. Lynce F, Barac A, Geng X, Dang C, Yu AF, Smith KL, et al. Prospective Evaluation of the Cardiac Safety of HER2-Targeted Therapies in Patients with HER2-Positive Breast Cancer and Compromised Heart Function: The SAFE-HEaRt Study. Breast Cancer Res Treat. 2019;175(3):595-603. doi: 10.1007/s10549-019-05191-2.

15. Leong DP, Cosman T, Alhussein MM, Kumar Tyagi N, Karampatos S, Barron CC, et al. Safety of Continuing Trastuzumab Despite Mild Cardiotoxicity: A Phase I Trial. JACC CardioOncol. 2019;1(1):1-10. doi: 10.1016/j.jaccao.2019.06.004.

16. Khoury K, Lynce F, Barac A, Geng X, Dang C, Yu AF, et al. Long-Term Follow-Up Assessment of Cardiac Safety in SAFE-HEaRt, a Clinical Trial Evaluating the Use of HER2-Targeted Therapies in Patients with Breast Cancer and Compromised Heart Function. Breast Cancer Res Treat. 2021;185(3):863-8. doi: 10.1007/s10549-020-06053-y.

17. Zhou S, Cirne F, Chow J, Zereshkian A, Bordeleau L, Dhesy-Thind S, et al. Three-Year Outcomes Following Permissive Cardiotoxicity in Patients on Trastuzumab. Oncologist. 2023;28(9):712-22. doi: 10.1093/oncolo/oyad086.

18. Slamon DJ, Leyland-Jones B, Shak S, Fuchs H, Paton V, Bajamonde A, et al. Use of Chemotherapy Plus a Monoclonal Antibody Against HER2 for Metastatic Breast Cancer that Overexpresses HER2. N Engl J Med. 2001;344(11):783-92. doi: 10.1056/NEJM200103153441101. P

19. Desai A, Mohammed T, Patel KN, Almnajam M, Kim AS. 5-Fluorouracil Rechallenge after Cardiotoxicity. Am J Case Rep. 2020;21:e924446. doi: 10.12659/AJCR.924446.

20. Inno A, Roviello G, Ghidini A, Luciani A, Catalano M, Gori S, et al. Rechallenge of Immune Checkpoint Inhibitors: A Systematic Review and Meta-Analysis. Crit Rev Oncol Hematol. 2021;165:103434. doi: 10.1016/j.critrevonc.2021.103434.

21. Bishnoi R, Xie Z, Shah C, Bian J, Murthy HS, Wingard JR, et al. Real-World Experience of Carfilzomib-Associated Cardiovascular Adverse Events: SEER-Medicare Data Set Analysis. Cancer Med. 2021;10(1):70-8. doi: 10.1002/cam4.3568.

22. Lancellotti P, Nkomo VT, Badano LP, Bergler-Klein J, Bogaert J, Davin L, et al. Expert Consensus for Multi-Modality Imaging Evaluation of Cardiovascular Complications of Radiotherapy in Adults: A Report from the European Association of Cardiovascular Imaging and the American Society of Echocardiography. Eur Heart J Cardiovasc Imaging. 2013;14(8):721-40. doi: 10.1093/ehjci/jet123.

23. Melo MDT, Paiva MG, Santos MVC, Rochitte CE, Moreira VM, Saleh MH, et al. Brazilian Position Statement on the Use Of Multimodality Imaging in Cardio-Oncology - 2021. Arq Bras Cardiol. 2021;117(4):845-909. doi: 10.36660/abc.20200266.

24. Almeida ALC, Melo MDT, Bihan DCSL, Vieira MLC, Pena JLB, Del Castillo JM, et al. Position Statement on the Use of Myocardial Strain in Cardiology Routines by the Brazilian Society of Cardiology's Department Of Cardiovascular Imaging - 2023. Arq Bras Cardiol. 2023;120(12):e20230646.. doi: 10.36660/abc.20230646.

Pericardial Agenesis: When Should This Diagnosis Be Considered?

Bruna Barbosa Chagas de Almeida,[1] Bruna Zanforlin Jácome,[1] Bernardo Nascimento Lourenço,[1] Alessandro Zakhia de Seixas,[1,2] Juliana Serafim da Silveira,[1,2] Eliza de Almeida Gripp[1,2]

Universidade Federal Fluminense,[1] Niterói, RJ – Brazil

Hospital Pró-cardiaco,[2] Rio de Janeiro, RJ – Brazil

Central Illustration: Pericardial Agenesis: When Should This Diagnosis Be Considered?

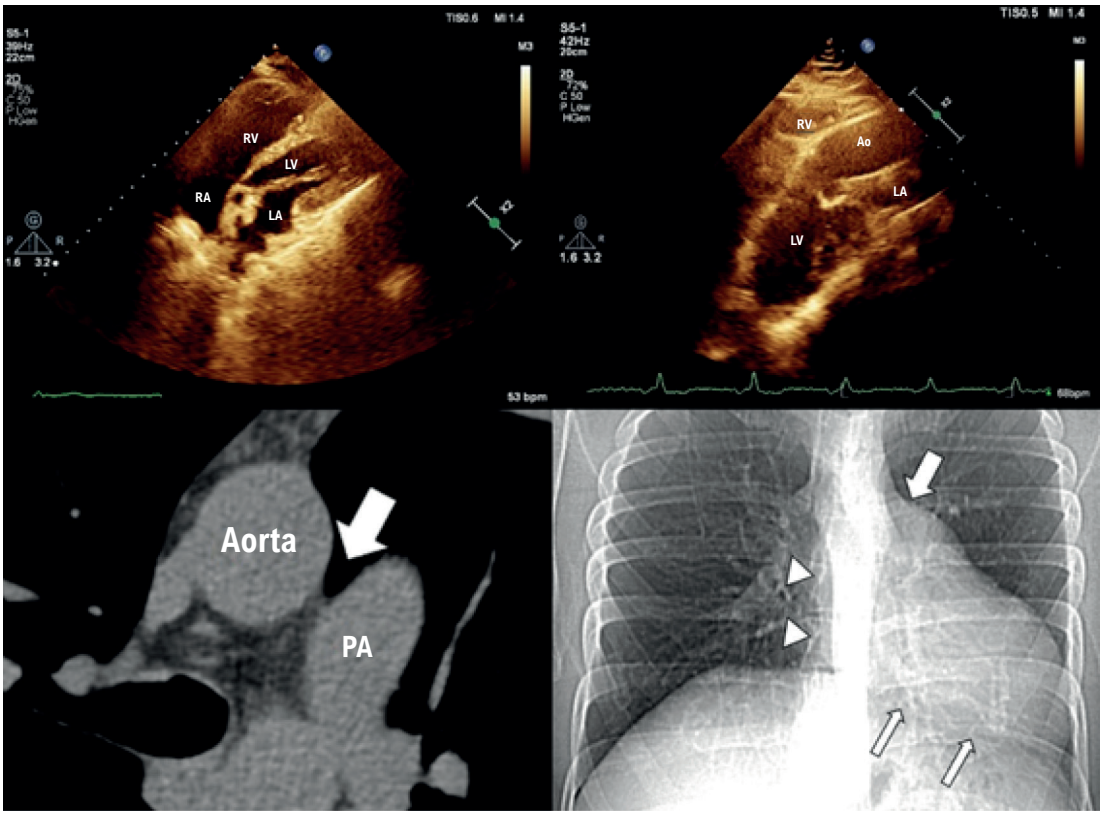

Arq Bras Cardiol: Imagem cardiovasc. 2025;38(1):e20250004

The importance of multimodality in the diagnosis of PA. Ao: aorta; PA: pericardial agenesis; LV: left ventricle; RV: right ventricle; LA: left atrium.

Keywords

Pericardium; Pericarditis; X-Ray Computed Tomography; Magnetic Resonance Imaging

Mailing Address: Eliza de Almeida Gripp •
Hospital Pró-Cardíaco. Rua General Polidoro, 192. Postal code: 22280-020. Botafogo, Rio de Janeiro, RJ – Brazil
E-mail: elizagripp@yahoo.com.br
Manuscript received January 29, 2025; revised January 30, 2025; accepted February 3, 2025
Editor responsible for the review: Marcelo Tavares

DOI: https://doi.org/10.36660/abcimg.20250004i

Abstract

Pericardial agenesis (PA) is a rare condition characterized by the partial or complete absence of the pericardium. The consequences associated with this condition can be quite serious. Therefore, understanding the peculiarities of this disease is essential for accurate diagnosis and treatment.

Introduction

PA prevalence is estimated at approximately 0.002% to 0.004% in the general population, often diagnosed incidentally.[1] Studies indicate that this condition occurs more frequently in

males, with a 3:1 ratio between males and females, and may be associated with other congenital anomalies.[2]

Although there is no specific gene directly responsible for the PA, this disease is associated with several genetic anomalies and structural congenital malformations,[2] which suggests a possible genetic predisposition.[2]

The consequences associated with this diagnosis can be serious and include ventricular herniation (which occurs in partial agenesis) and sudden death. To know the peculiarities of such disease is crucial, as the symptoms are nonspecific. Imaging tests such as chest X-ray, Doppler echocardiogram, computed tomography (CT), and cardiac magnetic resonance imaging (CMRI) play a key role in confirming the diagnosis (Central Illustration).

Embryogenesis

The pericardium is formed by the visceral and the parietal layers. It acts as a barrier against infections, maintaining the heart in a stable position and limiting cardiac volume.[3] It is innervated by the phrenic nerve, whose nociceptors are involved in pericardial pain transmission reflexes, and secretes prostaglandins and similar substances that modulate coronary tone and neural traffic.[3]

In the first week of fetal development, cavities are formed, which permeate the mesodermal tissue, which will later unite to form three primitive cavities: pericardium, peritoneum, and pleura.[4]

During the fourth week of gestation, a fragment of the mesoderm (transverse septum) separates the primitive pericardium from the peritoneum.[5] This separation completes between the fourth and fifth weeks when the right and left pleuropericardial membranes fuse, driven by the growth of the Ducts of Cuvier (common cardinal veins).[5,6] The pleuropericardial membrane later forms the fibrous pericardium. Failure in the closure of these membranes results in partial or total PA.[4]

One of the theories to explain AP is that the developing heart would stretch the pericardium. If the pleuropericardial membranes do not fuse before the heart enlarges, a pericardial defect is generated.[7] Another theory proposes that a traction-induced tear may develop in the pleuropericardial membrane, resulting in pericardial defect.[7] To illustrate this situation, Kaneko et al. describe a case of pericardial absence associated with the division of the phrenic nerve with its two bundles passing ventrally and dorsally to the defect.[8]

A third hypothesis suggests that pericardial membrane development fails due to premature atrophy of the cardinal veins (duct of Cuvier), which supply the pleuropericardial folds.[7,9] This theory explains the rarity of right-sided pericardial defects, as the right cardinal vein remains as the superior vena cava.[9] A percentage of pericardial defects may be attributed to each of these mechanisms.

Classification

PA is a rare anomaly that can be classified as total or partial based on the extent of pericardial absence. This condition results from failures in embryonic development, specifically during fusion of the pleuropericardial primordia.[7] Its classification is based primarily on the extent of the pericardium absence, in addition to its clinical and anatomical implications (Table 1).[10,11] The main categories are:

Total agenesis:

- Complete absence of the pericardium.
- The heart may have an abnormal position in the thorax (levoposition) and greater mobility.
- It is usually asymptomatic, but may be associated with a left side displacement of the heart and an increased risk of cardiac torsion.

Partial agenesis:

- Usually involves the absence of the left or right portion of the pericardium, with the first one being more common.
- It may cause herniation or strangulation of cardiac structures, leading to more serious complications.
- It is more associated with symptoms, such as chest pain or arrhythmias, due to compression or herniation of cardiac structures through the pericardial defect.

Circumscribed or localized defects:

- A subtype of partial agenesis affecting specific areas, such as the pericardium over the left atrium or the great vessels. Small defects in the pericardium, which may allow protrusion of structures such as the atrium or ventricle.

Clinical Presentation

The clinical presentation of PA is often heterogeneous, ranging from nonspecific symptoms to fatal complications. Although it is commonly asymptomatic, precordial pain

Table 1 – Prevalence, complications, and symptoms by category of PA.[8, 10-15]

	Partial on the right or left	Complete bilateral	Complete on the right	Complete on the left
Prevalence	3–4%	9%	17%	70%
Complications	Frequent	Rare	Rare	Rare
Symptoms	Chest pain, dyspnea, arrhythmias	Asymptomatic in most cases	Asymptomatic or with mild symptoms	Generally asymptomatic
Published cases	Balaji A et al.[12]	Pedrotti P et al.[13]	Minocha GK et al.[14]	Kaneko Y et al.[8]

may occur and is the most common symptom, followed by palpitations.[16-18] Other symptoms attributed to PA, such as dyspnea, trepopnea (dyspnea related to the side on which one lies, which is a characteristic feature of partial defects), arrhythmias (sick sinus syndrome and syncope are probably due to increased vagal tone or intermittent atrial herniation, which resolves with atropine or changing to lateral decubitus), and dizziness, are signs and symptoms normally attributed to increased cardiac mobility, anomalous heart positioning and herniation of cardiac tissue.[7,17] Moreover, increased cardiac mobility may produce a displaced and vigorous apical impulse, leading to the impression of cardiomegaly.[19] Patients with complete defects may present with precordial pain due to pleuropericardial adhesions, absence of the pericardial cushion, and torsion of the great vessels.[20]

The most severe documented manifestation is sudden death, caused by strangulation of the heart through an incomplete pericardium, as observed in patients with partial defects.[21] Strangulation typically leads to regional myocardial ischemia, resulting in precordial pain and electrocardiographic changes.[22] Cardiac displacement may cause severe tricuspid regurgitation due to the stretching of the anterior wall of the right ventricle (RV).[23]

Although rare, PA should be considered in the differential diagnosis of patients with atypical cardiovascular symptoms that are unusual for their age, particularly when echocardiographic images are acquired from nonstandard locations. Early identification is essential to avoid more serious complications and direct appropriate clinical management. Differential diagnoses of PA include post-surgical or post-traumatic defects, the latter after blunt thoracic trauma, which may result in pericardial rupture, herniation, and torsion of the cardiac cavities.[24]

Diagnosis: The role of multimodality

Chest X-ray

Chest X-ray may be altered in large pericardial defects, where the cardiac silhouette is displaced excessively to the left in the posteroanterior projection, and posteriorly in relation to the mediastinum. There is a loss of the right border of the heart, which overlaps the spine. Radiolucency and increased distance between the aorta and pulmonary artery, as well as between the lower heart border and diaphragm, occur due to lung tissue insinuation into these areas. The "Snoopy Sign" refers to leftward cardiac displacement, elongation of the left heart border with a rounded apex resembling Snoopy's nose, and prominence and convexity of the left atrial appendage resembling Snoopy's ear (Figure 1).[25]

Doppler echocardiogram

The Doppler echocardiogram is a widely-available non-invasive, low-cost exam and the first-line choice in the diagnostic suspicion not only for AP, but also for the evaluation of pericardial diseases.[26]

The first indication suggesting agenesis during examination relates to image acquisition in nonstandard positions due to abnormal cardiac positioning (Figures 2A and 2B). In the long parasternal plane, the apex deviates posteriorly, revealing a large segment of the RV, creating an impression of cavity enlargement[7,27] (Figures and Videos 1 and 2). The acquisition of the apical 4-chamber plane will occur beyond or in the posterior midclavicular line, different from the commonly located in the 5th intercostal space, in the mid-midclavicular line. (Figure and Video 3 and 4).

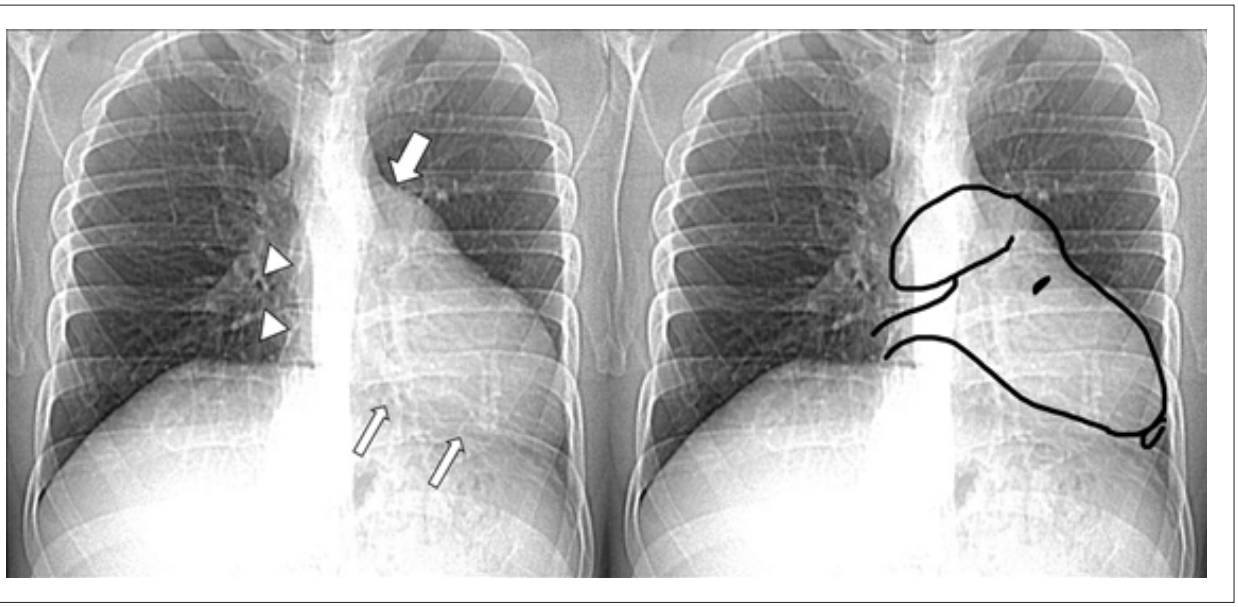

Figure 1 – *The "Snoopy sign" on chest radiography is composed of multiple abnormalities, namely: excessive levoposition with elongation of the LV edge, radiolucency separating the aorta and pulmonary artery (thick arrow), radiolucency separating the LV and diaphragm (thin arrows), and loss of the right edge of the heart (arrowheads).*

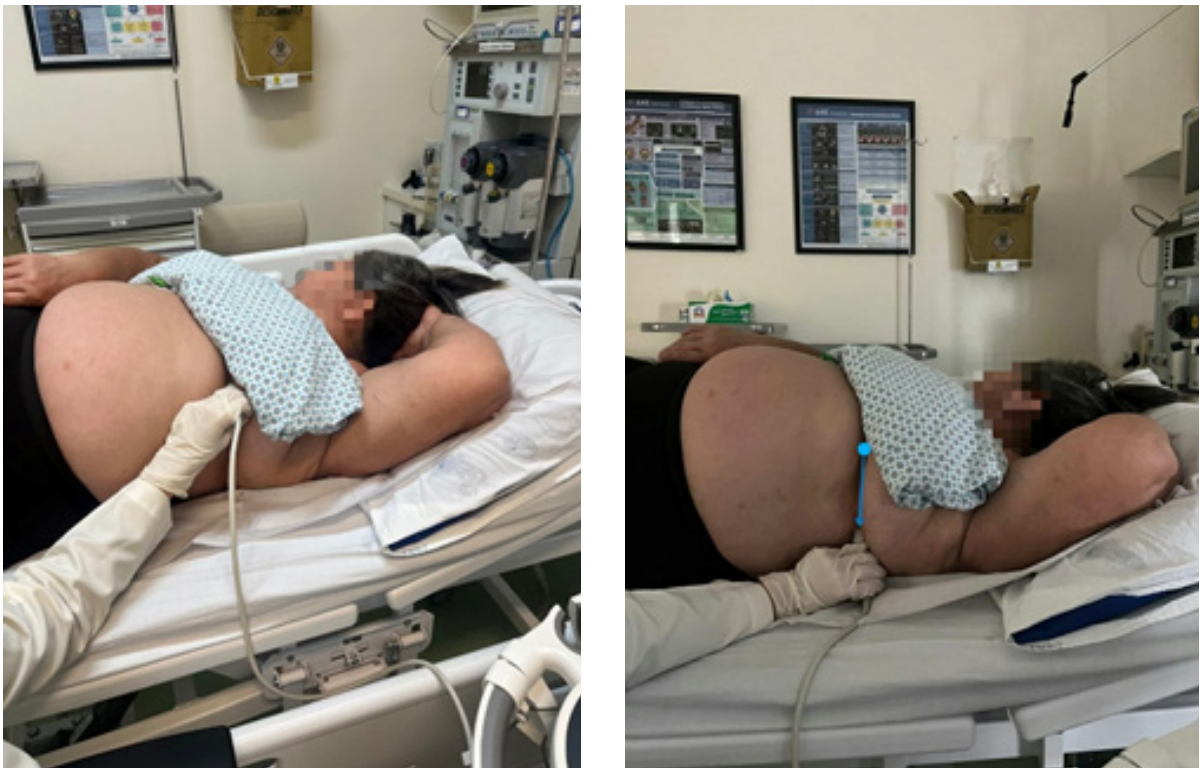

Figure 2 – *A) This image illustrates the positioning of the transducer on the patient, where the apical 4-chamber plane would normally be located. B) In partial PA, note the significant displacement through the inserted line (blue), from the site to the new location of the apical 4-chamber plane.*

In cases of left partial PA, 63% of patients present an apparent RV enlargement due to leftward cardiac displacement.[28] This finding can lead to a misdiagnosis of interatrial communication or arrhythmogenic cardiomyopathy. Additional findings relating to PA include exaggerated cardiac motion and paradoxical ventricular septum movement due to increased inferior wall motion. A teardrop-shaped heart results from atrial elongation, ventricular widening, and inferior wall bulging.[2,7,28] Right-sided agenesis may lead to RV and right atrium (RA) enlargement, along with severe tricuspid regurgitation due to chordal traction. Stress Doppler echocardiography may demonstrate a pendulum-like movement of the heart. Another significant spectral Doppler finding is reduced systolic flow and a lower systolic-diastolic ratio in the pulmonary vein as a result of the absence of negative intrapericardial pressure.[26]

However, this method depends on the quality of the acoustic window, especially in obese patients or those with lung disease.[26]

CT

CT imaging, with its high resolution and volumetric acquisition, provides excellent contrast between the pericardium's dense thin line and the low-density epicardial and mediastinal fat, making it highly effective for pericardial delineation. However, some pericardial segments in the left silhouette of the heart may be poorly delimited, even when present.

On CT, PA can be confirmed by the partial or complete absence of the thin dense line corresponding to the pericardium around the heart. There is excessive levoposition of the heart, which touches the rib cage. There may be an absence of hypodense fatty tissue between the myocardium and the costal arches. There is insinuated lung tissue between the aorta and the pulmonary arterial trunk, a site commonly covered by pericardium and containing fatty tissue that obliterates this space. Occasionally, there is bulging of the left atrial appendage through the defect (Figure 5).[28]

CMRI

CMRI is currently the gold standard for pericardial assessment thanks to its superior spatial resolution and inherent tissue characterization. T1- and T2-weighted "black blood" morphological acquisitions and cine steady-state-free-precession (SSFP) functional acquisitions are useful for delimiting the hypointense linear image corresponding to the pericardium, between the mediastinal and epicardial fat with hyperintense signal. However, similar to CT, some segments of the pericardium adjacent to the left ventricle (LV) may be difficult to individualize

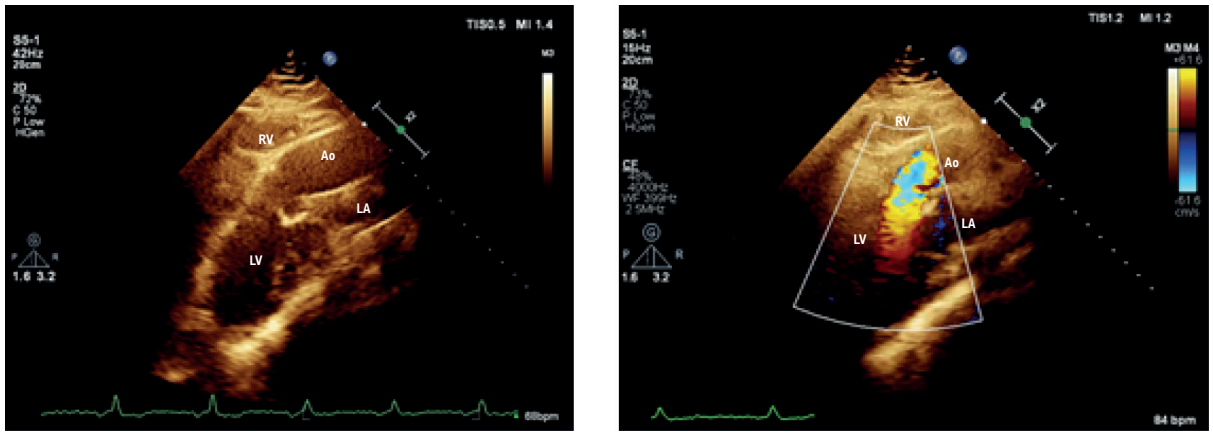

Figure 3 – *A) Visualization of the completely distorted longitudinal parasternal plane, with the apex deviated posteriorly (videos attached). B) The flow through the LV outflow tract confirms the position of the ascending aorta, LV and LA in a patient with partial PA. Ao: aorta; LV: left ventricle; RV: right ventricle; LA: left atrium.*

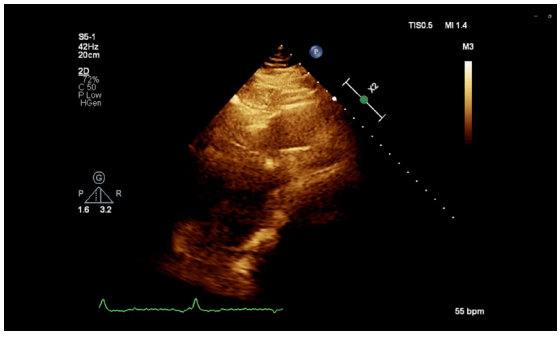

Video 1 – *Visualization of the completely distorted longitudinal parasternal plane, with the apex deviated posteriorly. Link: http://abcimaging.org/supplementary-material/2025/3801/2025-0004_video_1.mp4*

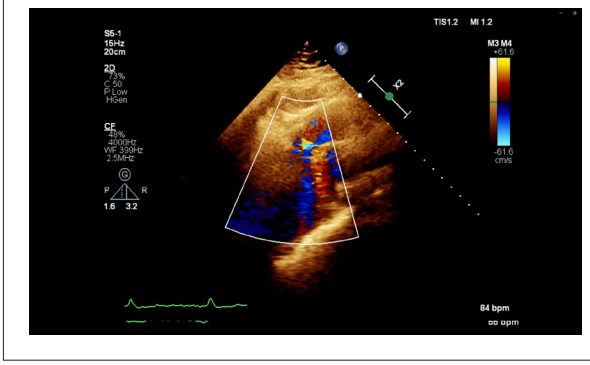

Video 2 – *The flow through the LV outflow tract confirms the position of the ascending aorta, LV and LA in a patient with partial PA. Link: http://abcimaging.org/supplementary-material/2025/3801/2025-0004_video_2.mp4*

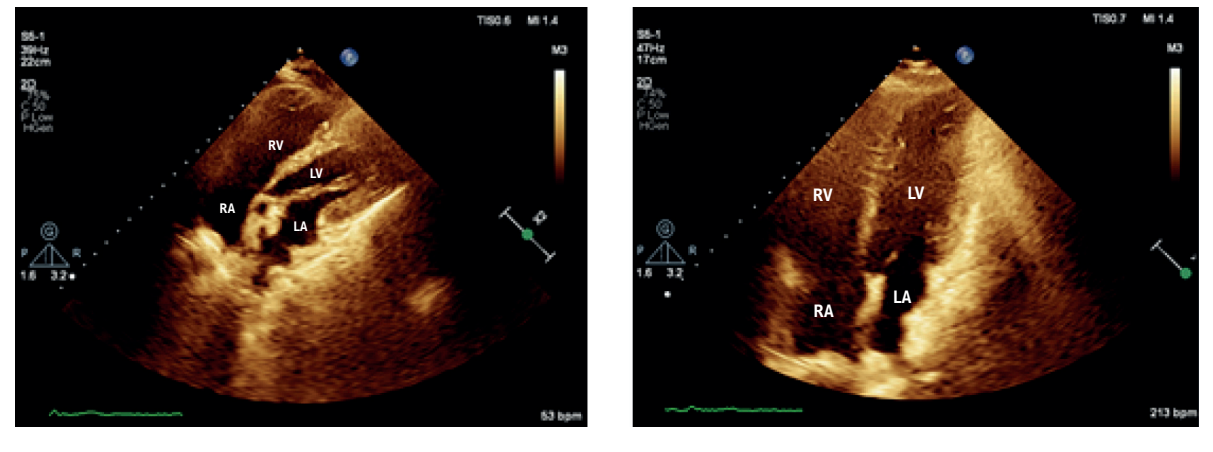

Figure 4 – *A) Case of partial PA showing the impression of enlarged right cavities due to the deviation caused by partial left agenesis (video attached). B) Case of partial PA showing the teardrop-like appearance of the heart (video attached). LV: left ventricle; RV: right ventricle; RA: right atrium; LA: left atrium.*

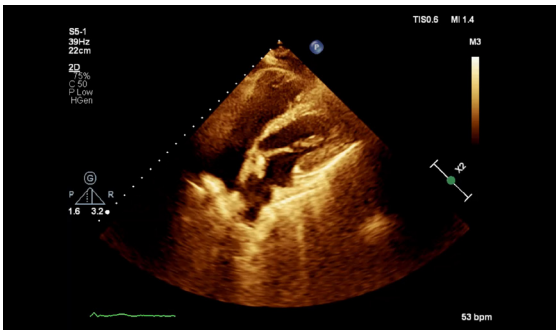

Video 3 – *Case of partial PA showing the impression of enlarged right cavities due to the deviation caused by partial left agenesis. Link: http://abcimaging.org/supplementary-material/2025/3801/2025-0004_video_3.mp4*

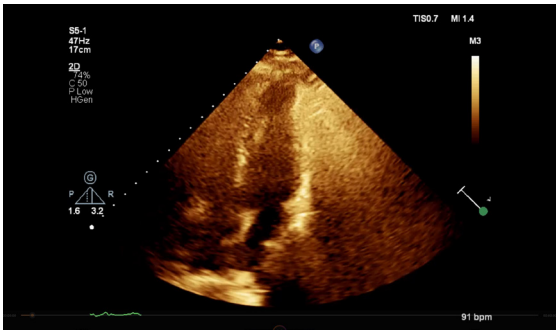

Video 4 – *Case of partial PA showing the teardrop-like appearance of the heart. Link: http://abcimaging.org/supplementary-material/2025/3801/2025-0004_video_4.mp4*

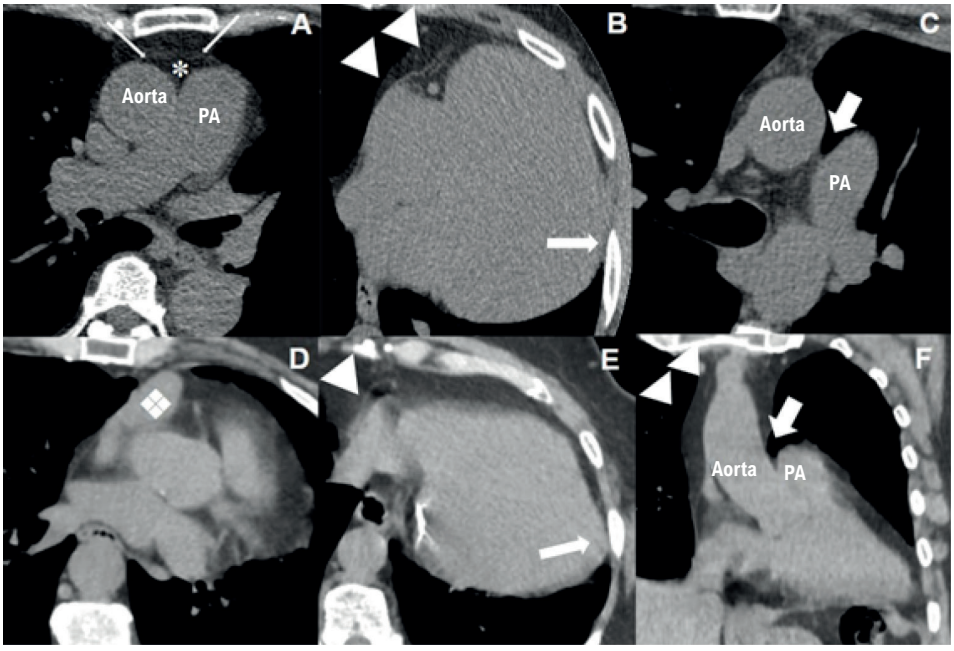

Figure 5 – *A) The non-contrast CT in the axial plane demonstrates the normal anatomy of the pericardium (thin arrows) outlining the fatty tissue (✻) between the aorta and the pulmonary trunk. (B-F) Non-contrast CT images in two patients with partial left pericardial agenesis, respectively, ♂, 41 years (B/C), and ♀, 58 years (D-F). The absence of pericardial covering is observed over almost the entire extent, visible only along the right atrial border (arrowheads in B, D, and E). There is excessive leftward positioning of the heart and posterior deviation of the apex touching the chest wall (thin arrows in B and E). D) Projection of the right atrial appendage (❖). (C/F) Lung interposition between the aorta and the pulmonary trunk (thick arrows). AP: pericardial agenesis.*

by the method. The absence of pericardial visualization, combined with excessive leftward cardiac displacement, hypermobility (particularly of the posterior LV wall), and lung interposition between the aorta and pulmonary trunk, are CMRI diagnostic criteria for PA (Figure 6). The presence of focal indentations in the ventricular walls suggests the presence of partial PA.[2, 28]

Treatment

Watchful waiting is the preferred approach for most patients with PA, as the majority remain asymptomatic.[26] Surgical treatment relies on small, uncontrolled observational studies.[26]

Surgical intervention (Table 2) is recommended for symptomatic patients with high-risk complicated partial defects or refractory symptoms, such as pain caused by abnormal cardiac motion.[10] Left partial defects presenting with compression, herniation, or strangulation of major vessels or coronary arteries also warrant surgical consideration.[29]

Recently, the detection of high-risk anatomic features by multimodal cardiovascular imaging, including (1) LV myocardial fold or hinge point on echocardiography, CMR, or

CT; (2) coronary compression on CT; (3) inducible ischemia on stress perfusion imaging – Single Photon Emission Computed Tomography (SPECT), Positron Emission Tomography (PET) or CMR – and (4) evidence of left atrial appendage herniation have been proposed for risk stratification.[30] Detection of these red flags can be used to tailor surgical planning.

Specific surgical options for pericardial defects vary, with pericardioplasty being the most common procedure. As an alternative to pericardial reconstruction, pericardiectomy with pericardioplasty, to enlarge the defect and prevent strangulation, has also been described.

Author Contributions

Conception and design of the research and acquisition of data: Almeida BBC, Jácome BZ, Lourenço BN, Gripp EA; analysis and interpretation of the data and statistical analysis: Gripp EA; writing of the manuscript and critical revision of the manuscript for intellectual content: Almeida BBC, Jácome BZ, Lourenço BN, Seixas AZ, Silveira JS, Gripp EA.

Potential Conflict of Interest

No potential conflict of interest relevant to this article was reported.

Sources of Funding

There were no external funding sources for this study.

Study Association

This study is not associated with any thesis or dissertation work.

Ethics Approval and Consent to Participate

This article does not contain any studies with human participants or animals performed by any of the authors.

Table 2 – Relationship between surgical intervention, possible indications and complications.[7,15]

Surgical interventions	Possible indications	Potential complications
Pericardioplasty	Major congenital defects	Failure to correct the defect
Pericardiectomy with pericardioplasty	Risk of strangulation	Formation of pericardial adhesions
Left atrial appendage resection/ligation	Left atrial appendage herniation	Damage to adjacent structures
Right atrial appendage correction	Right atrial appendage herniation	Right atrial appendage rupture
Video-assisted thoracic surgery (VATS)	Pneumopericardium/pneumothorax	Perforation of thoracic structures

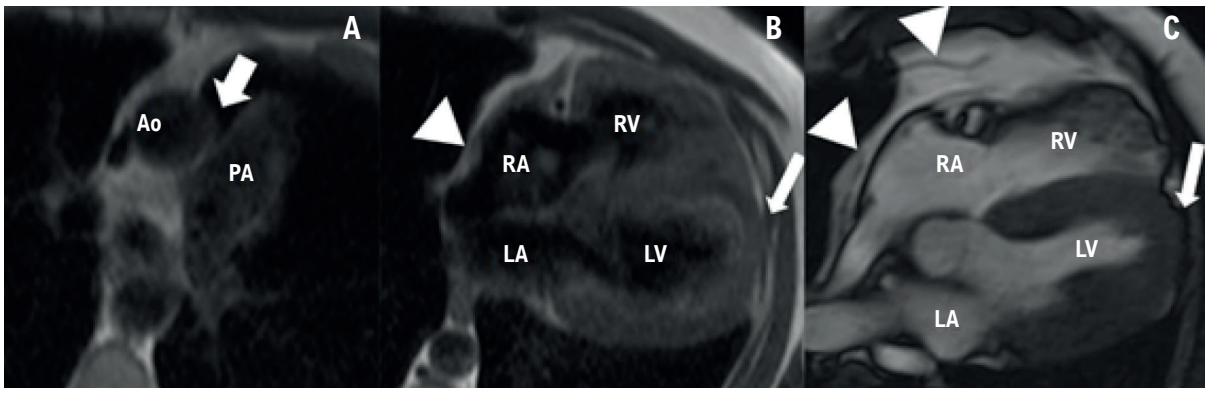

Figure 6 – *Black-blood T2-weighted CMR images in the axial plane (A,B) and cine SSFP (C) in a patient with left partial PA. A) Interposition of lung tissue between the aorta and pulmonary artery (thick arrow). (B,C) The pericardium is partially visible as a thin hypointense line along the right atrial border (arrowheads in B and C). It is observed excessive levoposition of the heart and posterior deviation of the apex, touching the rib cage (thin arrows in B and C). PA: pericardial agenesis; LV: left ventricle; RV: right ventricle; RA: right atrium; LA: left atrium: Ao: Aorta.*

References

1. Rayamajhi S, Shrestha R, Shahi K, Adhikari B, Mahaseth A. Congenital Pericardial Agenesis Presenting as Non-Specific Chest Pain: A Case Report. Radiol Case Rep. 2022;17(12):4462-5. doi: 10.1016/j.radcr.2022.08.075.
2. Abbas AE, Appleton CP, Liu PT, Sweeney JP. Congenital Absence of the Pericardium: Case Presentation and Review of Literature. Int J Cardiol. 2005;98(1):21-5. doi: 10.1016/j.ijcard.2003.10.021.

3. Mann DL, Zipes DP, Libby P, Bonow RO, editors. Braunwald's Heart Disease: A Textbook of Cardiovascular Medicine. 10th ed. Philadelphia: Elsevier Saunders; 2015.

4. Faridah Y, Julsrud PR. Congenital Absence of Pericardium Revisited. Int J Cardiovasc Imaging. 2002;18(1):67-73. doi: 10.1023/a:1014350814067.

5. Parmar YJ, Shah AB, Poon M, Kronzon I. Congenital Abnormalities of the Pericardium. Cardiol Clin. 2017;35(4):601-14. doi: 10.1016/j.ccl.2017.07.012.

6. Kronzon I. Introduction to Pericardial Diseases. In: Lang RM, Goldstein SA, Krozon I, Khandheria BK, Saric M, Mor-Avi V, editors. ASE's Comprehensive Echocardiography. 2nd ed. Philadelphia: Elsevier Health Sciences; 2016. p. 593-5.

7. Khayata M, Haouzi AA, Asher CR, Xu B. Multimodality Imaging Approach Evaluation of the Congenital Pericardial Defect: A Contemporary Review. Curr Cardiol Rep. 2023;25(12):1715-24. doi: 10.1007/s11886-023-02004-3.

8. Kaneko Y, Okabe H, Nagata N. Complete Left Pericardial Defect with Dual Passage of the Phrenic Nerve: A Challenge to the Widely Accepted Embryogenic Theory. Pediatr Cardiol. 1998;19(5):414-7. doi: 10.1007/s002469900338.

9. Koo CW, Newburg A. Congenital Absence of the Right Pericardium: Embryology and Imaging. J Clin Imaging Sci. 2015;5:12. doi: 10.4103/2156-7514.152338.

10. Lopez D, Asher CR. Congenital Absence of the Pericardium. Prog Cardiovasc Dis. 2017;59(4):398-406. doi: 10.1016/j.pcad.2016.12.002.

11. Xu B, Betancor J, Asher C, Rosario A, Klein A. Congenital Absence of the Pericardium: A Systematic Approach to Diagnosis and Management. Cardiology. 2017;136(4):270-8. doi: 10.1159/000452441.

12. Balaji A, Makam R, Hussein N, Loubani M. Congenital Absence of Pericardium: A Case Report and Technical Considerations in Cardiac Surgery. Cureus. 2024;16(3):e56885. doi: 10.7759/cureus.56885.

13. Pedrotti P, Peritore A, Cereda A, Giannattasio C, Imazio M. Total Pericardial Agenesis Mimicking Arrhythmogenic Right Ventricular Dysplasia. J Cardiovasc Med. 2016;17(Suppl 2):e216-e217. doi: 10.2459/JCM.0000000000000425.

14. Minocha GK, Falicov RE, Nijensohn E. Partial Right-Sided Congenital Pericardial Defect with Herniation of Right Atrium and Right Ventricle. Chest. 1979;76(4):484-6. doi: 10.1378/chest.76.4.484.

15. Cipriano A, Brunetti G, Bernardinello V, Baritussio A. Congenital Pericardial Agenesis. Expert Analysis [Internet]. Washington: American College of Cardiology: 2020 [cited 2025 07 Feb]. Available from: https://www.acc.org/Latest-in-Cardiology/Articles/2020/07/27/09/25/Congenital-Pericardial-Agenesis.

16. Glover LB, Barcia A, Reeves TJ. Congenital Absence of the Pericardium. A Review of the Literature with Demonstration of a Previously Unreported Fluoroscopic Finding. Am J Roentgenol Radium Ther Nucl Med. 1969;106(3):542-9.

17. Baim RS, MacDonald IL, Wise DJ, Lenkei SC. Computed Tomography of Absent Left Pericardium. Radiology. 1980;135(1):127-8. doi: 10.1148/radiology.135.1.7360949.

18. Nasser WK. Congenital Absence of the Left Pericardium. Am J Cardiol. 1970;26(5):466-70. doi: 10.1016/0002-9149(70)90703-4.

19. Ellis K, Leeds NE, Himmelstein A. Congenital Deficiencies in the Parietal Pericardium: A Review with 2 New Cases Including Successful Diagnosis by Plain Roentgenography. Am J Roentgenol Radium Ther Nucl Med. 1959;82(1):125-37.

20. Kojima S, Nakamura T, Sugiyama S, Sakamoto T, Yoshimura M, Arima T, et al. Cardiac Displacement with a Congenital Complete Left-Sided Pericardial Defect in a Patient with Exertional Angina Pectoris - A Case Report. Angiology. 2004;55(4):445-9. doi: 10.1177/000331970405500412.

21. Parchake MB, Pathak H, Vidhate S, Sukhadeve R, Tumram N, Kamble R. Sudden Death Due to Lethal Strangulation of Heart by Congenital Partial Pericardium. Egypt J Forensic Sci. 2016;6(4):520–3. doi: 10.1016/j.ejfs.2016.06.002.

22. Rice BJ, Espinosa SM, Parikh P, Pollak, P. ST-Elevation Myocardial Infarction Caused by Herniation of the Left Ventricle through a Partial Pericardial Defect. J Am Coll Cardiol. 2023;81(8 Suppl):2414. doi:10.1016/S0735-1097(23)02858-9.

23. Goetz WA, Liebold A, Vogt F, Birnbaum DE. Tricuspid Valve Repair in a Case with Congenital Absence of Left Thoracic Pericardium. Eur J Cardiothorac Surg. 2004;26(4):848-9. doi: 10.1016/j.ejcts.2004.06.004.

24. Lindenmann J, Matzi V, Neuboeck N, Porubsky C, Ratzenhofer B, Maier A, et al. Traumatic Pericardial Rupture with Cardiac Herniation. Ann Thorac Surg. 2010;89(6):2028-30. doi: 10.1016/j.athoracsur.2009.10.048.

25. Panagiotopoulos N, Barnard J, Wells F. The Snoopy Sign. Eur J Cardiothorac Surg. 2014;45(3):586. doi: 10.1093/ejcts/ezt331.

26. Klein AL, Abbara S, Agler DA, Appleton CP, Asher CR, Hoit B, et al. American Society of Echocardiography Clinical Recommendations for Multimodality Cardiovascular Imaging of Patients with Pericardial Disease: Endorsed by the Society for Cardiovascular Magnetic Resonance and Society of Cardiovascular Computed Tomography. J Am Soc Echocardiogr. 2013;26(9):965-1012.e15. doi: 10.1016/j.echo.2013.06.023.

27. Flosdorff P, Paech C, Riede FT, Dähnert I. Odd Acoustic Window and Elongated Ventricles: Echocardiographic Diagnosis of Congenital Absence of the Pericardium. Pediatr Cardiol. 2012;33(7):1220-1. doi: 10.1007/s00246-012-0339-z.

28. Shah AB, Kronzon I. Congenital Defects of the Pericardium: A Review. Eur Heart J Cardiovasc Imaging. 2015;16(8):821-7. doi: 10.1093/ehjci/jev119.

29. Brulotte S, Roy L, Larose E. Congenital Absence of the Pericardium Presenting as Acute Myocardial Necrosis. Can J Cardiol. 2007;23(11):909-12. doi: 10.1016/s0828-282x(07)70851-6.

30. Marzullo R, Capestro A, Cosimo R, Fogante M, Aprile A, Balardi L, et al. Congenital Absence of Pericardium: The Swinging Heart. J Imaging. 2024;10(8):199. doi: 10.3390/jimaging10080199.

Review Article

My Approach to HFpEF Considering Ventricular-Arterial Coupling and Ventricular Interdependence

João Carlos Moron Saes Braga,[1,2] *Jorge Eduardo Assef,*[3] *Fabio Villaça Guimarães Filho,*[2] *Raphael Aparecido Barreto da Silva*[2]

Faculdade de Medicina de Marília,[1] *Marília, SP – Brazil*
Instituto do Coração de Marília,[2] *Marília, SP – Brazil*
Instituto Dante Pazzanese de Cardiologia,[3] *São Paulo, SP – Brazil*

Abstract

Heart failure (HF) is a serious public health issue that impacts the mortality and morbidity of the global population. The prevalence of heart failure with preserved ejection fraction (HFpEF) is clearly increasing, associated with population aging, obesity, sedentary lifestyle, and cardiometabolic diseases. It is one of the most urgent diagnostic and therapeutic challenges nowadays. Additionally, the obesity phenotype of HFpEF may be associated with HF and occurs as a result of several mechanisms that are deleterious to cardiac function, including the direct action of epicardial adipose tissue (EAT), causing direct restraint of the pericardium and ventricular interdependence, with significant hemodynamic repercussions, decline in functional capacity, and a worse prognosis. The estimation of ventricular-arterial coupling (VAC) in a non-invasive manner by echocardiography allows a better understanding of the interaction between the heart and the arterial system by monitoring hemodynamic changes, which can guide medical therapy and have an impact on prognosis. Although these tools and parameters are promising, new technologies, such as artificial intelligence and machine learning, must be used to enable the applicability of VAC in clinical practice. Further studies are key to standardizing new methods and values in this context.

Introduction

Heart failure (HF) is a serious public health issue that affects millions of individuals worldwide and has a considerable impact on mortality and quality of life. Although epidemiological data indicate that the global incidence of HF tends to decrease, the prevalence of heart failure with preserved ejection fraction (HFpEF) continues to grow, being associated with population aging, obesity, sedentary lifestyle, and cardiometabolic diseases.[1-3]

The pathophysiology of HFpEF is associated with the primary morbidities that cause cardiac and vascular aggression from a chronic pro-inflammatory state. More specifically, this cardiac structural and functional impairment results from a complex interaction between metabolic abnormalities, damage to microcirculation, changes in the functioning of cellular organelles, autonomic dysfunction, exacerbation of the activity of the renin-angiotensin-aldosterone system (RAAS), and maladaptive immune responses.[4,5]

The diagnosis of HFpEF is challenging in most cases and is usually obtained in the advanced stages of the disease, which limits the therapeutic results. In summary, HFpEF can be diagnosed in the presence of clinical evidence of HF, left ventricular ejection fraction (LVEF) ≥ 50%, and evidence of elevated filling pressures and/or cardiac structural alteration. Therefore, a thorough clinical evaluation, echocardiographic examination, and natriuretic peptide levels remain fundamental diagnostic resources.[6]

Thus, HFpEF is one of the most pressing diagnostic and therapeutic challenges nowadays, considering its increasing prevalence, underdiagnosis, poor prognosis, limited therapeutic options, and considerable impact on healthcare systems.

HFpEF with obesity phenotype

HFpEF is characterized by the coexistence of multiple cardiac and non-cardiac diseases. In this way, distinct clinical phenotypes can be identified and determined by different risk factors, comorbidities, left ventricular (LV) remodeling, hemodynamic pattern, and organ dysfunction (Table 1).[6,7] Obesity, in addition to being unequivocally associated with systemic arterial hypertension (SAH), diabetes mellitus (DM), and insulin resistance, has been identified as the primary cause of HF, mediated by several elements that are deleterious to cardiac function due to altered cardiometabolism and direct restraint of the pericardium (epicardial fat), as well as systemic effects on the lung, skeletal muscle, kidney, and liver because of systemic inflammation, neurohormonal activation, autonomic dysregulation, and altered hemodynamic load (Table 1).[7-13]

Recent studies on obesity have given greater attention to the location of fat than to the amount of fat itself since subcutaneous adipose tissue (SAT), visceral adipose tissue (VAT), and epicardial adipose tissue (EAT) contribute differently to the overall cardiovascular risk (Figure 1).[12,14,15] EAT may

Keywords

Obesity Phenotipe; Ventricular-Arterial Coupling; Ventricular Interdependence

Mailing Address: João Carlos Moron Saes Braga •
Faculdade de Medicina de Marília. Avenida Monte Carmelo, 800. Postal code: 17519-030. Marília, SP – Brazil
E-mail: joaocbraga2002@yahoo.com.br
Manuscript received December 7, 2024; revised December 10, 2024; accepted January 17, 2025
Editor responsible for the review: Marcelo Tavares

DOI: https://doi.org/10.36660/abcimg.20240132i

CONTENTS

Central Illustration: My Approach to HFpEF Considering Ventricular-Arterial Coupling and Ventricular Interdependence

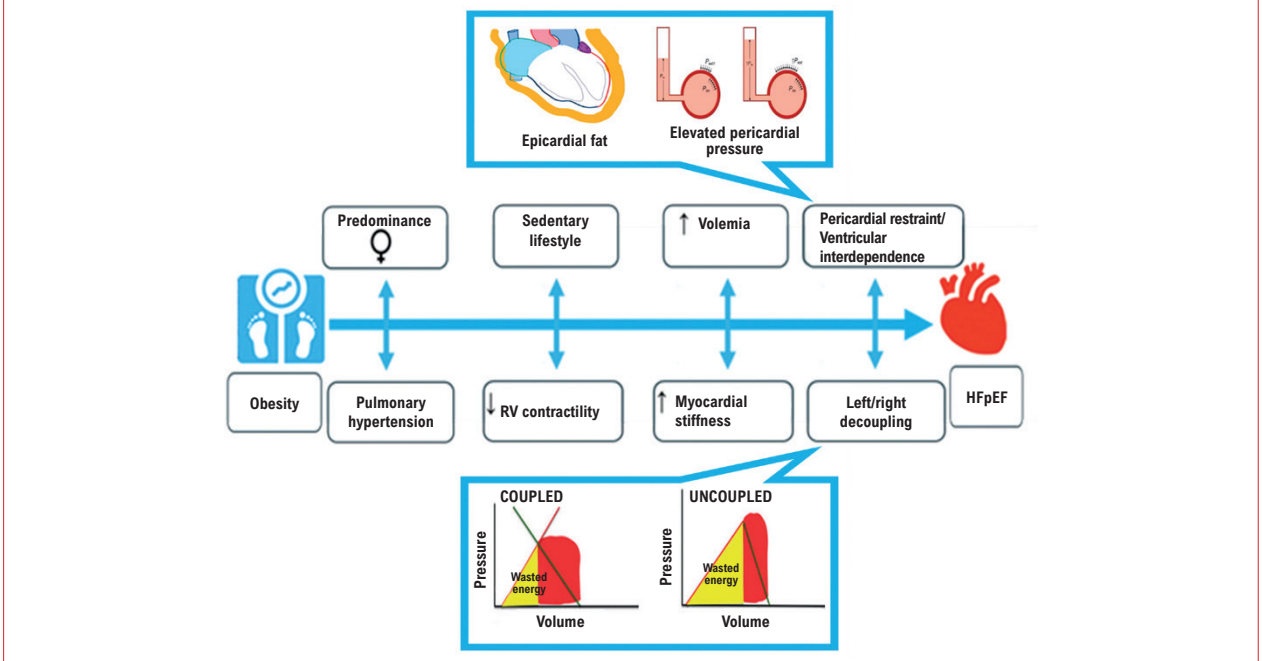

Arq Bras Cardiol: Imagem cardiovasc. 2025;38(1):e20240132

Development and progression of HFpEF with obesity phenotype. The implications for ventricular interdependence and VAC are highlighted. Source: Adapted from Borlaug et al., 2023.[13]

favor the onset of HFpEF due to pro-inflammatory paracrine effects, lipid infiltration, and pericardial restraint (Figure 1).[12,15]

It is worth emphasizing that, in HFpEF, arterial hypertension and other comorbidities coexist and lead to a scenario of chronic afterload elevation as a consequence of increased arterial stiffness and impaired vasodilation (dysregulation of the NO-sGC-cGMP-PKG pathway - nitric oxide, soluble guanylate cyclase, cyclic guanosine monophosphate, and protein kinase G), associated with an increase in blood volume and the appearance of early reflected pulse waves in the aorta (AO) (Figure 2). The stiffer (less compliant) artery causes a pulse wave that propagates at a higher speed, causing the corresponding reflex wave to return to the ascending AO earlier, still at the end of systole, with the aortic valve open. This results in an increase in systolic blood pressure (SBP), a reduction in diastolic blood pressure, and a reduction in coronary perfusion, i.e., a vicious cycle of progressive afterload increase and myocardial dysfunction (Figure 2). Ventricular-arterial coupling (VAC) has been used to assess the efficiency of the ventricular-arterial interaction process, and it also appears to represent an accurate marker of early LV dysfunction and potential therapeutic guidance in HFpEF.[13,16-22]

VAC

VAC assesses the relationship between two anatomically and functionally connected structures: the heart and the arteries. To investigate this interaction, a unit common to both systems is used: elastance, which measures changes in pressure for each unitary change in volume - unit: mmHg/ml. Originally, the elastance and VAC data came from the interpretation of the pressure-volume diagram of the cardiac cycle, derived from an invasive hemodynamic study (Figure 3).[16]

Arterial elastance (Ea) is defined as the ratio between ventricular end-systolic pressure and Stroke volume (ESP/Stroke volume), being influenced by vascular resistance, pulsatile load, and heart rate. It is characterized as an index of arterial load for the left ventricle. End-systolic elastance (Ees), usually known as ventricular elastance, is an index of LV contractility, independent of the load, and reflects the slope of the pressure-volume relationship curve at the end of systole (Figure 3), being the ratio between ventricular end-systolic pressure and ventricular end-systolic volume (ESP/ESV). The Ea/Ees ratio (ESP/Stroke volume)/(ESP/ESV) can be simplified as ESV/Stroke volume (removing ESP from the equation).[22]

VAC is defined as the ratio of Ea/Ees and investigates the contractile capacity of the heart and its ability to adapt to load impositions.[21] Previous studies have shown that the ideal VAC value, derived from the Ea/Ees ratio, should vary between 0.5 and 1, reflecting the state in which the LV systolic work is ideal (Figure 4). An Ea/Ees ratio > 1 suggests ventricular-arterial decoupling (Figure 4). Such ventricular-arterial incompatibility is frequently seen in HFpEF, being attributed to diastolic dysfunction induced by increased afterload and

Table 1 – Structural and functional changes in HFpEF

Cardiac Abnormality	Frequency, %
Alteration of LV geometry, concentric hypertrophy, or remodeling	60
Alteration of LV diastolic function (altered relaxation, increased stiffness)	80-90
Myocardial fibrosis	Mild 66 Moderate 17 Major 10
Microvascular myocardial dysfunction and/or reduced microvessel density	80
Increased LV stiffness	70
Left atrial enlargement and/or systolic and diastolic dysfunction	70
Increased epicardial fat	40-50 (patients with obesity)
Pericardial constriction with altered LV filling	30
Atrial fibrillation	40-50
Epicardial coronary artery disease	50-65
Pulmonary	
Post-capillary pulmonary hypertension or combined pre- and post-capillary pulmonary hypertension (group 2)	80
Pulmonary arterial, venous, and small vessel remodeling	
Restrictive pulmonary physiology	Mild 40-50 Moderate 10
Right heart	
RV diastolic dysfunction	50
RV enlargement and systolic dysfunction	30
Right atrial enlargement and/or right ventricular systolic/diastolic dysfunction	50
Vascular	
Increased arterial stiffness	70
Alteration of systemic microvascular function	70
Reduced systemic venous compliance and capacitance	70
Systemic	
Obesity	60-70
Dysglycemia/insulin resistance	60-70
Neurohumoral activation	30
Reduction of skeletal muscle and replacement with fat	60
Increased visceral fat	70
Renal	
Reduced glomerular filtration rate	60
Reduced sodium excretion	70
Hepatic	
Non-alcoholic fatty liver disease	40-50
Congestive liver disease	10

Table adapted from Redfield et al., 2023.[7] LV: left ventricle; RV: right ventricle.

subendocardial ischemia, and may be associated with a worse prognosis.[16]

Left VAC

The gold standard echocardiographic method for assessing LV-AO VAC is the so-called *single beat method*, developed by Chen et al.[23] (Figure 5). Simple non-invasive parameters that can be easily collected should be obtained: systolic and diastolic blood pressure, ejection volume, ejection fraction, pre-ejection period, and total ejection period. As the formulas are relatively complex, it is recommended to use an easy-to-use application (iElastance© - Apple iOS application)[24] (Figure 6), which yields fast and reliable results.

The proposed normal value for Ea is 2.2 (±0.8) mmHg/ml, and for Ees is 2.3 (±1.0) mmHg/ml.

$$Ea = (SBP \times 0.9) / \text{Stroke Volume}$$

$$Ees = [DBP - (E(nor)(est) \times SBP \times 0.9)]/E(nor)(est) \times \text{Stroke Volume}$$

where *DBP* and *SBP* are the diastolic and systolic cuff blood pressures, measured through the upper arm; *E(nor)(est)* is the normalized ventricular elastance, estimated at the beginning of ejection; and *Stroke volume* is derived from the product of the VTI (velocity-time integral) of the Doppler spectrum of the LV outflow tract flow by the measured LV outflow tract diameter.[22] Using the dedicated application avoids complex and time-consuming calculations. The user simply fills in the fields with the requested data: SBP (mmHg), diastolic blood pressure (mmHg), LV ejection fraction (%), stroke volume (ml), pre-ejection time (ms), and total ejection time (ms) (Figure 5). The result is immediate with the values of: Ea, Ees, and VAC (Figure 6).

Several methodologies have emerged to assess LV-AO VAC using echocardiography. The measurement of pulse wave velocity (PWV) appears to comprehensively represent arterial load (arterial stiffness, aortic impedance, and early reflected waves) (Figure 2), associated with the measurement of the global longitudinal strain (GLS) of the LV as a marker of myocardial performance. Therefore, the use of the PWV/

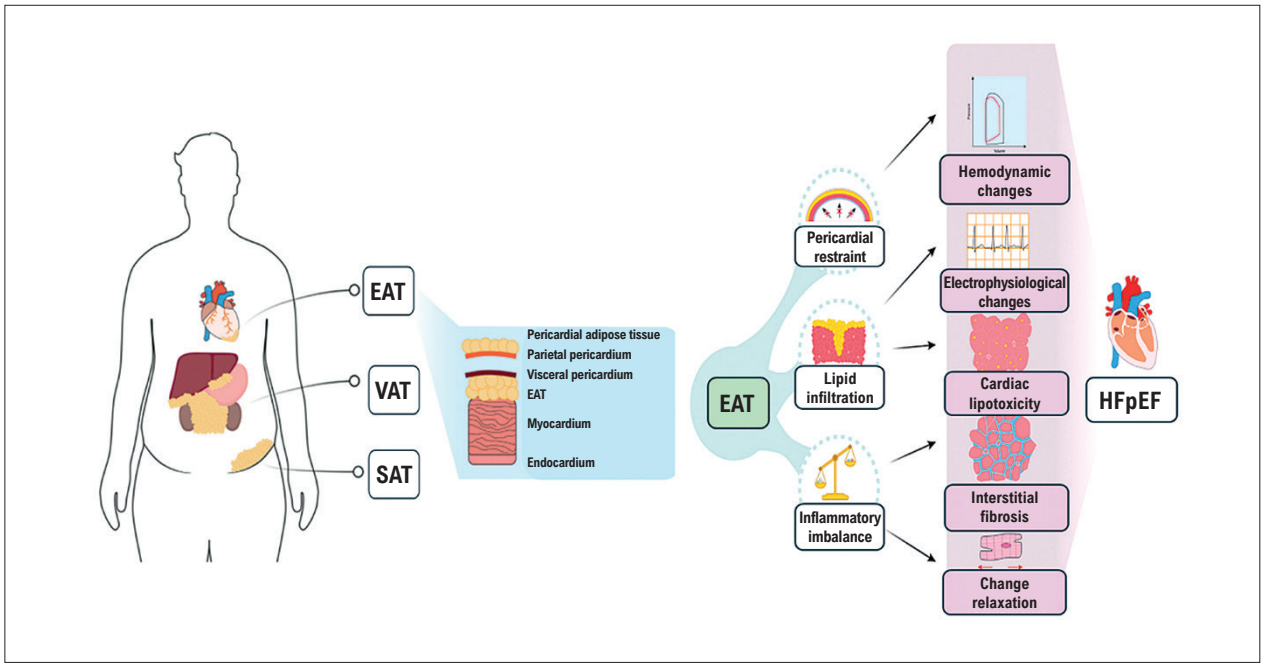

Figure 1 – *Different locations where fat can be deposited and the pathological potential of EAT. Source: Adapted from Dronkers et al., 2024.[12] EAT: epicardial adipose tissue; VAT: visceral adipose tissue; SAT: subcutaneous adipose tissue; HFpEF: heart failure with preserved ejection fraction.*

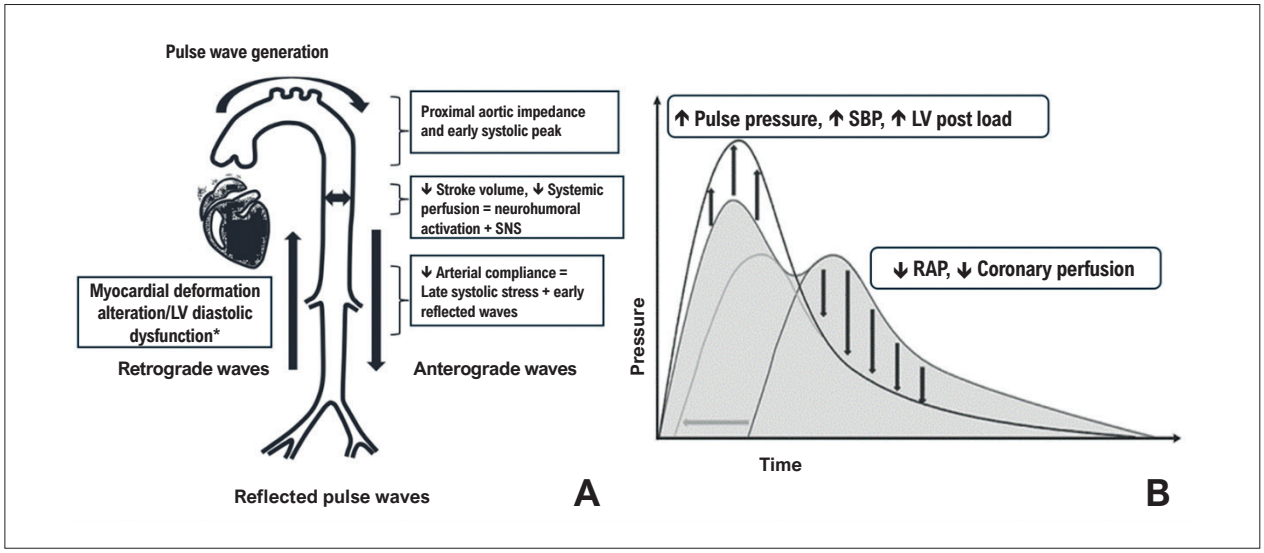

Figure 2 – *A: Pathophysiological mechanism that leads to LV dysfunction. B: Increased aortic stiffness and the emergence of early reflected waves that reach the heart at the end of systole, promoting increased pulse pressure, increased SBP, increased afterload, reduced diastolic blood pressure, and reduced coronary perfusion. Source: Adapted from Ikonomidis et al., 2019.[16] LV: left ventricle; SNS: sympathetic nervous system; SBP: systolic blood pressure; RAP: right atrial pressure.*

GLS ratio may be more appropriate in several scenarios to characterize VAC since it incorporates "gold standard" methods to assess arterial load (PWV) and LV contractility (GLS), with prognostic value.[16,22,25]

The use of 3D echocardiography to measure ventricular volumes, the use of myocardial work to analyze myocardial performance and the increasing incorporation of artificial intelligence and machine learning to calculate ventricular elastance (Ees) represent technical evolution and contribute to greater applicability of VAC in clinical practice in the future.[16,17] Studies will be necessary to standardize methods and values in this context.

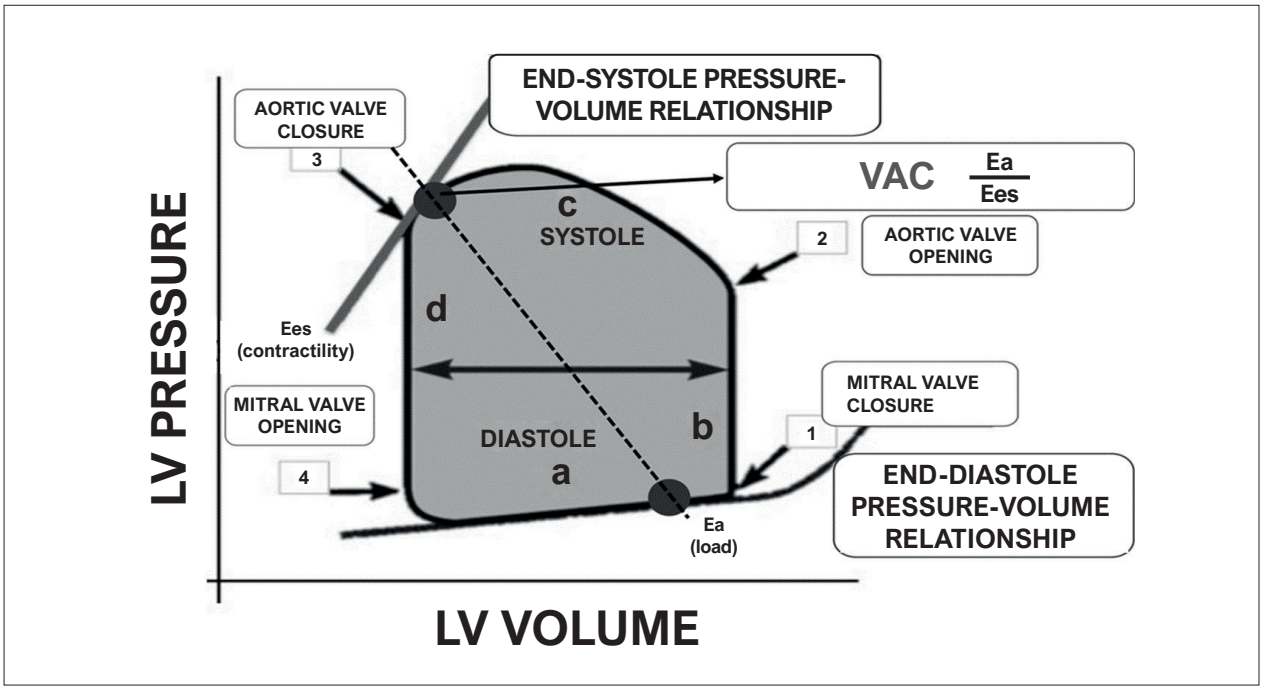

Figure 3 – *A classic Pressure-Volume diagram in the cardiac cycle demonstrating the Pressure-Volume relationship curves at the end of diastole and the Pressure-Volume relationship at the end of systole, determining Ea, Ees, and LV-AO VAC. Source: Adapted from Gamarra A et al., 2024.[17] Ea: arterial elastance; Ees: end-systolic elastance; LV: left ventricle; AO: aorta; VAC: ventricular-arterial coupling.*

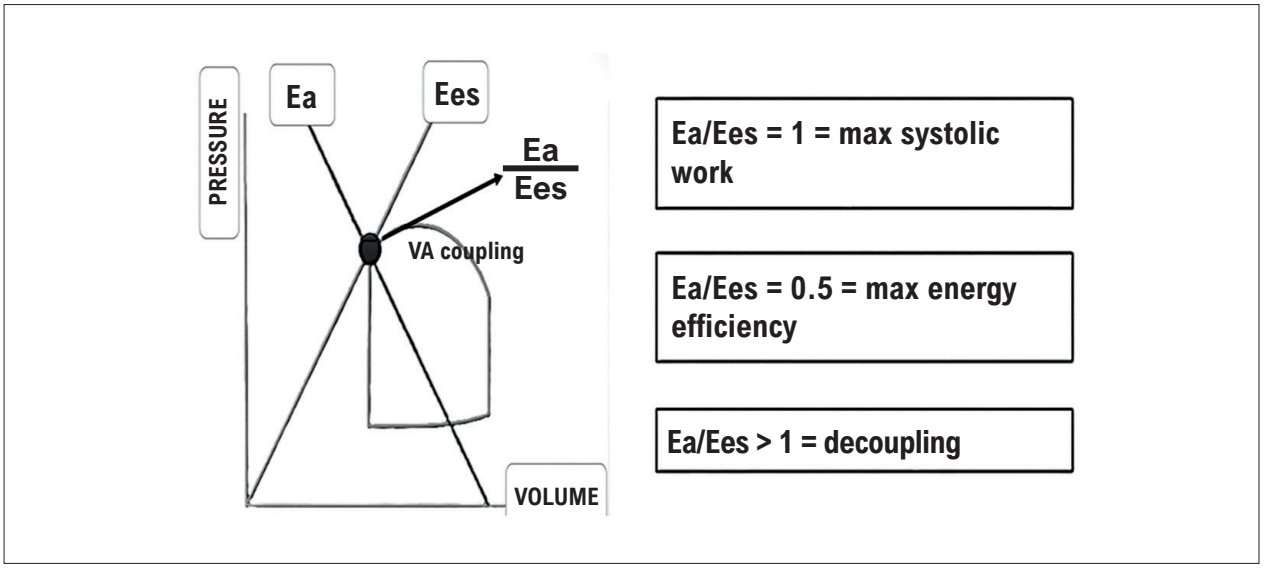

Figure 4 – *Assessment of energy efficiency in blood transfer from the ventricular to the arterial system by calculating VAC. Source: Adapted from Chirinos et al., 2013.[18] Ea: arterial elastance; Ees: end-systolic elastance; VE: left ventricle; VA: ventricular-arterial*

Right VAC

The TAPSE/PASP ratio (tricuspid annular plane systolic excursion/pulmonary artery systolic pressure) expresses the relationship between RV contractility and its afterload. It has been shown to have a good correlation with invasive methods deemed the "gold standard" for measuring RV (right ventricle)-PA (pulmonary artery) coupling. Consequently, the TAPSE/PASP ratio has been incorporated into the main guidelines for the assessment of RV and pulmonary hypertension.[26-28]

TAPSE is measured by M-mode echocardiography (Figure 7A) and assesses RV contractile function. To estimate RV afterload (PASP), the maximum velocity of the tricuspid

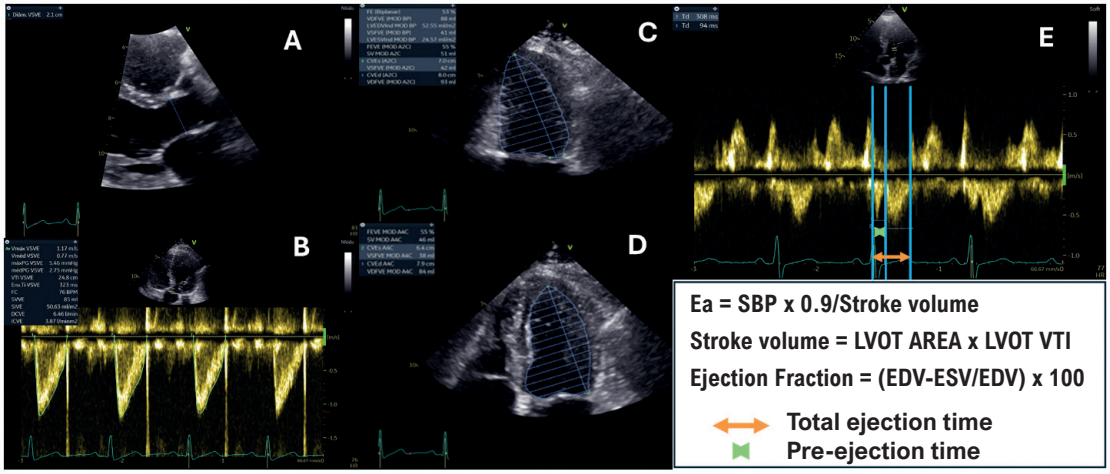

Figure 5 – *(A) Two-dimensional echocardiographic image in parasternal view, long axis, zooming in on the LV outflow tract diameter measurement. (B) VTI image of the Doppler spectrum of the LV outflow tract flow, which is obtained by tracing the fullest line of the spectrum to calculate the stroke volume. (C)/(D) Two-dimensional echocardiographic image in apical 4-chamber (D) and 2-chamber (C) views to obtain the LVEF value (Simpson method). (E) Apical 5-chamber view of the Doppler spectrum of the LV outflow tract flow and mitral inflow to obtain pre-ejection time (green) and total ejection time (orange). Ea: arterial elastance; SBP: systolic blood pressure; LVOT: left ventricular outflow tract; EDV: end-diastolic volume; ESV: end-systolic volume; VTI: velocity-time integral; LVEF: left ventricular ejection fraction.*

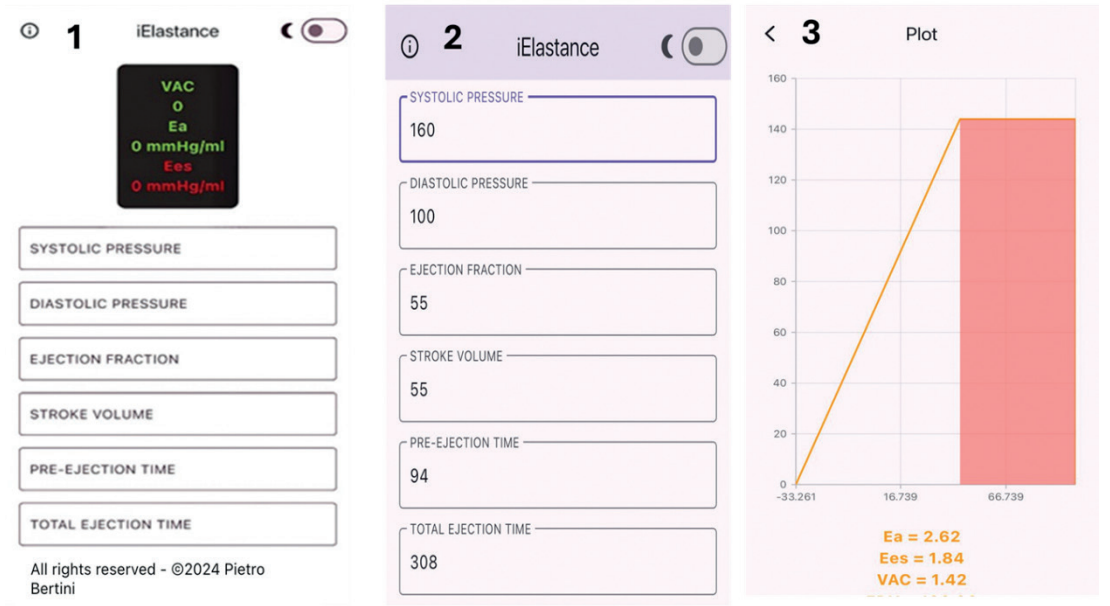

Figure 6 – *(1) Image reproduced from the mobile application showing how easy it is to use. It is only necessary to fill in the fields with the data obtained, as shown in Figure 5. (2) Practical example of filling in the fields. (3) Immediate result for Ea, Ees: end-systolic elastance, and VAC. Source: Bertini P. iElastance- Apple iOS App. Available at: https://apps.apple.com/br/app/ielastance/id556528864.*[24]

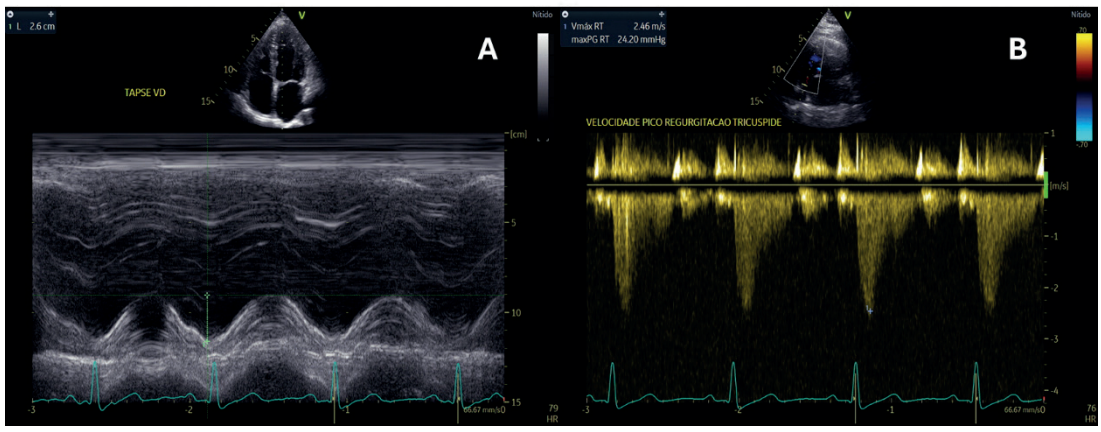

Figure 7 – *(A) Tricuspid annular displacement measured by M mode echocardiography - TAPSE. (B) Continuous Doppler spectral curve, demonstrating tricuspid regurgitation flow, allowing the systolic pressure in the pulmonary artery to be estimated. The TAPSE/PASP ratio estimates the value of RV-PA VAC. TAPSE: tricuspid annular plane systolic excursion; PASP: pulmonary artery systolic pressure; RV: right ventricle; PA: pulmonary artery.*

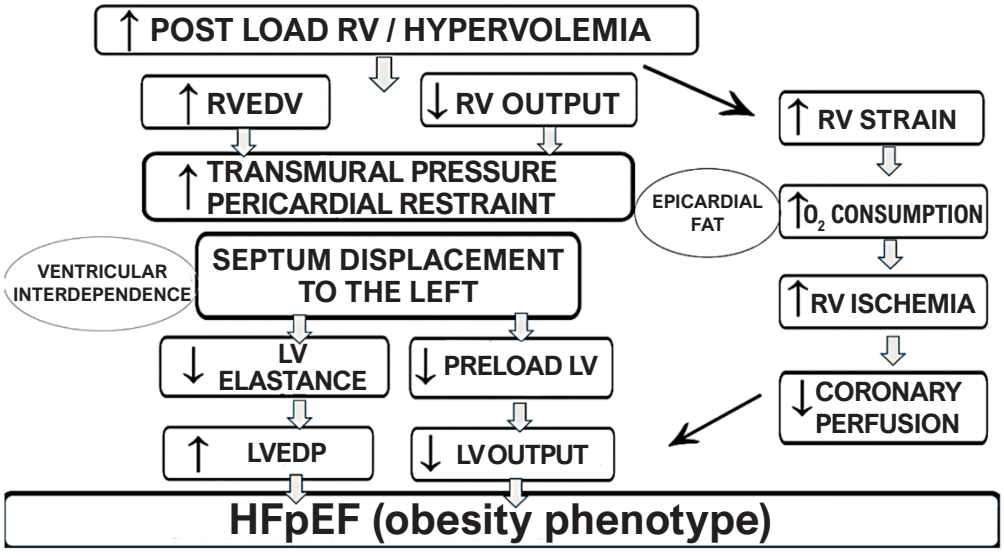

Figure 8 – *A proposed hemodynamic mechanism for HFpEF with obesity phenotype. LV: left ventricle; RV: right ventricle; O_2: oxygen; LVEDP: left ventricular end-diastolic pressure; RVEDV: right ventricular end-diastolic volume.*

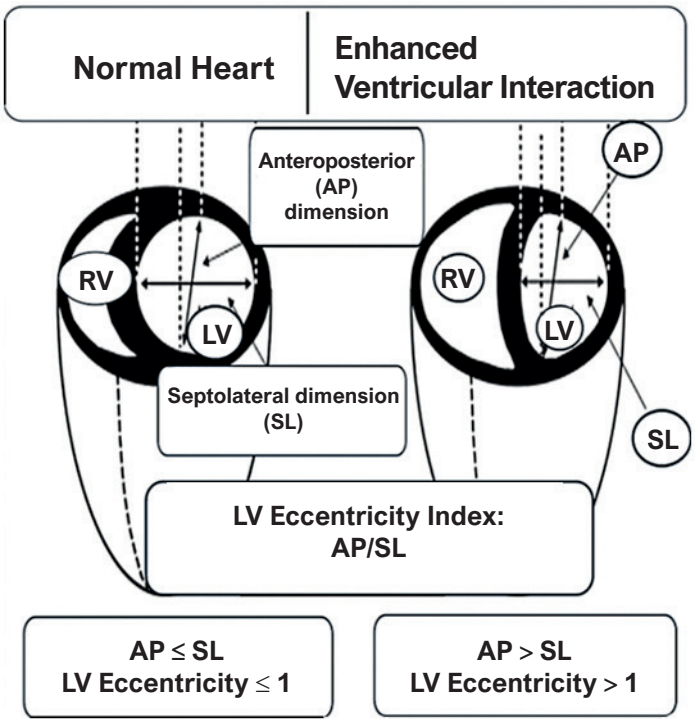

Figure 9 – *Illustration showing an increase in the LV eccentricity index due to ventricular interdependence, as proposed for HFpEF with obesity phenotype. Source: modified Borlaug et al., 2019.[39]*

regurgitation jet is determined by analyzing the continuous Doppler spectral curve and adding the right atrial pressure (RAP), which is estimated by observing the inferior vena cava. As a result, the RVSP (right ventricular systolic pressure) is obtained, which is calculated using the modified Bernoulli equation: 4 x peak velocity (Figure 7B). In the absence of right ventricular outflow tract obstruction or pulmonary stenosis, RVSP is equal to the PASP.

In HFpEF with obesity phenotype, right ventricular dysfunction results from several mechanisms acting on preload, afterload, and contractility of the right ventricle. Increased pulmonary pressure (combined pre- and post-capillary) is frequently present, as is right ventricular dilation, primary ventricular sarcomere dysfunction, pericardial constriction, and ventricular interdependence, which further aggravate biventricular filling and pulmonary hypertension.[27]

RV dysfunction is an independent predictor of mortality and hospitalization risk in HFpEF. Therefore, it should always be investigated. A TAPSE/PASP ratio < 0.48 mm/mmHg was associated with higher all-cause mortality and higher hospitalization for HF in a population with HF with preserved and reduced LVEF.[29] Another study has demonstrated that, in the subgroup of patients with HFpEF and pre-capillary pulmonary hypertension, a TAPSE/PASP ratio < 0.36 mm/mmHg was associated with poor clinical outcomes, but suggested that these individuals could respond more favorably to interventions targeting RV afterload.[30]

It is important to highlight that the RV-GSL/PASP ratio has also been used as an appropriate methodology to assess RV-PA coupling and has proven to be an accurate instrument for assessing patients in different scenarios.[26-28]

VAC X HFpEF

In the context of HFpEF, the calculation of the LVEF does not characterize broader aspects of the ventricular-arterial connection, particularly those related to afterload (Ea) or contractility (Ees), which are highly relevant for therapeutic management in patients with clinical symptoms of HF and preserved LVEF. In this scenario, Ees may be normal, while Ea may be increased, resulting in Ea/Ees > 1.0 (VA decoupling). However, Ea/Ees can often occur with a normal result (between 0.5 and 1.0), despite Ea and Ees being elevated. Therefore, it is crucial to identify the value of the elastances individually[22] (Figures 5 and 6). Some interventions have shown potential impact on elastances, in addition to improving VAC: antihypertensive drugs,[21] angiotensin receptor-neprilysin inhibitors (ARNIs),[31] sodium-glucose cotransporter-2 (SGLT2) inhibitors,[32] GLP-1 analogs,[33] and interleukin IL-1[34] and IL-12 inhibitors.[35]

The use of VAC to assess the population with HFpEF has proven to be an accurate tool for stratifying those individuals at greater risk. In a recent study involving patients with LVEF > 40%, it was shown that the subgroup of patients, despite having higher LVEF, had a greater degree of LV

hypertrophy, higher LV filling pressures, and a higher rate of LV-AO decoupling with a worse prognosis. On top of that, the subgroup that showed RV-PA decoupling, verified by the TAPSE/PASP ratio, also demonstrated a worse prognosis, regardless of LVEF values, E/e' ratio, and presence of atrial fibrillation.[34]

Pericardial restraint (HFpEF) X ventricular interdependence

Obese patients with HFpEF have peculiar pathophysiological characteristics, including hypervolemia, RV-PA decoupling, biventricular hypertrophy, right ventricular dysfunction, pre- and post-pulmonary capillary hypertension, elevated filling pressures in left chambers, and increased EAT[36] (Figure 8).

Due to its proximity to the myocardium, excess EAT can promote local inflammatory and mechanical constrictive effects on the cardiac muscle. Pericardial restraint associated with hypervolemia can increase pericardial pressure, promote competition for filling between the RV and LV, cause flattening of the ventricular septum, highlight ventricular interdependence, and lead to RV distension, reduced LV preload, increased LV end-diastolic pressure, and reduced cardiac output (Figure 8). On echocardiography, it is possible to quantify, using the parasternal short-axis plane, the LV eccentricity index, which becomes higher (LV eccentricity index > 1) (Figure 9) as greater pericardial constriction and higher intracardiac pressures are observed, including right atrial, pulmonary arterial, and RV end-diastolic pressures, which are concomitant with a significant reduction in functional physical capacity.[37-40]

Ventricular interdependence has been a therapeutic target of several current studies. Studies performing transcatheter interventions to reduce tricuspid regurgitation in patients with HFpEF have been designed to improve ventricular interdependence and increase LV filling.[40,41] Similarly, a pilot study has demonstrated the potential for surgical pericardiotomy in patients with HFpEF and restraint EAT.[42]

Final considerations

The magnitude of the global public health issue of HFpEF, in which obesity has a prevalence of approximately 70% (Table 1), has motivated, in recent years, a more specific investigation of the phenotype of subpopulations for better diagnostic, therapeutic, and prognostic results. Particular attention has been given to excess EAT in this population, which, associated with volume overload, can lead to pericardial restraint with ventricular interdependence, contributing to a more significant increase in left chamber filling pressures, worsening of pulmonary pressure, reduction in cardiac output, low physical capacity, and a worse prognosis. This hemodynamic condition can be identified by echocardiogram (LV eccentricity index > 1).

Non-invasive analysis of VAC by echocardiography appears to be a promising tool to assess hemodynamics in a more individualized manner and customize the treatment of patients with HFpEF. The single-beat echocardiographic method, coupled with a dedicated application, is becoming increasingly feasible. Besides, physicians are gaining more experience with this technology, having a better understanding of the complex interaction between the heart and the vessels. Yet, efforts to develop new methods must continue, both through advanced imaging techniques and new software solutions, artificial intelligence, and machine learning. It is clear that the earlier an accurate diagnosis, etiological definition, and severity estimation are made, and preventive and therapeutic efforts are implemented, the greater the benefits in terms of disease progression and the associated outcomes.

Author Contributions

Conception and design of the research, acquisition of data, analysis and interpretation of the data and writing of the manuscript: Braga JCMS; critical revision of the manuscript for intellectual content: Braga JCMS, Assef JE, Guimarães Filho FV, Silva RAB.

Potential Conflict of Interest

No potential conflict of interest relevant to this article was reported.

Sources of Funding

There were no external funding sources for this study.

Study Association

This study is not associated with any thesis or dissertation work.

Ethics Approval and Consent to Participate

This article does not contain any studies with human participants or animals performed by any of the authors.

References

1. Maryniak A, Maisuradze N, Ahmed R, Biskupski P, Jayaraj J, Budzikowski AS. Heart Failure with Preserved Ejection Fraction Update: A Review of Clinical Trials and New Therapeutic Considerations. Cardiol J. 2022;29(4):670-9. doi: 10.5603/CJ.a2022.0051.
2. Kittleson M, Panjrath G, Amancherla K, Davis LL, Deswal A, Dixon DL, et al. 2023 ACC Expert Consensus Decision Pathway on Management of Heart Failure with Preserved Ejection Fraction: A Report of the American College of Cardiology Solution Set Oversight Committee. J Am Coll Cardiol. 2023;81(18):1835-78. doi: 10.1016/j.jacc.2023.03.393
3. Logeart D. Heart Failure with Preserved Ejection Fraction: New Challenges and New Hopes. Presse Med. 2024;53(1):104185. doi: 10.1016/j.lpm.2023.104185.

4. Jasinska-Piadlo A, Campbell P. Management of Patients with Heart Failure and Preserved Ejection Fraction. Heart. 2023;109(11):874-83. doi: 10.1136/heartjnl-2022-321097.

5. Bozkurt B, Coats AJ, Tsutsui H, Abdelhamid M, Adamopoulos S, Albert N, et al. Universal Definition and Classification of Heart Failure: A Report of the Heart Failure Society of America, Heart Failure Association of the European Society of Cardiology, Japanese Heart Failure Society and Writing Committee of the Universal Definition of Heart Failure. J Card Fail. 2021;27(4):387-413. doi: 10.1016/j.cardfail.2021.01.022.

6. Hamo CE, De Jong C, Hartshorne-Evans N, Lund LH, Shah SJ, Solomon S, et al. Heart Failure with Preserved Ejection Fraction. Nat Rev Dis Primers. 2024;10(1):55. doi: 10.1038/s41572-024-00540-y.

7. Redfield MM, Borlaug BA. Heart Failure with Preserved Ejection Fraction: A Review. JAMA. 2023;329(10):827-38. doi: 10.1001/jama.2023.2020.

8. Donal E, L'Official G, Kosmala W. Heart Failure with Preserved Ejection Fraction: Defining Phenotypes. J Card Fail. 2020;26(11):929-31. doi: 10.1016/j.cardfail.2020.09.013.

9. Khan SS, Ning H, Wilkins JT, Allen N, Carnethon M, Berry JD, et al. Association of Body Mass Index with Lifetime Risk of Cardiovascular Disease and Compression of Morbidity. JAMA Cardiol. 2018;3(4):280-7. doi: 10.1001/jamacardio.2018.0022.

10. Cercato C, Fonseca FA. Cardiovascular Risk and Obesity. Diabetol Metab Syndr. 2019;11:74. doi: 10.1186/s13098-019-0468-0.

11. Shams E, Kamalumpundi V, Peterson J, Gismondi RA, Oigman W, Correia MLG. Highlights of Mechanisms and Treatment of Obesity-Related Hypertension. J Hum Hypertens. 2022;36(9):785-93. doi: 10.1038/s41371-021-00644-y.

12. Dronkers J, van Veldhuisen DJ, van der Meer P, Meems LMG. Heart Failure and Obesity: Unraveling Molecular Mechanisms of Excess Adipose Tissue. J Am Coll Cardiol. 2024;84(17):1666-77. doi: 10.1016/j.jacc.2024.07.016.

13. Borlaug BA, Sharma K, Shah SJ, Ho JE. Heart Failure with Preserved Ejection Fraction: JACC Scientific Statement. J Am Coll Cardiol. 2023;81(18):1810-34. doi: 10.1016/j.jacc.2023.01.049.

14. Ferrara D, Montecucco F, Dallegri F, Carbone F. Impact of Different Ectopic Fat Depots on Cardiovascular and Metabolic Diseases. J Cell Physiol. 2019;234(12):21630-41. doi: 10.1002/jcp.28821.

15. Gosh S. Ectopic Fat: The Potential Target for Obesity Management. J Obes Metab Res 2014;1(1):30-8. doi: 10.4103/2347-9906.123883.

16. Ikonomidis I, Aboyans V, Blacher J, Brodmann M, Brutsaert DL, Chirinos JA, et al. The Role of Ventricular-Arterial Coupling in Cardiac Disease and Heart Failure: Assessment, Clinical Implications and Therapeutic Interventions. A Consensus Document of the European Society of Cardiology Working Group on Aorta & Peripheral Vascular Diseases, European Association of Cardiovascular Imaging, and Heart Failure Association. Eur J Heart Fail. 2019;21(4):402-24. doi: 10.1002/ejhf.1436.

17. Gamarra A, Díez-Villanueva P, Salamanca J, Aguilar R, Mahía P, Alfonso F. Development and Clinical Application of Left Ventricular-Arterial Coupling Non-Invasive Assessment Methods. J Cardiovasc Dev Dis. 2024;11(5):141. doi: 10.3390/jcdd11050141.

18. Chirinos JA. Ventricular-Arterial Coupling: Invasive and Non-Invasive Assessment. Artery Res. 2013;7(1):1-24.doi: 10.1016/j.artres.2012.12.002.

19. Laurent S, Cockcroft J, van Bortel L, Boutouyrie P, Giannattasio C, Hayoz D, et al. Expert Consensus Document on Arterial Stiffness: Methodological Issues and Clinical Applications. Eur Heart J. 2006;27(21):2588-605. doi: 10.1093/eurheartj/ehl254.

20. Shah AM, Claggett B, Sweitzer NK, Shah SJ, Anand IS, Liu L, et al. Prognostic Importance of Impaired Systolic Function in Heart Failure with Preserved Ejection Fraction and the Impact of Spironolactone. Circulation. 2015;132(5):402-14. doi: 10.1161/CIRCULATIONAHA.115.015884.

21. Iakovou I, Karpanou EA, Vyssoulis GP, Toutouzas PK, Cokkinos DV. Assessment of Arterial Ventricular Coupling Changes in Patients Under Therapy with Various Antihypertensive Agents by a Non-Invasive Echocardiographic Method. Int J Cardiol. 2004;96(3):355-60. doi: 10.1016/j.ijcard.2003.07.022.

22. Holm H, Magnusson M, Jujić A, Bozec E, Girerd N. How to Calculate Ventricular-Arterial Coupling? Eur J Heart Fail. 2022;24(4):600-2. doi: 10.1002/ejhf.2456.

23. Chen CH, Fetics B, Nevo E, Rochitte CE, Chiou KR, Ding PA, et al. Noninvasive Single-Beat Determination of Left Ventricular End-Systolic Elastance in Humans. J Am Coll Cardiol. 2001;38(7):2028-34. doi: 10.1016/s0735-1097(01)01651-5.

24. Bertini P. iElastance - Apple iOS App [Internet]. Cupertino: Apple; 2024 [cited 2025 Jan 6]. Available from: https://apps.apple.com/br/app/ielastance/id556528864.

25. Ikonomidis I, Katsanos S, Triantafyllidi H, Parissis J, Tzortzis S, Pavlidis G, et al. Pulse Wave Velocity to Global Longitudinal Strain Ratio in Hypertension. Eur J Clin Invest. 2019;49(2):e13049. doi: 10.1111/eci.13049.

26. Humbert M, Kovacs G, Hoeper MM, Badagliacca R, Berger RMF, Brida M, et al. 2022 ESC/ERS Guidelines for the Diagnosis and Treatment of Pulmonary Hypertension. Eur Heart J. 2022;43(38):3618-731. doi: 10.1093/eurheartj/ehac237.

27. Li H, Ye T, Su L, Wang J, Jia Z, Wu Q, et al. Assessment of Right Ventricular-Arterial Coupling by Echocardiography in Patients with Right Ventricular Pressure and Volume Overload. Rev Cardiovasc Med. 2023;24(12):366. doi: 10.31083/j.rcm2412366.

28. Houston BA, Brittain EL, Tedford RJ. Right Ventricular Failure. N Engl J Med. 2023;388(12):1111-25. doi: 10.1056/NEJMra2207410.

29. Bosch L, Lam CSP, Gong L, Chan SP, Sim D, Teo D, et al. Right Ventricular Dysfunction in Left-Sided Heart Failure with Preserved versus Reduced Ejection Fraction. Eur J Heart Fail. 2017;19(12):1664-71. doi: 10.1002/ejhf.873.

30. Gorter TM, van Veldhuisen DJ, Voors AA, Hummel YM, Lam CSP, Berger RMF, et al. Right Ventricular-Vascular Coupling in Heart Failure with Preserved Ejection Fraction and Pre- Vs. Post-Capillary Pulmonary Hypertension. Eur Heart J Cardiovasc Imaging. 2018;19(4):425-32. doi: 10.1093/ehjci/jex133.

31. Williams B, Cockcroft JR, Kario K, Zappe DH, Brunel PC, Wang Q, et al. Effects of Sacubitril/Valsartan versus Olmesartan on Central Hemodynamics in the Elderly with Systolic Hypertension: The PARAMETER Study. Hypertension. 2017;69(3):411-20. doi: 10.1161/HYPERTENSIONAHA.116.08556.

32. Ikonomidis I, Papadavid E, Makavos G, Andreadou I, Varoudi M, Gravanis K, et al. Lowering Interleukin-12 Activity Improves Myocardial and Vascular Function Compared with Tumor Necrosis Factor-a Antagonism or Cyclosporine in Psoriasis. Circ Cardiovasc Imaging. 2017;10(9):e006283. doi: 10.1161/CIRCIMAGING.117.006283.

33. Kosiborod MN, Verma S, Borlaug BA, Butler J, Davies MJ, Jensen TJ, et al. Effects of Semaglutide on Symptoms, Function, and Quality of Life in Patients with Heart Failure with Preserved Ejection Fraction and Obesity: A Prespecified Analysis of the STEP-HFpEF Trial. Circulation. 2024;149(3):204–16. doi: 10.1161/CIRCULATIONAHA.123.067505.

34. Ikonomidis I, Tzortzis S, Lekakis J, Paraskevaidis I, Andreadou I, Nikolaou M, et al. Lowering Interleukin-1 Activity with Anakinra Improves Myocardial Deformation in Rheumatoid Arthritis. Heart. 2009;95(18):1502-7. doi: 10.1136/hrt.2009.168971.

35. Reddy YNV, Carter RE, Sorimachi H, Omar M, Popovic D, Alogna A, et al. Effect of Dapagliflozin on Right Heart-Pulmonary Vascular Interaction in Heart Failure with Preserved Ejection Fraction: A Secondary Analysis of a Randomized Clinical Trial. JAMA Cardiol. 2024;9(9)843-51. doi: 10.1001/jamacardio.2024.1914.

36. Ohte N, Kikuchi S, Iwahashi N, Kinugasa Y, Dohi K, Takase H, et al. Distinctive Left Ventricular-Arterial and Right Ventricular-Pulmonary Arterial Coupling Observed in Patients with Heart Failure and a Higher Left Ventricular Ejection Fraction Range. Eur Heart J Cardiovasc Imaging. 2024;25(6):774-81. doi: 10.1093/ehjci/jeae033.

37. Obokata M, Reddy YNV, Pislaru SV, Melenovsky V, Borlaug BA. Evidence Supporting the Existence of a Distinct Obese Phenotype of Heart Failure with Preserved Ejection Fraction. Circulation. 2017;136(1):6-19. doi: 10.1161/CIRCULATIONAHA.116.026807.

38. Oduah MT, Sundaram V, Reddy YN. Epicardial Fat in Heart Failure with Preserved Ejection Fraction: Bad Actor or Just Lying Around? Card Fail Rev. 2023;9:e06. doi: 10.15420/cfr.2022.25.

39. Borlaug BA, Reddy YNV. The Role of the Pericardium in Heart Failure: Implications for Pathophysiology and Treatment. JACC Heart Fail. 2019;7(7):574-85. doi: 10.1016/j.jchf.2019.03.021.

40. Elsanhoury A, Nelki V, Kelle S, van Linthout S, Tschöpe C. Epicardial Fat Expansion in Diabetic and Obese Patients with Heart Failure and Preserved Ejection Fraction-A Specific HFpEF Phenotype. Front Cardiovasc Med. 2021;8:720690. doi: 10.3389/fcvm.2021.720690.

41. Kresoja KP, Rosch S, Schober AR, Fengler K, Schlotter F, Bombace S, et al. Implications of Tricuspid Regurgitation and Right Ventricular Volume Overload in Patients with Heart Failure with Preserved Ejection Fraction. Eur J Heart Fail 2024;26(4):1025-35. doi: 10.1002/ejhf.3195.

42. Borlaug BA, Schaff HV, Asirvatham SJ, Koepp KE, Mauermann WJ, Rowse PG. Surgical Pericardiotomy to Treat Heart Failure with Preserved Ejection Fraction: A First Clinical Study. Eur Heart J. 2023;44(44):4719–21. doi: 10.1093/eurheartj/ehad620.

My Approach To Myocardial Extracellular Volume Quantification Using Cardiac Computed Tomography

Gabriel C. Camargo,[1,2] *Leticia R. Sabioni*[1]
Instituto Nacional de Cardiologia,[1] *Rio de Janeiro, RJ – Brazil*
Instituto D'Or de Pesquisa e Ensino,[2] *Rio de Janeiro, RJ – Brazil*

Central Illustration: My Approach To Myocardial Extracellular Volume Quantification Using Cardiac Computed Tomography

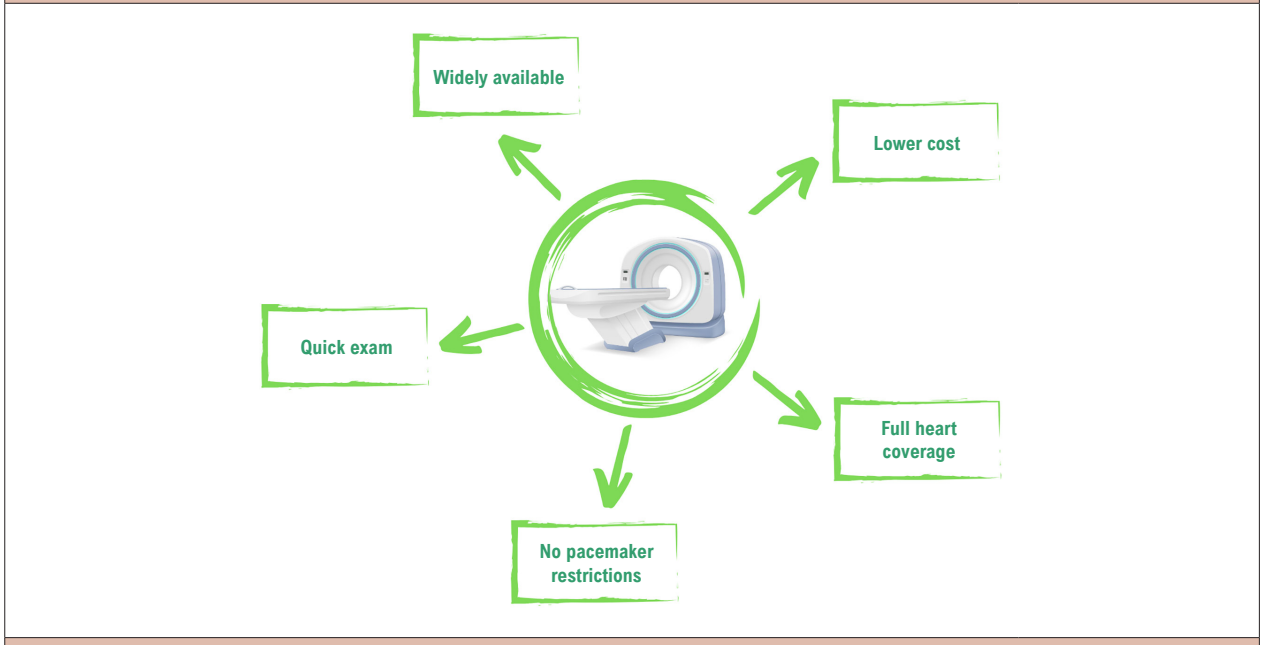

Arq Bras Cardiol: Imagem cardiovasc. 2025;38(1):e20240112

Advantages of using computed tomography compared to magnetic resonance imaging for the calculation of myocardial ECV.

Abstract

The quantification of myocardial extracellular volume (ECV) has demonstrated both diagnostic and prognostic value in various heart diseases. While ECV is typically assessed using cardiac magnetic resonance imaging (CMR), it can also be measured through cardiac computed tomography (CCT) imaging. This article discusses the application of CCT for myocardial ECV calculation, detailing the technique, its advantages and disadvantages, and its potential clinical applications.

Keywords

X-Ray Computed Tomography; Cardiomyopathies; Evidence-Based Practice.

Mailling Address: Gabriel C. Camargo •
National Institute of Cardiology. R das Laranjeiras, 374. Postal code: 22240-006. Rio de Janeiro, RJ – Brazil
E-mail: gabccamargo@gmail.com
Manuscript received October 30, 2024; revised October 31, 2024; accepted October 31, 2024
Editor responsible for the review: Marcelo Tavares

DOI: https://doi.org/10.36660/abcimg.20240112i

Introduction

Myocardial tissue characterization through non-invasive imaging methods is essential for evaluating heart diseases, offering additional diagnostic and prognostic benefits beyond morphological and functional assessments.[1] Among the available techniques, myocardial extracellular volume (ECV) quantification has recently shown value in differential diagnosis and disease staging, particularly for cardiomyopathies with a hypertrophic phenotype, such as hypertrophic cardiomyopathy and amyloidosis.[2-4]

Myocardial ECV is typically obtained through cardiac magnetic resonance imaging (CMR) using gadolinium-based contrast. However, it can also be calculated using

CONTENTS

cardiac computed tomography (CCT) with iodinated contrast, providing an alternative when CMR is unavailable or contraindicated.[5]

The technical process for obtaining this data in CCT examinations is outlined below.

My Approach To

Image acquisition

To calculate myocardial ECV, images of the heart must be acquired before and after the administration of iodine-based contrast, using identical acquisition and reconstruction parameters. Tomographs suitable for cardiac evaluation (minimum of 64 detector rows) are required.[6]

Given that slices with a thickness of 3 mm or more are suitable for myocardial analysis, we recommend that pre- and post-contrast acquisitions adhere to the institutional calcium scoring protocol. This protocol, which routinely employs a low radiation dose (< 1.5 mSv),[7] is widely available and easy to implement. Therefore, the pre-contrast image used for myocardial ECV calculation may also provide additional information, such as the coronary and/or aortic valve calcium score, if needed.

The protocol typically involves a prospective acquisition synchronized with the electrocardiogram, capturing images of the entire heart in diastole for patients with a heart rate of 75 bpm or lower, or in systole for those with a heart rate above 75 bpm. The tube power is set at 120 kVp, with the tube current adjusted based on the patient's weight, and the reconstructed images are generated with 3 mm thick slices.[7]

Iodinated contrast, usually in a concentration of 350 mg I/ml, should be administered at an average dose of 1 mL/kg of body weight, although this may vary depending on the patient's clinical condition and the primary indication for the examination. The contrast infusion rate does not affect the calculation of myocardial ECV and can be adjusted based on the purpose of the study (e.g., approximately 6 mL/s for coronary angiography). Post-contrast images should be obtained during the equilibrium phase (5 to 15 minutes after contrast administration),[8] using the same acquisition and reconstruction parameters as those for pre-contrast images.

Premedication, such as sublingual nitrate or beta-blockers, is not required for myocardial ECV calculation. However, these medications may be used at the physician's discretion if cardiac angiography is also performed during the same examination.

ECV calculation

Since iodinated contrast distributes within the extracellular space, the difference in myocardial signal between the equilibrium-phase contrast images and the non-contrast images (ΔHU myocardium) reflects the extracellular space volume in this tissue.[8] By using a reference tissue, such as blood, where the ECV is readily determined by measuring hematocrit, myocardial ECV can be calculated with the following formula:

$$ECV = (1 - Hematocrit) \times (\Delta HU\ myocardium / \Delta HU\ blood)$$

Myocardial ECV can be measured either globally or regionally, depending on the clinical context. The regions of interest (ROI) selected for measurement should be identical or as closely matched as possible between the pre- and post-contrast images. These ROIs can be outlined using proprietary or open-source DICOM image analysis tools on axial, sagittal, coronal, or other oblique planes of interest. To ensure reproducibility and minimize distortions from non-isotropic acquisition and reconstruction, myocardial ECV is typically measured in the axial plane at the mid-left ventricular level. A freehand ROI is drawn in the interventricular septum, covering its entire visible thickness and length while avoiding partial volume effects at the edges (Figure 1). For the blood signal measurement, a circular ROI of approximately 1 cm^2 is placed in the center of the left ventricular cavity within the same plane, ensuring trabeculae and papillary muscles are excluded.

The hematocrit value used in the calculation should be obtained as close as possible to the imaging exam date.[9]

Discussion

Myocardial ECV is a quantitative measure of the myocardial extracellular matrix and may be elevated in the presence of interstitial fibrosis[10] or in cases of storage diseases such as amyloidosis, where insoluble fibrillar proteins can accumulate in the heart muscle.[3]

As a quantitative measure, myocardial ECV has diagnostic and prognostic utility and holds potential for use in longitudinal follow-up.[11]

Although most commonly assessed by CMR, myocardial ECV can also be calculated using contrast-enhanced CCT, as the distribution pattern and kinetics of contrast media are equivalent in both imaging methods.[5]

In a meta-analysis conducted by Han et al., comparing myocardial ECV measurements by CCT and CMR, a high grouped correlation coefficient (0.90) and a small, grouped difference (0.96%) were observed, with a slight overestimation of values obtained by CCT.[12]

Although guidelines do not yet provide clear recommendations for the use of CCT in assessing myocardial ECV, its future utility has already been suggested.[13] However, CCT can be considered a viable option in cases where this measurement is clinically significant but cannot be obtained through CMR. This typically occurs due to factors such as limited availability of equipment, T1 mapping sequences, or analysis software; contraindications to performing the examination (e.g., presence of implantable devices incompatible with magnetic resonance imaging); or contraindications to the use of gadolinium-based contrast media (e.g., renal failure requiring dialysis). Chart 1 outlines the main advantages and disadvantages of using CCT compared to CMR for myocardial ECV assessment.

In addition to these scenarios, it may be beneficial to consider obtaining myocardial ECV in contrast-enhanced CT scans performed for other purposes, such as pre-transcatheter intervention coronary or aortic valve assessment, with a small modification to the protocol (e.g.,

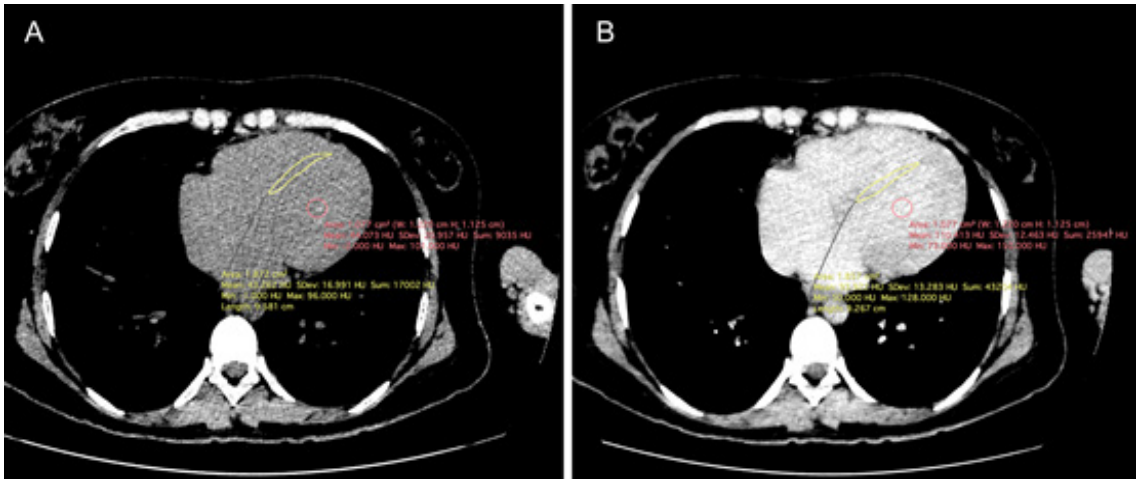

Figure 1 – *Calculation of myocardial ECV through CCT. Myocardial and blood signals are quantified through ROIs drawn on pre- (A) and post-contrast (B) images, in a patient with left ventricular hypertrophy, referred for coronary angiotomography due to complaints of shortness of breath. The myocardial ECV was elevated and calculated at 47% (hematocrit of 39.8%). Subsequent investigation led to the diagnosis of cardiac amyloidosis due to transthyretin.*
ROI: region of interest.

Chart 1 – Advantages and Disadvantages of Myocardial ECV Calculation through CCT versus CMR

Advantages:
More widely available equipment
Generally lower cost
Faster procedure and routinely well tolerated by claustrophobic patients
No restrictions for patients with implanted cardiac devices or metallic fragments in the body
High-resolution images with complete myocardial coverage
Does not require dedicated software for calculation
Disadvantages:
Exposure to ionizing radiation
Use of potentially nephrotoxic contrast

adding a late post-contrast acquisition). In patients referred for these exams, it is not uncommon, for example, to encounter the coexistence of heart failure with preserved ejection fraction and/or left ventricular hypertrophy, clinical situations where knowledge of myocardial ECV may indicate an etiological diagnosis still unknown, in addition to providing incremental prognostic data.[14,15]

Conclusion

Myocardial ECV is a measure of increasing clinical utility and can be obtained through contrast-enhanced CCT, using a low-dose radiation protocol and rapid execution. This approach eliminates the need for sequences and proprietary software required for calculation by CMR, without compromising accuracy compared to the latter.

Author Contributions

Conception and design of the research: Camargo GC; writing of the manuscript and critical revision of the manuscript for intellectual content: Camargo GC, Sabioni LR.

Potential Conflict of Interest

No potential conflict of interest relevant to this article was reported.

Sources of Funding

There were no external funding sources for this study.

Study Association

This study is not associated with any thesis or dissertation work.

Ethics Approval and Consent to Participate

This article does not contain any studies with human participants or animals performed by any of the authors.

References

1. Arbelo E, Protonotarios A, Gimeno JR, Arbustini E, Barriales-Villa R, Basso C, et al. 2023 ESC Guidelines for the Management of Cardiomyopathies. Eur Heart J. 2023;44(37):3503-626. doi: 10.1093/eurheartj/ehad194.
2. Li Y, Liu X, Yang F, Wang J, Xu Y, Fang T, et al. Prognostic Value of Myocardial Extracellular Volume Fraction Evaluation Based on Cardiac Magnetic Resonance T1 Mapping with T1 Long and Short in Hypertrophic Cardiomyopathy. Eur Radiol. 2021;31(7):4557-67. doi: 10.1007/s00330-020-07650-7.
3. Gama F, Rosmini S, Bandula S, Patel KP, Massa P, Tobon-Gomez C, et al. Extracellular Volume Fraction by Computed Tomography Predicts Long-term Prognosis Among Patients with Cardiac Amyloidosis. JACC Cardiovasc Imaging. 2022;15(12):2082-94. doi: 10.1016/j.jcmg.2022.08.006.
4. Hammer Y, Talmor-Barkan Y, Abelow A, Orvin K, Aviv Y, Bar N, et al. Myocardial Extracellular Volume Quantification by Computed Tomography Predicts Outcomes in Patients with Severe Aortic Stenosis. PLoS One. 2021;16(3):e0248306. doi: 10.1371/journal.pone.0248306.
5. Scully PR, Bastarrika G, Moon JC, Treibel TA. Myocardial Extracellular Volume Quantification by Cardiovascular Magnetic Resonance and Computed Tomography. Curr Cardiol Rep. 2018;20(3):15. doi: 10.1007/s11886-018-0961-3.
6. Abbara S, Blanke P, Maroules CD, Cheezum M, Choi AD, Han BK, et al. SCCT Guidelines for the Performance and Acquisition of Coronary Computed Tomographic Angiography: A Report of the Society of Cardiovascular Computed Tomography Guidelines Committee: Endorsed by the North American Society for Cardiovascular Imaging (NASCI). J Cardiovasc Comput Tomogr. 2016;10(6):435-49. doi: 10.1016/j.jcct.2016.10.002.
7. Voros S, Rivera JJ, Berman DS, Blankstein R, Budoff MJ, Cury RC, et al. Guideline for Minimizing Radiation Exposure During Acquisition of Coronary Artery Calcium Scans with the use of Multidetector Computed Tomography: A Report by the Society for Atherosclerosis Imaging and Prevention Tomographic Imaging and Prevention Councils in Collaboration with the Society of Cardiovascular Computed Tomography. J Cardiovasc Comput Tomogr. 2011;5(2):75-83. doi: 10.1016/j.jcct.2011.01.003.
8. Treibel TA, Bandula S, Fontana M, White SK, Gilbertson JA, Herrey AS, et al. Extracellular Volume Quantification by Dynamic Equilibrium Cardiac Computed Tomography in Cardiac Amyloidosis. J Cardiovasc Comput Tomogr. 2015;9(6):585-92. doi: 10.1016/j.jcct.2015.07.001.
9. Su MY, Huang YS, Niisato E, Chow K, Juang JJ, Wu CK, et al. Is a Timely Assessment of the Hematocrit Necessary for Cardiovascular Magnetic Resonance-derived Extracellular Volume Measurements? J Cardiovasc Magn Reson. 2020;22(1):77. doi: 10.1186/s12968-020-00689-x.
10. Wang S, Hu H, Lu M, Sirajuddin A, Li J, An J, et al. Myocardial Extracellular Volume Fraction Quantified by Cardiovascular Magnetic Resonance is Increased in Hypertension and Associated with Left Ventricular Remodeling. Eur Radiol. 2017;27(11):4620-30. doi: 10.1007/s00330-017-4841-9.
11. Rettl R, Mann C, Duca F, Dachs TM, Binder C, Ligios LC, et al. Tafamidis Treatment Delays Structural and Functional Changes of the Left Ventricle in Patients with Transthyretin Amyloid Cardiomyopathy. Eur Heart J Cardiovasc Imaging. 2022;23(6):767-80. doi: 10.1093/ehjci/jeab226.
12. Han D, Lin A, Kuronuma K, Gransar H, Dey D, Friedman JD, et al. Cardiac Computed Tomography for Quantification of Myocardial Extracellular Volume Fraction: A Systematic Review and Meta-analysis. JACC Cardiovasc Imaging. 2023;16(10):1306-17. doi: 10.1016/j.jcmg.2023.03.021.
13. Magalhães TA, Carneiro ACC, Moreira VM, Trad HS, Lopes MMU, Cerci RJ, et al. Cardiovascular Computed Tomography and Magnetic Resonance Imaging Guideline of the Brazilian Society of Cardiology and the Brazilian College of Radiology - 2024. Arq Bras Cardiol. 2024;121(9):e20240608. doi: 10.36660/abc.20240608.
14. Scully PR, Patel KP, Saberwal B, Klotz E, Augusto JB, Thornton GD, et al. Identifying Cardiac Amyloid in Aortic Stenosis: ECV Quantification by CT in TAVR Patients. JACC Cardiovasc Imaging. 2020;13(10):2177-89. doi: 10.1016/j.jcmg.2020.05.029.
15. Koike H, Fukui M, Treibel T, Stanberry LI, Cheng VY, Enriquez-Sarano M, et al. Comprehensive Myocardial Assessment by Computed Tomography: Impact on Short-term Outcomes after Transcatheter Aortic Valve Replacement. JACC Cardiovasc Imaging. 2024;17(4):396-407. doi: 10.1016/j.jcmg.2023.08.008.

Prosthetic Valve Endocarditis: A Multidisciplinary Challenge

Ana Beatriz Aisemann Goulart Paiva,[1] Ana Carolina de Azevedo Pastori,[1] Gabriel Silva Vaz Martins,[1] Lucas Norambuena Aulicino,[1] Marcelo Goulart Paiva[2]

UNILUS,[1] Santos, SP – Brazil

Hospital 9 de Julho,[2] São Paulo, SP – Brazil

Clinical case

We report the case of a 55-year-old male patient who was admitted to the hospital in July 2019 with sudden left hemiplegia, mitral systolic murmur 4+, and aortic systolic and diastolic murmurs 2+. He had a history of aortic valve replacement in 2015, with a mechanical prosthetic aortic valve (PAV) due to infective endocarditis (IE). Cranial computed tomography (CT) revealed a right frontoparietal hematoma (Figure 1C), and blood tests revealed hyperglycemia and elevated C-reactive protein. His electrocardiogram (ECG) showed sinus rhythm with repolarization abnormalities (Figure 1A), and a chest X-ray showed cardiomegaly +/4 (Figure 1B). Transthoracic echocardiography (TTE) showed preserved function, thickening of the mobile elements of the mechanical PAV, mild double aortic lesion, pseudoaneurysm of the mitral-aortic intervalvular fibrosa, and important eccentric mitral regurgitation (Figure 1D). Blood cultures were requested, and ceftriaxone 4 g/d and teicoplanin 800 mg/d were started. Transesophageal echocardiography (TEE) showed vegetations on the ventricular side of the mechanical PAV leaflets and periprosthetic abscess (Figure 2). Group B *Streptococcus agalactiae* was identified, and surgical treatment was indicated after 4 weeks due to cardiovascular stability and hemorrhagic stroke.

On day 22 of hospitalization, the patient presented pulmonary congestion and respiratory failure. Repeated TTE revealed partial loosening of the mechanical PAV and severe periprosthetic leak. Emergency surgery was performed to clean and replace the mechanical PAV with a biological PAV, without mitral valve approach. Culture of the explanted prosthesis revealed no bacterial growth.

The postoperative period was complicated, with fungemia due to *Candida guilliermondii*. On postoperative day 14, TTE and TEE identified a periprosthetic abscess with the presence of a fistula (Figure 3). CT angiography showed that the biological PAV had periaortic and perivalvular contrast extravasation (Figure 4). On postoperative day 18, a diastolic murmur appeared, and a new TTE showed a fistula from the ventricular outflow tract to the right atrium, with systolic flow, that was 2 mm in diameter (Gerbode defect), as shown in Figure 5.

The heart team contraindicated further surgery, maintaining meropenem, teicoplanin and caspofungin for 42 days. After repeat TEE without any change in progression, inflammatory tests and negative blood cultures normalized, and the patient was discharged from the hospital.

The patient was readmitted with fever 30 days later, and the previous antibiotic regimen was restarted, with no infectious focus and negative blood cultures. Positron emission tomography with computed tomography (PET/CT) with 18FDG showed focal glycolytic hypermetabolism in the biological PAV and abscess surrounding the ascending aorta (Figure 6). Surgery was again contraindicated, and amoxicillin 3 g/day was chosen for an indefinite period.

In November 2019, 18FDG PET/CT showed no uptake, suggesting resolution of prosthetic valve endocarditis (PVE). At the last evaluation, in July 2023, the patient was stable, without infectious complications. ETT showed dilation of the left cavities, periprosthetic fistula, Gerbode defect, moderate pulmonary hypertension, and biological PAV with maintained gradients.

Discussion

The incidence of PVE varies from 1% to 6% per year; it is more common in biological prostheses, and it represents 20% to 30% of IE cases.[1] The diagnosis of PVE still poses challenges, leading to delays in management, which is sometimes decided on an almost individual basis.[2]

Asymptomatic neurological symptoms or neuroimaging findings may indicate embolism, and they can be the first manifestation of IE, associated with higher mortality and indication for early surgery.[1,3,4] Blood cultures were collected and, because it was a case of late PVE (1 year after the first surgery), coverage against Gram-positive pathogens was considered.[1,5]

The reported case was diagnosed by the modified Duke criteria,[1] with nonspecific ECG, but PVE can manifest with atrioventricular block. Laboratory findings assisted in risk stratification and evaluation of therapeutic response. The most frequent agents in late PVE are as follows: *S. aureus*, 22.9%; coagulase negative staphylococci, 17.2%; and viridans streptococci, 16%.[3] *S agalactiae* was isolated, which rarely causes PVE and, unlike cases of late PVE, progresses rapidly with valve destruction, embolism, 20% mortality, and need for surgery in 40% to 50% of cases.[6]

Keywords

Endocarditis; Multimodal Imaging; Heart Valve Prosthes

Mailling Address: Marcelo Goulart Paiva •
Rua Periquito, 210, 92B. Postal code: 04023-062. São Paulo, SP – Brazil
E-mail: mgpaiva123@gmail.com
Manuscript received December 14, 2024; revised January 10, 2025; accepted January 17, 2025
Editor responsible for the review: Marcelo Tavares

DOI: https://doi.org/10.36660/abcimg.20240133i

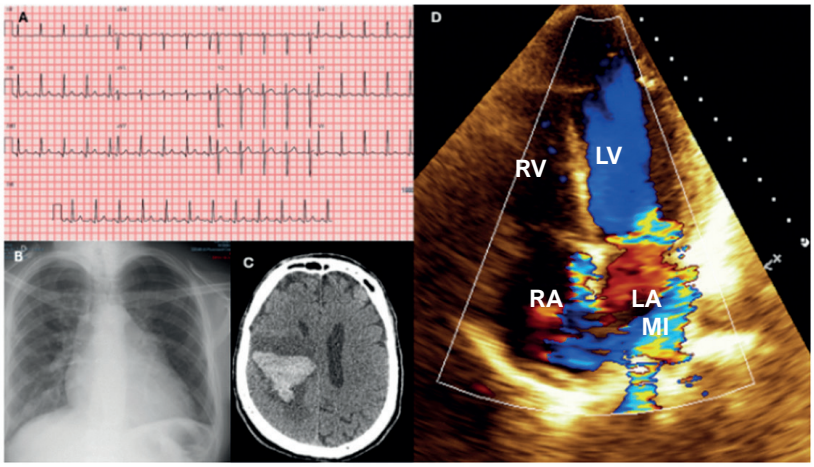

Figure 1 – *(A) ECG; (B) Posteroanterior chest X-ray; (C) Cranial CT; (D) Transthoracic echocardiogram. LA: left atrium; LV: left ventricle; MI: mitral insufficiency; RA: right atrium; RV: right ventricle.*

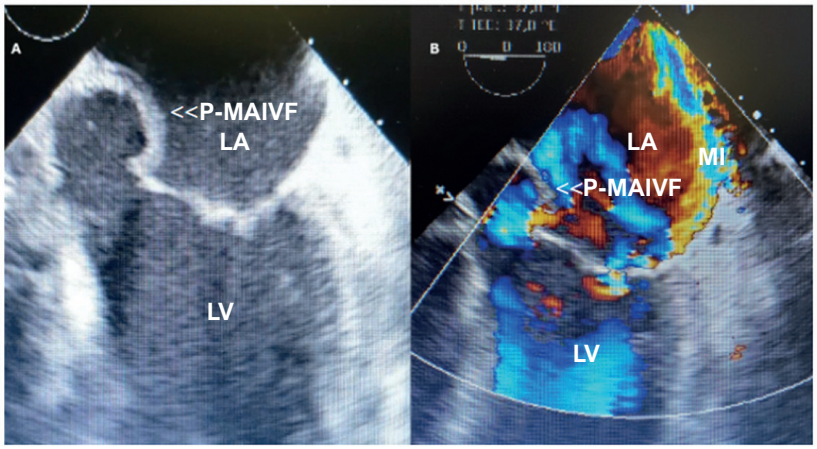

Figure 2 – *Transesophageal echocardiogram. LA: left atrium; LV: left ventricle; MI: mitral insufficiency; P-MAIVF: pseudoaneurysm of the mitral-aortic intervalvular fibrosa.*

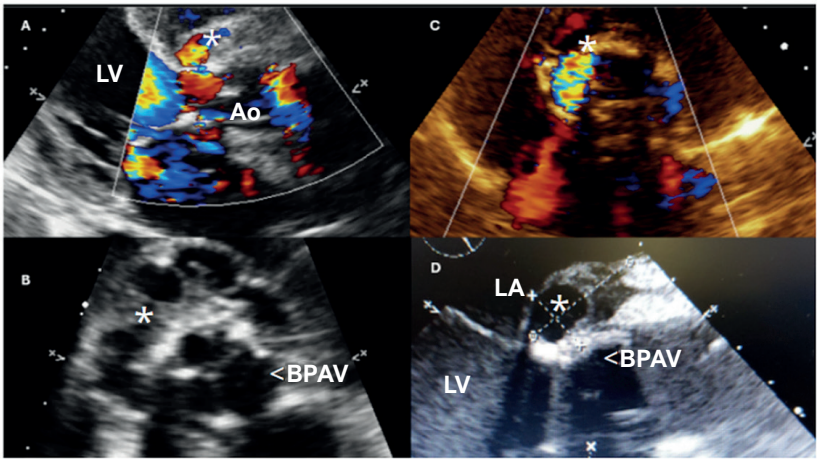

Figure 3 – *(A, B, and C) Transthoracic echocardiogram; (D) Transesophageal echocardiogram. BPAV: biological prosthetic aortic valve; LA: left atrium; LV: left ventricle. Asterisk (*) indicates abscess.*

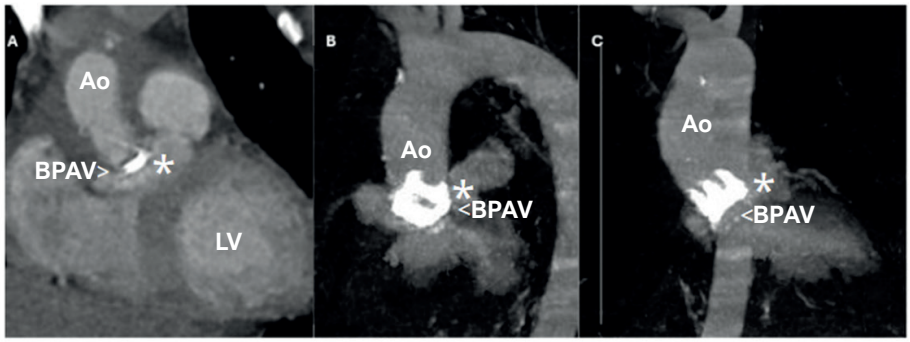

Figure 4 – *T angiography of the aorta. Ao: ascending aorta; BPAV: biological prosthetic aortic valve; LV: left ventricle. Asterisk (*) indicates perivalvular leak.*

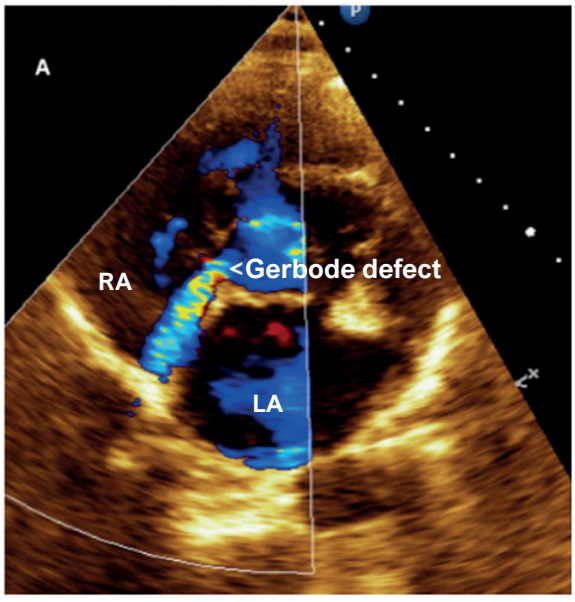

Figure 5 – *Transthoracic echocardiogram. LA: left atrium; RA: right atrium.*

The specificity of TTE for PVS is 96%, and the sensitivity ranges from 40% to 50%, lower than in native valve IE, most often involving the prosthetic ring (mainly in mechanical prostheses).[1,7] The European guideline indicates TEE when TTE is inconclusive or in suspected complications, whereas the United States guideline advises that it should always be performed.[1,8] The sensitivity of TEE ranges from 82% to 96%, and the specificity is 86%.[1,7,8] On day 3 of hospitalization, TEE revealed a pseudoaneurysm of the mitral-aortic intervalvular fibrosa, which can lead to coronary compression, pericardial effusion, and fistulization. The sensitivity on TEE and TTE is 90% and 43%, respectively, with indication for surgery.[9]

On day 22 of hospitalization, the patient presented a mechanical complication, which is responsible for 30% of urgent surgeries, as well as congestive heart failure, abscess and persistent fever. Failure to perform surgery is a marker of worse prognosis.[1,3,5]

Postoperative mortality ranges from 6% to 29% in observational studies, and it is associated with age, urgent or emergency surgery, prior cardiac surgery, prosthetic valve, multivalvular involvement, perivalvular abscess, and kidney failure.[10,11]

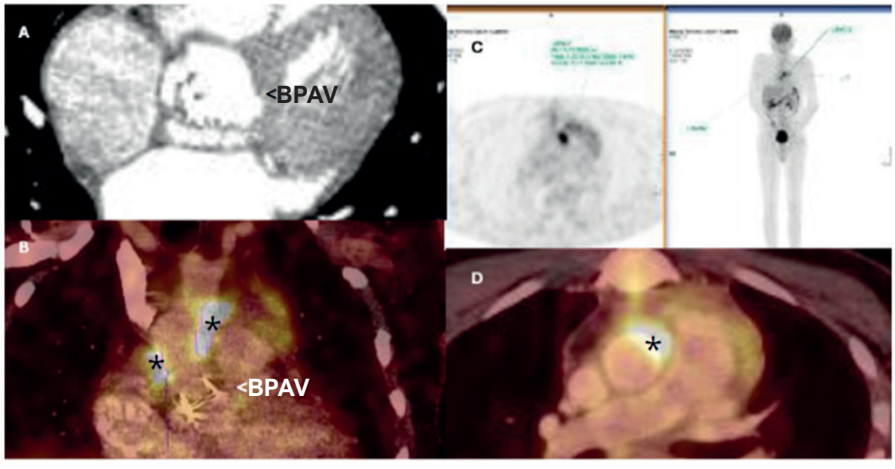

Figure 6 – *18FDG PET/CT. BPAV: Biological prosthetic aortic valve. Asterisk (*) indicates glycolytic hypermetabolism with maximum standardized uptake value (SUVmax) = 11.2.*

After fungemia, TEE and CT showed a periaortic abscess with fistula and Gerbode defect, which can be found rarely in complications after cardiac surgery or IE.[7,12] Since the prosthesis culture was negative, a new PVE was suspected, given that fungi are a cause of acute PVE.[1,3,5]

CT became more important in the latest revision of the Duke criteria and in the European guideline, going on to be considered a major criterion for diagnosis, with a sensitivity of 88% and a specificity of 93%, surpassing TEE in the identification of paravalvular abscess.[1] TEE, on the other hand, has a specificity of 100% for paravalvular leak. Nuclear magnetic resonance imaging has limited use compared to CT, since prosthetic valves impair assessment.

In spite of the indication for reoperation, the patient improved and was discharged, being readmitted after 4 weeks. Patients with surgical indication who did not undergo surgery, usually due to clinical complications, present reinfection and recurrence of 5% during 1-year follow-up. When comparing mortality between operated and non-operated patients, recurrence is 9% and 34%, respectively.[13]

In cases of inconclusive diagnosis, 18FDG PET/CT can be requested. Positive findings are predictors of complications, recurrence of IE, and new embolic events. It is important to differentiate uptake in the recent postoperative period (diffuse and homogeneous) from PVE (intense, heterogeneous, focal, or multifocal), with sensitivity of 54% to 87% and specificity of 56% to 93%, reclassifying the Duke criteria on admission and increasing sensitivity to 82% to 96% without loss of specificity.[1,14]

Prolonged antibiotic therapy is recommended in cases of IE caused by *Candida* or as an alternative in patients with surgical indications who did not undergo surgery.[1] In a study with 31 patients who did not undergo surgery and received prolonged oral antibiotic therapy, the event-free survival rate at 1 year was 74%; the overall survival rate was 84.3%; and the recurrence rate was 12% (mean after 111 days).[15] The absence of uptake on the control PET/CT allows for safe suspension of treatment with a low risk of complications.[14]

The following are associated with worse prognosis in IE: advanced age, diabetes mellitus, *S. aureus*, fungi, acute PVE, congestive heart failure, stroke, abscesses, and failure to perform surgery when indicated.[10,16] The patient was at high risk, with an estimated mortality rate of 60% in 6 months. In fungal IE, the prognosis is significantly worse, and, even with early diagnosis and appropriate treatment, mortality rates of 10% to 75% have been reported.

Despite the risk factors and various complications related to PVE, the patient remains stable to date, reinforcing the importance of multimodal imaging and a multidisciplinary approach.

Author Contributions

Conception and design of the research and acquisition of data: Paiva ABAG, Paiva MG; Analysis and interpretation of the data, writing of the manuscript and critical revision of the manuscript for intellectual content: Paiva ABAG, Pastori ACA, Martins GSV, Aulicino LN, Paiva MG.

Potential Conflict of Interest

No potential conflict of interest relevant to this article was reported.

Sources of Funding

There were no external funding sources for this study.

Study Association

This study is not associated with any thesis or dissertation work.

Ethics Approval and Consent to Participate

This study was approved by the Ethics Committee of the Hospital 9 de Julho under the protocol number 19795619.9.0000.5455. All the procedures in this study were in accordance with the 1975 Helsinki Declaration, updated in 2013. Informed consent was obtained from all participants included in the study.

References

1. Delgado V, Marsan NA, Waha S, Bonaros N, Brida M, Burri H, et al. 2023 ESC Guidelines for the Management of Endocarditis. Eur Heart J. 2023;44(39):3948-4042. doi: 10.1093/eurheartj/ehad193.
2. Cuervo G, Quintana E, Regueiro A, Perissinotti A, Vidal B, Miro JM, et al. The Clinical Challenge of Prosthetic Valve Endocarditis: JACC Focus Seminar 3/4. J Am Coll Cardiol. 2024;83(15):1418-30. doi: 10.1016/j.jacc.2024.01.037.
3. Habib G, Erba PA, Iung B, Donal E, Cosyns B, Laroche C, et al. Clinical Presentation, Aetiology and Outcome of Infective Endocarditis. Results of the ESC-EORP EURO-ENDO (European Infective Endocarditis) Registry: A Prospective Cohort Study. Eur Heart J. 2019;40(39):3222-32. doi: 10.1093/eurheartj/ehz620.
4. Cuervo G, Escrihuela-Vidal F, Gudiol C, Carratalà J. Current Challenges in the Management of Infective Endocarditis. Front Med. 2024;8:641243. doi: 10.3389/fmed.2021.641243.
5. Shah ASV, McAllister DA, Gallacher P, Astengo F, Pérez JAR, Hall J, et al. Incidence, Microbiology, and Outcomes in Patients Hospitalized with Infective Endocarditis. Circulation. 2020;141(25):2067-77. doi: 10.1161/CIRCULATIONAHA.119.044913.
6. Machado C, Almeida C, Santos E, Pelicano N, Dourado R, Martins D. Endocardite a Streptococcus Agalactiae. Rev Port Cardiol. 2012;31(9):619-21. doi: 10.1016/j.repc.2012.01.017.
7. Arockiam AD, Agrawal A, El Dahdah J, Honnekeri B, Kafil TS, Halablab S, et al. Contemporary Review of Multi-Modality Cardiac Imaging Evaluation of Infective Endocarditis. Life. 2023;13(3):639. doi: 10.3390/life13030639.
8. Baddour LM, Wilson WR, Bayer AS, Fowler VG, Tleyjeh IM, Rybak MJ, et al. Infective Endocarditis in Adults: Diagnosis, Antimicrobial Therapy, and Management of Complications: A Scientific Statement for Healthcare Professionals from the American Heart Association. Circulation. 2015;132(15):1435-86. doi: 10.1161/CIR.0000000000000296.
9. Kuroda M, Yamamoto H, Nakamura Y. Infective Endocarditis Complicated by Pseudoaneurysm of the Mitral-Aortic Intervalvular Fibrosa without

Valvular Involvement. JACC Case Rep. 2020;2(8):1212-6. doi: 10.1016/j.jaccas.2020.05.071.

10. Marques A, Cruz I, Caldeira D, Alegria S, Gomes AC, Broa AL, et al. Risk Factors for In-Hospital Mortality in Infective Endocarditis. Arq Bras Cardiol. 2020;114(1):1-8. doi: 10.36660/abc.20180194.

11. Sousa C, Pinto FJ. Infective Endocarditis: Still More Challenges Than Convictions. Arq Bras Cardiol. 2022;118(5):976-88. doi: 10.36660/abc.20200798.

12. Takagui ASM, Baggio TC, Savariz MB, Theilacker G, Baggio TE. Left Ventricular-to-Right Atrial Shunt (Gerbode Defect) Associated with Interventricular Communication in a 42-Year-Old Patient. ABC Imagem Cardiovasc. 2021;34(1):1-4. doi: 10.47593/2675-312X/20213401eabc142.

13. Camazón NV, Cediel G, Aragón RN, Mateu L, Llibre C, Sopena N, et al. Short- and Long-Term Mortality in Patients with Left-Sided Infective Endocarditis Not Undergoing Surgery Despite Indication. Rev Esp Cardiol. 2020;73(9):734-40. doi: 10.1016/j.rec.2019.09.011.

14. Lancellotti P, Go YY. The Power of Negative Metabolic Imaging: Negative FDG-PET/CT Predicts Infective Endocarditis Resolution. Eur Heart J Cardiovasc Imaging. 2023;24(11):1489-90. doi: 10.1093/ehjci/jead175.

15. Beaumont AL, Mestre F, Decaux S, Bertin C, Duval X, Iung B, et al. Long-Term Oral Suppressive Antimicrobial Therapy in Infective Endocarditis (SATIE Study): An Observational Study. Open Forum Infect Dis. 2024;11(5):ofae194. doi: 10.1093/ofid/ofae194.

16. Gatti G, Perrotti A, Obadia JF, Duval X, Iung B, Alla F, et al. Simple Scoring System to Predict In-Hospital Mortality after Surgery for Infective Endocarditis. J Am Heart Assoc. 2017;6(7):e004806. doi: 10.1161/JAHA.116.004806.

Percutaneous Closure of the Aortopulmonary Window in an Infant Using an Amplatzer Duct Occluder II Prosthesis

Edmundo Clarindo Oliveira,[1] José Augusto Almeida Barbosa,[1,2] Marco Antonio Gonçalves Moura,[1] Marcelo Frederigue de Castro,[2] Renata Fonseca Mendoza,[3,4] Maria Carmo Pereira Nunes[4]

Felicio Rocho Hospital,[1] Belo Horizonte, MG – Brazil

Vila da Serra Hospital,[2] Nova Lima, MG – Brazil

Universidade Estadual de Feira de Santana,[3] Feira de Santana, BA – Brazil

Universidade Federal de Minas Gerais,[4] Belo Horizonte, MG – Brazil

Introduction

The Aortopulmonary Window (APW) is a rare congenital malformation, representing approximately 0.2% of all congenital heart diseases. It is typically nonrestrictive and requires early surgical intervention to prevent complications such as pulmonary congestion, respiratory infections, and obstructive pulmonary vascular disease. In cases like ours, where the surgical risk is exceedingly high, percutaneous closure may present a viable alternative.

Case Report

A 1.5-month-old male infant, born with a weight of 2180 g, presented with multiple comorbidities, including esophageal atresia, congenital chylothorax, and Meckel's diverticulum. The patient underwent several surgeries within the first few days of life. He also experienced recurrent infections and required prolonged mechanical ventilation. During evaluation, cardiomegaly was noted alongside a continuous murmur at the upper left sternal border. The echocardiogram revealed a 5.0 mm APW (Figures 1 and 2). The echocardiogram revealed a large left-to-right shunt, resulting in left chamber enlargement. Following a multidisciplinary discussion with the cardiology team and given the high surgical risk, percutaneous closure of the APW was chosen as the best approach. The procedure was performed after informed consent was obtained.

Cardiac catheterization was performed under general anesthesia using ultrasound-guided puncture of the right carotid artery and right femoral vein, with a 4F sheath in the artery and a 5F sheath in the vein. Heparin was administered at 100 IU/kg. Mean aortic and pulmonary pressures were measured at 44 and 29 mmHg, respectively. The ascending aortogram confirmed a 5.0 mm APW located distant from the left aortic cusp (Figure 3). The defect was crossed via the aorta using a 4F Judkins catheter with a 3.5 bend and a 0.0035 Terumo guidewire. The guidewire was captured and exteriorized through the femoral vein, forming a venoarterial loop. A long 5F sheath and a delivery system were then advanced from the femoral vein, through the APW, and into the descending aorta. Initially, an Amplatzer Duct Occluder II (ADOII 6/6) prosthesis (St. Jude Medical, St. Paul, MN, USA) was advanced; the aortic disc was delivered followed by the pulmonary disc, which did not fix properly. The device was then replaced by an ADO II 4/4. After confirming proper device positioning using transthoracic echocardiography and fluoroscopy, ensuring no interference with aortic and pulmonary flows or proximity to the coronary arteries, the device was successfully implanted (Fig. 4). Two weeks post-procedure, the patient showed no signs of heart failure, and the echocardiogram confirmed the device was well-positioned, with no significant vessel obstruction or residual shunt. The patient remained in the ICU due to other comorbidities.

Discussion

APW is a defect resulting from incomplete separation of the aorta and pulmonary trunk walls at the conotruncal septum during early embryogenesis. APW is classified into three morphological types. Type I defects (60-70%) are located proximally, in the aorta above the sinus of Valsalva. Type II defects (20-25%) are distal, situated in the upper ascending aorta before the emergence of the aortic branches. Type III defects, which are less common, are extensive and combine features of types I and II, involving most of the ascending aorta, the pulmonary trunk, and the right pulmonary artery. The Type II defect reported in this case accounts for 20% of APW cases and is particularly amenable to percutaneous correction due to its location. Surgery is the gold standard treatment and has been performed for many years. However, when a patient's clinical condition is critical, with a prohibitively high surgical risk, as the case presented. In these cases, percutaneous closure becomes a valuable alternative when the defect allows for it. Reports in the literature on transcatheter closure of APW are limited, especially for patients weighing less than 3 kg, and they describe various vascular access methods and devices.[1-13] Table 1 presents a summary of the literature review. The defect's position was conducive to percutaneous intervention, while the infant's multiple comorbidities made surgery exceedingly high-risk.

Keywords

Cardiovascular Surgical Procedures; Aortopulmonary Septal Defect; Infant.

Mailing Address: Edmundi Clarindo de Oliveira •
Vila da Serra Hospital. Alameda Oscar Niemeyer, 499. Postal Code: 34006-056. Nova Lima, MG – Brazil
E-mail: jalmeidabarbosa@uol.com.br

Manuscript received August 12, 2024, revised manuscript October 27, 2024, accepted November 19, 2024
Editor responsible for the review: Márcio Brito

DOI: https://doi.org/10.36660/abcimg.20240079i

The optimal device choice remains unclear. Device selection depends on the hemodynamicist's experience with different types of devices designed for closing cardiac and extracardiac shunts. Given the patient's low weight, arterial access via the internal carotid artery was selected, which is our preferred approach for infants under 3.0 kg. In this specific case, we anticipated that crossing the window would be relatively straightforward, as it ultimately proved to be.

Conclusion

Although cardiac surgery is the gold standard for APW closure, high-risk patients with anatomy favorable to percutaneous closure should be considered for this approach, as a viable and effective alternative in the management of such cases.

Author Contributions

Conception and design of the research: Oliveira EC, Castro MF; acquisition of data: Moura MAG; writing of the manuscript: Barbosa JAA; critical revision of the manuscript for intellectual content: Nunes MCP; translation: Mendoza RF.

Potential Conflict of Interest

No potential conflict of interest relevant to this article was reported.

Sources of Funding

There were no external funding sources for this study.

Study Association

This study is not associated with any thesis or dissertation work.

Ethics Approval and Consent to Participate

This article does not contain any studies with human participants or animals performed by any of the authors.

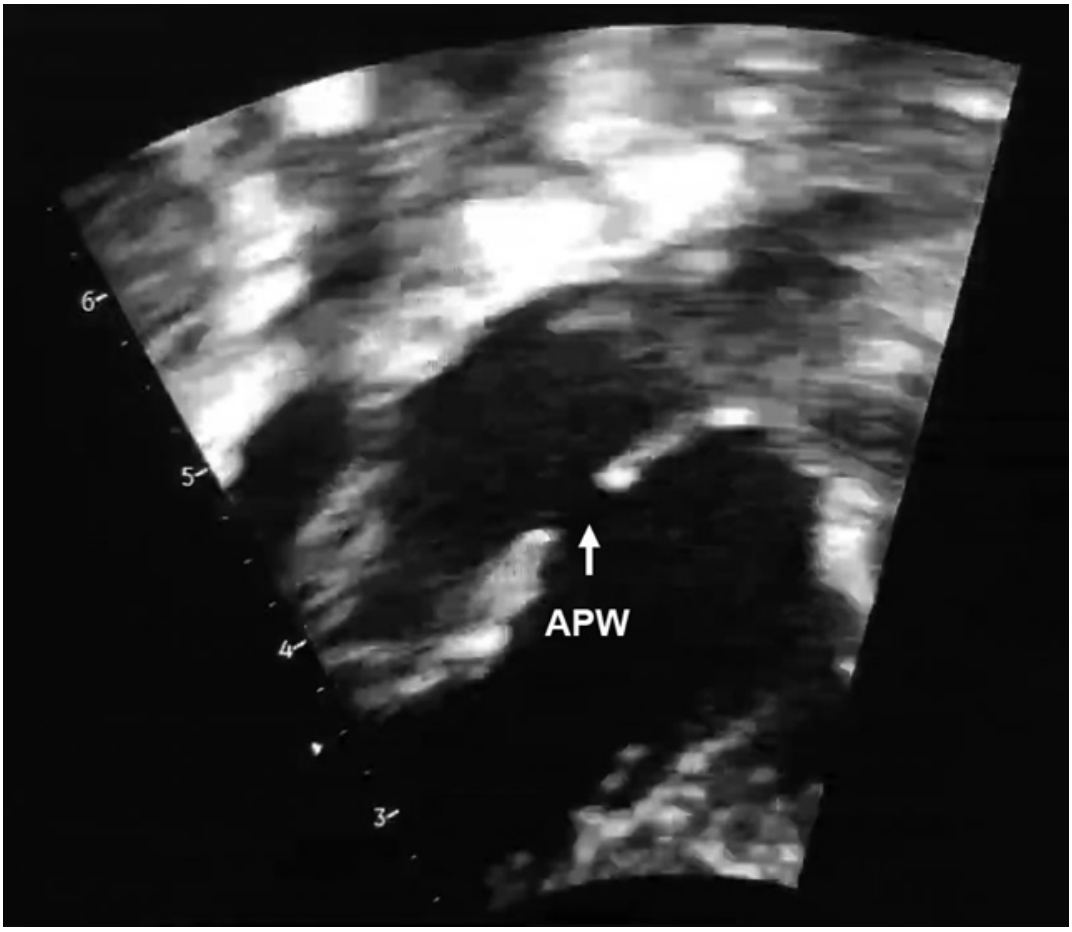

Figure 1 – *Echocardiogram showed a large 5.0 mm APW (white arrow). APW: Aortopulmonary Window.*

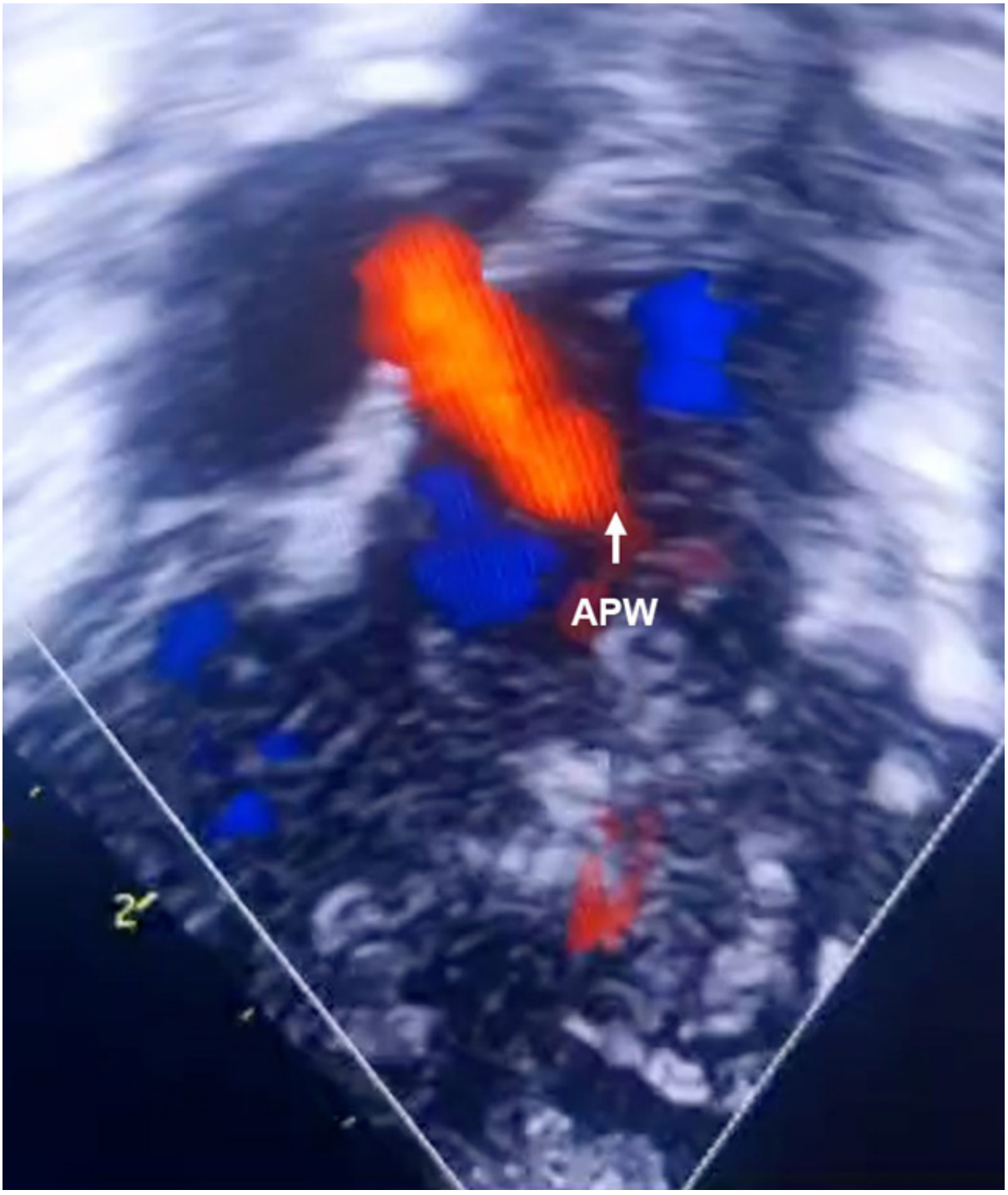

Figure 2 – *Echocardiogram with Color Doppler revealed a significant left-to-right shunt. APW: Aortopulmonary Window*

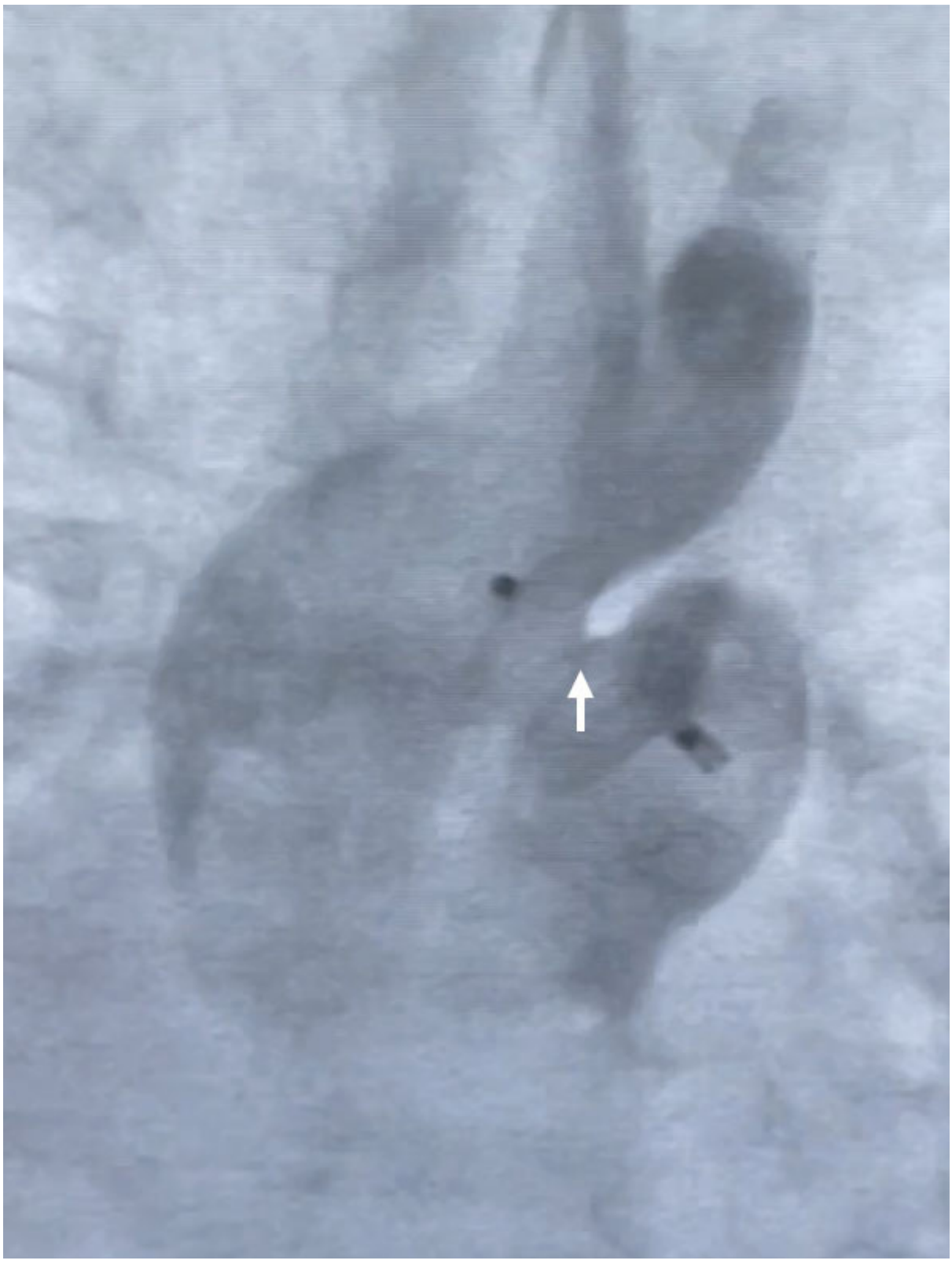

Figure 3 – *Ascending aortogram confirmed an APW.*

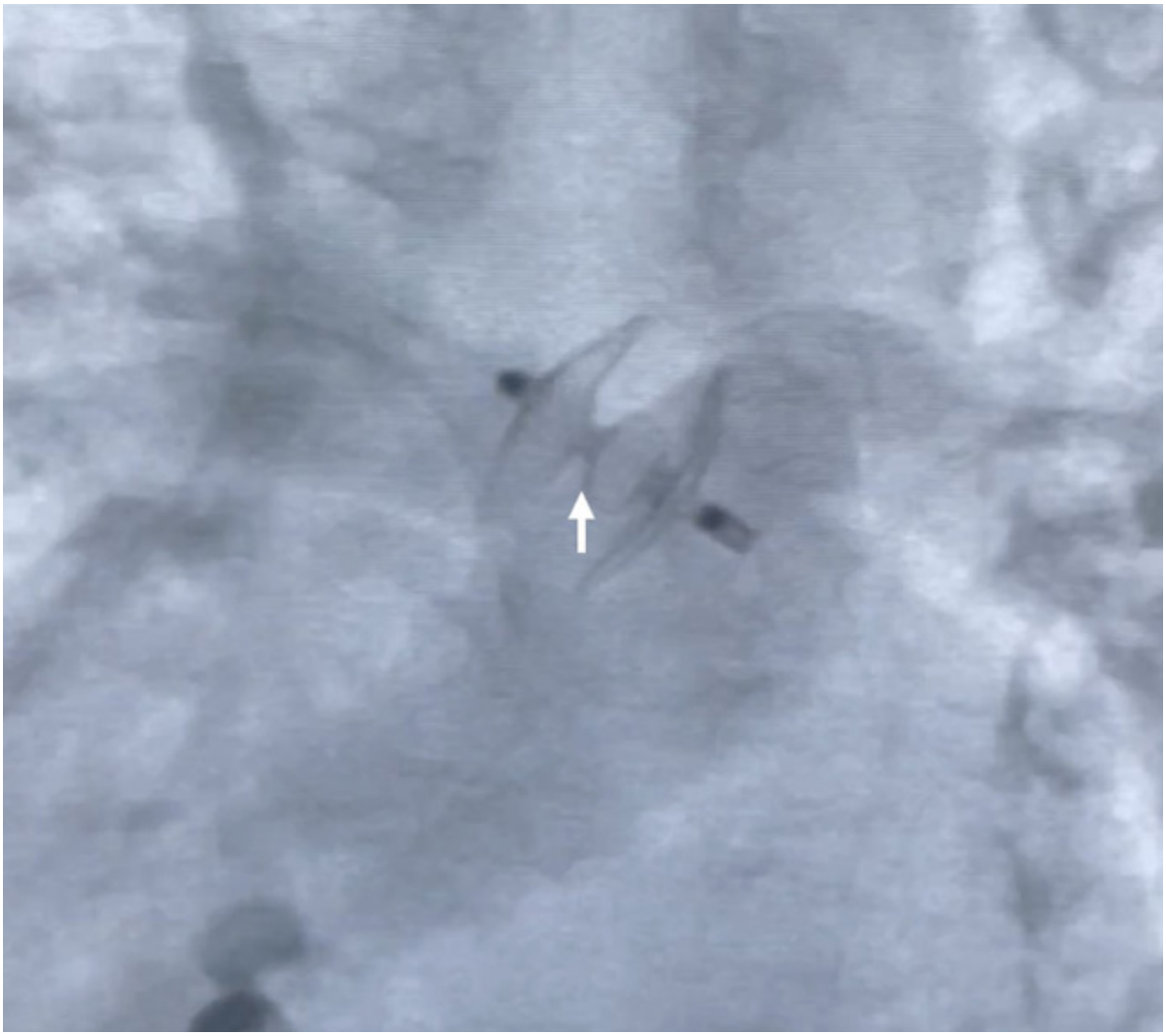

Figure 4 – *Confirmation of the position by fluoroscopy, without interfering in the aorta and pulmonary flow (white arrow).*

Table 1 – Overview of percutaneous closure of the APW as described in the literature.

Reference	Year	Country	Age	Weight (kg)	Sex	Prosthesis	Prosthesis size (mm)
Stamato et al.[1]	1995	Canada	3 y	11	NI	Modified Double Umbrella Occluder System	12
Sivakumar et al.[2]	2006	Sri Lanka	8 m	6.5	M	Amplatzer Duct Occluder 12/10	8.7
			5 y	6.5	F	Amplatzer Duct Occluder 10/8	6
Trehan et al.[3]	2008	India	5 m	5	F	Blockaid PDA occluder (12/10mm)	10
			9 m	6.5	F	Amplatzer muscular VSD occluder (12mm)	10
			5.5 y	5.5	M	Blockaid VSD occluder perimembane (9mm)	8
Zhao-feng et al.[5]	2011	China	11 m	8	M	A 6-8 mm Amplatzer duct occluder	3
			2 y	NI	F	An 18 mm HeartR muscular ventricular septal defect occluder (Lifetech Scientific Co, China)	10.4
			14 y	NI	M	An 18-20 mm HeartR Duct Occluder (Lifetech Scientific Co, China)	14

Kosmač B.[4]	2013	German	25 m	3.9	F	Amplatzer perimembranous VSD occluder (5mm)	4/6
Fiszer et al.[6]	2017	Poland	4.5 y	6	NI	Amplatzer Duct Occluder 4/2	2.3
Sabnis et al.[7]	2018	India	27 d	2.6	M	ADOI (St. Jude Medical, USA)	5
Campos-Quinteiro et al.[8]	2019	Mexico	9 m	6.3	NI	Amplatzer Duct Occluder 5/4	25
			15 y	45	NI	Amplatzer Duct Occluder 10/8	30
			1 y 7 m	8.4	NI	Amplatzer Duct Occluder 8/6	30
			22 d	3.1	NI	Amplatzer Duct Occluder II 6/4	80
			4 y 7 m	15	NI	Amplatzer Duct Occluder 14/12	80
			1 y 5 m	14.2	NI	Cera 16/18	60
Uçar et al.[9]	2020	Türkiye	9 m	NI	F	Amplatzer Duct Occluder AS 5/2	3.7
Giordano et al.[10]	2020	Italy	25 y	51	F	Amplatzer Muscular Septal occluder device 16mm (Abbot)	9/12
Guzeltas A.[11]	2021	Türkiye	1 m	3.5	M	8/6 Amplatzer Muscular Septal occluder (Abbot)	4/7
			6 m	5.3	F	10/8 Amplatzer Muscular Septal occluder (Abbot)	4.7
Yildirim et al.[12]	2021	Türkiye	3 m	4	M	A 7-mm symmetric membranous VSD occlude (Lifetech Scientific Co, China)	5.1
Abdelrazek Ali et al.[13]	2022	Egipt	12 m	7	M	A multifunctional occluder device 12 x 10 mm (Lifetech Scientific Co, China)	7/8

Note: NI = no information available; y = years; m = months; d = days. PDA: patent ductus arteriosus; VSD: ventricular septal defect.

References

1. Stamato T, Benson LN, Smallhorn JF, Freedom RM. Transcatheter Closure of an Aortopulmonary Window with a Modified Double Umbrella Occluder System. Cathet Cardiovasc Diagn. 1995;35(2):165-7. doi: 10.1002/ccd.1810350218.
2. Sivakumar K, Francis E. Transcatheter Closure of Distal Aortopulmonary Window Using Amplatzer Device. Congenit Heart Dis. 2006;1(6):321-3. doi: 10.1111/j.1747-0803.2006.00055.x.
3. Trehan V, Nigam A, Tyagi S. Percutaneous Closure of Nonrestrictive Aortopulmonary Window in Three Infants. Catheter Cardiovasc Interv. 2008;71(3):405-11. doi: 10.1002/ccd.21366.
4. Kosmač B, Eicken A, Kühn A, Heinrich M, Ewert P. Percutaneous Device Closure of an Aortopulmonary Window in a Small Infant. Int J Cardiol. 2013;168(3):e102-3. doi: 10.1016/j.ijcard.2013.07.218.
5. Zhao-Feng X, Zhi-Wei Z, Yu-Me X, Jun-Jie L. Transcatheter Closure of Aortopulmonary Window in Children: Case Reports and Literature Review. CAJ. 2011;12(2):131-5.
6. Fiszer R, Zbroński K, Szkutnik M. Percutaneous Closure of an Aortopulmonary Window Using Amplatzer Duct Occluder II: Additional Sizes: The First Reported Case. Cardiol Young. 2017;27(4):812-5. doi: 10.1017/S1047951116002134.
7. Sabnis GR, Shah HC, Lanjewar CP, Malik S, Kerkar PG. Transcatheter Closure of Large Aortopulmonary Window in a Neonate. Ann Pediatr Cardiol. 2018;11(2):228-30. doi: 10.4103/apc.APC_158_17.
8. Campos-Quintero A, García-Montes JA, Zabal-Cerdeira C, Cervantes-Salazar JL, Calderón-Colmenero J, Sandoval JP. Transcatheter Device Closure of Aortopulmonary Window. Is There a Need for an Alternative Strategy to Surgery? Rev Esp Cardiol (Engl Ed). 2019;72(4):349-51. doi: 10.1016/j.rec.2018.03.020.
9. Uçar T, Karagözlü S, Ramoğlu MG, Tutar E. Transcatheter Closure of Aortopulmonary Window with Amplatzer Duct Occluder II: Additional Size. Cardiol Young. 2020;30(3):424-6. doi: 10.1017/S1047951119003342.
10. Giordano M, Butera G. Percutaneous Closure of an Aortopulmonary Window in a Young Adult Patient: A Case Report of Transcatheter Closure with an Occluder Device. Eur Heart J Case Rep. 2020;4(3):1-4. doi: 10.1093/ehjcr/ytaa059.
11. Guzeltas A, Ugan Atik S, Tanidir IC. Transcatheter Closure of Aortopulmonary Window in Infants with Amplatzer Duct Occluder-I. Acta Cardiol Sin. 2021;37(3):305-8. doi: 10.6515/ACS.202105_37(3).20201019A.
12. Yıldırım A, Erdem A, Karaağaç AT. Transcatheter Closure of the Aortopulmonary Window in a Three-Month-Old Infant with a Symmetric Membranous Ventricular Septal Defect Occluder Device. Turk Gogus Kalp Damar Cerrahisi Derg. 2021;29(1):101-4. doi: 10.5606/tgkdc.dergisi.2021.20988.
13. Abdelrazek Ali Y, Nour A, Rashad M, Sayed Tawfik A, Habachi S, Roushdy AM. Transcatheter Closure of a Large Aortopulmonary Window with the Novel Device Multifunctional Occluder (Konar) Under TEE Guidance (A Case Report). J Cardiol Cases. 2022;25(6):370-2. doi: 10.1016/j.jccase.2021.12.014.

Atrial Myxoma as a Rare Cause of Stroke: Case Report

Maurício Ângelo de Almeida Junior,[1] *Ana Flavia Parreira de Morais,*[1] *Jamil Alli Murad Junior*[1]
FAMERP,[1] *São José do Rio Preto, SP – Brazil*

Introduction

Atrial myxoma (AM) is the most common primary benign tumor affecting the heart. Its prevalence is rare, estimated at 0.03% in the general population. Surgical intervention should be introduced as soon as diagnosed due to the increased risk of cardiac complications, such as intracardiac obstructions or systemic embolizations.[1]

Cardiac myxomas are commonly observed in the left atrium in >75% of cases, predominantly attached with a stalk to the fossa ovalis (>90%). However, they can be seen in other locations (left ventricle, right atrium, and, though quite rarely, the right ventricle).[2]

Approximately 7% of all cardiac myxomas are associated with Carney complex, an autosomal dominant disease characterized by the presence of cardiac and cutaneous lesions, myxomas, skin hyperpigmentation and primary pigmented nodules, with adrenocortical disease leading to Cushing's syndrome.[2]

In up to one third of the cases of myxomas, there is evidence of systemic embolism, even in the brain, which may be silent or cause neurological symptoms. Neurological deficits may often be the first **sign** of the manifestation of a cardiac myxoma.[3]

Following surgical removal, myxomas may recur, and wide excision of the tumor with adjacent cardiac tissue is necessary to prevent recurrence. Surgery is usually recommended when the diagnosis of cardiac myxoma is made, regardless of whether or not systemic embolism has already occurred.[4]

The present case report demonstrates a case of AM in an elderly patient with stroke as the first symptom, diagnosed with transthoracic echocardiography (TTE) and transesophageal echocardiography (TEE), and with a favorable clinical outcome after surgical removal of a benign tumor.

Case report

A 72-year-old male patient with a history of systemic arterial hypertension and type 2 diabetes mellitus was admitted to the emergency room three months ago with vertigo, left hemiparesis, rhyme deviation, spatial disorientation, and ataxia. He was referred for neurological evaluation with a diagnostic hypothesis of ischemic stroke (***acidente vascular encefálico isquêmico*** – **AVEi**), of probable cardioembolic origin, confirmed by magnetic resonance imaging of the skull. **The findings in the aforementioned imaging exam that describe this hypothesis of cardioembolic origin were described as a small hyperintense lesion on T2 weighting and with restriction in the diffusion study used to examine the right thalamus, suggesting acute ischemic vascular injury and small lesions with the same characteristics in the dorsal region of the midbrain and in the right cerebral peduncle.** During the investigation of the neurological condition, the electrocardiogram showed sinus rhythm and nonspecific ventricular repolarization alteration, while the TTE (Figure 1) showed a mobile echogenic image measuring 1.4 x 1.6 cm near the opening of the mitral valve in the region of the anterior leaflet and interatrial septum. Continuing the investigation with TEE (Figures 2 and 3), an echogenic image was confirmed, attached to the septal portion of the mitral annulus, interatrial septum, and anterior leaflet of the mitral valve, measuring 22 x 13 mm, with contrast enhancement within a lesion compatible with vascularization, suggesting AM.

The patient was referred for outpatient cardiovascular surgery, and tumor resection was recommended. During the preoperative period, a multivessel lesion was identified by cardiac catheterization, and therefore a combined procedure of intracardiac tumor resection and coronary artery bypass grafting was recommended, which was performed without complications. The material was sent for anatomopathological examination, which confirmed AM.

Following the surgery, the patient showed clinical improvement, with no new cardioembolic events. Upon hospital discharge, he was asymptomatic and was referred for outpatient follow-up with clinical cardiology.

Discussion

AM is responsible for less than 0.5% of cases of ischemic stroke.[5] Recent studies report that 9% to 22% of patients with MA suffer from cardioembolic stroke. Its incidence is higher in females, at a ratio of 2:1, which most commonly appears between the third and sixth decades of life.[6]

AM is increasingly diagnosed in the elderly and its predominance in females disappears after the age of 65. Its most frequent location is in the left atrium (75 to 80%), inserted in the interatrial septum around the fossa ovalis.[7]

The main etiology of AM is unknown, with approximately 10% of the cases presenting an autosomal dominant genetic component. The classic clinical triad of AM

Keywords

Myxoma; Heart Neoplasms; Stroke.

Mailling Address: Maurício Ângelo de Almeida Junior
FAMERP. Avenida Brigadeiro Faria Lima, 5544. Postal code: 15090-000. São José do Rio Preto, SP – Brazil
E-mail: mauricio_bh@hotmail.com
Manuscript received October 15, 2024; revised October 29, 2024; accepted October 31, 2024
Editor responsible for the review: Marcelo Tavares

DOI: https://doi.org/10.36660/abcimg.20240099i

CONTENTS

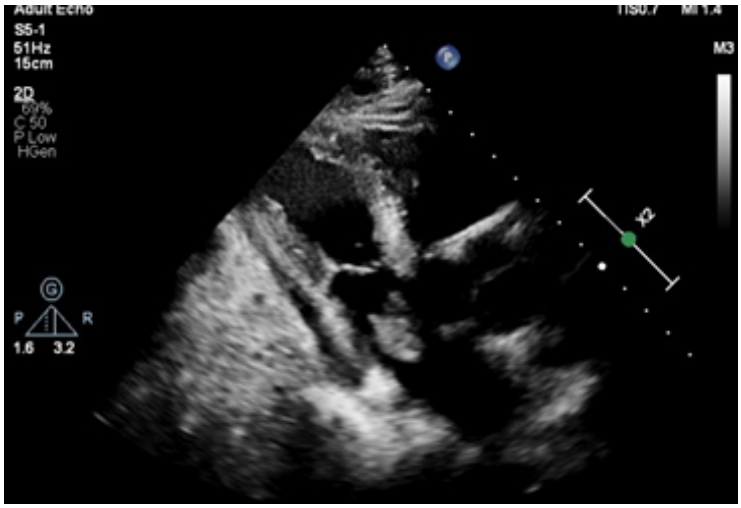

Figure 1 – *Left longitudinal parasternal TTE demonstrating left interatrial myxoma.*

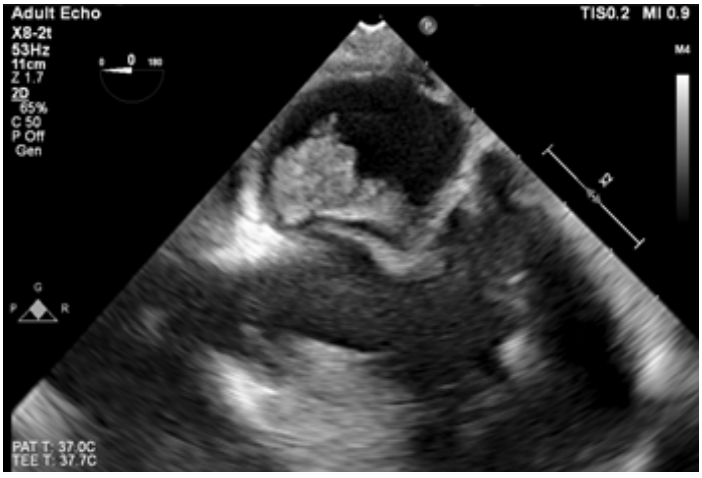

Figure 2 – *TEE in mid-esophagus at 0 degrees. (left interatrial myxoma visible – with largest diameters of 2.5 cm x 1.5 cm).*

includes obstructive symptoms, such as **valve obstruction** and ventricular failure; embolic manifestations in any arterial territory, with the cerebral artery being the most frequently involved; and constitutional symptoms, such as fever, asthenia, myalgias, arthralgias, and weight loss. Approximately 20% of all cases are asymptomatic, with the diagnosis being made incidentally through imaging exams. Obstructive (40% to 60%) and constitutional (30% to 90%) cardiac symptoms are the most frequent in clinical presentation, and embolic manifestations may occur in 30% to 40% of all patients.[6]

Patients with AM who present neurological complications are mostly young, and stroke or transient ischemic attack are the most common neurological manifestations (82%), occurring due to embolization of tumor fragments, thrombus formation, or both.[8]

AMs are usually solitary, with sizes ranging from 0.4 to 6.5 cm. Morphologically, they are divided into two types: type 1, with an irregular or villous surface and long pedicle, which are associated with a higher risk of embolization, and type 2, with a smooth surface and soft consistency.[7]

TTE is the initial examination used to detect cardiac masses, with a sensitivity of 90% and a specificity of 95%. TEE enables a more detailed visualization of the anatomical structures, which is useful in determining the size, location, adhesion, relationship with adjacent structures, and mobility of the tumor.[9]

Differential diagnoses of AM include vegetations, intracardiac thrombi, or artifacts.[10]

Surgical resection is considered curative and is recommended whenever AM is diagnosed, regardless of

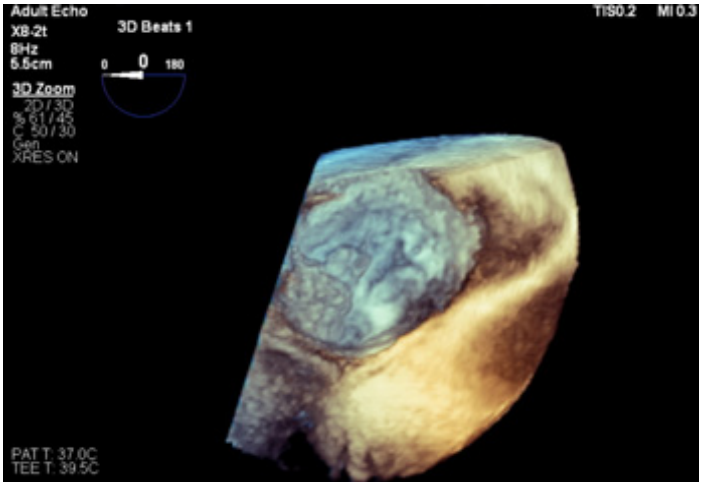

Figure 3 – *Three-dimensional (3D) TEE (3D zoom of the left atrium with visualization of myxoma attached to the membrane in the oval fossa).*

previous embolization. It should be performed as early as possible due to the risk of recurrence of embolism or valve obstruction. The postoperative prognosis is variable and depends on the patient's age, comorbidities, preoperative clinical status, and possible need to perform other surgical procedures associated with AM resection.[7]

Most AM recurrences occur in the first 4 years after tumor resection, although the risk is low. For this reason, regular follow-up with echocardiography should be performed.[7]

Conclusion

AM is a rare cause of **AVEi**, which, although it has a low population prevalence, has important clinical relevance for early surgical intervention in an attempt to reduce morbidity and mortality due to systemic embolisms caused by the tumor.

Author Contributions

Conception and design of the research, acquisition of data, analysis and interpretation of the data and writing of the manuscript: Almeida Junior MA, Morais AFP; critical revision of the manuscript for intellectual content: Murad Junior JA.

Potential Conflict of Interest

No potential conflict of interest relevant to this article was reported.

Sources of Funding

There were no external funding sources for this study.

Study Association

This study is not associated with any thesis or dissertation work.

Ethics Approval and Consent to Participate

This article does not contain any studies with human participants or animals performed by any of the authors.

References

1. Gupta A, Darbari A, Mishra A. Excision of a Left Atrial Myxoma with Mitral and Tricuspid Valve Repair. Multimed Man Cardiothorac Surg. 2020;2020. doi: 10.1510/mmcts.2020.080.
2. Saric M, Armour AC, Arnaout MS, Chaudhry FA, Grimm RA, Kronzon I, et al. Guidelines for the Use of Echocardiography in the Evaluation of a Cardiac Source of Embolism. J Am Soc Echocardiogr. 2016;29(1):1-42. doi: 10.1016/j.echo.2015.09.011.
3. Pucci A, Gagliardotto P, Zanini C, Pansini S, di Summa M, Mollo F. Histopathologic and Clinical Characterization of Cardiac Myxoma: Review of 53 Cases from a Single Institution. Am Heart J. 2000;140(1):134-8. doi: 10.1067/mhj.2000.107176.
4. Shapiro LM. Cardiac Tumours: Diagnosis and Management. Heart. 2001;85(2):218-22. doi: 10.1136/heart.85.2.218.
5. Eira C, Mota A, Silvério R, Monteiro R, Monteiro A. Atrial Myxoma: A Rare Cause of Ischemic Stroke. Rev Soc Bras Clin Med. 2018;16(1):48-51.
6. Iyer P, Aung MM, Awan MU, Kososky C, Barn K. A Case of Large Atrial Myxoma Presenting as an Acute Stroke. J Community Hosp Intern Med Perspect. 2016;6(1):29604. doi: 10.3402/jchimp.v6.29604.
7. Bordalo AD, Alves I, Nobre AL, Silva F, Lemos A, Serpa C, et al. New Clinical Aspects of Cardiac Myxomas: A Clinical and Pathological Reappraisal. Rev Port Cardiol. 2012;31(9):567-75. doi: 10.1016/j.repc.2012.05.008.

8. Baek SH, Park S, Lee NJ, Kang Y, Cho KH. Effective Mechanical Thrombectomy in a Patient with Hyperacute Ischemic Stroke Associated with Cardiac Myxoma. J Stroke Cerebrovasc Dis. 2014;23(9):e417-9. doi: 10.1016/j.jstrokecerebrovasdis.2014.05.006.

9. Kebede S, Edmunds E, Raybould A. A Large Left Atrial Myxoma Causing Multiple Cerebral Infarcts. BMJ Case Rep. 2013;2013:bcr2013010007. doi: 10.1136/bcr-2013-010007.

10. Ha JW, Kang WC, Chung N, Chang BC, Rim SJ, Kwon JW, et al. Echocardiographic and Morphologic Characteristics of Left Atrial Myxoma and their Relation to Systemic Embolism. Am J Cardiol. 1999;83(11):1579-82, A8. doi: 10.1016/s0002-9149(99)00156-3.

Successful Occlusion of a Giant Subclavian Artery Aneurysm Sac with a Vascular Plug: A Case Report

Fuat Polat,[1] *Osman Eren Karpuzoğlu*[1]

Health Sciences University Dr. Siyami Ersek Thoracic and Cardiovascular Surgery Education and Research Hospital,[1] *İstanbul – Turkey*

Abstract

Subclavian artery aneurysms are rare vascular anomalies that carry significant risks, including thromboembolism, ischemia, and rupture. This case report describes a 71-year-old female patient presenting with left arm ischemia, including pain, numbness, and weakness, caused by a left subclavian artery aneurysm complicated by distal thrombosis. Imaging revealed a 65 × 55 mm aneurysm with a 2.5 cm thrombotic occlusion. The aneurysm was treated with an endovascular approach, utilizing a vascular plug deployed via femoral access. This was preceded by failed attempts to access the lesion through the radial approach due to the presence of thrombotic occlusion and complex vascular anatomy. After the procedure, the patient experienced significant symptom relief, and follow-up imaging confirmed thrombosis of the aneurysm sac. This case highlights the effectiveness of endovascular techniques in managing complex subclavian artery aneurysms and emphasizes the importance of individualized treatment strategies and close follow-up.

Introduction

Subclavian artery aneurysms are rare, accounting for less than 1% of peripheral artery aneurysms.[1] They may be associated with trauma, atherosclerosis, thoracic outlet syndrome, or congenital abnormalities.[2] While many remain asymptomatic, symptomatic cases can present with ischemic symptoms due to arterial compression, thromboembolism, or aneurysmal rupture.[3] These symptoms often include pain, numbness, weakness, or diminished pulses in the affected arm, along with differential blood pressures between the upper limbs. Given the risk of severe complications such as embolization or rupture, early diagnosis and treatment are crucial. Endovascular repair has emerged as the preferred treatment for subclavian artery aneurysms, offering a minimally invasive alternative to open surgery with lower perioperative risk.[4] However, challenges may arise, particularly when aneurysms are complicated by thrombotic occlusion or extensive collateralization. This report presents a 71-year-old woman with symptomatic left arm ischemia caused by a subclavian artery aneurysm with distal thrombosis, successfully treated with endovascular intervention.

Keywords

Subclavian Artery; Endovascular Aneurysm Repair; Thrombosis

Mailing Address: Fuat Polat •
Selimiye, Tıbbiye St. No:25. Postal code: 34668 Uskudar, Istanbul – Turkey
E-mail: drfuatpolat@gmail.com
Manuscript received October 18, 2024, revised manuscript December 7, 2024, accepted February 24, 2025
Editor responsible for the review: Tiago Magalhães

DOI: https://doi.org/10.36660/abcimg.20240101i

Case report

A 71-year-old woman with hypertension presented with pain, numbness, and weakness in her left arm, which had worsened over the past few months. Her heart rate was 80 beats per minute, regular, with no murmurs. Electrocardiogram showed sinus rhythm and incomplete right bundle branch block. Transthoracic echocardiography revealed a left ventricular ejection fraction of 60%, interventricular septal thickness of 12 mm, stage 1 diastolic dysfunction, and mild aortic regurgitation. Physical examination revealed a weak right radial pulse. Blood pressure was 130/70 mmHg in the right arm and 105/65 mmHg in the left arm. A posterior-anterior chest X-ray showed a well-circumscribed round mass in the left hemithorax (Figure 1). Subsequent computed tomographic angiography (CTA) of the thoracic aorta and upper extremities revealed a 65 × 55 mm aneurysm of the left subclavian artery, located just distal to the origin of the vertebral artery. The occluded segment, measuring approximately 2.5 cm, exhibited non-calcified thrombotic material filling the lumen, without evidence of significant extrinsic compression or surrounding soft tissue abnormalities. The mechanism of occlusion appeared to be thrombus formation within the aneurysmal sac, likely due to stasis of blood flow. The aneurysm's etiology was suspected to be degenerative in nature, potentially related to chronic hypertension and atherosclerotic changes, as no history of trauma or congenital abnormality was reported. Collateral vessels reconstructed the left axillary artery, and both the left vertebral artery and the left internal mammary artery (LIMA) demonstrated normal flow (Figure 2). Endovascular repair was planned using stent-graft placement. Access was obtained via the right femoral artery and the left radial artery. However, despite advanced guidewires, the aneurysm could not be reached from the radial approach. An Amplatzer Vascular Plug II (AVP II; Abbott, Plymouth, MN, USA), measuring 10 mm in diameter, was deployed in the left subclavian artery near the aneurysm via the femoral route. The device was delivered using a 6 French guiding catheter, which provided sufficient support for precise positioning of the vascular plug, while preserving access to the left

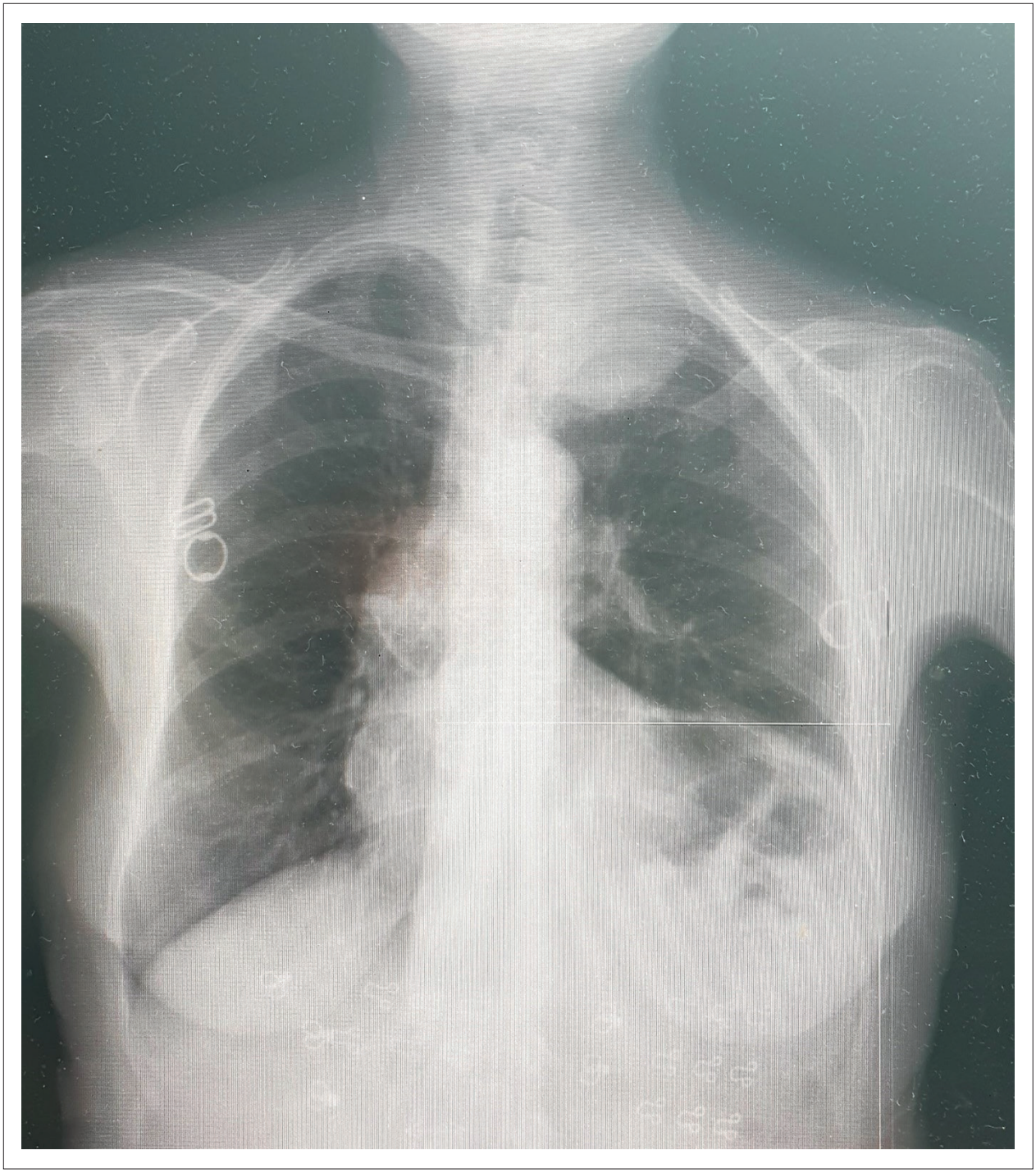

Figure 1 – *Posterior-anterior chest X-ray showing a well-circumscribed round mass in the left hemithorax.*

vertebral artery and LIMA. Post-procedural angiography confirmed cessation of aneurysmal flow with preserved flow in the left vertebral artery and LIMA (Figure 3). Following the procedure, the patient was initiated on dual antiplatelet therapy (aspirin 100 mg daily and clopidogrel 75 mg daily) to prevent thromboembolic complications associated with the vascular plug and to maintain patency of critical collateral vessels. The antithrombotic strategy was selected based on the patient's risk profile and the nature of the intervention. At a 1-month follow-up, the patient reported significant improvement in her left arm symptoms, and repeat CTA demonstrated complete thrombosis of the aneurysm sac with cessation of flow (Figure 4). Continued follow-up at 3 and 6 months, including clinical evaluations

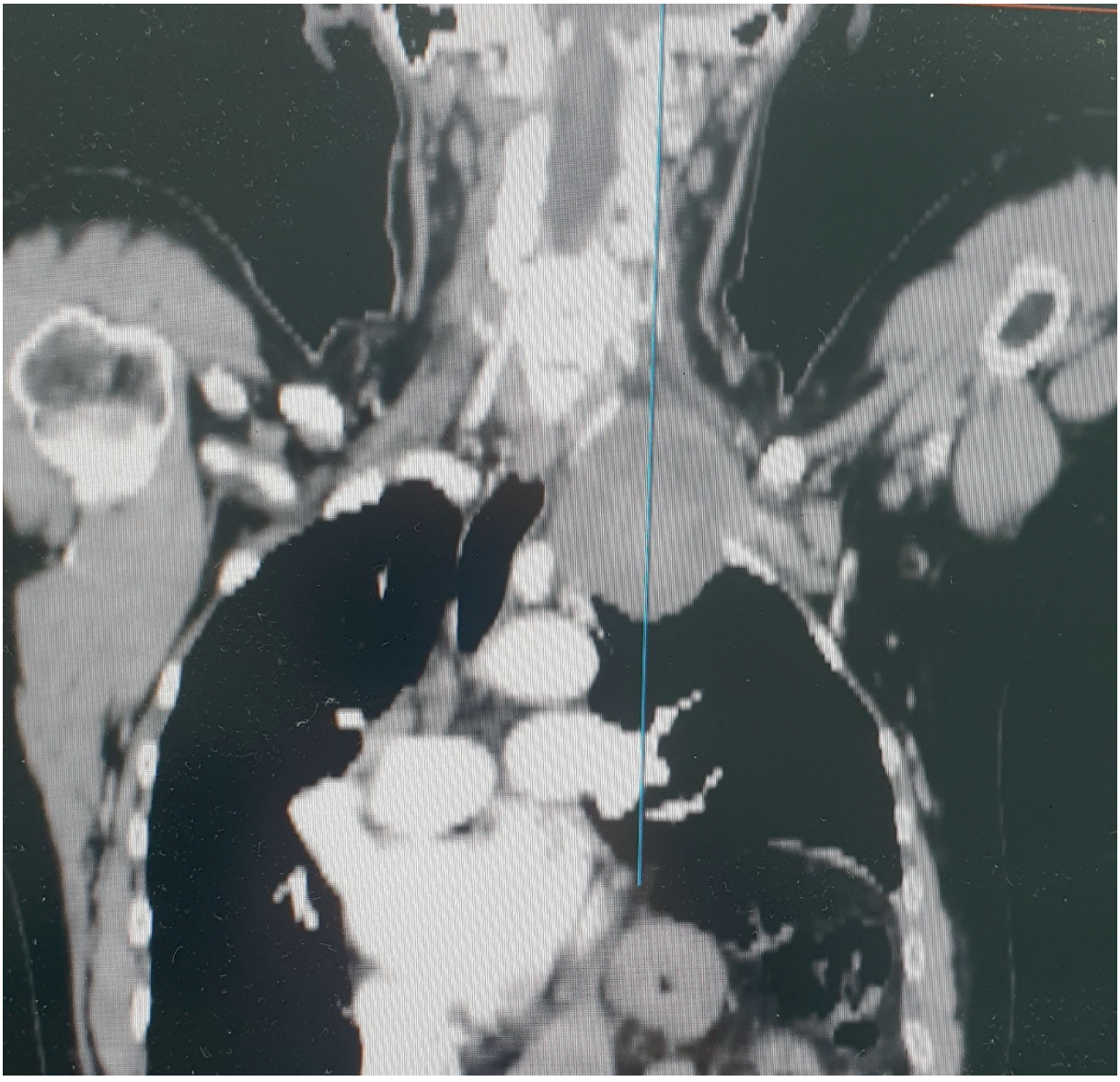

Figure 2 – *Computed tomography angiography of the thoracic aorta and upper extremities shows a left subclavian artery aneurysm distal to the origin of the vertebral artery.*

and imaging, was scheduled to monitor for complications such as migration of the vascular plug, residual flow, or recurrence of ischemic symptoms.

Discussion

Subclavian artery aneurysms, although rare, carry significant risks, including embolization, thrombosis, and rupture.[5] In this case, the patient presented with upper extremity ischemia, which is typical of symptomatic subclavian aneurysms, manifesting as pain, numbness, weakness, and differential blood pressure. These clinical findings were pivotal in diagnosing a left subclavian artery aneurysm with thrombotic occlusion. Endovascular repair is increasingly preferred due to its minimally invasive nature, reduced morbidity, and faster recovery compared to open surgery.[6] However, this case illustrates the technical difficulties that can arise, particularly in navigating complex vascular anatomy complicated by thrombosis and collateralization. In this case, despite initial challenges accessing the aneurysm via the radial route, a vascular plug was successfully deployed via the femoral approach, achieving cessation of aneurysmal flow while preserving perfusion in critical vessels such as the left vertebral artery and LIMA. The patient's favorable outcome, with significant symptom

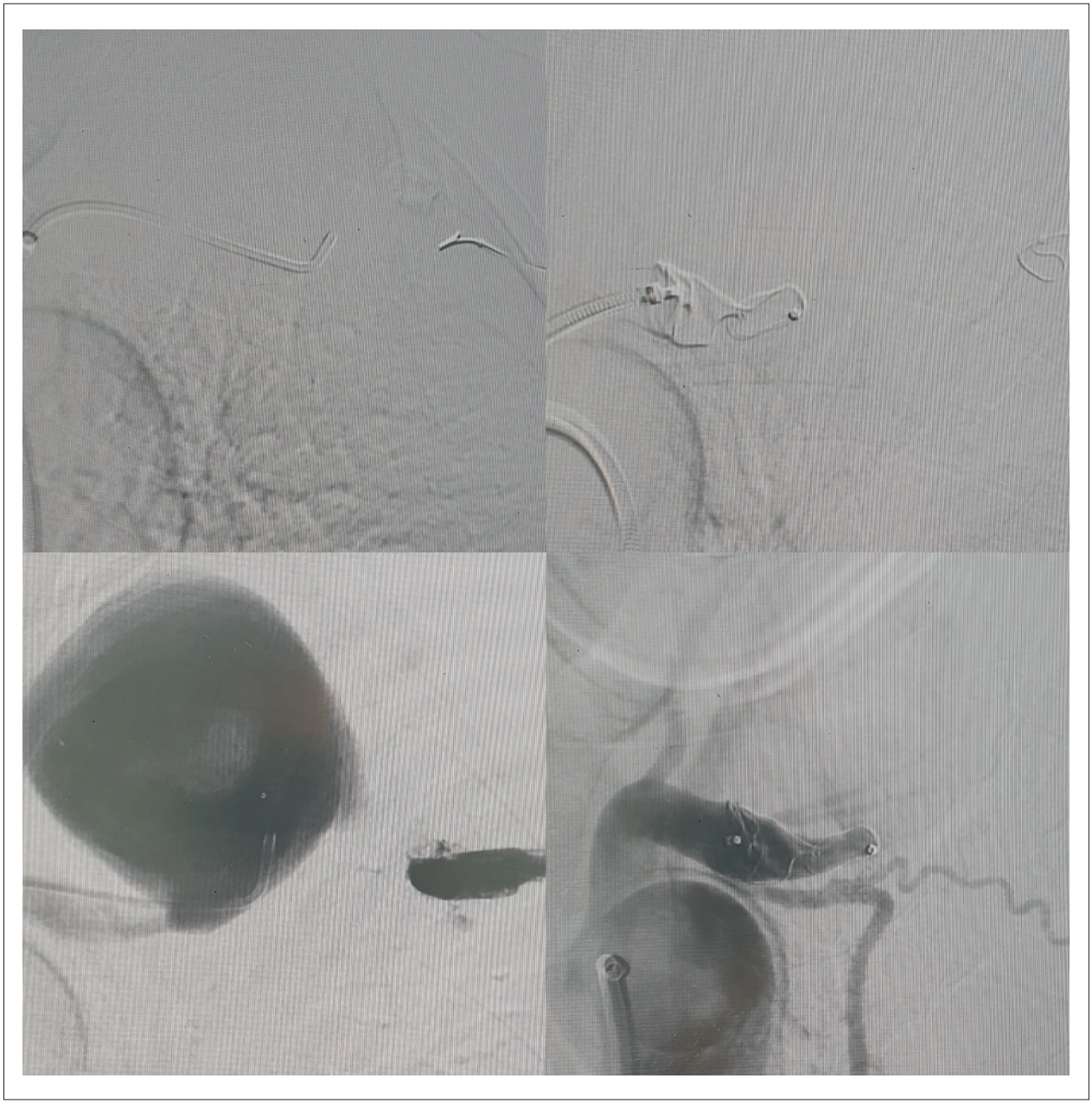

Figure 3 – *A Destination sheath and vertebral catheter were positioned in the proximal subclavian artery via the femoral artery, while a right Judkins catheter was advanced into the distal subclavian artery through the radial approach (top left). Despite using stiff guidewires, access to the aneurysmal region from the distal end was unsuccessful (bottom left). A 10 mm vascular plug was placed proximal to the aneurysm sac through the vertebral catheter via the femoral route (top right). Post-procedural cine angiography confirmed preserved flow in both the left vertebral artery and the LIMA, with near-complete occlusion of flow within the aneurysm sac (bottom right).*

improvement and imaging-confirmed thrombosis of the aneurysm, underscores the efficacy of endovascular management. This case also highlights the importance of thorough imaging assessment and individualized intervention strategies for complex vascular lesions.[7] While the outcome in this case was successful, it serves as a reminder of the potential complications of subclavian artery aneurysms and the need for timely diagnosis and intervention to prevent more severe consequences, such as rupture or embolization. Continued follow-up is essential to monitor for recurrence or complications related to the vascular plug.

Conclusion

This case demonstrates the successful endovascular treatment of a rare subclavian artery aneurysm complicated

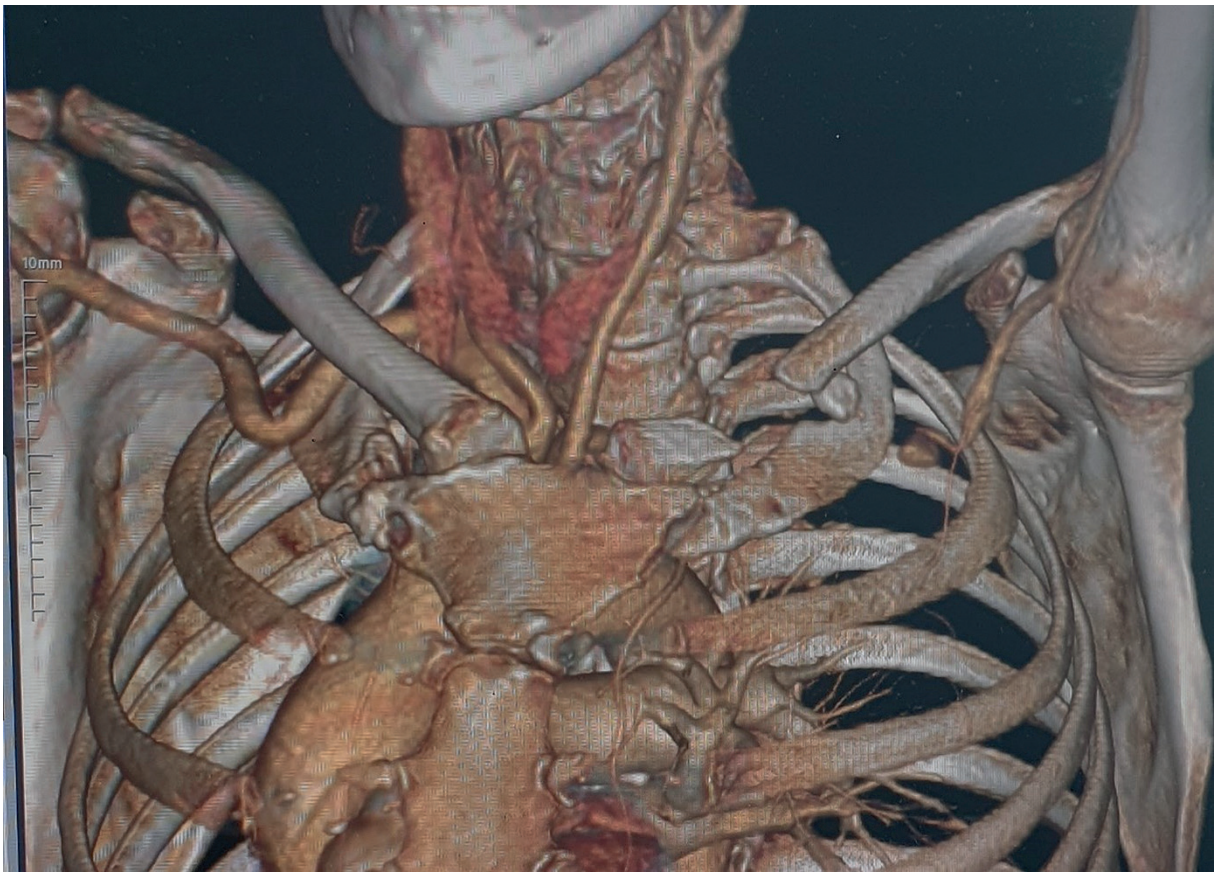

Figure 4 – *Computed tomography angiography performed 1 month after vascular plug placement in the subclavian artery revealed complete cessation of flow within the aneurysm sac.*

by thrombosis and presenting with upper extremity ischemia. Despite procedural challenges, the deployment of a vascular plug effectively halted aneurysmal flow while preserving critical vessel patency. Early diagnosis, tailored intervention, and ongoing follow-up are crucial to achieving optimal outcomes in such complex cases.

Author Contributions

Conception and design of the research and analysis and interpretation of the data: Polat F, Karpuzoğlu OE; acquisition of data, statistical analysis and writing of the manuscript: Polat F; critical revision of the manuscript for intellectual content: Karpuzoğlu OE.

Potential Conflict of Interest

No potential conflict of interest relevant to this article was reported.

Sources of Funding

There were no external funding sources for this study.

Study Association

This study is not associated with any thesis or dissertation work.

Ethics Approval and Consent to Participate

This article does not contain any studies with human participants or animals performed by any of the authors.

References

1. Counts S, Zeeshan A, Elefteriades J. Giant Subclavian Artery Aneurysm. Int J Angiol. 2016;25(2):128-30. doi: 10.1055/s-0034-1372245.
2. Maślanka K, Zielinska N, Karauda P, Balcerzak A, Georgiev G, Borowski A, et al. Congenital, Acquired, and Trauma-Related Risk Factors for Thoracic Outlet Syndrome-Review of the Literature. J Clin Med. 2023;12(21):6811. doi: 10.3390/jcm12216811.
3. Dougherty MJ, Calligaro KD, Savarese RP, Laurentis DA. Atherosclerotic Aneurysm of the Intrathoracic Subclavian Artery: A Case Report and

Review of the Literature. J Vasc Surg. 1995;21(3):521-9. doi: 10.1016/s0741-5214(95)70297-0.

4. Zha B, Chen Z, Ou-Yang H. Endovascular Repair for Giant Right Subclavian Artery Aneurysm with Gore Viabahn and Pull-Through Procedure: A Case Report. Front Surg. 2022;9:939818. doi: 10.3389/fsurg.2022.939818.

5. Banning SK, Ur R, Malleis J, Hamlat CA, Byers PH, Shalhub S. Extrathoracic Subclavian Artery Aneurysm in a Patient with Suspected Genetic Arteriopathy. J Vasc Surg Cases Innov Tech. 2020;7(1):46-50. doi: 10.1016/j.jvscit.2020.11.008.

6. Daye D, Walker TG. Complications of Endovascular Aneurysm Repair of the Thoracic and Abdominal Aorta: Evaluation and Management. Cardiovasc Diagn Ther. 2018;8(Suppl 1):S138-S156. doi: 10.21037/cdt.2017.09.17.

7. Christie A, Roditi G. Vascular Imaging: The Evolving Role of the Multidisciplinary Team Meeting in Peripheral Vascular Disease. Semin Intervent Radiol. 2014;31(4):320-9. doi: 10.1055/s-0034-1393968.

Late Evolution of Takotsubo Cardiomyopathy Following Transcatheter Aortic Valve Implantation

Merve Akbulut Çakır,[1] *Emirhan Çakır,*[1] *Çağlar Kaya,*[1] *Kenan Yalta*[1]
Trakya University Faculty of Medicine,[1] *Edirne – Turkey*

Introduction

Transcatheter aortic valve implantation (TAVI) is recognized as a first-line treatment for symptomatic patients with advanced aortic stenosis who are at high surgical risk. In inoperable patients with poor prognosis, it carries a risk for complications, such as myocardial infarction due to coronary occlusion, stroke, annular rupture, etc.[1] Takotsubo Cardiomyopathy (TTC) is a syndrome that usually develops in the absence of overt coronary occlusion and signs of alternative diagnosis, including myocarditis. It presents with electrocardiographic changes, increased cardiac biomarkers, and typical echocardiographic findings.[2,3] In this article, we describe a patient with TTC who previously underwent TAVI and subsequent implantable cardiac defibrillator (ICD) implantation.

Case report

A 77-year-old woman was admitted with symptoms of shortness of breath and wheezing. Physical examination demonstrated a blood pressure value of 111/76 mmHg, respiratory rate of 28/min, pulse rate of 70 bpm, and oxygen saturation of 88%. Cardiovascular examination exhibited a pattern of left-sided apical impulse, 2-3/6 systolic murmur, and bilateral 2 + pitting edema of lower limbs. Examination of the lungs revealed bilateral rales up to the middle zones. Left ventricular ejection fraction (LVEF) value was 42%. The left ventricular apex was akinetic, suggesting a pattern of apical ballooning. High sensitive-troponin and brain natriuretic peptide (BNP) levels on admission were 256 ng/l (normal range: 0-19 ng/l) and 114.3 pg/ml (normal range: 0-100 pg/ml), respectively. The patient's detailed anamnesis included hypertension and TAVI performed due to aortic stenosis four months ago. After TAVI, a complete atrioventricular block persisted in the patient, and non-sustained VT was observed in the follow-up. For this reason, the patient was implanted with an ICD instead of a permanent pacemaker. In the transthoracic echocardiography performed after TAVI, LVEF was calculated as 55% and left ventricular systolic functions were normal. No pericardial effusion or paravalvular leakage was observed in the implanted aortic valve. The patient, who had no complaints, no physical examination findings, and no deterioration in laboratory parameters, was called for a cardiology outpatient clinic control and then discharged. After detailed evaluation, the patient was hospitalized with the prediagnoses of acute coronary syndrome and decompensated heart failure. Coronary angiography performed after urgent stabilization of the patient revealed no critical stenosis in the coronary arteries (Figure 1). Subsequent cardiac magnetic resonance imaging excluded acute myocarditis and revealed a pattern of global hypokinesia with severe apical and mid-ventricular involvement (Figure 2). Based on these findings, TTC was considered as the most likely diagnosis. Following successful management, she was discharged uneventfully under acute coronary syndrome and heart failure medications. An outpatient visit was planned for the patient following one month. During the scheduled cardiology outpatient clinic visit, the patient's complaints related to heart failure disappeared after medical treatment. In the transthoracic echocardiography, it was seen that the left ventricular contractions returned to normal, and LVEF was calculated as 50%. The patient continues to be followed up with medical treatment.

Discussion

TC was first described in 1991, and it was generally considered to occur due to emotional or physical triggers, including mourning, trauma, sepsis or metabolic abnormalities.[2,4] It is known that high catecholamine levels associated with these triggers play a pivotal role in its pathogenesis.[2,5] The findings that prompted us to make the diagnosis of TTC, in this case, were the presence of specific abnormalities in left ventricular wall motion beyond a single arterial perfusion zone, absence of occlusive coronary artery disease, increased cardiac troponin levels, and absence of findings in favor of myocarditis.[2]

Acute coronary syndromes and arrhythmias may develop frequently after TAVI.[1] Most of the acute cardiomyopathies occurring after TAVI may be due to occlusive coronary artery disease.[1] TAVI is a less invasive procedure compared to cardiac surgery but may cause severe emotional and/or physical stress in high-risk patients, potentially leading to TTC evolution. However, in the present case, TTC emerged long after TAVI, potentially indicating the null impact of procedure-related stress on TTC evolution. However, TTC (in the form of apical ballooning) was also previously suggested to occur as a consequence of mechanical factors,

Keywords

Takotsubo Cardiomyopathy;Transcatheter Aortic Valve Replacement; Echocardiography

Mailing Address: Emirhan Çakır •
Trakya University Faculty of Medicine Cardiology Department. CEP: 22030. Edirne – Turkey
E-mail: emir.cakir05@gmail.com
Manuscript received December 6, 2024; revised February 19, 2025; accepted February 24, 2025
Editor responsible for the review: Maria Otto

DOI: https://doi.org/10.36660/abcimg.20240130i

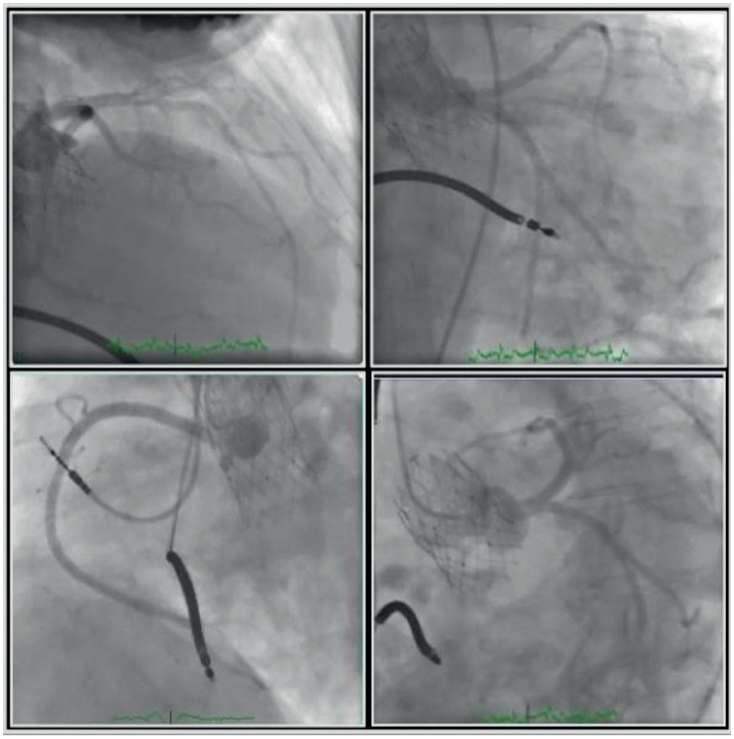

Figure 1 – *Non-occlusive coronary arteries, TAVI device, and ICD leads on coronary angiogram.*

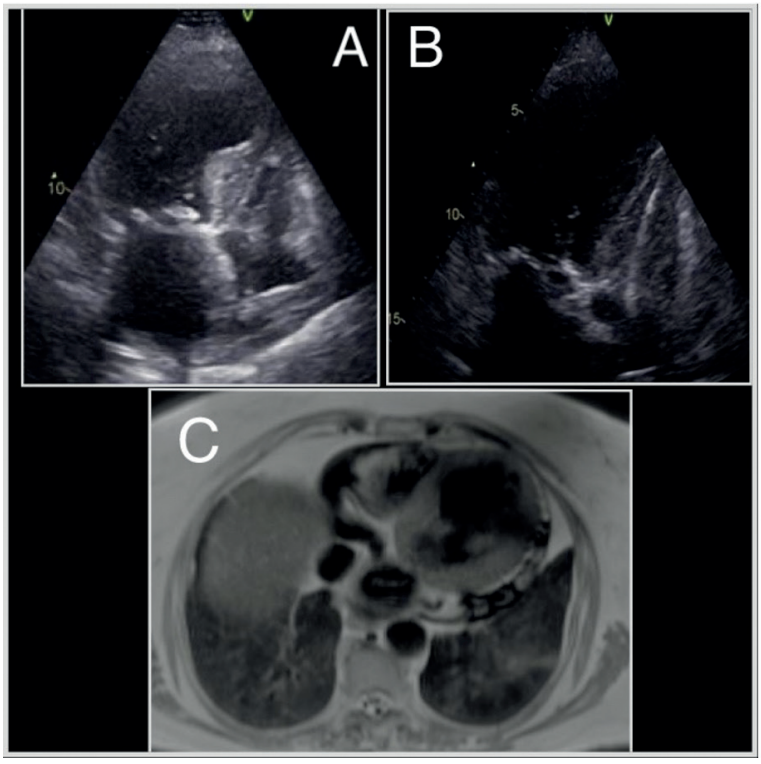

Figure 2 – *A-B: Transthoracic echocardiogram demonstrating left ventricular apical ballooning and lead image in the right chambers on apical four-chamber view C: Apical ballooning on cardiac MRI.*

including acute intraventricular gradient, possibly due to afterload mismatch in patients with a modest degree of pre-existing left ventricular hypertrophy.[3,6] Accordingly, our case might have possibly incurred acute midventricular or outflow tract gradient due to certain mechanical factors, including enhanced contractility and reduced preload or afterload,[3] most of which might, to some extent, be associated with the relief of aortic valve stenosis following TAVI. However, this notion remains speculative, and certain tests, including dobutamine stress echocardiogram, are required to reveal provoked intraventricular gradient[3] in our patient. To date, TTC, regardless of the underlying actual trigger, has been rarely reported following TAVI.[7] The present case might be regarded as an epitome of late TTC evolution following TAVI.

Author Contributions

Conception and design of the research, acquisition of data, analysis and interpretation of the data, statistical analysis, writing of the manuscript and critical revision of the manuscript for intellectual content: Çakır MA, Çakır E, Kaya Ç, Yalta K.

Potential Conflict of Interest

No potential conflict of interest relevant to this article was reported.

Sources of Funding

There were no external funding sources for this study.

Study Association

This study is not associated with any thesis or dissertation work.

Ethics Approval and Consent to Participate

This article does not contain any studies with human participants or animals performed by any of the authors.

References

1. Yalta K, Kaya Ç, Aksoy Y, Yılmaztepe M, Kardaş F. Acute Myocardial Infarction Shortly after Valve-in-Valve Transcatheter Aortic Valve Implantation Successfully Managedwith Challenging Percutaneous Coronary Intervention. Turk Kardiyol Dern Ars. 2018;46(1):61-5. doi: 10.5543/tkda.2017.03256.
2. Yalta K, Madias JE, Kounis NG, Y-Hassan S, Polovina M, Altay S, et al. Takotsubo Syndrome: An International Expert Consensus Report on Practical Challenges and Specific Conditions (Part-1: Diagnostic and Therapeutic Challenges). Balkan Med J. 2024;41(6):421-41. doi: 10.4274/balkanmedj.galenos.2024.2024-9-98.
3. Yalta K, Madias JE, Kounis NG, Y-Hassan S, Polovina M, Altay S, et al. Takotsubo Syndrome: An International Expert Consensus Report on Practical Challenges and Specific Conditions (Part-2: Specific Entities, Risk Stratification and Challenges after Recovery). Balkan Med J. 2024;41(6):442-57. doi: 10.4274/balkanmedj.galenos.2024.2024-9-99.
4. Zhang L, Piña IL. Stress-Induced Cardiomyopathy. Heart Fail Clin. 2019;15(1):41-53. doi: 10.1016/j.hfc.2018.08.005.
5. Ghadri JR, Wittstein IS, Prasad A, Sharkey S, Dote K, Akashi YJ, et al. International Expert Consensus Document on Takotsubo Syndrome (Part I): Clinical Characteristics, Diagnostic Criteria, and Pathophysiology. Eur Heart J. 2018;39(22):2032-46. doi: 10.1093/eurheartj/ehy076.
6. Yalta K, Kaya C, Yalta T. Left Ventricular Aneurysm Formation in Patients with Takotsubo Syndrome: A Peculiar Phenomenon with Subtle Implications. Kardiol Pol. 2023;81(10):1034-5. doi: 10.33963/KP.a2023.0161.
7. Harhash A, Koulogiannis KP, Marcoff L, Kipperman R. Takotsubo Cardiomyopathy after Transcatheter Aortic Valve Replacement. JACC Cardiovasc Interv. 2016;9(12):1302-4. doi: 10.1016/j.jcin.2016.04.017.

ATTRwt Cardiac Amyloidosis and Aortic Regurgitation in a Patient with Acute Myelomonocytic Leukemia: an Unusual Combination

Diego Chemello,[1] *Patricia Chagas,*[1] *Camila Sales Fagundes,*[1] *Juliana Chiodelli Salvador,*[1] *Marcelo Tavares*[2]
Universidade Federal de Santa Maria,[1] *Santa Maria, RS – Brazil*
Universidade Federal da Paraíba,[2] *João Pessoa, PB – Brazil*

Introduction

Systemic amyloidosis is a relatively rare multisystem disease caused by the deposition of misfolded protein in various tissues and organs. Cardiac amyloidosis (CA) is recognized as an underlying cause of left ventricular wall thickening, heart failure, and arrhythmia with variable clinical presentation. The clinical diagnosis of cardiac involvement in amyloidosis is challenging, requiring a patient-centered diagnostic work-up that ensures an appropriate diagnosis.[1,2]

Although amyloidosis has been associated with multiple malignant disorders, its association with leukemia is rather uncommon.[3-5] Also, there is a relationship between CA and valvular heart disease, particularly aortic stenosis (AS).[6] The association of ATTRwt CA and aortic regurgitation (AR) in a patient with acute myelomonocytic leukemia (MML) is unique and has not been described so far.

Description

A 72-year-old hypertensive male patient diagnosed with acute AML was referred to the emergency department with a recent onset of chest discomfort at rest and signs of mild pulmonary congestion. At presentation, physical examination revealed blood pressure of 195/62 mmHg, heart rate of 96 beats per minute, respiratory rate of 26 movements per minute, and oxygen saturation of 90%. There were jugular venous distention and bilateral rales. The cardiac auscultation revealed an S3-gallop and a diastolic murmur in the aortic position. The electrocardiogram (ECG) revealed sinus rhythm, with no signs of ST segment changes or T-wave abnormalities (Figure 1A). The cardiac troponin was 2,025 ng/L (reference of 58 ng/L). The patient was started on treatment for non-ST elevation acute coronary syndrome (ACS). After clinical stabilization, a coronary angiogram was performed, revealing a critical lesion in the proximal aspect of the left anterior descending artery and the left trunk (Figure 1B, Supplementary Video 1). The patient was then treated with drug-eluting stents in the left trunk and left anterior descending artery (LAD) with success (Figure 1C, Supplementary Video 2).

The patient's past medical history was characterized by acute MML, which had been treated with decitabine for 18 months with a good clinical response. Other medications included losartan 50 mg twice a day, hydrochlorothiazide 25 mg once a day, and rosuvastatin 10 mg once a day. During his admission, laboratory exams showed hemoglobin of 9.5 g/dL, platelets of 172,000 /mm^3, and leucocyte count of 6,560/mm^3 with 9% immature forms. A transthoracic echocardiogram was performed for risk stratification post-ACS, showing findings suggestive of CA: there was concentric thickening of the cardiac chambers, with grade 2 diastolic impairment function. The ejection fraction was 53%, and the global longitudinal strain (GLS) was -15.9% with strain magnitude preserved exclusively at the apex (apical sparring pattern) (Figure 2A). There was also aortic valvular thickening with moderate AR (Figure 2B).

A work-up for amyloidosis was then started. There was no evidence of monoclonal protein. The serum free light chain (sFLC) assay revealed a normal ratio of kappa and lambda free light chain (0.77, considering a glomerular filtration rate of 52 ml/min). The serum (SIFE) and urine immunofixation electrophoresis (UIFE) revealed the absence of monoclonal protein.

A technetium-pyrophosphate cardiac single-photon emission computed tomography (Tc-PYP SPECT) was performed, revealing heart uptake equal to rub uptake (grade 2 visual scale, as described by Perugini et al.).[7] The quantitative analysis revealed a heart-to-contralateral lung uptake ratio (H/CL) of 1.5 in the first hour and 1.3 in the third hour (Figure 2C).

A cardiac magnetic resonance imaging (MRI) revealed biventricular function within normal limits, with a left ventricular ejection fraction (LVEF) of 56% and a right ventricular ejection fraction (RVEF) of 38.5%. The was increased thickening of the LV walls, particularly in the mid septum (1.6 cm). There were mild irregular and diffuse areas of late gadolinium enhancement within basal and mid segments of LV (Figure 2D).

Genetic testing for transthyretin (TTR) gene mutation was negative for TTR variants known to cause CA. A diagnosis of wild-type transthyretin amyloidosis (ATTRwt) was performed. Despite this diagnosis, tafamidis was not utilized, based on the decision made by the National Committee for the

Keywords

Amyloidosis; Aortic Valve Insufficiency; Acute Myelomonocytic Leukemia

Mailing Address: Diego Chemello •
Universidade Federal de Santa Maria. Av. Presidente Vargas, 2084. Postal code: 97015-51. Santa Maria, RS – Brazil
E-mail: chemello.diego@gmail.com
Manuscript received November 27, 2024; revised November 27, 2024; accepted January 26, 2025
Editor responsible for the review: Marcelo Tavares

DOI: https://doi.org/10.36660/abcimg.20240127i

CONTENTS

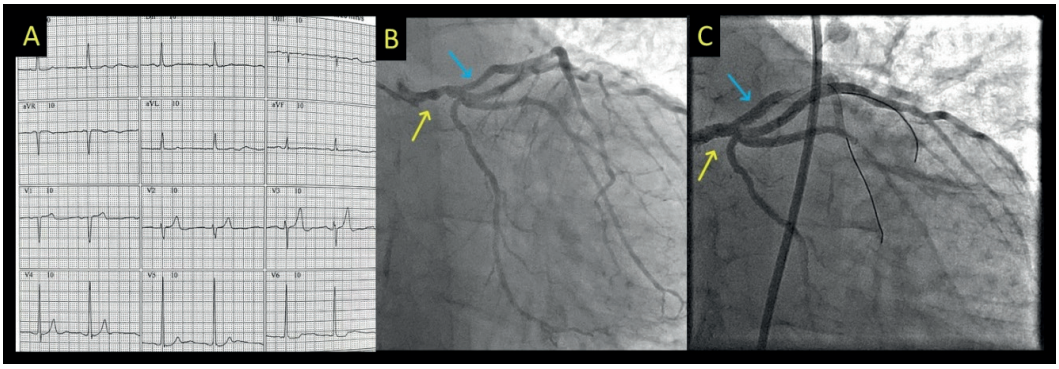

Figure 1 – *(1A): The 12-lead ECG at the presentation showed no significant ST/T abnormalities. (1B): Coronary angiogram showing severe lesion in the left coronary trunk (yellow arrow) and left anterior descending artery (blue arrow). (1C): coronary angiogram after drug-eluting stents in the left coronary trunk (yellow arrow) and left anterior descending artery (blue arrow).*

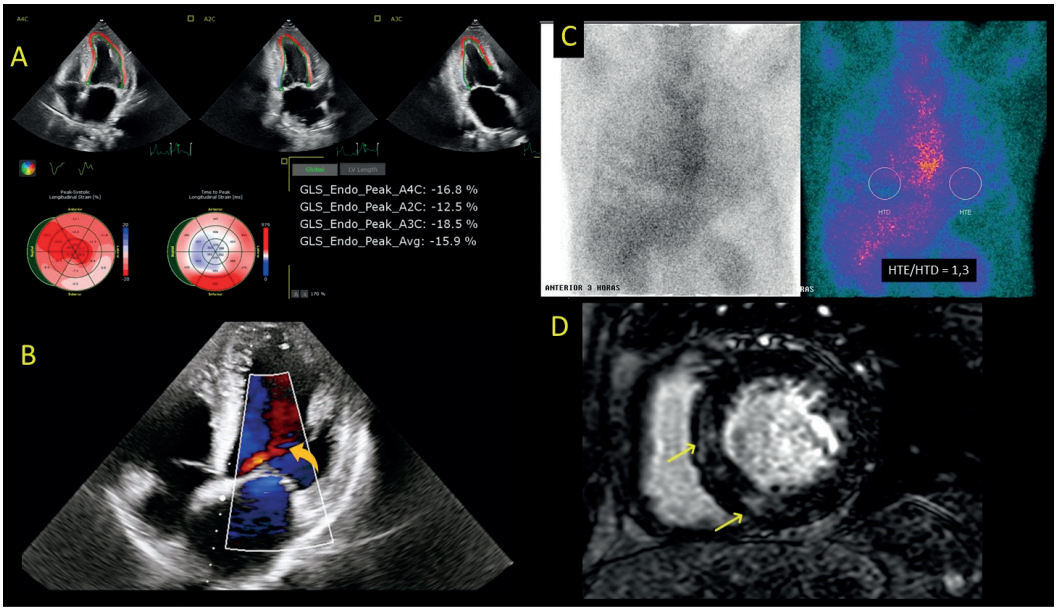

Figure 2 – *(2A): Echocardiogram showing GLS of 15.9% with apical sparring pattern. (2B): Echocardiogram (5-chamber view) with color Doppler showing AR (orange arrow). (2C): Technetium-pyrophosphate cardiac single-photon emission computed tomography (Tc-PYP SPECT) revealing heart uptake equal to rub uptake (grade 2 visual scale) and quantitative analysis with heart-to-contralateral lung uptake ration (H/CL) of 1.3 in the third hour. (2D): Cardiac MRI reveals mild irregular and diffuse areas of late gadolinium enhancement within basal and mid segments of the LV (yellow arrows).*

Incorporation of Technologies (Conitec), an institution to assist the Brazilian Ministry of Health in decision-making (Conitec, Brazilian Ministry of Health, 2022)*.

The patient continued hematological treatment for MML and control of other cardiac risk factors with good clinical evolution. His pharmacological treatment consisted of losartan, hydrochlorothiazide, amlodipine, hydralazine, spironolactone, bisoprolol, and dapagliflozin. After two years of good cardiac evolution and no further complications, the patient experienced a hematological progression of his disease and died after an episode of respiratory sepsis.

Discussion

Systemic amyloidoses consist of protein misfolding disorders that form insoluble amyloid fibrils, which, in turn, are deposited in the tissues leading to organ damage. Two types of amyloid account for 95% of CA: light-chain amyloid (AL), due to immunoglobin light-chain deposition, and TTR cardiac amyloidosis (ATTR-CM), which can be due to hereditary mutation (ATTRh) or ATTRwt. Hereditary transthyretin cardiac amyloidosis (hATTR-CM) is caused by one of the known heritable mutations in the TTR gene. In contrast, ATTRwt is caused by age-related changes in the

wild-type TTR.[1,2] According to the most recent guidelines, AL can be excluded by obtaining a monoclonal protein screen comprising three laboratory tests: sFLC, SIFE, and UIFE. Additionally, the combined finding of positive bone radiotracer scintigraphy in patients with no evidence of detectable monoclonal protein in urine or serum was found to be 100% specific for ATTR-CM.[1,8]

Although systemic amyloidosis has been associated with multiple malignant disorders, its association with leukemia is rather uncommon. In 1970, Kyle et al. described a rapidly progressive acute MML development in a patient with systemic amyloidosis of five years' duration who had received a prolonged course of melphalan.[3] Chronic lymphocytic leukemia can also be related to AL amyloidosis involving the heart. Cases of chronic MML were described in association with primary systemic amyloidosis by Cohen et al.[5] and Okuda et al.[4] As far as we are concerned, this is the first report of the coexistence of acute MML and ATTRwt amyloidosis. Although a non-biopsy diagnosis of ATTRwt can be obtained when certain diagnostic criteria are fulfilled, tissue characterization still represents the gold standard for the diagnosis and typing of CA. In this case, however, financial constraints and limitations of cardiac biopsy in our health system made this procedure unsuitable.[1,2]

Among valvular heart diseases, AS is the most prevalent disease in amyloidosis, with a prevalence of 16% in patients with severe AS planned to undergo transcatheter aortic valve replacement (TAVR).[9] Treibel et al. described that approximately 1 in 7 patients undergoing TAVR has occult CA.[6] Cases of mitral and tricuspid regurgitation seem to be increased in patients with CA.[10] The presence of AR has not been associated with CA. As far as we are concerned, this is the first description of CA in a patient with aortic insufficiency. Higher quality treatment of hematological and cardiological conditions has possibly led to an improvement in this patient's survival, which reinforces the role of cardio-oncology specialists in regular monitoring of these patients.

Conclusion

CA is an infiltrative disease that requires a high clinical suspicion for an appropriate diagnosis. In this case, we describe a very unusual association between ATTRwt CA and AR in a patient with acute MML. The increasing knowledge of CA and the improved prognosis of oncology diseases are possible causes for such association.

Author Contributions

Conception and design of the research: Chemello D, Salvador JC, Tavares M; acquisition of data: Chemello D, Salvador JC; analysis and interpretation of the data: Chemello D, Fagundes CS, Tavares M; writing of the manuscript: Chemello D, Chagas P, Fagundes CS; critical revision of the manuscript for intellectual content: Chemello D, Chagas P, Salvador JC, Tavares M.

Potential Conflict of Interest

No potential conflict of interest relevant to this article was reported.

Sources of Funding

There were no external funding sources for this study.

Study Association

This article is part of the Final Paper of the Specialization in Cardio-Oncology submitted by Diego Chemello, from Sociedade Brasileira de Cardiologia, Instituto Nacional do Câncer.

Ethics Approval and Consent to Participate

This study was approved by the Ethics Committee of the Universidade Federal de Santa Maria under the protocol number 83537224.0.0000.5346. All the procedures in this study were in accordance with the 1975 Helsinki Declaration, updated in 2013. Informed consent was obtained from all participants included in the study.

References

1. Simões MV, Fernandes F, Marcondes-Braga FG, Scheinberg P, Correia EB, Rohde LEP, et al. Position Statement on Diagnosis and Treatment of Cardiac Amyloidosis - 2021. Arq Bras Cardiol. 2021;117(3):561-98. doi: 10.36660/abc.20210718.
2. Kittleson MM, Ruberg FL, Ambardekar AV, Brannagan TH, Cheng RK, Clarke JO, et al. 2023 ACC Expert Consensus Decision Pathway on Comprehensive Multidisciplinary Care for the Patient with Cardiac Amyloidosis: A Report of the American College of Cardiology Solution Set Oversight Committee. J Am Coll Cardiol. 2023;81(11):1076-126. doi: 10.1016/j.jacc.2022.11.022.
3. Kyle RA, Pierre RV, Bayrd ED. Multiple Myeloma and Acute Myelomonocytic Leukemia. N Engl J Med. 1970;283(21):1121-5. doi: 10.1056/NEJM197011192832101.
4. Okuda T, Yumoto Y, Kamakari K, Kano T. Primary Amyloidosis Complicated with Chronic Myelomonocytic Leukemia. Rinsho Ketsueki. 1996;37(9):858-62.
5. Cohen AM, Mittelman M, Gal R, Halperin M, Djaldetti M. Chronic Myelomonocytic Leukemia Associated with Primary Amyloidosis. Leuk Lymphoma. 1994;16(1-2):183-7. doi: 10.3109/10428199409114157.
6. Treibel TA, Fontana M, Gilbertson JA, Castelletti S, White SK, Scully PR, et al. Occult Transthyretin Cardiac Amyloid in Severe Calcific Aortic Stenosis: Prevalence and Prognosis in Patients Undergoing Surgical Aortic Valve Replacement. Circ Cardiovasc Imaging. 2016;9(8):e005066. doi: 10.1161/CIRCIMAGING.116.005066.
7. Perugini E, Guidalotti PL, Salvi F, Cooke RM, Pettinato C, Riva L, et al. Noninvasive Etiologic Diagnosis of Cardiac Amyloidosis Using 99mTc-3,3-Diphosphono-1,2-Propanodicarboxylic Acid Scintigraphy. J Am Coll Cardiol. 2005;46(6):1076-84. doi: 10.1016/j.jacc.2005.05.073.
8. Gillmore JD, Maurer MS, Falk RH, Merlini G, Damy T, Dispenzieri A, et al. Nonbiopsy Diagnosis of Cardiac Transthyretin Amyloidosis. Circulation. 2016;133(24):2404-12. doi: 10.1161/CIRCULATIONAHA.116.021612.

9. Castaño A, Narotsky DL, Hamid N, Khalique OK, Morgenstern R, De Luca A, et al. Unveiling Transthyretin Cardiac Amyloidosis and its Predictors among Elderly Patients with Severe Aortic Stenosis Undergoing Transcatheter Aortic Valve Replacement. Eur Heart J. 2017;38(38):2879-87. doi: 10.1093/eurheartj/ehx350.

10. Aimo A, Camerini L, Fabiani I, Morfino P, Panichella G, Barison A, et al. Valvular Heart Disease in Patients with Cardiac Amyloidosis. Heart Fail Rev. 2024;29(1):65-77. doi: 10.1007/s10741-023-10350-1.

*Supplemental Materials

See the Supplemental Video 1, please click here.

See the Supplemental Video 2, please click here.

Asymptomatic Non-Bacterial Thrombotic Endocarditis Leading to a Diagnosis of Pancreatic Cancer

Diego Chemello,[1] Patricia Chagas,[2] Daniel Marques Barreiro,[3] Camila Sales Fagundes,[1] Rafael Coelho,[3] Marcelo Dantas Tavares de Melo[4]

Universidade Federal de Santa Maria,[1] Santa Maria, RS – Brazil
Hospital Universitário de Santa Maria,[2] Santa Maria, RS – Brazil
Hospital de Caridade Dr. Astrogildo de Azevedo,[3] Santa Maria, RS – Brazil
Universidade Federal da Paraíba,[4] João Pessoa, PB – Brazil

Introduction

Non-bacterial thrombotic endocarditis (NBTE) is a phenomenon associated with sterile vegetations composed of fibrin and platelets aggregating on healthy heart valves. Most cases are diagnosed after death or in patients experiencing systemic embolization. Diagnosis relies on clinical suspicion and a compatible echocardiographic image. The correct treatment is long-term systemic anticoagulation to avoid arterial embolization, which often presents as multiple and recurrent ischemic strokes.[1]

The first antemortem report of NBTE as the initial presentation of underlying pancreatic cancer was published in 2008.[2] However, incidental diagnosis of uncomplicated NBTE that leads to a subsequent discovery of carcinoma is rare.

Description

A 72-year-old male patient with a previous history of valvular heart disease presented for an elective consultation due to weight loss, fatigue, and depressive symptoms. His past medical history was characterized by biologic aortic valve replacement in 2014 due to severe aortic insufficiency. He also had mild mitral stenosis, without valvular replacement. There were no signs of coronary artery disease. He had recently received a diagnosis of major depressive disorder and was started on escitalopram 15 mg with minor improvement after 2 months. His other medications included enalapril 20 mg/day, metoprolol succinate 50 mg/day, and rosuvastatin 10 mg/day. Physical examination revealed blood pressure of 143/73 mmHg, heart rate of 62 beats per minute, and no fever. His weight was 78 kg, compared to the previous consultation of 88 kg, registered 6 months prior. Cardiac auscultation revealed regular rhythm, a systolic ejection murmur (grade 2/6) in aortic focus, and a diastolic murmur (grade 2/6) at the apex. Laboratory exams showed hemoglobin of 10.1 g/dL, platelets of 365,000/mm^3 and normal leucocyte count (8,120/mm^3 with 4% immature forms).

A transthoracic echocardiogram was performed, showing a 10 mm filamentous mobile echodense mass implanted on the anterior leaflet of the native mitral valve (Figure 1, Video 1). This valve also presented signs of moderate regurgitation and moderate stenosis (effective regurgitant orifice area of 0.29 cm^2). The aortic bioprosthetic valve mobility was normal, and there was mild perivalvular posterior leak. There was also concentric left ventricular hypertrophy (septum and posterior wall of 14 mm), severe left atrial enlargement (volume of 77 ml/mm^2) and left ventricular ejection fraction of 58%.

The patient was admitted for investigation with the main clinical suspicion of infective endocarditis. Multiple blood cultures were collected. The rheumatoid factor was negative, and there were no abnormalities in the urine analysis. The workup for bacterial endocarditis was negative. As a consequence, anticoagulation with low-molecular weight heparin was initiated. An abdominal computed tomography was also performed for additional investigation, revealing a large mass in the pancreas head, with extension to the superior mesenteric artery. The CA19-9 levels were 54.3 U/ml (normal values < 37 U/ml). A needle biopsy by echoendoscopy revealed the diagnosis of pancreatic adenocarcinoma. Complementary evaluation revealed absence of metastasis but an unresectable tumor. Anticoagulation was maintained despite the bleeding risks, considering the diagnosis of marantic endocarditis. After 4 weeks, echocardiogram was repeated, with complete disappearance of the filamentous mass in the mitral valve (Figure 2, Video 2). No signs of embolization were observed.

The patient received 5 cycles of chemotherapy with nab-paclitaxel (Abraxane©) and gemcitabine.[3] There was significant clinical improvement, with tumor size reduction. At this point, anticoagulation was switched to apixaban 5 mg twice daily. The oncology team also opted for complementary treatment with local radiotherapy (45 Gy × 25 cycles) with capecitabine (Xeloda©).[4] During chemotherapy treatment, all cardiac medications were temporarily interrupted due to hypotension. In the following months, there was significant clinical improvement in his depressive symptoms, with weight maintenance and reduction of tumor dimensions. Progressive pancreatic and peritoneal disease was identified 13 months after chemoradiation. Chemotherapy was performed first with rechallenge of nab-paclitaxel and gemcitabine[4] and after with modified FOLFIRINOX.[5] The patient had poor response to treatments and died 24 months after the diagnosis of unresectable pancreatic adenocarcinoma.

Keywords

Non-Infective Endocarditis; Pancreatic Neoplasms; Aortic Valve Insufficiency; Heart Valve Prosthesis.

Mailing Address: Diego Chemello •
Universidade Federal de Santa Maria. Av Presidente Vargas, 2084. Postal code: 97015-51. Santa Maria, RS – Brazil
E-mail: chemello.diego@gmail.com
Manuscript received November 27, 2024; revised November 27, 2024; accepted January 26, 2025
Editor responsible for the review: Marcelo Tavares

DOI: https://doi.org/10.36660/abcimg.20240126i

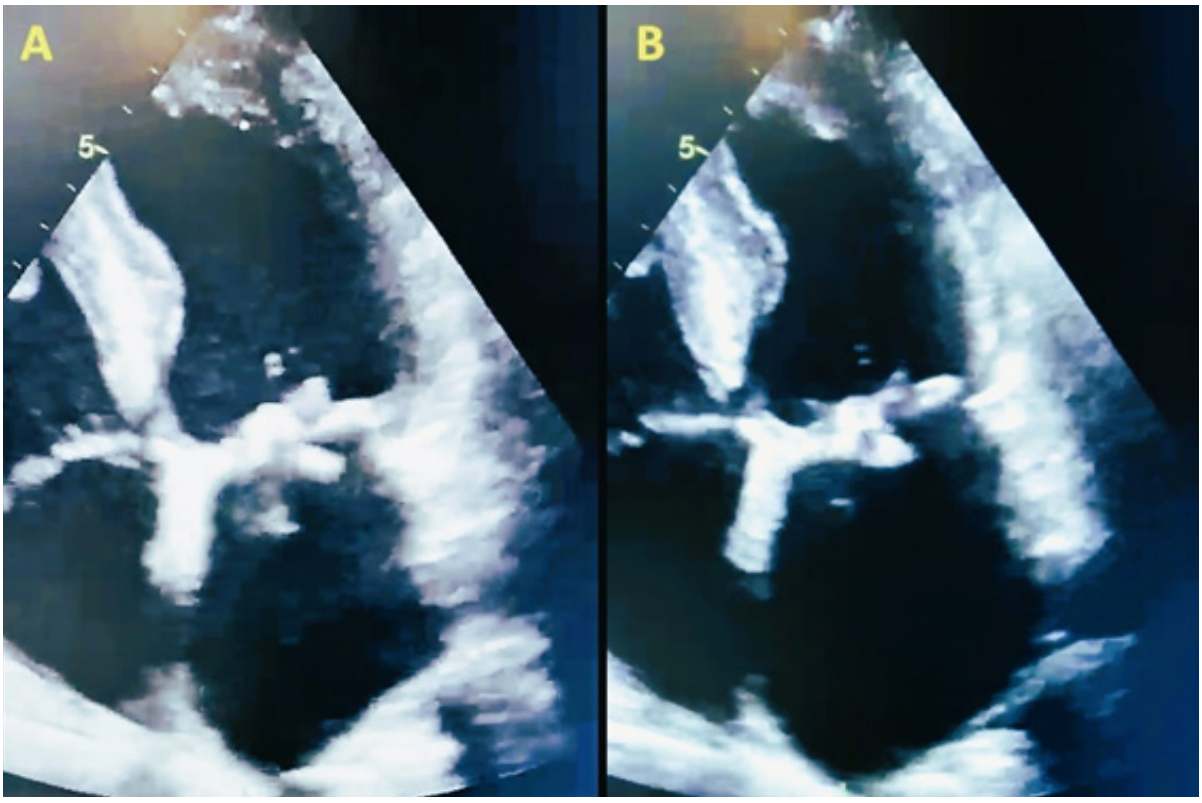

Figure 1 – *Transthoracic echocardiogram (apical 4-chamber view) showing a 10 mm filamentous mobile echodense mass implanted on the anterior leaflet of the native mitral valve (A and B).*

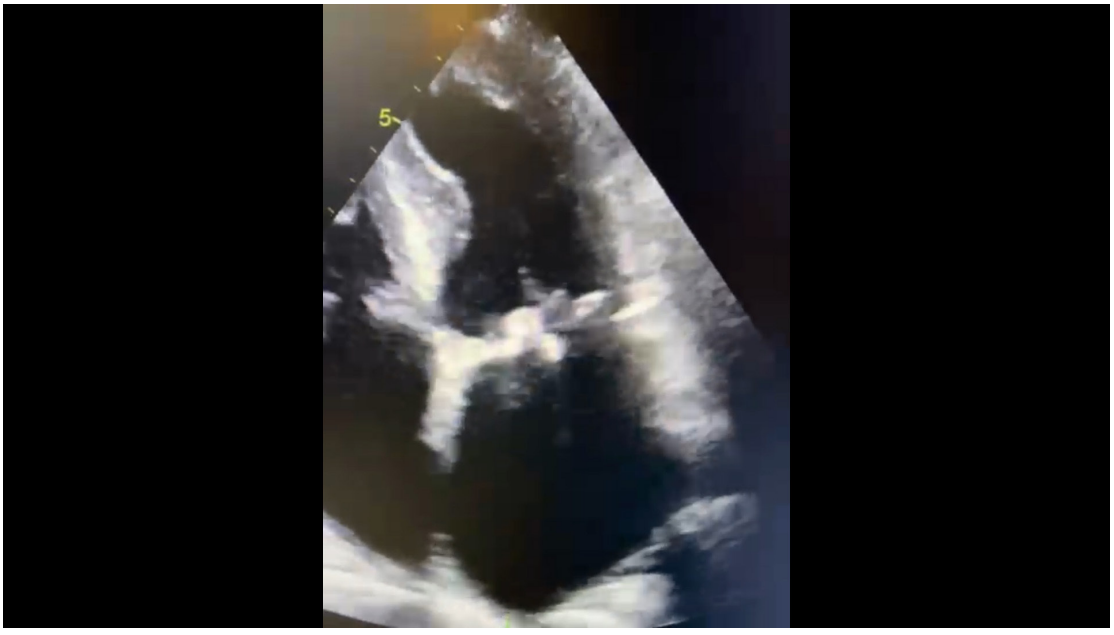

Video 1 – *Transthoracic echocardiogram (apical 4-chamber view) showing a 10 mm filamentous mobile echodense mass implanted on the anterior leaflet of the native mitral valve.*
http://abcimaging.org/supplementary-material/2025/3801/2024-0126_video_01.mp4

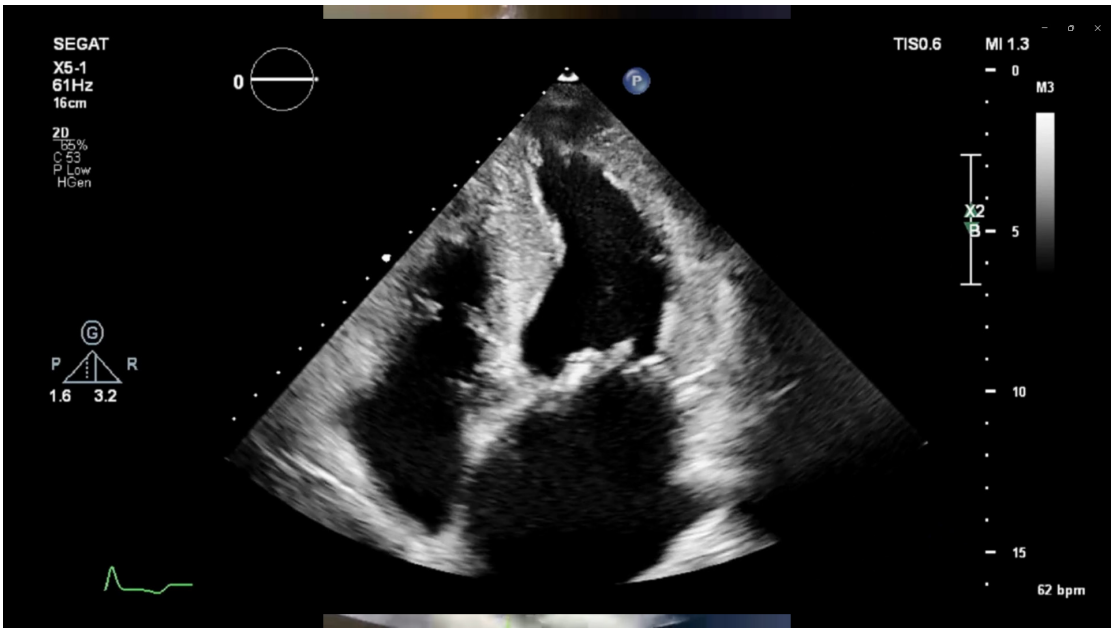

Video 2 – *New transthoracic echocardiogram (apical four-chamber view) after systemic anticoagulation showing complete disappearance of the filamentous mass on the mitral valve.*
http://abcimaging.org/supplementary-material/2025/3801/2024-0126_video_02.mp4

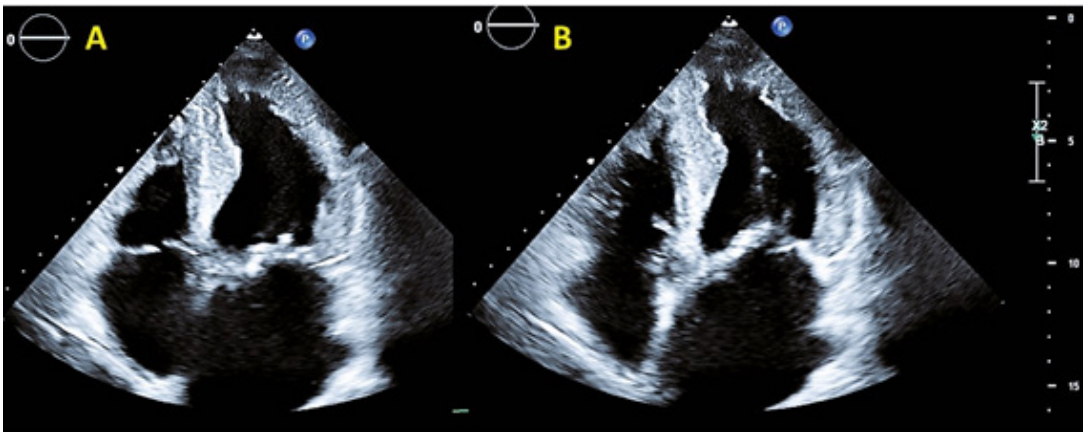

Figure 2 – *New transthoracic echocardiogram (apical 4-chamber view) after systemic anticoagulation showing complete disappearance of the filamentous mass in the mitral valve.*

Discussion

NBTE, also known as marantic or Libman-Sacks endocarditis, refers to a rare condition characterized by cardiac valve thickening or vegetation formation due to non-infective mechanisms.[1] Although the exact pathogenesis is unknown, these lesions are not associated with an inflammatory response or bacteremia, and they commonly happen as the result of fibrin deposition and platelet aggregation. Several conditions are related to the formation of sterile vegetations, including hypercoagulable states, autoimmune diseases, and malignancy. Potential mechanisms responsible for this association are increased production of circulation cytokines and clotting factors, which cause endothelial damage and hypercoagulable state.[6,7] According to contemporary reports, NBTE is more prevalent in females. Embolic complications are the most common presentation (up to 79%), with stroke representing the most common embolic event.

The diagnosis is currently based on echocardiographic image in association with a low index of clinical suspicion. Once the valvular lesion has been identified, investigation should be aimed at differentiating NBTE from infective endocarditis.[1] Treatment

consists of reducing the risk of systemic embolism, as well as identification and treatment of underlying conditions. Unless there is a clear contraindication, all patients with clinical diagnosis of NBTE should receive systemic anticoagulation.[1,8]

There is a well-known association of NBTE with malignancy, particularly adenocarcinomas of the pancreas and lung.[9,10] Most reports are usually associated with advanced or metastatic disease, or they are diagnosed during a postmortem examination.[11-13] The first antemortem report of NBTE as the initial presentation of underlying pancreatic cancer was published in 2008 by Smeglin et al.[2] Since then, several case reports have been described, all in patients with advanced disease or embolic phenomena.[13,14] The incidental finding of a sterile vegetation in a patient with depression and recent-onset weight loss makes our case report unique.

The incidence of depression is 2 to 3 times higher in patients with cancer compared to their healthy counterparts.[15] The strikingly closed relationship between pancreatic cancer and major depression has been known since 1931, when Yaskin reported the association between this cancer and the triad of anxiety, depression, and "sense of impending doom."[16] One of the largest studies published in this field found a significantly increased risk of psychiatric diseases nearly a year before the cancer was diagnosed.[17] Interestingly, our case presented a similar timeline, potentially contributing to an early diagnosis.

Regarding the echocardiographic image, there were potential differential diagnosis with NBTE, including papillary fibroelastoma, vegetations due to subacute bacterial endocarditis, or multiple large Lambl excrescences. Transthoracic echocardiography is the mainstay imaging modality to describe the vegetation. Cardiac imaging workup for papillary fibroelastoma, bacterial endocarditis, and NBTE is somewhat similar. Papillary fibroelastoma is being recognized as the most common primary tumor to arise in cardiac valves. It has a typical form of pedunculated mass with small fronds and a stalk. On the other hand, vegetations of infective and non-infective endocarditis are usually small (< 1 cm), broad-based, and irregular in shape.[1,15] In the present report, although the image was not conclusive for differential diagnosis, the complete disappearance of the lesion with systemic anticoagulation and the absence of positive cultures and signs of embolization confirmed NBTE as the diagnosis.

The present case highlights the importance of correct diagnosis and investigation after diagnosis of NBTE without an underlying cause. It also emphasizes the management by a multidisciplinary team comprised of a cardiologist, thrombosis specialist, and oncologist.[18]

Conclusion

Marantic endocarditis (or NBTE) is a rare condition commonly associated with malignancy. Most cases have been reported in postmortem examination or in patients with advanced neoplastic disease. A high index of suspicion is necessary for a correct diagnosis. The echocardiographic image, associated with complementary exams to rule out infectious endocarditis is therefore required. Management requires prevention of systemic embolism with long-term systemic anticoagulation.

Author Contributions

Conception and design of the research and analysis and interpretation of the data: Chemello D, Coelho R, Tavares M; acquisition of data: Chemello D, Barreiro DM, Fagundes CS, Coelho R; writing of the manuscript: Chemello D, Chagas P; critical revision of the manuscript for intellectual content: Chemello D, Chagas P, Barreiro DM, Fagundes CS, Coelho R, Tavares M.

Potential Conflict of Interest

No potential conflict of interest relevant to this article was reported.

Sources of Funding

There were no external funding sources for this study.

Study Association

This article is part of the thesis of Postgraduate course in Cardio-Oncology submitted by Diego Chemello, from Instituto Nacional de Cardiologia.

Ethics Approval and Consent to Participate

This study was approved by the Ethics Committee of the Universidade Federal de Santa Maria under the protocol number 83549924.0.0000.5346. All the procedures in this study were in accordance with the 1975 Helsinki Declaration, updated in 2013. Informed consent was obtained from all participants included in the study.

References

1. Hurrell H, Roberts-Thomson R, Prendergast BD. Non-Infective Endocarditis. Heart. 2020;106(13):1023-9. doi:10.1136/heartjnl-2019-315204.
2. Smeglin A, Ansari M, Skali H, Oo TH, Maysky M. Marantic Endocarditis and Disseminated Intravascular Coagulation with Systemic Emboli in Presentation of Pancreatic Cancer. J Clin Oncol. 2008;26(8):1383-5. doi:10.1200/JCO.2007.12.9148.
3. von Hoff DD, Ervin T, Arena FP, Chiorean EG, Infante J, Moore M, et al. Increased Survival in Pancreatic Cancer with Nab-Paclitaxel Plus Gemcitabine. N Engl J Med. 2013;369(18):1691-703. doi:10.1056/NEJMoa1304369.
4. Mukherjee S, Hurt CN, Bridgewater J, Falk S, Cummins S, Wasan H, et al. Gemcitabine-Based or Capecitabine-Based Chemoradiotherapy for Locally Advanced Pancreatic Cancer (SCALOP): A Multicentre, Randomised, Phase 2 Trial. Lancet Oncol. 2013;14(4):317-26. doi:10.1016/S1470-2045(13)70021-4.
5. Sawada M, Kasuga A, Mie T, Furukawa T, Taniguchi T, Fukuda K, et al. Modified FOLFIRINOX as a Second-Line Therapy Following Gemcitabine Plus Nab-Paclitaxel Therapy in Metastatic Pancreatic Cancer. BMC Cancer. 2020;20(1):449. doi:10.1186/s12885-020-06945-8.

6. Bick RL. Cancer-Associated Thrombosis: Focus on Extended Therapy with Dalteparin. J Support Oncol. 2006;4(3):115-20.

7. Liu J, Frishman WH. Nonbacterial Thrombotic Endocarditis: Pathogenesis, Diagnosis, and Management. Cardiol Rev. 2016;24(5):244-7. doi:10.1097/CRD.0000000000000106.

8. Habib G, Lancellotti P, Antunes MJ, Bongiorni MG, Casalta JP, Zotti DF, et al. 2015 ESC Guidelines for the Management of Infective Endocarditis: The Task Force for the Management of Infective Endocarditis of the European Society of Cardiology (ESC). Endorsed by: European Association for Cardio-Thoracic Surgery (EACTS), the European Association of Nuclear Medicine (EANM). Eur Heart J. 2015;36(44):3075-128. doi:10.1093/eurheartj/ehv319.

9. Quintero-Martinez JA, Hindy JR, El Zein S, Michelena MI, Nkomo VT, DeSimone DC, et al. Contemporary Demographics, Diagnostics and Outcomes in Non-Bacterial Thrombotic Endocarditis. Heart. 2022;108(20):1637-43. doi:10.1136/heartjnl-2022-320970.

10. Quintela AG, Candela MJ, Vidal C, Román J, Aramburo P. Non-Bacterial Thrombotic Endocarditis in Cancer Patients. Acta Cardiol. 1991;46(1):1-9.

11. Chen L, Li Y, Gebre W, Lin JH. Myocardial and Cerebral Infarction Due to Nonbacterial Thrombotic Endocarditis as an Initial Presentation of Pancreatic Adenocarcinoma. Arch Pathol Lab Med. 2004;128(11):1307-8. doi:10.5858/2004-128-1307-MACIDT.

12. Rogers LR, Cho ES, Kempin S, Posner JB. Cerebral Infarction from Non-Bacterial Thrombotic Endocarditis. Clinical and Pathological Study Including the Effects of Anticoagulation. Am J Med. 1987;83(4):746-56. doi:10.1016/0002-9343(87)90908-9.

13. Jameson GS, Ramanathan RK, Borad MJ, Downhour M, Korn R, von Hoff D. Marantic Endocarditis Associated with Pancreatic Cancer: A Case Series. Case Rep Gastroenterol. 2009;3(1):67-71. doi:10.1159/000207195.

14. Starobinska E, Robinson EA, Brucks E, Scott S. Marantic Endocarditis: Incidental Infarcts Leading to Diagnosis of Pancreatic Cancer. BMJ Case Rep. 2018;2018:bcr2018224529. doi:10.1136/bcr-2018-224529.

15. Currier MB, Nemeroff CB. Depression as a Risk Factor for Cancer: From Pathophysiological Advances to Treatment Implications. Annu Rev Med. 2014;65:203-21. doi:10.1146/annurev-med-061212-171507.

16. Yaskin JC. Nervous Symptoms as Earliest Manifestations of Carcinoma of the Pancreas. J Am Med Ass. 1931;96(20):1664-8. doi: 10.1001/jama.1931.02720460010003.

17. Lu D, Andersson TM, Fall K, Hultman CM, Czene K, Valdimarsdóttir U, et al. Clinical Diagnosis of Mental Disorders Immediately Before and after Cancer Diagnosis: A Nationwide Matched Cohort Study in Sweden. JAMA Oncol. 2016;2(9):1188-96. doi:10.1001/jamaoncol.2016.0483.

18. Itzhaki Ben Zadok O, Spectre G, Leader A. Cancer-Associated Non-Bacterial Thrombotic Endocarditis. Thromb Res. 2022;213(Suppl 1):S127-S132. doi:10.1016/j.thromres.2021.11.024.

A Common Primary Cardiac Tumor With an Uncommon Presentation

Juan Felipe Vasquez-Rodriguez,[1] *Carolina Paola Idrovo-Turbay,*[2] *Jaime Alberto Rodríguez,*[3,4] *Lorena Montes Villalobos*[3]

Fundación Cardioinfantil Instituto de Cardiología,[1] *Bogotá – Colombia*
Servicios Médicos Especializados AR SAS,[2] *Bogotá – Colombia*
Fundación Cardiovascular de Colombia,[3] *Floridablanca – Colombia*
Cardiovascular Imaging Society of the Inter-American Society of Cardiology (SISIAC),[4] *Bogotá – Colombia*

Abstract

Background

Cardiac tumors are rare, and most are secondary (metastatic) lesions. Primary tumors, though uncommon, are typically benign, with myxomas being the most frequent and occasionally displaying unique features. Diagnosis often requires multimodality imaging.

Case summary

A 41-year-old man with a history of ischemic stroke and resection of an apical left ventricular myxoma presented for evaluation after a follow-up transthoracic echocardiogram (TTE) revealed a mobile, ovoid apical lesion with high embolic risk, despite being asymptomatic. Cardiac magnetic resonance (CMR) imaging suggested recurrence of the ventricular myxoma. Surgical resection was performed, and histopathology confirmed the diagnosis of cardiac myxoma (CM).

Discussion

CMs are the most common primary benign cardiac tumors, typically located in the left atrium and attached to the interatrial septum. They are less frequently found in the ventricular cavities. About half of cases are asymptomatic, and recurrence is possible after resection. This case highlights a rare instance of late recurrence in an atypical location.

Keywords

Heart Neoplasms; Myxoma; Magnetic Resonance Imaging; Echocardiography.

Mailing Address: Juan Felipe Vasquez-Rodriguez •
Fundación Cardioinfantil Instituto de Cardiología. Clle 163a No 13b-60. Postal code: 111111. Bogota – Colombia
E-mail: jvasquez@lacardio.org
Manuscript received December 27, 2024; revised January 10, 2025; accepted January 26, 2025
Editor responsible for the review: Marcelo Tavares

DOI: https://doi.org/10.36660/abcimg.20240123i

Introduction

Cardiac tumors are rare, and mostly secondary (metastatic), benign (90%) lesions.[1] Among these, CMs are the most common, representing 50-60% of benign cases.[2,3] Myxomas predominantly occur in the left atrium (75-85%), with fewer cases in the right atrium, ventricles, or valve structures.[4,5] Once resected, tumor recurrence is possible, highlighting the need for proper postoperative follow-up. We report a case of a rapidly growing, late recurrent myxoma in an uncommon location.

Clinical case

A 41-year-old man with a history of ischemic stroke and resected left ventricular myxoma presented to the emergency room following a follow-up TTE that revealed a mobile, ovoid lesion in the left ventricular apex with high embolic risk, despite being asymptomatic. His stroke in 2014 had led to the diagnosis of a 20x15 mm pedunculated mass in the ventricular apex, which was resected via a transapical approach. Histology confirmed the lesion as a CM. The patient had no personal or family history of malignancy or primary cardiac tumors.

After the initial resection, serial TTEs were performed every two years to monitor for recurrence. In January 2023, a TTE revealed apical akinesia and a poorly characterized, linear, mobile structure. Due to the lack of ultrasound contrast, CMR was performed, showing apical scarring with akinesia, mild systolic dysfunction, and a 20x8 mm linear structure adherent to the apex, consistent with thrombus (Figure.1). Warfarin therapy was initiated, but the patient did not achieve adequate anticoagulation (INR: 1.5).

In March 2023, follow-up TTE revealed a large (40x20 mm), highly mobile, pedunculated lesion with a heterogeneous appearance (Video.1). A repeat CMR confirmed a 36x20 mm lesion at the apex with heterogeneous T2 hyperintensity, mild gadolinium perfusion, and peripheral late enhancement, suggesting CM recurrence with possible thrombus (Figures.2-3 and Video.2).

The patient underwent surgical resection of the lesion, which was identified as a fibrotic lesion with a thrombotic component. Histopathology confirmed the diagnosis of recurrent CM (Figure.4). Postoperative recovery was uneventful, and the patient remains under regular follow-up without complications or further hospitalizations.

Discussion

Myxomas are the most frequent benign primary cardiac tumors, generally diagnosed in patients aged 40–70 years, with a female predominance. Left ventricular involvement is rare, accounting for 0.7–3.6% of cases.[6] Up to half of patients are asymptomatic, while symptomatic presentations depend on the lesion's location and its effect on adjacent structures. Obstructive

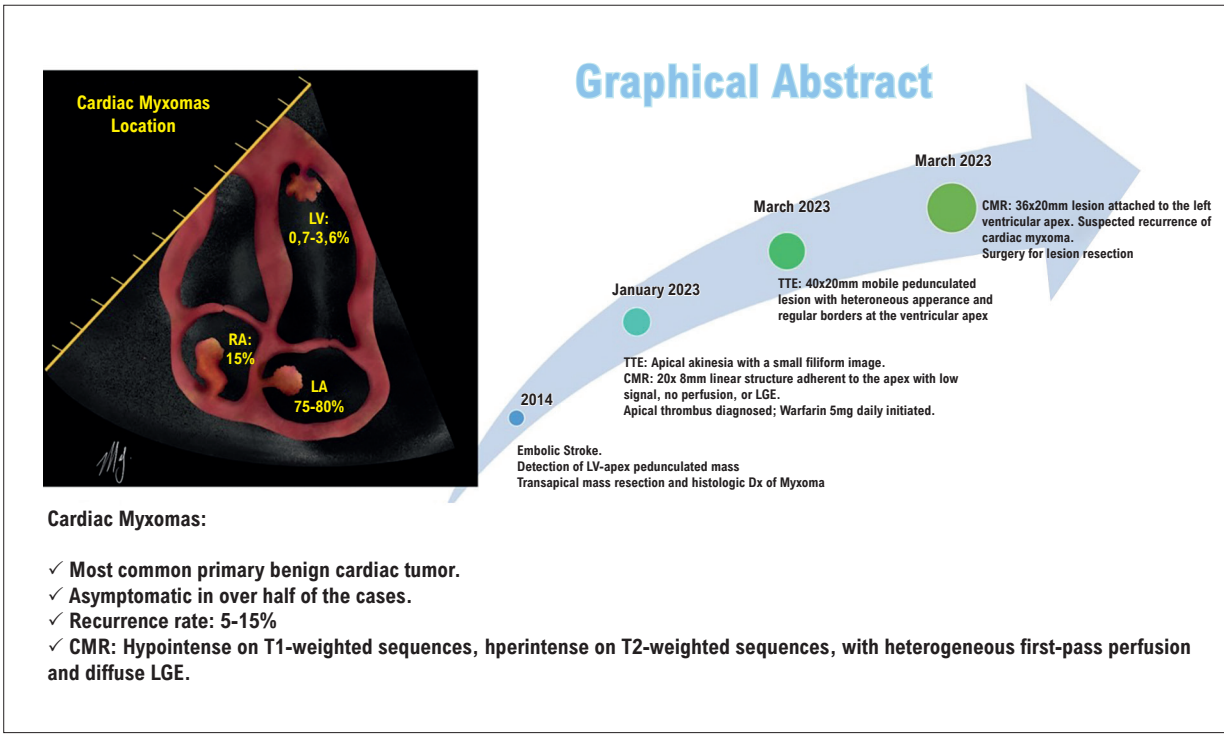

Figure 1 – *Graphical Abstract. LV: left ventricle; RA: right atrium; LA: left atrium; CMR: cardiac magnetic resonance; LGE: late gadolinium enhancement; TTE: transthoracic echocardiogram.*

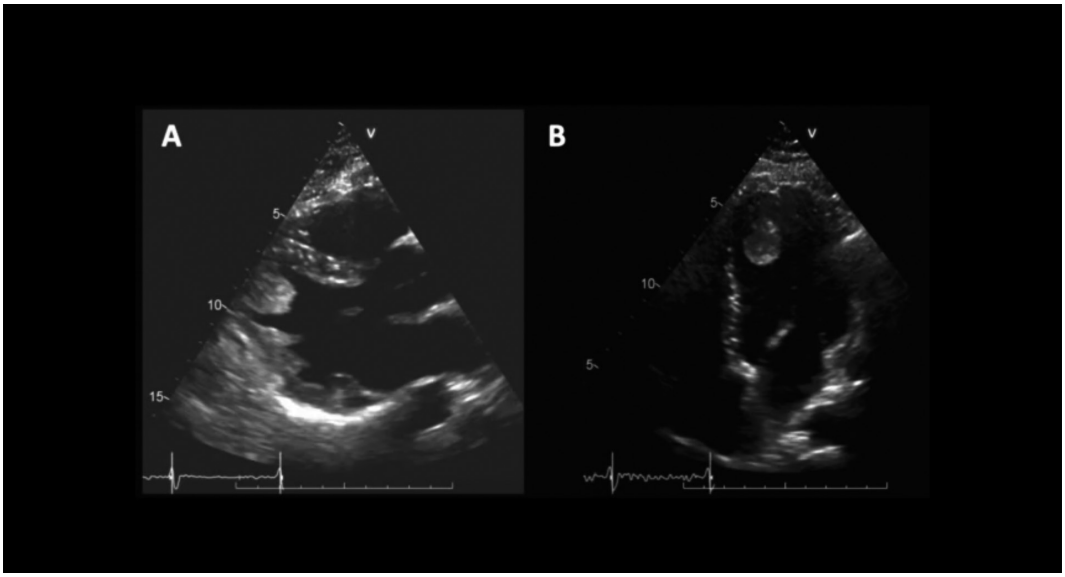

Video 1 – *TTE (A-B): Mobile, ovoid lesion in the left ventricular apex with a small pedicle, smooth edges, and heterogeneous content. http://abcimaging.org/supplementary-material/2025/3801/2024-0123_video_01.mp4*

symptoms (dyspnea, syncope, palpitations, lower extremity edema) occur in about two-thirds of symptomatic patients, especially with larger tumors, whereas the remaining third experience systemic or pulmonary embolism (depending on tumor location), particularly when lesions are small and friable. Rarely, systemic symptoms (anemia, fever, weight loss, fatigue, arthralgia, myalgia, Raynaud's phenomenon) occur, linked to elevated cytokine (particularly IL-6) secretion by the tumor.[7]

Echocardiography is essential for diagnosing CM, offering a 90–96% sensitivity [8] During evaluation, key features such as

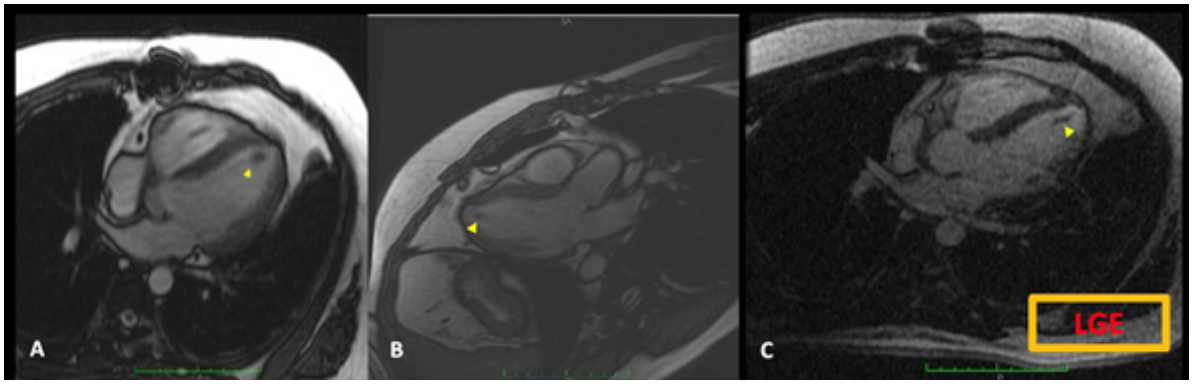

Figure 2 – *CMR. A-B: Four-chamber and three-chamber cine showing a low-intensity lesion at the left ventricular apex; C: no late enhancement with gadolinium; LGE: late gadolinium enhancement.*

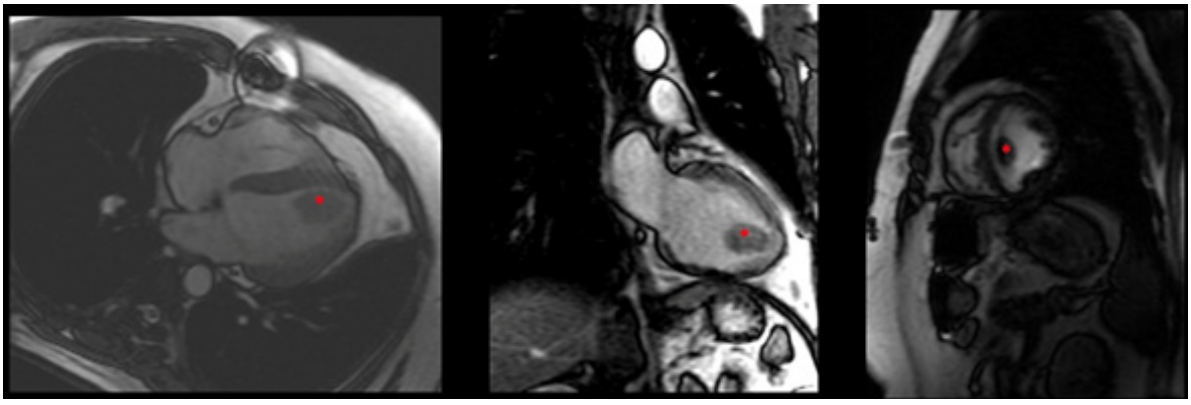

Figure 3 – *CMR (four-chamber and two-chamber, short-axis images) showing a low-intensity lesion at the left ventricular apex*

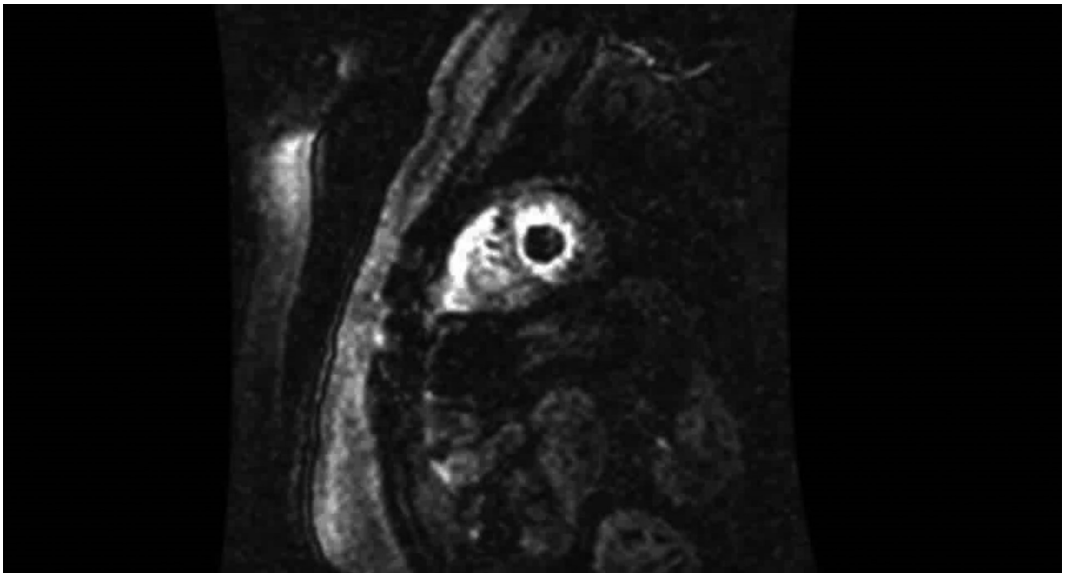

Video 2 – *CMR perfusion revealing mild, heterogeneous perfusion of the lesion. http://abcimaging.org/supplementary-material/2025/3801/2024-0123_video_02.mp4*

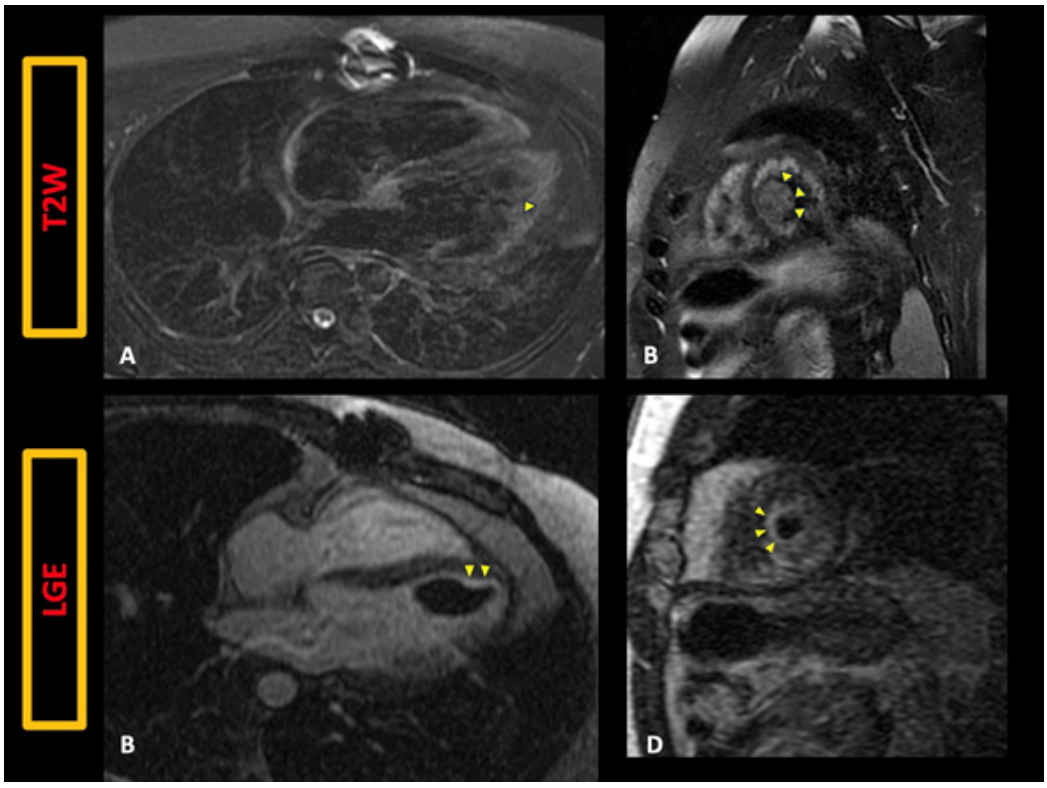

Figure 4 – *CMR. A-B: T2W sequences showing heterogeneous hyperintensity at the apical lesion; C-D: LGE around the lesion's periphery. LGE: late gadolinium enhancement; T2W: T2-weighted.*

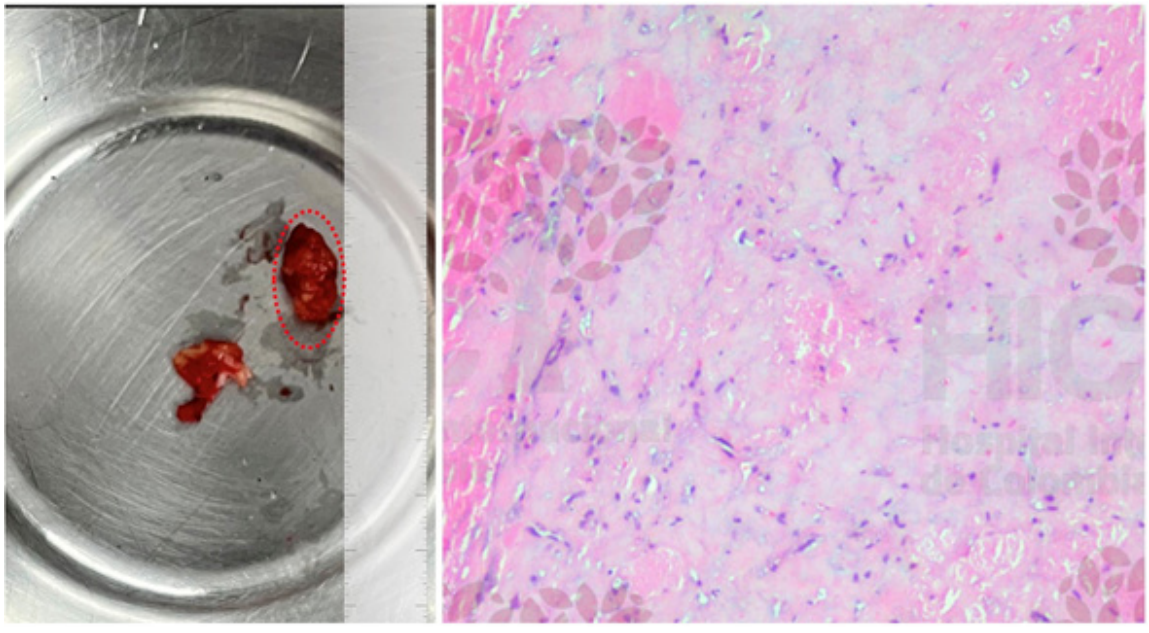

Figure 5 – *Cardiac mass specimen. A: Ovoid lesion resected from the ventricular apex (dotted red line). B: Hematoxylin–eosin revealing myxomatous tissue with spindle-shaped cells (Myxoma Cells). Histology image includes a watermark from the pathology laboratory of Hospital Internacional de Colombia (HIC).*

the lesion's location and impact should be noted. Myxomas exhibit two main morphologies: polypoid and papillary. Polypoid tumors are larger, with a smooth surface, small pedicle, and heterogeneous interior (including cystic or hemorrhagic areas), whereas papillary tumors are smaller, have a villous surface, and are more prone to embolic events.[9] In this case, a polypoid CM was identified.

One of the primary differential diagnoses of CM is intracavitary thrombus, especially in the ventricles. In some cases, both may coexist. Additional imaging techniques, such as cardiac computed tomography and CMR, refine lesion characterization. On CMR, myxomas typically appear hypointense on T1-weighted sequences and hyperintense on T2-weighted sequences, reflecting their high extracellular water content.[10] With gadolinium, they often show variable first-pass perfusion due to poor vascularity and display heterogeneous late enhancement with possible necrosis, as observed in our patient.

An important aspect with CMs is the recurrence rate, which range from 5% to 15% in retrospective studies and case series.[1,11] Recurrences typically occur at the same location but may also appear elsewhere. Proposed causes include incomplete resection, metastatic spread, totipotent multicentricity, and familial inheritance.[12] In a registry of 207 CMs followed for 9.5 ± 6.6 years, only multicentric myxomas were independently associated with recurrence.[11]

Another consideration is the recurrence-free interval after resection. In our case, the late recurrence was unexpected. Data from long-term registries indicate that most recurrences occur within the first five years, although there are isolated reports of recurrences 5–10 years after resection.[11,13]

Finally, the lesion's rapid progression was striking, doubling in size (from 20×8mm to 40×20mm) over 2.5 months, indicating a growth rate of about 8mm/month. Some studies, based on echocardiography, report a growth rate of 4,9mm/month,[14] while tomographic analyses suggest 1,2–2,2 mm/month.[15] Notably, echocardiography often underestimates tumor size compared to surgical specimens. This case not only underscores the high growth potential of CM, but also its characteristics, including unusual location, recurrence, and complications.

Highlights

CMs are the most frequent benign tumors of the heart. The ventricular location of these is infrequent.

The main differential diagnosis for myxoma is the presence of thrombi. CMR is very useful for lesion characterization and differentiation. CMs have a significant recurrence rate as well as high growth rates.

Conclusion

CMs are the most common benign primary cardiac tumors. Their features can vary markedly in size, location, complications, recurrence, and growth. Although the most frequent patterns are well described, it is essential to recognize and understand the possibilities of less common presentations.

Author Contributions

Conception and design of the research: Vasquez-Rodriguez JF; acquisition of data: Idrovo-Turbay CP, Rodríguez JÁ, Villalobos LM; analysis and interpretation of the data: Vasquez-Rodriguez JF, Villalobos LM; writing of the manuscript: Vasquez-Rodriguez JF, Idrovo-Turbay CP; critical revision of the manuscript for intellectual content: Vasquez-Rodriguez JF, Rodríguez JÁ, Villalobos LM.

Potential Conflict of Interest

No potential conflict of interest relevant to this article was reported.

Sources of Funding

There were no external funding sources for this study.

Study Association

This study is not associated with any thesis or dissertation work.

Ethics Approval and Consent to Participate

This article does not contain any studies with human participants or animals performed by any of the authors.

References

1. Tyebally S, Chen D, Bhattacharyya S, Mughrabi A, Hussain Z, Manisty C, et al. Cardiac Tumors: JACC CardioOncology State-of-the-Art Review. JACC CardioOncol. 2020;2(2):293-311. doi:10.1016/j.jaccao.2020.05.009.
2. Paolisso P, Foà A, Bergamaschi L, Graziosi M, Rinaldi A, Magnani I, et al. Echocardiographic Markers in the Diagnosis of Cardiac Masses. J Am Soc Echocardiogr. 2023;36(5):464-73. doi:10.1016/j.echo.2022.12.022.
3. Bussani R, Castrichini M, Restivo L, Fabris E, Porcari A, Ferro F, et al. Cardiac Tumors: Diagnosis, Prognosis, and Treatment. Curr Cardiol Rep. 2020;22(12):169. doi: 10.1007/s11886-020-01420-z.
4. Mando R, Barbat JJ, Vivacqua A. The Mysterious Mitral Mass: A Case of Valvular Myxoma. Case Rep Cardiol. 2018;1(1):3927948. doi:10.1155/2018/3927948.
5. Rahmanian PB, Castillo JG, Sanz J, Adams DH, Filsoufi F. Cardiac Myxoma: Preoperative Diagnosis Using a Multimodal Imaging Approach and Surgical Outcome in a Large Contemporary Series. Interact Cardiovasc Thorac Surg. 2007;6(4):479-83. doi:10.1510/icvts.2007.154096.
6. Samanidis G, Khoury M, Balanika M, Perrea DN. Current Challenges in the Diagnosis and Treatment of Cardiac Myxoma. Kardiol Pol. 2020;78(4):269-77. doi:10.33963/KP.15254.
7. Seino Y, Ikeda U, Shimada K. Increased Expression of Interleukin 6 mRNA in Cardiac Myxomas. Br Heart J. 1993;69(6):565-7. doi:10.1136/HRT.69.6.565.
8. Koritnik P, Pavsic N, Bervar M, Prokselj K. Echocardiographic Characteristics of Cardiac Myxoma. Eur Heart J. 2021;42(Suppl 1). doi:10.1093/EURHEARTJ/EHAB724.0146.

9. Mankad R, Herrmann J. Cardiac Tumors: Echo Assessment. Echo Res Pract. 2016;3(4):R65-R77. doi:10.1530/ERP-16-0035.

10. Aiello VD, Campos FPF. Cardiac Myxoma. Autops Case Rep. 2016;6(2):5-7. doi:10.4322/ACR.2016.030.

11. Wang Z, Chen S, Zhu M, Zhang W, Zhang H, Li H, et al. Risk Prediction for Emboli and Recurrence of Primary Cardiac Myxomas after Resection. J Cardiothorac Surg. 2016;11(1):22. doi:10.1186/S13019-016-0420-4/FIGURES/4.

12. Carvalho MS, Andrade MJ, Abecasis J, Gouveia R, Branco L, Neves JP, et al. Understanding Cardiac Myxoma Recurrence: A Case Report. Rev Port Cardiol. 2013;32(3):239-42. doi:10.1016/J.REPCE.2013.04.002.

13. Elbardissi AW, Dearani JA, Daly RC, Mullany CJ, Orszulak TA, Puga FJ, et al. Survival after Resection of Primary Cardiac Tumors: A 48-Year Experience. Circulation. 2008;118(14 Suppl):7-15. doi:10.1161/CIRCULATIONAHA.107.783126.

14. Gewehr DM, Neiverth A, Cavalcanti MS, Maestri TC, Haurani S, Kubrusly FB, et al. Fast Growth Rate of a Right Atrial Myxoma. Einstein. 2022;20:eRC6478. doi:10.31744/EINSTEIN_JOURNAL/2022RC6478.

15. Hsi DH, Sosa A, Miller W, Oren T, Koulova A, Coady MA. A Giant Right Atrial Myxoma-The Growth Rate and Multi-Modality Imaging. Echocardiography. 2021;38(6):1057-60. doi:10.1111/echo.15049.

Persistent Cephalgia Secondary to Carotid Web

José Aldo Ribeiro Teodoro,[1] Pedro Bution Teodoro,[2] Lucas Bution Teodoro,[2] Marco Antonio Zandoni Junior,[2] Antônio Pio Maria Jemma[3]

PRENOTO Clínica Médica Diagnóstica,[1] Ribeirão Preto, SP – Brazil
Universidade do Oeste Paulista,[2] Presidente Prudente, SP – Brazil
Hospital São Paulo,[3] Ribeirão Preto, SP – Brazil

Introduction

The Carotid Web (CW) consists of an intraluminal projection of the carotid artery's intima, forming either as a membrane or tissue fold, and may cause arterial lumen stenosis, disrupt blood flow patterns, leading to vascular embolic events such as a Cerebrovascular Accident (CVA).[1] The Carotid Web can be asymptomatic or symptomatic, with symptoms most often presenting as persistent cephalgia (headache). CW is a congenital anomaly of embryological development at the carotid bifurcation level. Currently, due to technological advances, CW is more easily diagnosed through the following diagnostic methods: Color Doppler Echocardiography (CDE), Computed Tomography Angiography (CTA), Magnetic Resonance Angiography (MRA) and Angiography (AGP). CDE is a highly accurate exam, demonstrating high sensitivity (94%) and specificity (92%). However, its positive and negative predictive values can be influenced by the disease's low prevalence, making the exam highly reliant on a qualified, experienced examiner.[4-10]

Case Report

Patient P.F.A., a 33-year-old female, consulted a neurologist on December 6, 2023, with a primary complaint of intense, pulsating headaches, typically lasting long periods and predominantly affecting the left side of her head, suggesting possible vasospasm. Physical examination showed no apparent abnormalities, leading to a referral to a vascular surgeon for further investigation of possible vascular-related headache. A Color Doppler exam of the bilateral carotid and vertebral arteries was performed, diagnosing a Carotid Web in the left carotid artery (Figure 1 and 7). Imaging revealed a focal, triangular thickening of the intimal-media layer with parietal irregularities and a small fibrotic area within the intimal layer, where a thin, mobile membrane was observed projecting into the lumen, intermittently contacting the vessel wall. The membrane's proximal and distal ends were anchored in the internal carotid artery's proximal segment (Figure 2 and Video 2), which maintained a normal diameter but showed slight bulging and altered flow patterns consistent with the characteristics of a Carotid Membrane. (Figure 3 and Video 2). Additionally, an anatomical variation related to the left vertebral artery, originating directly from the aortic arch was also observed in the CDE (Figure 7 and 8 and Video 1).

The carotid system on the right side showed normal calibers and preserved flows.

Angiography (AGP) (Figure 12 and Video 3) confirmed the presence of the Carotid Web (CW), showing local flow pattern alterations without significant stenosis. Treatment options included clinical, open surgery and endovascular approaches with stent implantation, from which the patient decided on the endovascular therapeutic intervention with placement of a stent[3] in the left carotid, supported by the justification of minimizing the risks for cerebrovascular events, which was performed without angioplasty, having no complications or other relevant findings. At the end of the procedure, a control AGP was performed, still intraoperative (Figure 13 and Video 5), where it was possible to note the absence of the aforementioned alterations, presenting only an episode of vasospasm. One month post-procedure, follow-up CDE confirmed that the stent was well-positioned at the site of the CW, with normal, low-resistance anterograde flow and no abnormalities or structural changes (Figures 9, 10 and 11 and Video 4). At follow-ups one and five months later, the patient reported no recurrence of the pulsating headache experienced pre-intervention.

Literature Review

The Carotid Web has a 1-7%[4] prevalence, representing up to 37% of cryptogenic ischemic CVAs, that is, of unidentified cause. It is responsible for thrombogenic hemodynamic changes distal to it, which can eventually cause embolization and consequent stroke.[4] Histopathologically, this variation (CW) represents a form of fibromuscular dysplasia characterized by intimal fibroelastic hyperplasia in the vascular endothelium, which forms a triangular intraluminal projection, possibly resulting in stenosis, aneurysm, or arterial dissection, and being most commonly found in the renal and carotid arteries.[6] In cases involving cervical arteries, typical symptoms include headache, vertigo, and pulsatile tinnitus, with presentation varying based on the CW pattern and degree of arterial narrowing. The carotid murmur may also be noted.[6] As described in other cases, distinctive changes have been observed in various blood flow imaging

Keywords

Headache; Internal Carotid Artery; Vascular Echo Doppler; Carotid Web.

Mailing Address: José Aldo Ribeiro Teodoro •
PRENOTO Clínica Médica Diagnóstica. Avenida Presidente Vargas, 2001, sala 113. Postal Code: 14020-260. Ribeirão Preto, SP – Brazil
E-mail: jarteodoro@gmail.com
Manuscript received August 20, 2024; revised October 25, 2024; accepted November 5, 2024
Editor responsible for the review: Simone Nascimento dos Santos

DOI: https://doi.org/10.36660/abcimg.20240080i

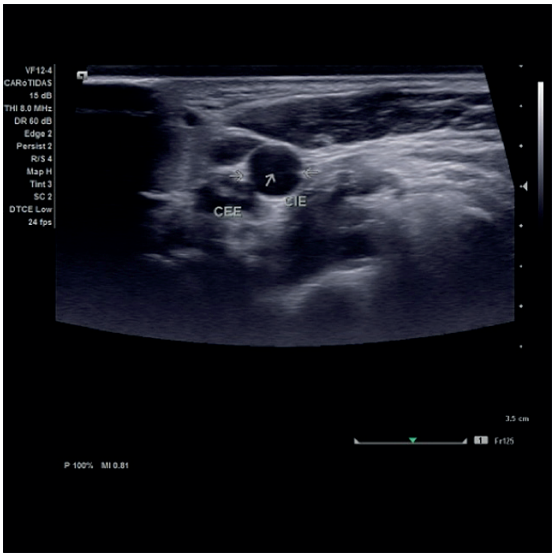

Figure 1 – *Cross-section in two-dimensional mode showing a thin membrane crossing the lumen with insertion into the wall of the left proximal internal carotid artery.*

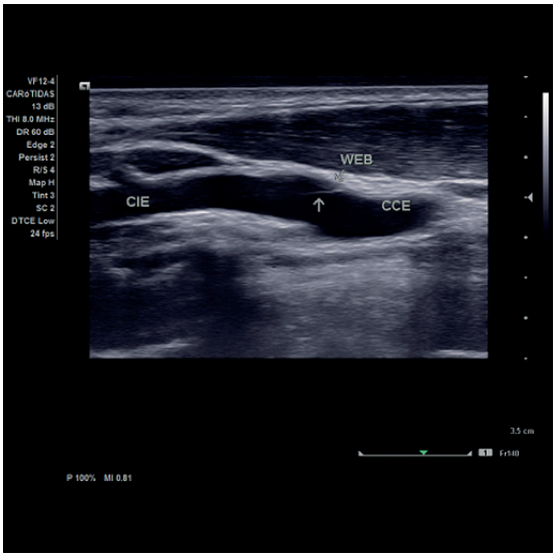

Figure 2 – *Longitudinal section in two-dimensional mode showing a triangular shape with a fibrosis point in the intimal layer where the thin membrane projecting into the lumen of the left proximal internal carotid artery is inserted. WEB: Carotid Web; CIE: Left Internal Carotid; CCE: Left Common Carotid.*

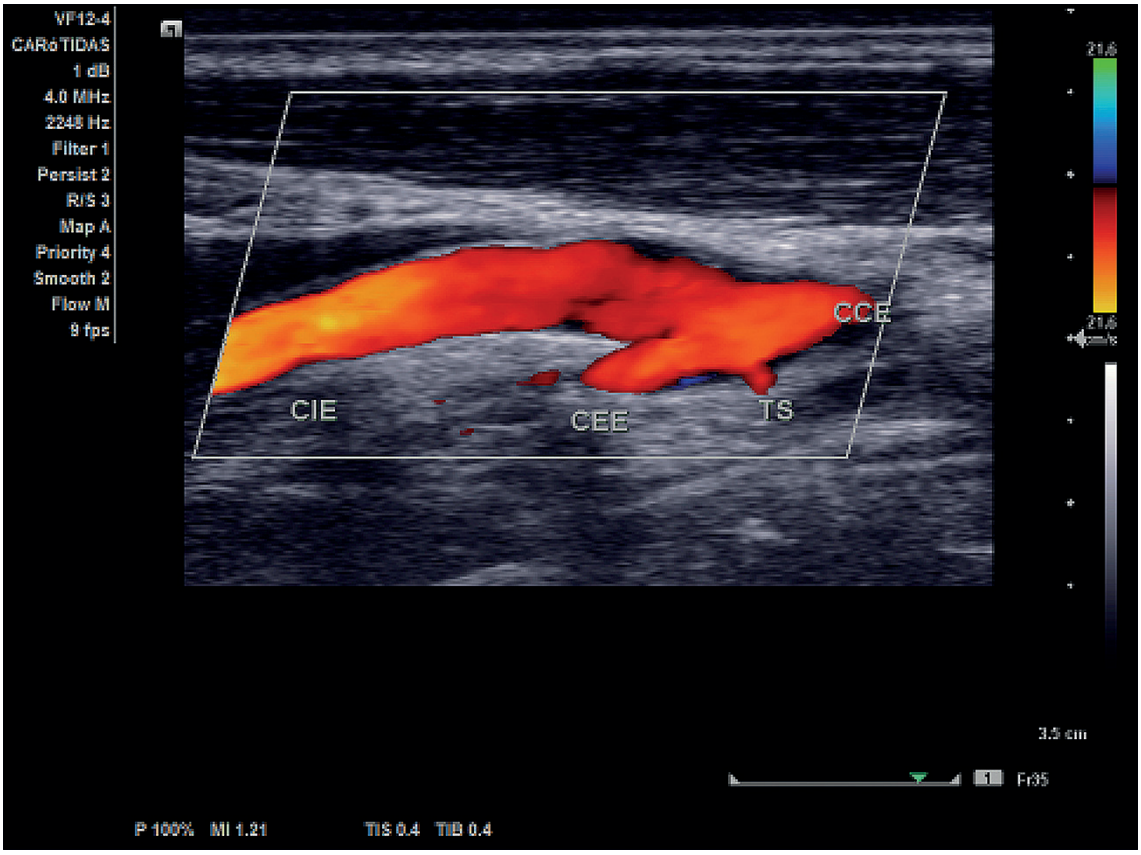

Figure 3 – *Longitudinal section with color Doppler showing a thin membrane inside the lumen of the left proximal internal carotid artery. CIE: Left Internal Carotid; CCE: Left Common Carotid; CEE: Left External Carotid; TS: Superior Thyroid.CEE: Left External Carotid; TS: Superior Thyroid.*

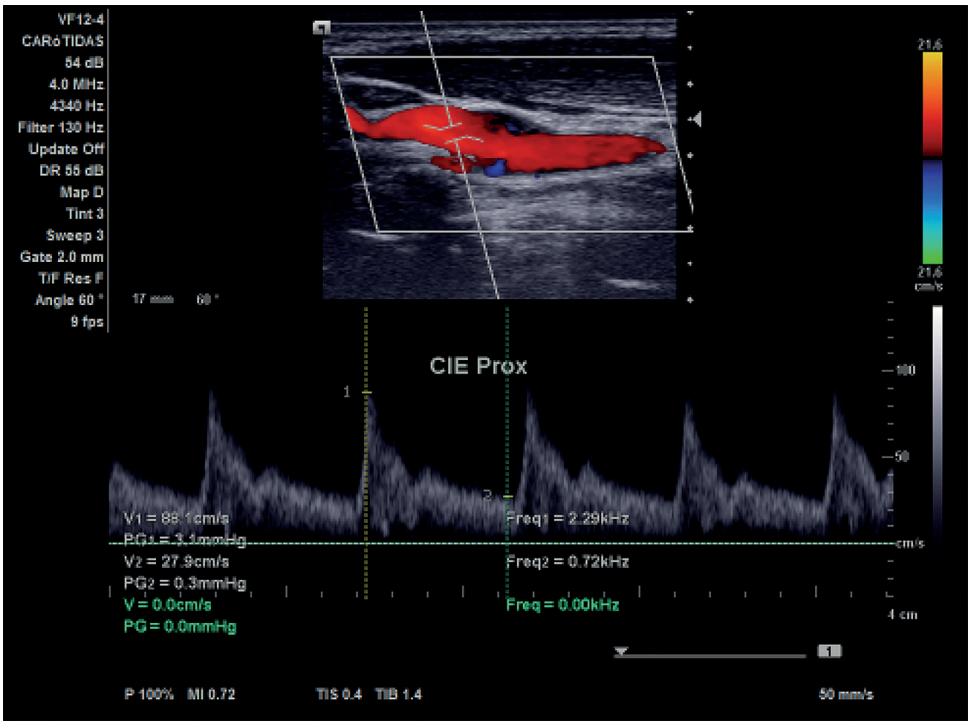

Figure 4 – *Longitudinal section with spectral pulsed Doppler showing the anterograde flow pattern and no significant increase in velocity in the left proximal internal carotid artery. CIE: Left Internal Carotid.*

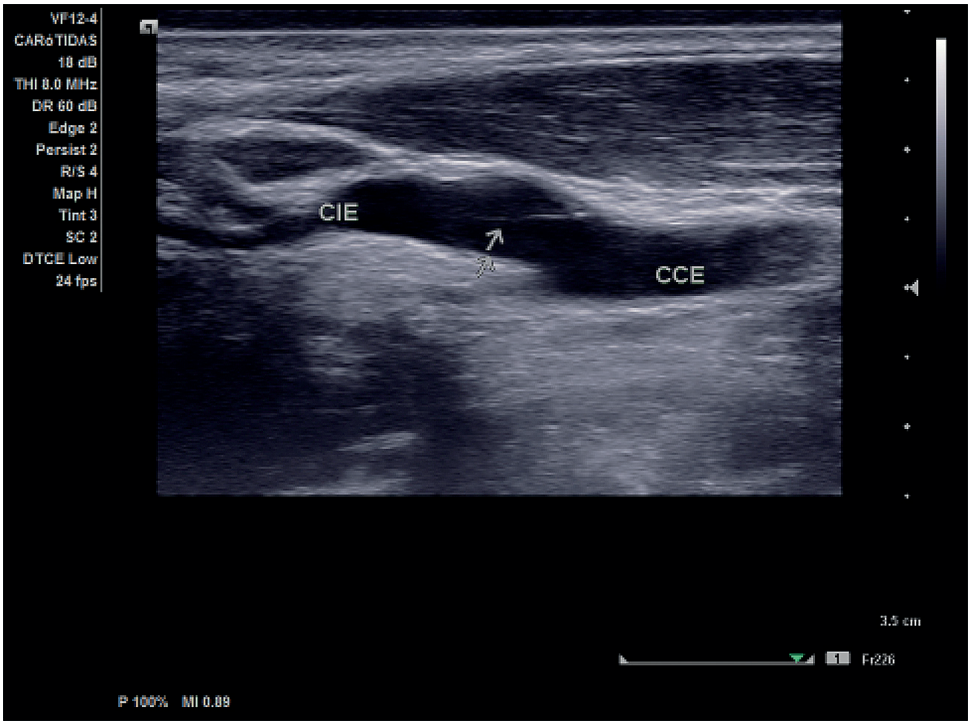

Figure 5 – *Longitudinal section with two-dimensional mode showing intimal thickening and slight bulging of the proximal left internal carotid artery wall. CIE: Left Internal Carotid; CCE: Left Common Carotid.*

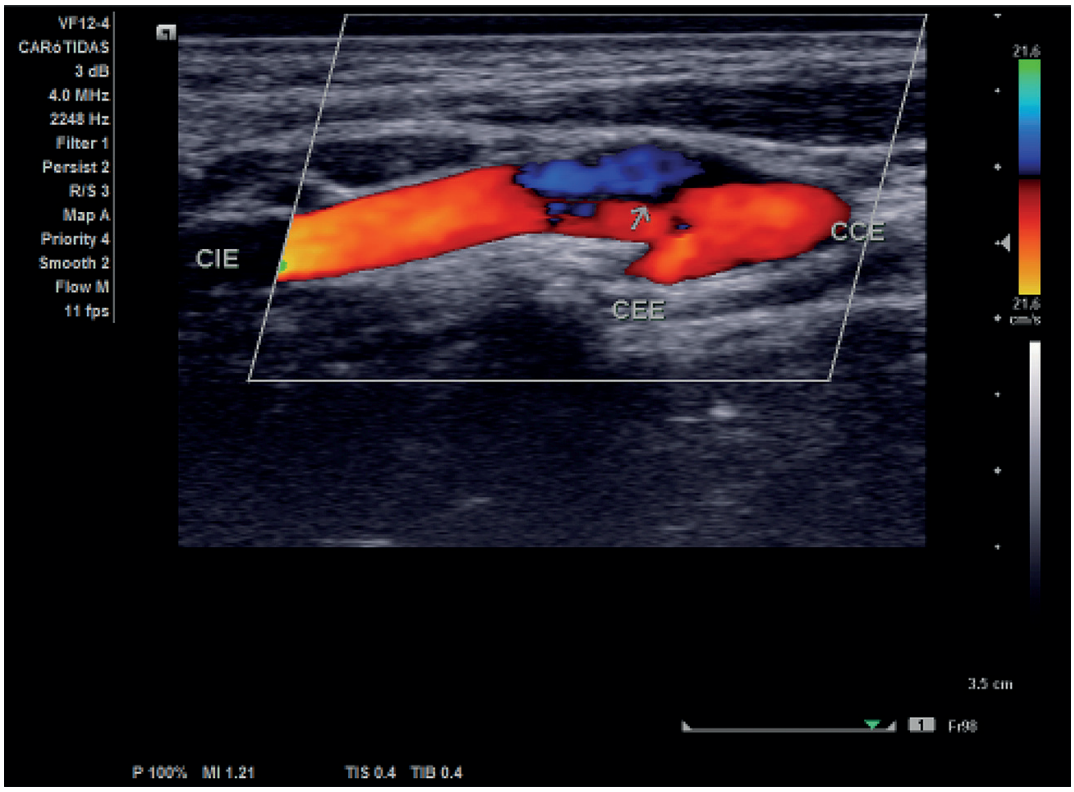

Figure 6 – *Longitudinal section with color Doppler showing the reverse flow division pattern through the presence of the membrane, and slight bulging of the proximal left internal carotid artery wall. CIE: Left Internal Carotid; CCE: Left Common Carotid; CEE: Left External Carotid.*

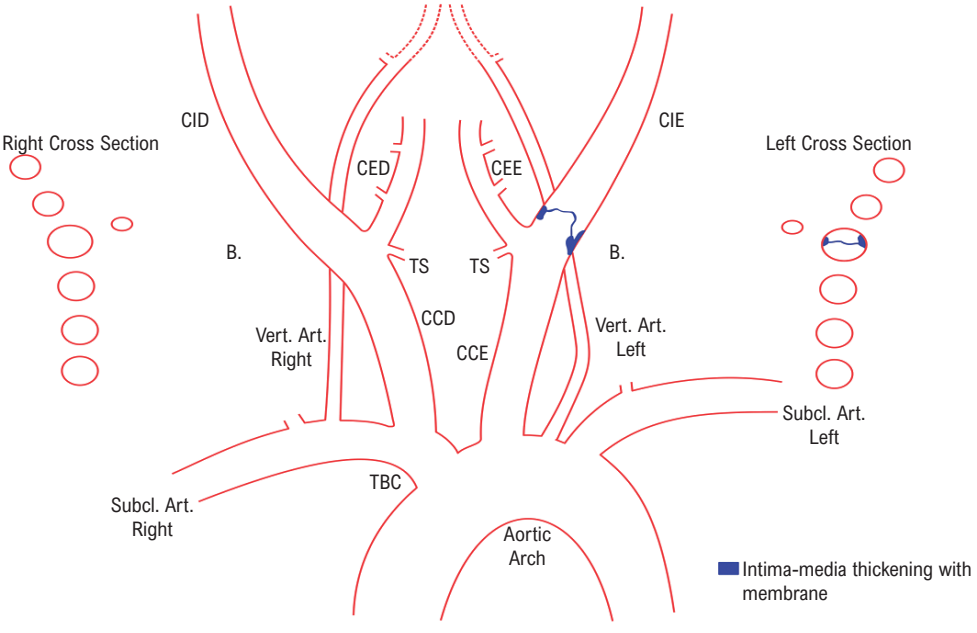

Figure 7 – *Cartographic drawing showing the site of the carotid web in the left carotid artery. CED: Right External Carotid; CID: Right Internal Carotid; CCD: Right Common Carotid; CIE: Left Internal Carotid; CCE: Left Common Carotid; CEE: Left External Carotid; TBC: Brachiocephalic Trunk.*

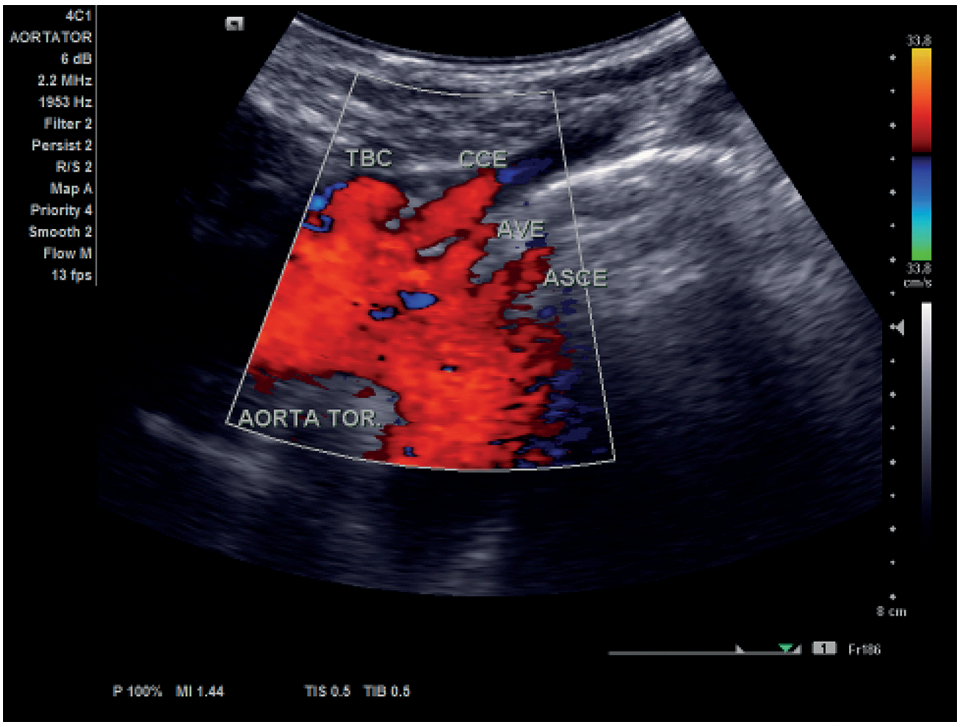

Figure 8 – *Longitudinal section with convex transducer and color Doppler demonstrating the anatomical variation of the left vertebral artery origin in the aortic arch, and the origins of the other supra-aortic trunk vessels. TBC: Brachiocephalic Trunk; AVE: Left Vertebral Artery; ASCE: Left Subclavian Artery; CEE: Left External Carotid.*

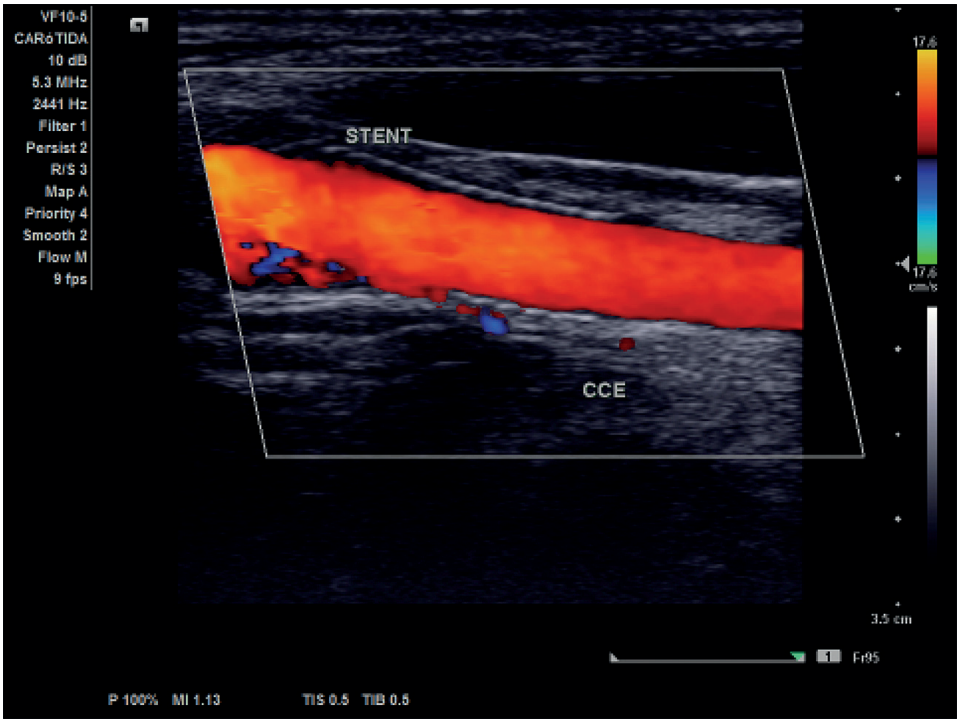

Figure 9 – *Longitudinal section with color Doppler showing a patent stent and normal anterograde flow within the left distal common carotid artery, without abnormalities. CCE: Left Common Carotid.*

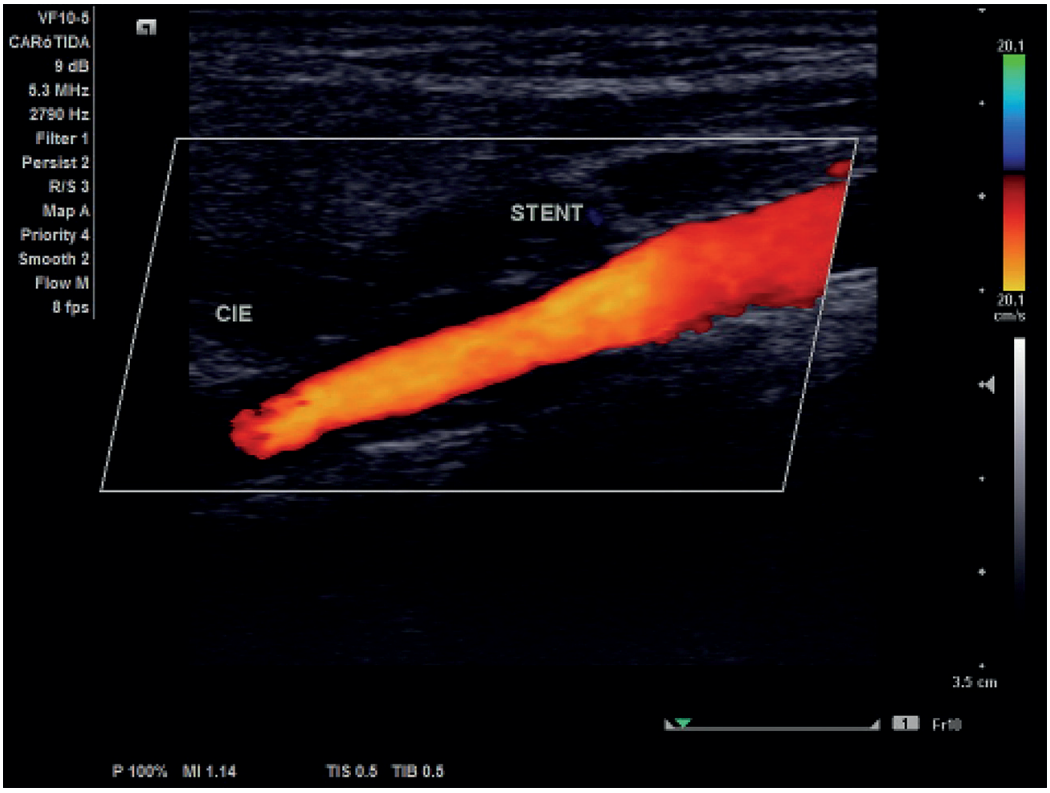

Figure 10 – *Longitudinal section with color Doppler showing a patent stent and normal anterograde flow supporting the carotid web within the left proximal internal carotid artery, without abnormalities. CIE: Left Internal Carotid.*

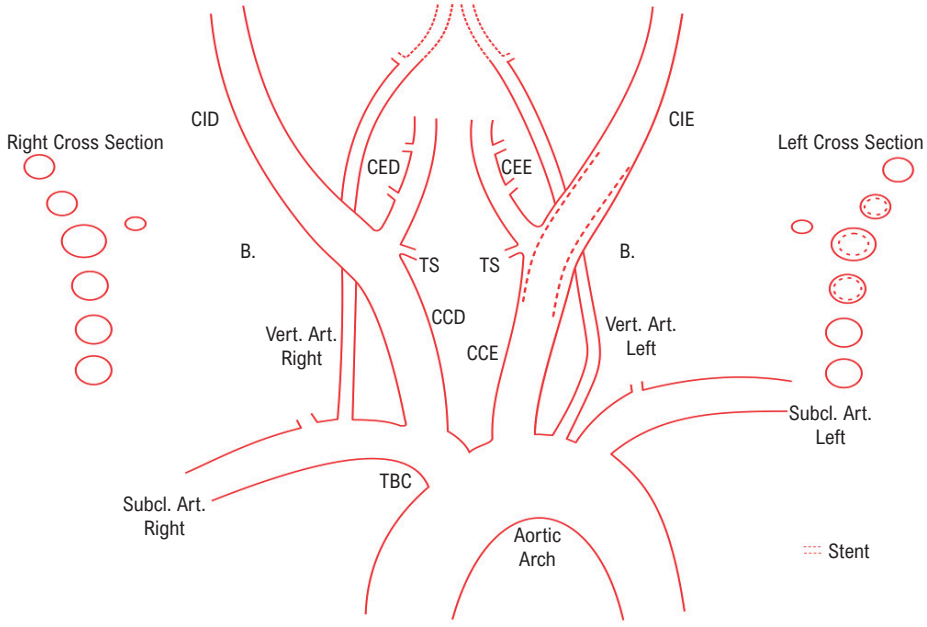

Figure 11 – *Cartographic drawing showing the stent site in the left carotid artery. CED: Right External Carotid; CID: Right Internal Carotid; CCD: Right Common Carotid; CIE: Left Internal Carotid; CEE: Left External Carotid; CCE: Left Common Carotid; TBC: Brachiocephalic Trunk.*

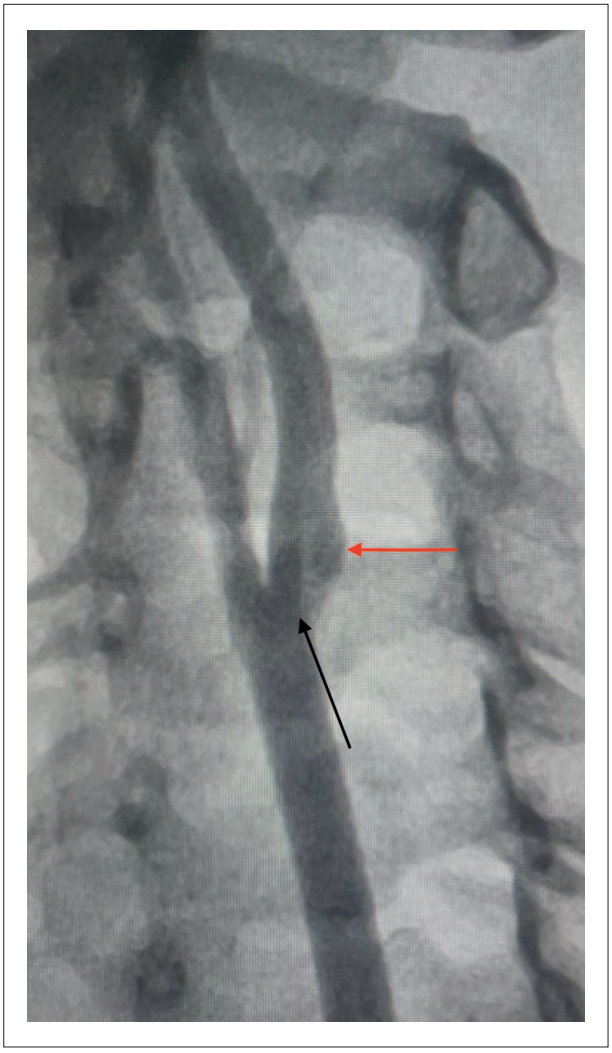

Figure 12 – *Preoperative AGP with carotid web (red and black arrow).*

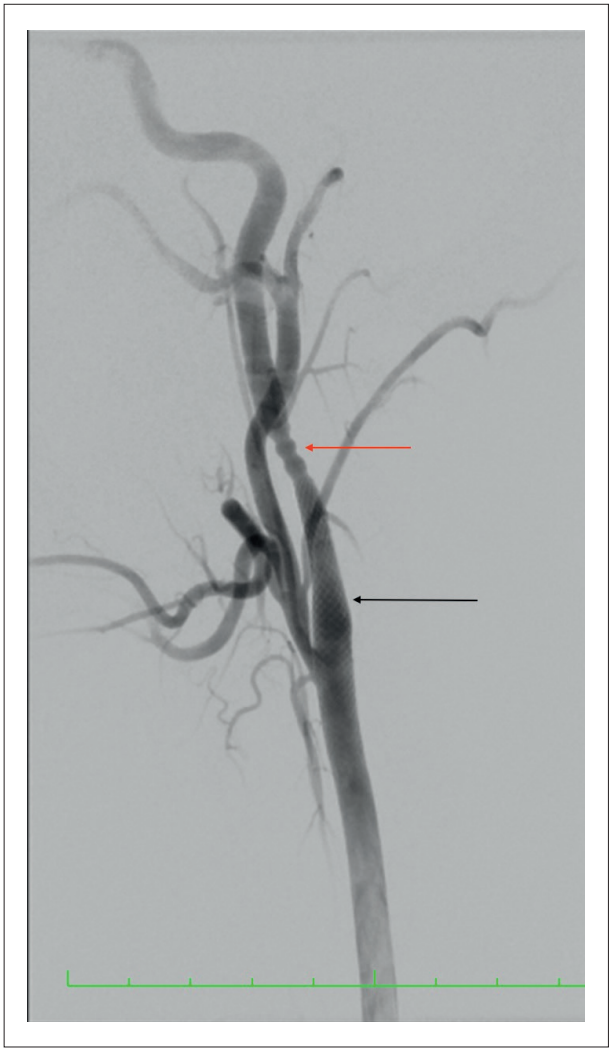

Figure 13 – *Trans-operative AGP of the carotid web stent (black arrow), with a slight final vasospasm (red arrow).*

techniques, which may show a triangular isohypoechoic lesion that protrudes, with or without an accompanying membrane, appearing as a punctiform spicule, short or long trabeculae, or web-like structures seen in both axial and longitudinal ultrasound scans. At the same time, color-coded Doppler typically reveals areas of turbulence and reduced flow velocities behind the membrane.[5] Though often asymptomatic, this membrane can be redundant and mobile, causing hemodynamic disruptions that may exceed those associated with atherosclerotic disease.[4] The main differential diagnosis should consider segmental carotid dissection. Therapeutic follow-up should be tailored to each patient, as no standardized treatment approach is widely accepted in clinical practice. One potential therapeutic strategy includes the use of anticoagulant or antiplatelet medications, recommended for both symptomatic and asymptomatic patients when the goal is to lower the risk of cerebrovascular events, combined with healthier lifestyle changes.[6] In patients with a history of CVA, intervention in the affected carotid artery is recommended by the endovascular technique with stent[3], or open surgery.

Remarks

The patient mentioned in this report did not experience thrombotic events, and her symptoms were limited to intense, pulsating, and persistent headaches. The diagnosis was established with Color Doppler Echocardiography (CDE), which detected structural changes, including a mobile and redundant membrane and alterations in the local flow pattern, later confirmed with Carotid Angiography.

Conclusion

CDE is a non-invasive and cost-effective method, comprising a valuable and accurate diagnostic tool for identifying the Carotid Web, and it plays an essential role in treatment planning, directly contributing to improved survival and quality of life for individuals with this condition.

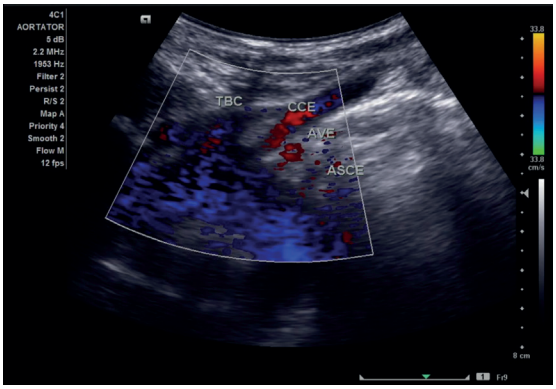

Video 1 – *Longitudinal section with convex transducer and color Doppler demonstrating the anatomical variation of the left vertebral artery origin in the aortic arch, and the origins of the other supra-aortic trunk vessels. Em: https://abcimaging.org/supplementary-material/2025/3801/2024_0080_video_01.mp4*

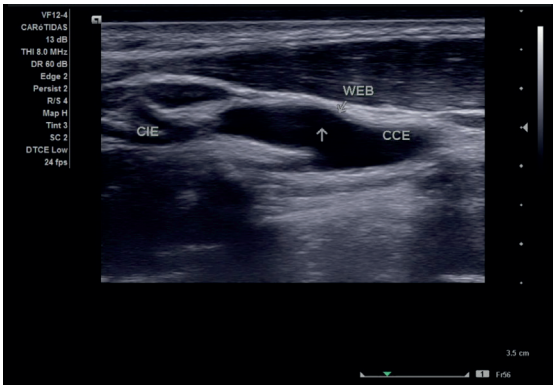

Video 2 – *CDE showing the redundant membrane and flow alteration. Em: https://abcimaging.org/supplementary-material/2025/3801/2024_0080_video_02.mp4*

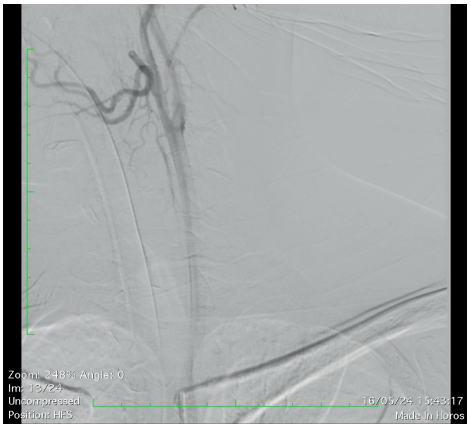

Video 3 – *Trans-operative AGP showing the intra-carotid web (Black arrow) and rarefaction of contrast at the site of blood turbulence (Red arrow). Em: https://abcimaging.org/supplementary-material/2025/3801/2024_0080_video_03.mp4*

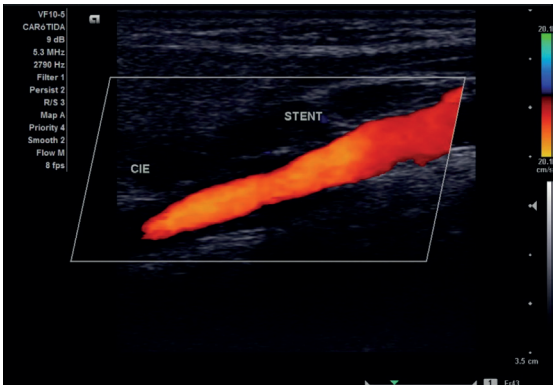

Video 4 – *CDE showing normal flow in the stent. Em: https://abcimaging.org/supplementary-material/2025/3801/2024_0080_video_04.mp4*

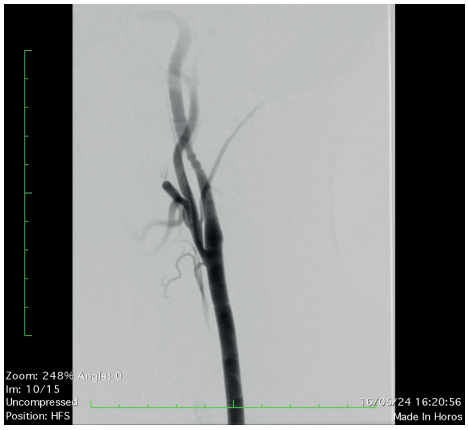

Video 5 – *Trans-operative AGP showing well positioned Wallstent Carotid/Boston stent, with disappearance of the mobile membrane (Black arrow). Note the spasm induced by the presence of the stent - "rosary beads" aspect (Red arrow). Em: https://abcimaging.org/supplementary-material/2025/3801/2024_0080_video_05.mp4*

Author Contributions

Conception and design of the research, analysis and interpretation of the data, statistical analysis and writing of the manuscript: Teodoro JAR, Teodoro PB, Teodoro LB, Zandoni Junior MA; acquisition of data: Teodoro JAR, Teodoro PB, Teodoro LB, Zandoni Junior MA, Jemma APM; critical revision of the manuscript for intellectual content: Teodoro JAR, Teodoro PB, Teodoro LB, Jemma APM.

Potential Conflict of Interest

No potential conflict of interest relevant to this article was reported.

Sources of Funding

There were no external funding sources for this study.

Study Association

This study is not associated with any thesis or dissertation work.

Ethics Approval and Consent to Participate

This article does not contain any studies with human participants or animals performed by any of the authors.

References

1. Natarajan S, Rahul S, Archana R, Sivarajan T. Carotid Web – An Unusual Cause for Ischemic Stroke in a Young Woman. IJVES CInI- Case reports, Innovations and Images. 2023;2(1):21-3. doi: 10.4103/IJCR.IJCR_8_24.
2. Patel SD, Otite FO, Topiwala K, Saber H, Kaneko N, Sussman E, et al. Interventional Compared with Medical Management of Symptomatic Carotid Web: A Systematic Review. J Stroke Cerebrovasc Dis. 2022;31(10):106682. doi: 10.1016/j.jstrokecerebrovasdis.2022.106682.
3. Kamatani K, Yoshida S, Tashiro N, Hashiguchi Y, Takigawa K, Yasaka M, et al. The Case of Treatment for Carotid Web - Double-Layer Micromesh Stent Implantation in Our Hospital. Surg Neurol Int. 2023;14:339. doi: 10.25259/SNI_525_2023.
4. Park CC, El Sayed R, Risk BB, Haussen DC, Nogueira RG, Oshinski JN, et al. Carotid Webs Produce Greater Hemodynamic Disturbances than Atherosclerotic Disease: A DSA Time-density Curve Study. J Neurointerv Surg. 2022;14(7):729-33. doi: 10.1136/neurintsurg-2021-017588.
5. Fontaine L, Guidolin B, Viguier A, Gollion C, Barbieux M, Larrue V. Ultrasound Characteristics of Carotid Web. J Neuroimaging. 2022;32(5):894-901. doi: 10.1111/jon.13022.
6. Touzé E, Southerland AM, Boulanger M, Labeyrie PE, Azizi M, Bouatia-Naji N, et al. Fibromuscular Dysplasia and Its Neurologic Manifestations: A Systematic Review. JAMA Neurol. 2019;76(2):217-26. doi: 10.1001/jamaneurol.2018.2848.
7. Ristow AVB, Massière B, Meirelles GV, Casella IB, Morales MM, Moreira RCR, et al. Brazilian Angiology and Vascular Surgery Society Guidelines for the Treatment of Extracranial Cerebrovascular Disease. J Vasc Bras. 2024;23:e20230094. doi: 10.1590/1677-5449.202300942.
8. Ben Z, Wang J, Zhan J, Chen S. Ultrasonic Characteristics of Carotid Webs. Neuroradiology. 2022;64(1):95-98. doi: 10.1007/s00234-021-02757-0.
9. Vukasović R, Pintarić M, Lovrenčić-Huzjan A. Headache as a Symptom of Carotid Web. Archives of Psychiatry Research. 2023; 59:133-6. DOI:10.20471/may.2023.59.01.19.
10. Engelhorn AN, Engelhorn CA, Morais DM Filho, Barros FS, Coelho NA, editors. Guia Prático de Ultrassonografia Vascular. Rio de Janeiro: DiLivros; 2019.

A Prosthetic Dysfunction Earlier Than Expected

Mariana Laranjeira,[1] *Maria Inês Bertão,*[2] *Rodolfo Pereira,*[3] *Olga Sousa*[3]

Unidade Local de Saúde Gaia/Espinho,[1] *Vila Nova de Gaia, Porto – Portugal*

Figueira da Foz District Hospital,[2] *Figueira da Foz – Portugal*

Vila Nova de Gaia Espinho Hospital Center,[3] *Vila Nova de Gaia, Porto – Portugal*

Prosthetic Heart Valves, despite their improvements over the last few decades, can be subject to complications and dysfunction. Mechanical prosthetic valves have an expected lifespan of approximately 10 to 20 years, with many lasting longer. For biological valves, the lifespan is generally shorter (5 to 15 years). However, the durability varies according to individual factors, valve type, and patient health. Although their greater durability, Mechanical Heart Valves are more pro-thrombotic than biological valves, and their dysfunction may be associated, for example, with thrombotic events and the formation of *pannus*.[1] *Pannus* is an inflammatory tissue composed of inflammatory cells, fibroblasts, and blood vessels, and its presence can lead to dysfunction or other complications such as valve obstruction or endocarditis. The prevalence of *pannus* in cardiac valve prostheses varies depending on several factors, such as the type of prosthesis (biological or mechanical) and the patients' clinical conditions. It is estimated that the formation of *pannus* occurs in about 1% to 5% of patients with valve prostheses, although it may be more common in biological ones. The annual rate of thrombus formation can reach 5.7-8%, being higher in tricuspid and mitral valve prostheses.[1,2] A multimodality-based approach can provide useful data for differential diagnosis, complementing clinical assessment and offering an appropriate and optimized therapeutic approach. Valve dysfunction, in case of delayed diagnosis, can progress to cardiogenic shock.[1] Valvular dysfunctions can be structural (valve dysfunction due to changes related to the valve itself) or non-structural (dysfunctions not related to the valve resulting in stenosis or regurgitation, which include the formation of *pannus*), which arises from the accumulation of fibrous tissue in the valve, causing its dysfunction. It forms less frequently than thrombi and its risk is higher in the mitral position compared to the tricuspid.[2]

The authors present a case of mechanical mitral valve prosthesis dysfunction due to *pannus*. A Caucasian 43 years-old woman, with dyslipidaemia and hypertension with a history of infectious endocarditis of the mitral valve in 04/2022, presented with signs of infectious infiltration of both leaflets and severe mitral regurgitation. At this point, a cycle of antibiotic therapy was performed with ampicillin and flucloxacillin, with no agent being isolated (neither in blood cultures nor microbiological examination of the explanted valve). A double-disc mechanical valve prosthesis was implanted in the mitral position. The patients were hypocoagulated with a vitamin K antagonist (warfarin, with target INR levels of 2.5-3.5) and discharged from the hospital for outpatient follow-up.

About a year after the intervention, she reported fatigue with moderate exertion. The INR value was 4.56, with adequate hypocoagulation in previous evaluations. A transthoracic echocardiogram was performed showing signs of prosthesis obstruction (transprosthetic mean gradient of 8 mmHg), due to a fixed disc in a closed position, and preserved Left Ventricular Ejection Fraction (58%). Faced with an abnormally high gradient, fluoroscopy was performed to assess valve function. Fluoroscopy, despite not being able to distinguish whether the valve dysfunction is due to *pannus* or thrombus, is extremely important because it allows us to understand that the valve movement is anomalous.[3] Fluoroscopy was performed confirming immobility of one of the discs (Figure 1)**.** The histological examination of the surgical material was compatible with *pannus*.

Pannus formation is usually indolent, occurring several years later. In this case, the authors present a case in which *pannus* formation occurred with significant obstruction shortly after surgery. In the case of hemodynamically significant *pannus*, the only therapeutic choice is surgery, and a differential diagnosis with thrombosis must be made. In this case, although the INR was at supra-therapeutic values, it was not expected that a *pannus* dysfunction would occur so early. The timely mechanism evaluation and its contextualization are essential, in order to personalize and optimize potential interventions. The use of an integrated strategy (clinical, laboratory, and imaging) is essential for the adequate guidance of these complex cases.

Keywords

Heart Valve Prosthesis; General Surgery; Thrombosis; Pannus

Mailing Address: Mariana Ribas Laranjeira •
Unidade Local de Saúde Gaia/Espinho. R. Conceição Fernandes, S/N. Postal Code: 4434-502. Vila Nova de Gaia – Portugal
E-mail: mariribaslaranjeira@gmail.com
Manuscript received August 8, 2024; revised October 18, 2024; accepted December 7, 2024
Editor responsible for the review: Andrea Vilela

DOI: https://doi.org/10.36660/abcimg.20240078i

Author Contributions

Conception and design of the research, acquisition of data, analysis and interpretation of the data: Laranjeira M, Bertão MI, Sousa O, Pereira R; statistical analysis: Laranjeira M; writing of the manuscript: Laranjeira M, Bertão MI; critical revision of the manuscript for intellectual content: Bertão MI, Sousa O, Pereira R.

Potential Conflict of Interest

No potential conflict of interest relevant to this article was reported.

Sources of Funding

There were no external funding sources for this study.

Study Association

This study is not associated with any thesis or dissertation work.

Ethics Approval and Consent to Participate

This article does not contain any studies with human participants or animals performed by any of the authors.

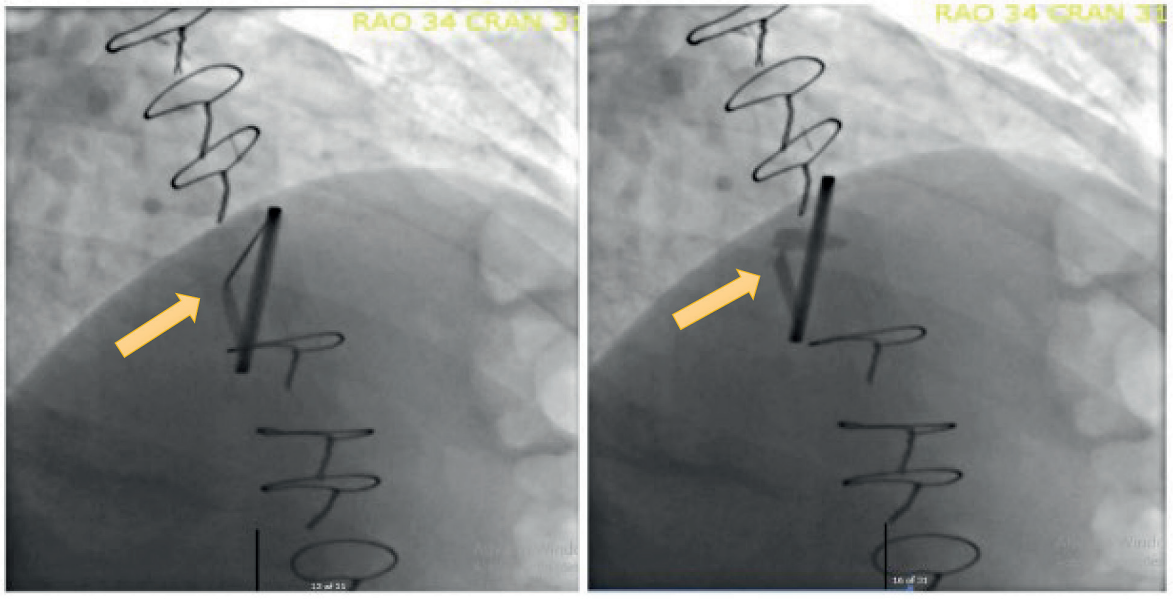

Figure 1 – *Fluoroscopy with evidence of immobility of one of the discs of the mitral valve prosthesis (arrows).*

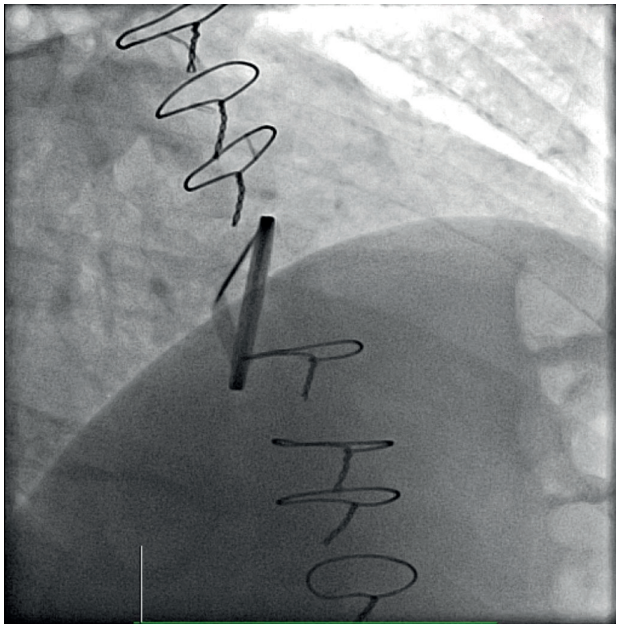

Video 1 – *In: http://abcimaging.org/supplementary-material/2025/3801/2024-0078_IM_video1_fluoroscopia.mp4*

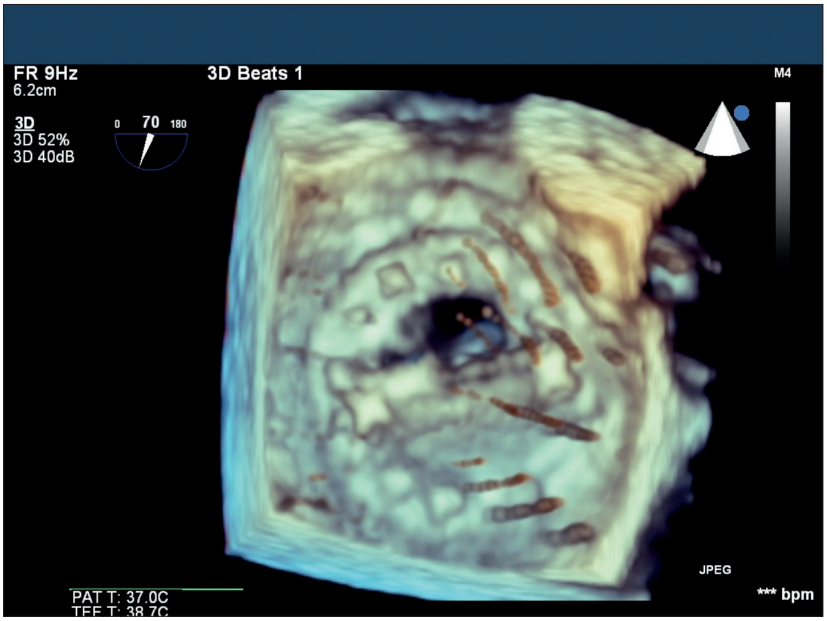

Video 2 – *In: http://abcimaging.org/supplementary-material/2025/3801/2024-0078_IM_video2_reconstrucao_da_valvula.mp4*

References

1. Jiménez CES, Papolos AI, Kenigsberg BB, Ben-Dor I, Satler LF, Waksman R, et al. Management of Mechanical Prosthetic Heart Valve Thrombosis: JACC Review Topic of the Week. J Am Coll Cardiol. 2023;81(21):2115-27. doi: 10.1016/j.jacc.2023.03.412.
2. Lancellotti P, Pibarot P, Chambers J, Edvardsen T, Delgado V, Dulgheru R, et al. Recommendations for the Imaging Assessment of Prosthetic Heart Valves: A Report from the European Association of Cardiovascular Imaging Endorsed by the Chinese Society of Echocardiography, the Inter-American Society of Echocardiography, and the Brazilian Department of Cardiovascular Imaging. Eur Heart J Cardiovasc Imaging. 2016;17(6):589-90. doi: 10.1093/ehjci/jew025.
3. Faraj R, Diallo TH, Dib H, Sarsari M, Diafarou R, Zarzur J, et al. Mechanical Prosthetic Mitral Valve Obstruction: Pannus or Thrombus? A Case Report. Radiol Case Rep. 2023;18(8):2685-8. doi: 10.1016/j.radcr.2023.05.016.

Crawford 2 Thoracoabdominal Aneurysm Associated with Bicarotid Trunk and Aberrant Right Subclavian Artery

Milton Sérgio Bohatch Junior,[1] Fernando Reis Neto,[1] Daniel Gustavo Miquelin,[1] Andre Rodrigo Miquelin,[1] Henrique Amorim Santos,[1] Amanda Fernandes Vidal da Silva,[1] Luiz Fernando Reis,[1] Jose Maria Pereira de Godoy[1]

Hospital de Base, Departamento de Cirurgia Vascular,[1] São José do Rio Preto, São Paulo, SP – Brazil

A 73-year-old woman with a history of hypertension was referred to the vascular surgery department for severe chest pain and signs of shock, including tachycardia and a tendency toward hypotension. An angiotomography revealed a thoracoabdominal aneurysm (Crawford Classification type 2 – Figure 1) with rupture signs (Figures 2A and 2B) and anatomical variations in the supra-aortic trunks, including an aberrant right subclavian artery (ARSA) (Figures 3A and 3B) and a bicarotid trunk (Figure 4). She underwent emergency surgery with a hybrid approach, which included visceral branching via laparotomy and endovascular repair of the aneurysm. Unfortunately, she developed hemodynamic instability and refractory shock during the procedure, resulting in death. Her family authorized the publication and signed the consent form.

An ARSA is a rare anomaly with a 0.2% to 13.3% prevalence.[1,2] It is more common among females, individuals with congenital anomalies (up to 3%), and those with Down syndrome (up to 35%).[3] ARSA may be associated with a bicarotid trunk in 0.8% to 20% of cases, where common carotid arteries originate from the same point on the aortic arch.[2] Thoracoabdominal Aortic Aneurysms (TAAAs) represent 10% of all aortic aneurysms. These aneurysms are potentially fatal if not treated early, as they may progress to rupture or dissection.[4] In a São Paulo epidemiological study, the mortality rate for emergency TAAA repairs was nearly double that of elective repairs (42.10% vs. 26.78%). This difference is often attributed to the hemodynamic instability of ruptured aneurysms and the lack of timely preoperative preparation in urgent cases.[5] Anatomical assessment is essential for treating TAAAs, whether through open surgery, endovascular surgery, or hybrid techniques. Anatomical variations in the supra-aortic trunks increase surgical complexity, regardless of the chosen technique.[6]

This "hybrid" approach, was first proposed by Quinones-Baldrich *et al*. in 1999 and involves a sequential revascularization of the visceral vessels, followed by endovascular aortic repair. Blood supply to the visceral organs is maintained by connecting an uncovered donor artery (often the iliac arteries).[7] This approach limits open surgery time to laparotomy, theoretically reducing the physiological stress associated with a larger thoracoabdominal incision and repair. By sparing patients from some disadvantages of open surgeries, such as thoracotomy, one-lung ventilation, extracorporeal pump perfusion, aortic cross-clamping, and ischemia of the visceral organs, spine, and limbs, it can be a valuable option.[8] In emergencies, there is insufficient time to customize stents for a fully endovascular repair in complex cases. Therefore, one alternative is surgeon-modified stents to create scallops or fenestrae. Yang *et al*. compared outcomes for TAAA patients treated with surgeon-modified stents and the hybrid technique, and reported low overall mortality (3.4% at 30 days) but a higher reintervention rate in patients who underwent endovascular surgery (13% vs. 0%).[9] Here, we report a rare case of anatomic variations in the supra-aortic trunks associated with a ruptured Crawford type 2 thoracoabdominal aneurysm.

Keywords

Aneurysm; Anatomic Variation; Cardiovascular Abnormalities.

Mailing Address: Milton Sérgio Bohatch Junior •
FAMERP. Avenida Brigadeiro Faria Lima, 5544. Postal code: 15090-000. São José do Rio Preto, SP – Brazil
E-mail: milton.jr87@hotmail.com
Manuscript received July 19, 2024; revised October 30 2024; accepted November 1, 2024.
Editor responsible for the review: Tiago Magalhães

DOI: https://doi.org/10.36660/abcimg.20240071i

Author Contributions

Conception and design of the research: Bohatch Junior MS, Reis Neto F, Miquelin DG, Godoy JMP; acquisition of data: Bohatch Junior MS, Santos HA, Silva AFV; analysis and interpretation of the data and critical revision of the manuscript for intellectual content: Bohatch Junior MS, Reis Neto F, Miquelin DG, Miquelin AR, Silva AFV, Godoy JMP; writing of the manuscript: Bohatch Junior MS, Reis Neto F, Santos HA, Reis LF.

Potential Conflict of Interest

No potential conflict of interest relevant to this article was reported.

Sources of Funding

There were no external funding sources for this study.

Study Association

This study is not associated with any thesis or dissertation work.

Ethics Approval and Consent to Participate

This study was approved by the Ethics Committee of the CEP-FAMERP under the protocol number 567/9522300005415/Report 6778289. All the procedures in this study were in accordance with the 1975 Helsinki Declaration, updated in 2013. Informed consent was obtained from all participants included in the study.

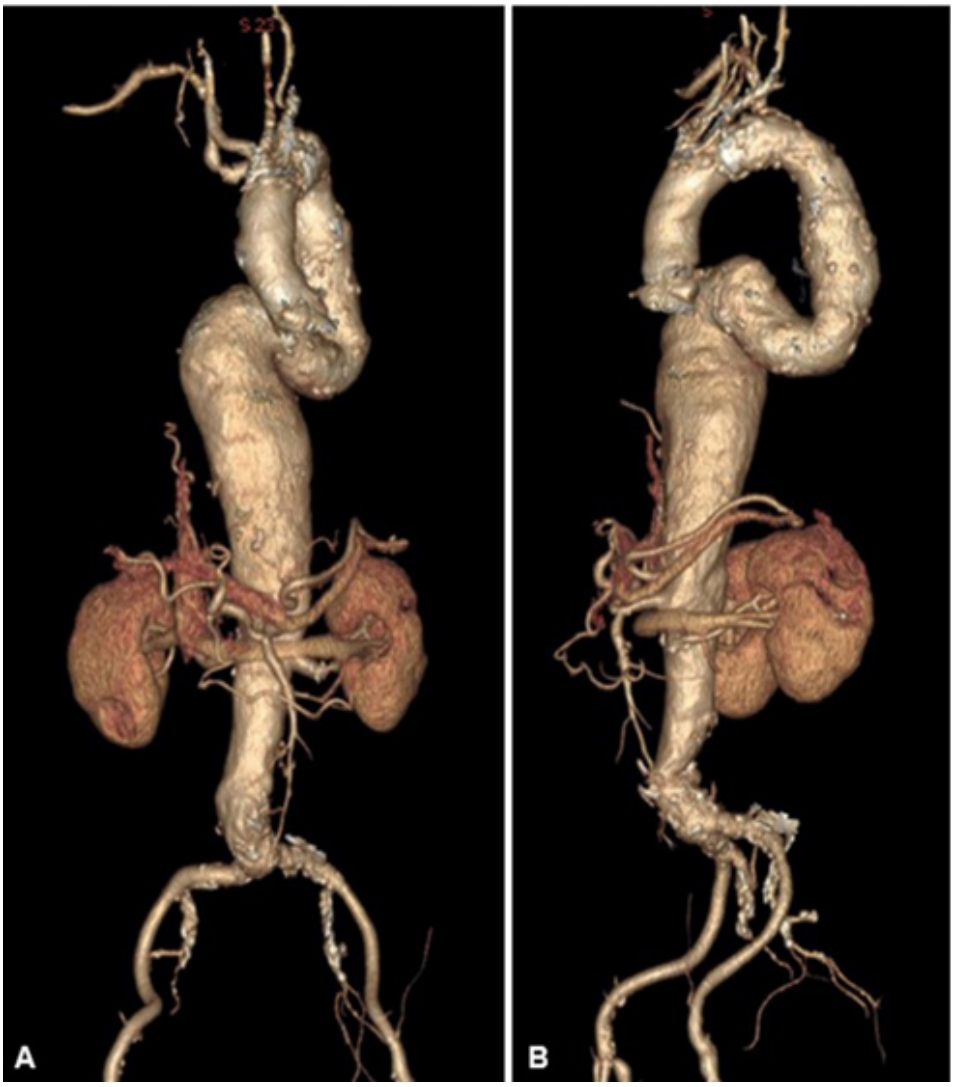

Figure 1 – *Angiotomography with 3D reconstruction. Overview of the thoracoabdominal aneurysm and variations of the supra-aortic trunks in anteroposterior (A) and lateral (B) views.*

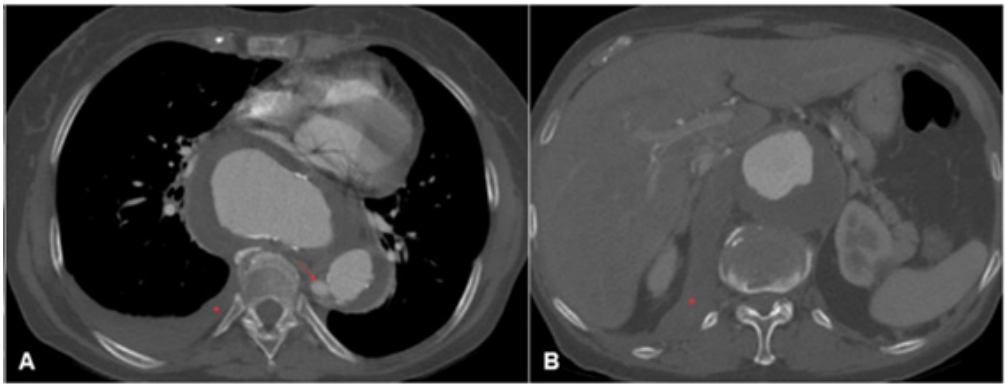

Figure 2 – *Axial angiotomography. A – Rupture of a Crawford 2 aneurysm with contrast extravasation (red arrow) and hemothorax (*); B – Rupture of a Crawford 2 aneurysm with retroperitoneal hematoma (*).*

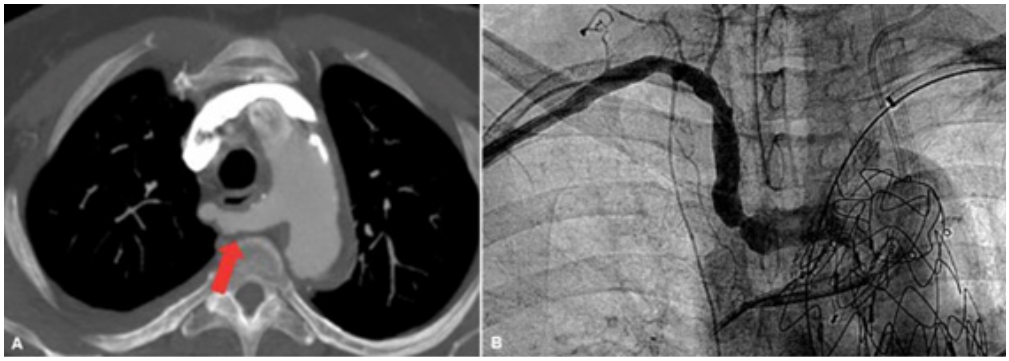

Figure 3 – *Demonstration of the ARSA in axial angiotomography (A; red arrow) and intraoperative angiography (B).*

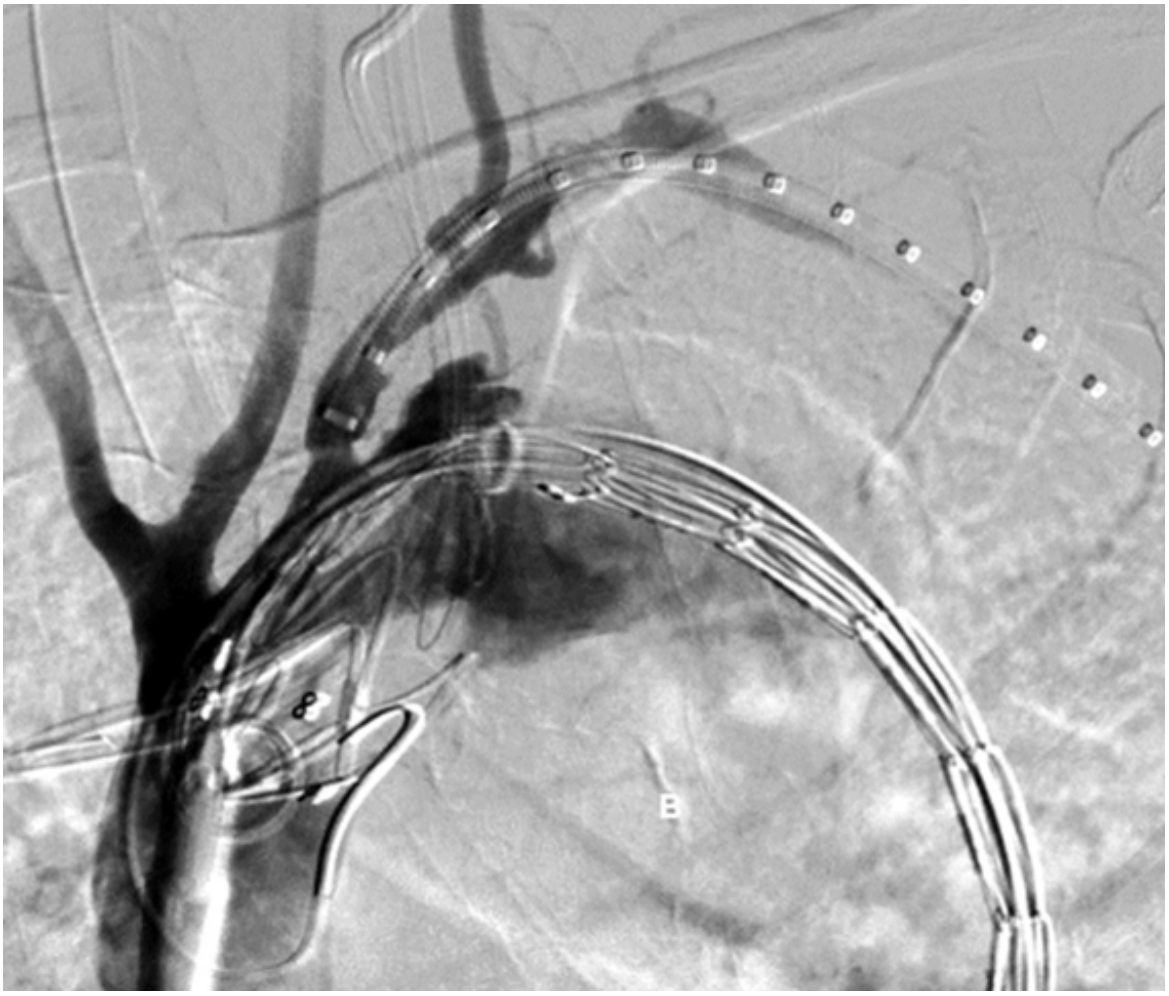

Figure 4 – *Intraoperative angiography with the highlighted bicarotid trunk.*

References

1. Polednak AP. Prevalence of the Aberrant Right Subclavian Artery Reported in a Published Systematic Review of Cadaveric Studies: The Impact of an Outlier. Clin Anat. 2017;30(8):1024-28. doi: 10.1002/ca.22905.
2. Hanžič N, Čizmarević U, Lesjak V, Caf P. Aberrant Right Subclavian Artery with a Bicarotid Trunk: The Importance of Diagnosing This Rare Incidental Anomaly. Cureus. 2019;11(11):e6094. doi: 10.7759/cureus.6094.
3. Buffoli B, Verzeletti V, Hirtler L, Rezzani R, Rodella LF. Retroesophageal Right Subclavian Artery Associated with a Bicarotid Trunk and an Ectopic Origin of Vertebral Arteries. Surg Radiol Anat. 2021;43(9):1491-5. doi: 10.1007/s00276-021-02746-1.
4. Rocha RV, Friedrich JO, Elbatarny M, Yanagawa B, Al-Omran M, Forbes TL, et al. A Systematic Review and Meta-analysis of Early Outcomes after Endovascular Versus Open Repair of Thoracoabdominal Aortic Aneurysms. J Vasc Surg. 2018;68(6):1936-45. doi: 10.1016/j.jvs.2018.08.147.
5. Anacleto AM, Morales MM, Teivelis MP, Silva MFAD, Portugal MFC, Stabellini N, et al. Epidemiological Analysis of 556 Procedures of Open Thoracoabdominal Aortic Aneurysm Repair in the Public Health System in the Largest Brazilian city. Einstein. 2022;20:eAO6724. doi: 10.31744/einstein_journal/2022AO6724.
6. Pandalai U, Pillay M, Moorthy S, Sukumaran TT, Ramakrishnan S, Gopalakrishnan A, et al. Anatomical Variations of the Aortic Arch: A Computerized Tomography-Based Study. Cureus. 2021;13(2):e13115. doi: 10.7759/cureus.13115.
7. Quiñones-Baldrich WJ, Panetta TF, Vescera CL, Kashyap VS. Repair of Type IV Thoracoabdominal Aneurysm with a Combined Endovascular and Surgical Approach. J Vasc Surg. 1999;30(3):555-60. doi: 10.1016/s0741-5214(99)70084-4.
8. Escobar GA, Oderich GS, Farber MA, Souza LR, Quinones-Baldrich WJ, Patel HJ, et al. Results of the North American Complex Abdominal Aortic Debranching (NACAAD) Registry. Circulation. 2022;146(15):1149-58. doi: 10.1161/CIRCULATIONAHA.120.045894.
9. Yang G, Zhang M, Muzepper M, Du X, Wang W, Liu C, et al. Comparison of Physician-Modified Fenestrated/Branched Stent-Grafts and Hybrid Visceral Debranching Plus Stent-Graft Placement for Complex Thoracoabdominal Aortic Aneurysm Repair. J Endovasc Ther. 2020;27(5):749-56. doi: 10.1177/1526602820934466.